

# Interactions of HPV E6 Oncoproteins with Binding Partners: Implications on E6 Stability and Cellular Functions

---

Đukić, Anamaria

Doctoral thesis / Disertacija

2023

Degree Grantor / Ustanova koja je dodijelila akademski / stručni stupanj: **University of Rijeka / Sveučilište u Rijeci**

Permanent link / Trajna poveznica: <https://um.nsk.hr/um:nbn:hr:193:148163>

Rights / Prava: [In copyright](#)/[Zaštićeno autorskim pravom.](#)

Download date / Datum preuzimanja: **2024-12-22**

Repository / Repozitorij:



[Repository of the University of Rijeka, Faculty of Biotechnology and Drug Development - BIOTECHRI Repository](#)



UNIVERSITY OF RIJEKA  
DEPARTMENT OF BIOTECHNOLOGY

Anamaria Đukić

**INTERACTIONS OF HPV E6  
ONCOPROTEINS WITH BINDING  
PARTNERS:  
IMPLICATIONS ON E6 STABILITY AND  
CELLULAR FUNCTIONS**

**DOCTORAL DISSERTATION**

Rijeka, 2023

UNIVERSITY OF RIJEKA  
DEPARTMENT OF BIOTECHNOLOGY

Anamaria Đukić

**INTERACTIONS OF HPV E6  
ONCOPROTEINS WITH BINDING  
PARTNERS:  
IMPLICATIONS ON E6 STABILITY AND  
CELLULAR FUNCTIONS**

**DOCTORAL DISSERTATION**

Supervisor:  
Assist Prof Vjekoslav Tomaić, PhD

Rijeka, 2023

SVEUČILIŠTE U RIJECI  
ODJEL ZA BIOTEHNOLOGIJU

Anamaria Đukić

**INTERAKCIJE ONKOPROTEINA E6  
HPV-a S VEZUJUĆIM PARTNERIMA:  
UTJECAJ NA STABILNOST I STANIČNE  
FUNKCIJE E6**

**DOKTORSKI RAD**

Mentor:  
doc. dr. sc. Vjekoslav Tomaić

Rijeka, 2023.

Supervisor: Assist Prof Vjekoslav Tomaić, PhD

Doctoral thesis was defended on July 7, 2023, at the Department of Biotechnology, University of Rijeka, in front of the committee:

1. Assoc Prof Igor Jurak, PhD (president of the committee)
2. Assoc Prof Felix Wensveen, PhD (member)
3. Assist Prof Dragomira Majhen, PhD (member)

Doctoral thesis contains 218 pages, 46 figures, 21 tables and 390 references.

This doctoral thesis was prepared in the Laboratory of Molecular Virology and Bacteriology, Department of Molecular Medicine of the Ruđer Bošković Institute in Zagreb, under the supervision of Assist Prof Vjekoslav Tomaić, PhD, as part of the postgraduate doctoral study Medicinal Chemistry at the Department of Biotechnology, University of Rijeka.

The dissertation was prepared with the support of two projects: *Elucidating the HPV E6/E7 Oncogenic Functions at Different Anatomical Sites* (IP-2016-06-224) of the Croatian Science Foundation and *Biological Factors Determining Human Papillomavirus (HPV) Driven Carcinogenesis* - ICGEB Early Career Return Grant (CRP/HRV16-05\_EC) (Supervisor: Assist Prof Vjekoslav Tomaić, PhD).

## ***Acknowledgments***

*Prije svega htjela bih zahvaliti svom mentoru doc.dr.sc. Vjekoslavu Tomaiću što je još davne 2016. godine u Trstu prepoznao moju veliku želju za radom u znanosti i izradom doktorata te mi je pružio priliku da dođem u Zagreb u Laboratorij za molekularnu virologiju i bakteriologiju Instituta Ruđer Bošković i provedem 6 predivnih godina ispunjenih predanim radom i druženjem sa divnim kolegama. Zahvaljujem mentoru što me uključio na projekt rada sa MAML1 proteinom i silnom trudu, energiji i volji koju je uložio u sva istraživanja provedena u sklopu svojih projekata, na prenesenom znanju i vremenu uloženom u moje znanstveno usavršavanje, a poglavito tijekom procesa pisanja doktorske disertacije. Nesebično je uložio sate rada kako bi ova disertacija bila na najbolji mogući način izrađena i napisana. Zahvaljujem svojoj kolegici dr.sc. Josipi Skelin Ilić što je tijekom cijelog našeg zajedničkog rada bila moj veliki uzor radi svoje efikasnosti, odličnih laboratorijskih sposobnosti i visokog stupnja znanja. Bez nje ova disertacija nebi bila ista i na tome sam joj iznimno zahvalna. Ovim putem želim vam puno uspjeha u daljnjem znanstvenom radu jer ste ga itekako zaslužili!*

*Zahvaljujem svim članovima Laboratorija za molekularnu virologiju i bakteriologiju što su bili divni kolege i dragi prijatelji tijekom cijelog perioda mog boravka s vama. Posebno zahvaljujem Nini što je postala moja vjerna prijateljica i najveća podrška dijeleći sa mnom sve zgone i nezgone iz našeg poslovnog i privatnog života. Veselim se svakom našem novom odlasku na espresso martini u Fogg. Zahvaljujem Jasminki što je uvijek bila divna prema meni, saslušala me, savjetovala i bodrila, te mi pomagala i nastojala olakšati mnogobrojne laboratorijske zadatke. Zahvaljujem našoj bivšoj šefici Magdalenii što je od prvog dana prepoznala moje zalaganje, štitila me i podupirala od prvog do zadnjeg dana izrade mog doktorata i nastojala mi u što većoj mjeri olakšati ovaj proces. Zahvaljujem Ivanu na njegovoj podršci i nesebičnoj pomoći vezano uz statističku obradu rezultata. Zahvaljujem Ivani što sam sa njom dijelila svoje brige i uživala u opuštrenom razgovoru. Hvala mojoj Tini što je godinama bila moja divna kolegica s kojom sam se uživala družiti na poslu i u slobodno vrijeme. Hvala Kseniji, Nathanielu i Eli što su postali moji bliski prijatelji s kojima sam osim posla dijelila brojne sretne trenutke u mojim prvim godinama provedenim u Zagrebu.*

*Hvala Andrei što je moja najdraža suputnica za putovanja radi koje se radujem svim novim anegdotama koje nas čekaju putujući i izlazeći. Divno je dijeliti sa tobom istu životu energiju i strast prema novim izazovima. Hvala Ani što je uvijek bila uz mene, pažljivo me slušala i savjetovala te postala jedan od mojih najvećih oslonaca čiji savjet cijenim i volim. Ana, želim ti prije svega da uživaš u majčinstvu i kad dođe vrijeme da nastaviš sa svojom znanstvenom karijerom jer znam da te čeka još mnogo uspjeha.*

*Također, zahvaljujem svim kolegama sa Zavoda za molekularnu medicinu te kolegama u 5. krilu što su mi godinama uljepšavali svaki radni dan, bio mi je zaista užitak raditi sa svima. Hvala svim prijateljima koje sam upoznala tijekom svog boravka na Ruđeru, bilo je tu puno smijeha i lijepih trenutaka koje ću zauvijek pamtiti.*

*Htjela bih se također zahvaliti svojim najdražim prijateljicama Nini i Nataliji što su moje vjerne družice još od studentskih dana, znaju svaki detalj vezan uz mene te me neizmjerljivo vole i podržavaju kao i ja njih (i danas na dan dok pišem ovu zahvalu moja Nati mi je javila da očekuje bebu i toliko me razveselila). Hvala Igoru i Mariji na velikoj podršci i prijateljstvu koje dobivam od njih, radujem se njihovom proširenju obitelji novom malom članicom. Hvala mojoj Anamariji i Nensi što su moj oslonac, podrška i najdraže društvo. Ne znam što bih bez vaše ljubavi i iskrenih savjeta.*

*Naposljetku, htjela bih zahvaliti svojoj obitelji što je cijeli život tu za mene, podupirala me od prvih koraka pa kroz cijeli ovaj dugačak put obrazovanja. Hvala mojim bakama i djedovima (koji više nažalost nisu tu) što su me na sve moguće načine podržavali i bodrili u mom školovanju. Znam da njima moj uspjeh vrijedi više nego meni samoj. Najveće hvala ide naravno mojim roditeljima Nataši i Predragu koji su mi sve omogućili, pogotovo što se tiče mog preseljenja u Zagreb i tijekom cijelog perioda izrade doktorata. Uvijek su bili tu za mene i znam da će to zauvijek tako i ostati. Neizmjerljivo vas volim i ovaj doktorat posvećujem vama radi svega što ste uložili u mene. Za kraj ostavljam zahvalu mom najdražem biću na cijelome svijetu, a to je moja mala sekica Nina. Hvala ti miško što sa mnom dijeliš sva ova veselja i nedaće akademskog života. Hvala ti za Oxford, to nas je zbližilo više od svega. Ti si moja najveća podrška i radost.*

*Hvala svima,*

*Ana*



## ABSTRACT

### **Interactions of HPV E6 Oncoproteins with Binding Partners: Implications on E6 Stability and Cellular Functions**

**Anamaria Đukić**

Ruđer Bošković Institute

Human papillomaviruses (HPVs) are a group of small DNA viruses that cause various human malignancies, with cervical cancer being the most significant disease associated with a persistent HPV infection. Only a small number of HPV types has been shown to be responsible for these malignancies. These HPVs are referred as high-risk (HR) types, with HPV-16 and -18 being the most prominent ones. Two major viral oncoproteins, E6 and E7, directly contribute to the development of cancers by interfering with various cellular signaling pathways. A number of HPV-16 variants has been identified in different geographical locations, with some variants exhibiting higher oncogenic potential than others. The first part of thesis focuses on the analysis of the HPV-16 E6 D25N L83V variant, which was shown to be strongly associated with the development of cervical cancer. It was shown that this variant exhibits an increased capacity for interacting with E6AP ubiquitin ligase and consequently degraded it more efficiently, in comparison to the other analyzed mutants HPV-16 E6 D25N and E6 L83V. The HPV-16 E6 mutants' abilities to degrade key cellular target proteins, including the p53 tumor suppressor and PDZ-domain containing substrates, were investigated through *in vitro* and overexpression degradation assays. The analyses revealed no significant differences in the degradatory activities among the evaluated E6 mutant oncoproteins. Furthermore, the second part of this thesis demonstrates that multiple  $\alpha$ -E6 oncoproteins can bind to MAML1 via LXXLL motif, resulting in an increased  $\alpha$ -E6 protein stability.  $\beta$ -E6 oncoprotein stability was also shown to be dependent on the interaction with MAML1, whilst the absence of MAML1 led to both HPV-8 E6 and HPV-18

E6 oncoprotein rapid turnover at the proteasome. The study proposed a model by which most of  $\beta$ -E6s interact exclusively with MAML1, whereas it appears that two cellular pools of HR  $\alpha$ -E6 are present, one forms a complex with MAML1, while the other one interacts with E6AP. Although HR  $\alpha$ -E6/MAML1 complex does not affect the targeting of cellular substrates such as p53 and DLG1, co-expression of MAML1 and E6AP with HR  $\alpha$ -E6 modulates MAML1's normal cellular activities leading to a significant increase in cellular proliferation. Silencing MAML1 decreases wound closure in HeLa cells, suggesting its role in the regulation of cellular migration in HPV-positive cells and maintenance of the transformed phenotype. Overall, this doctoral thesis provides novel insights into the functions of both  $\alpha$ - and  $\beta$ -E6 oncoproteins and their roles in HPV-induced pathogenesis.

(218 pages, 46 figures, 21 tables, 390 references, original in English)

**Keywords:** HPV, E6, E6 variants, cervical cancer, skin cancer, E6AP, MAML1, oncogenesis, protein stability, proliferation, migration

**Supervisor:** Assist Prof Vjekoslav Tomaić, PhD

**Reviewers:** Assoc Prof Igor Jurak, PhD (president of the committee)

Assoc Prof Felix Wensveen, PhD (member)

Assist Prof Dragomira Majhen, PhD (member)

**SAŽETAK****Interakcije onkoproteina E6 HPV-a s vezujućim partnerima:  
utjecaj na stabilnost i stanične funkcije E6****Anamaria Đukić**

Institut Ruđer Bošković

Humani papilomavirusi (HPVs) pripadaju skupini malih DNA virusa koji uzrokuju različita maligna oboljenja, pri čemu je rak vrata maternice najznačajnija bolest povezana sa dugotrajnom HPV infekcijom. Samo mali broj HPV tipova uzrokuje zloćudne bolesti. Spomenuti tipovi nazivaju se visokorizičnim (HR), među kojima su HPV-16 i HPV-18 najistaknutiji. Dva glavna virusna onkoproteina E6 i E7 svojim djelovanjem izravno pridonose razvoju raka djelujući na različite stanične signalne puteve. Postoje mnoge varijante HPV-16 zastupljene na različitim geografskim lokacijama te se pokazalo da neke od varijanti imaju veći onkogeni potencijal. Prvi dio doktorske disertacije usmjeren je na analizu HPV-16 E6 D25N L83V varijante koja je usko povezana s nastankom raka vrata maternice. Utvrđeno je da varijanta D25N L83V ostvaruje povećanu interakciju sa ubikvitinskom ligazom E6AP te je posljedično najučinkovitija u poticanju njezine razgradnje u usporedbi sa ostalim ispitanim mutantima HPV-16 E6 D25N i E6 L83V. Svojstva mutanata da izazovu razgradnju ključnih staničnih ciljnih proteina, uključujući tumor-supresor p53 i stanične proteine koji sadrže PDZ-domene ispitana su *in vitro* esejima razgradnje i esejima razgradnje provedenim korištenjem kulture stanica. Međutim, nisu otkrivene značajne razlike u aktivnostima razgradnje među ispitivanim HPV-16 E6 mutantima. Drugi dio doktorske disertacije otkriva da se različiti  $\alpha$ -E6 onkoproteini vežu za MAML1 putem LXXLL strukturalnog motiva, što rezultira povećanom stabilnošću onkoproteina E6. Nadalje, stabilnost onkoproteina  $\beta$ -E6 također ovisi o interakciji s MAML1, dok utišavanjem MAML1 dolazi do brže proteasomske razgradnje onkoproteina HPV-8 E6 i HPV-18 E6 u HPV-pozitivnim stanicama. Studija predlaže

molekularni model prema kojemu većina onkoproteina  $\beta$ -E6 stupa u interakciju isključivo s MAML1, dok su prisutna dva stanična skupa HR  $\alpha$ -E6, od kojih jedan tvori kompleks s MAML1, a drugi stupa u interakciji s E6AP. Iako kompleks HR  $\alpha$ -E6/MAML1 nema ulogu u razgradnji važnih staničnih ciljnih proteina kao što su p53 i DLG1, zajednička ekspresija MAML1 i E6AP sa HR  $\alpha$ -E6 mijenja uobičajene stanične aktivnosti MAML1 dovodeći do značajnog povećanja stanične proliferacije. Dodatno, utišavanje MAML1 smanjuje „proces cijeljenja rane“ u HeLa stanicama ukazujući na njegovu ulogu u regulaciji stanične migracije HPV-pozitivnih stanica i održavanju transformiranog fenotipa. Sveobuhvatno, doktorska disertacija donosi nove uvide o funkcijama onkoproteina  $\alpha$ - i  $\beta$ -E6 i njihovoj ulozi u patogenezi izazvanoj HPV infekcijom.

(218 stranica, 46 slika, 21 tablicu, 390 literaturnih navoda, jezik izvornika: engleski)

**Ključne riječi:** HPV, E6, E6 varijante, rak vrata maternice, rak kože, E6AP, MAML1, onkogeneza, stabilnost proteina, proliferacija, migracija

**Mentor:** doc.dr.sc. Vjekoslav Tomaić

**Članovi stručnog povjerenstva:** izv. prof. dr.sc Igor Jurak (predsjednik)  
izv. prof. dr. sc. Felix Wensveen (član)  
doc. dr. sc. Dragomira Majhen (član)

## PROŠIRENI SAŽETAK

Humani papilomavirusi (HPVs, *engl.* human papillomaviruses) raznolika su obitelj virusa sa malom kružnom dvolančanom DNA bez ovojnice. Inficiraju bazalni sloj epitelnog tkiva sluznice i kože na različitim anatomskim mjestima u ljudskom tijelu, a dugotrajna infekcija može dovesti do različitih kliničkih simptoma u rasponu od benignih bradavica do invazivnih karcinoma. Identificirano je više od 440 različitih tipova HPV-a, s razlikama u tropizmu i sposobnosti promicanja maligne transformacije. Alfa-papilomavirusi ( $\alpha$ -HPV) prvenstveno inficiraju anogenitalnu i oralnu sluznicu te se dijele temeljem njihove etiološke uloge u razvoju lezija koje mogu izazvati nastanak raka vrata maternice, brojnih anogenitalnih karcinoma i karcinoma glave i vrata. Četrnaest tipova HPV-a ubraja se u visokorizične (HR, *engl.* high-risk) tipove budući da posjeduju sposobnost promicanja maligne transformacije. HPV-16 je najzastupljeniji tip HPV-a koji uzrokuje karcinome različitih anatomskih sjela, ali je prvenstveno prepoznat kao glavni uzročnik raka vrata maternice. Dva glavna virusna onkoproteina E6 i E7 svojim djelovanjem izravno pridonose razvoju malignosti posredovane HPV infekcijom. Identificirane su mnogobrojne prirodno prisutne varijante HPV-16 zastupljene na različitim geografskim lokacijama te se pokazalo da neke od varijanti imaju veći onkogeni potencijal ukazujući na važne razlike u njihovoj sposobnosti izazivanja maligne progresije. Unatoč tome, molekularni mehanizmi odgovorni za povećani rizik od razvoja raka kod određenih varijanti HPV-16 još su uvijek vrlo slabo definirani. Prvi dio doktorskog istraživanja usmjeren je na analizu bioloških karakteristika HPV-16 E6 D25N L83V varijante koja je u visokom postotku povezana s nastankom raka vrata maternice. Proces mutageneze korišten je za stvaranje mutiranih formi HPV-16 E6 L83V, HPV-16 E6 D25N i HPV-16 E6 D25N L83V, a utvrđeno je da varijanta 16 E6 D25N L83V ostvaruje povećanu interakciju sa staničnom ubikvitinskom ligazom E6AP te je najučinkovitija u poticanju njezine proteasomske razgradnje. Stanična lokalizacija analiziranih HPV-16 E6 mutanata se ne razlikuje. *In vitro* eseji razgradnje i eseji provedeni korištenjem kulture stanica nisu otkrili značajne razlike u svojstvima mutanata da izazovu razgradnju ključnih staničnih ciljnih proteina, uključujući p53 tumor-supresor i stanične proteine koji posjeduju PDZ-domene (MAGI-1, DLG1, Scrib), no dobiveni rezultati pružaju detaljniji uvid u molekularne mehanizme kancerogeneze koji stoje u pozadini promijenjenih funkcija HPV-16 D25N L83V varijante te mogu dovesti do nastanka raka.

Beta-papilomavirusi ( $\beta$ -HPV) inficiraju kožni epitel te iako se smatraju nekancerogenim, pojedini tipovi  $\beta$ -HPV-a predstavljaju potencijalni rizik za razvoj raka u određenim rizičnim skupinama, stoga se  $\beta$ -HPV tipovi karakteriziraju kao kofaktori koji u kombinaciji s ultraljubičastim zračenjem pridonose razvoju nemelanomskih karcinoma kože. Stanični protein MAML1 koji djeluje kao koaktivator Notch transaktivacijskog kompleksa, identificiran je za interakcijskog partnera i ciljnu staničnu metu  $\beta$ -HPV E6 onkoproteina. Putem ove interakcije  $\beta$ -HPV E6 vrši represiju Notch transkripcijske aktivacije. Interakcija E6 onkoproteina sa MAML1 predstavlja ciljni mehanizam putem kojeg HPV može pridonijeti napredovanju maligne transformacije epitelnih stanica, upućujući na važnu ulogu koju MAML1 ima u molekularnim procesima koji stoje u pozadini infekcije  $\beta$ -HPV tipovima.  $\alpha$ - i  $\beta$ -E6 onkoproteini posjeduju u svojoj strukturi LXXLL motiv koji omogućuje  $\alpha$ -E6 onkoproteinima da tvore kompleks s E6AP te  $\beta$ -E6 onkoproteinima da ostvaruju interakciju sa MAML1. Drugi dio doktorskog istraživanja otkriva da se različiti  $\alpha$ -E6 onkoproteini vežu za MAML1 upravo putem LXXLL strukturalnog motiva, što rezultira povećanom stabilnošću onkoproteina E6. Nadalje, stabilnost onkoproteina  $\beta$ -E6 također ovisi o interakciji s MAML1. Utišavanjem MAML1 dolazi do brže proteasomske razgradnje onkoproteina HPV-8 E6 i HPV-18 E6 u HPV-pozitivnim stanicama. Sukladno dobivenim rezultatima predstavljen je molekularni model temeljem kojeg većina  $\beta$ -E6 onkoproteina stupa u interakciju isključivo s MAML1, dok su prisutna dva stanična skupa HR  $\alpha$ -E6, od kojih jedan tvori kompleks s MAML1, a drugi stupa u interakciju s E6AP. Različiti stanični skupovi E6 pokazuju različitu distribuciju unutar staničnih odjeljaka. Iako kompleks HR  $\alpha$ -E6/MAML1 nema ulogu u razgradnji važnih staničnih ciljnih proteina kao što su p53 i DLG1, zajednička ekspresija MAML1 i E6AP s HR  $\alpha$ -E6 dovodi do značajnog povećanja stanične proliferacije. Dodatno, utišavanje MAML1 smanjuje „proces cijeljenja rane“ u HeLa stanicama ukazujući na njegovu ulogu u regulaciji stanične migracije HPV-pozitivnih stanica. Konačno, dobiveni rezultati pokazuju da interakcija HR  $\alpha$ -E6 s MAML1 rezultira stabilizacijom HR  $\alpha$ -E6 kompleksa, posljedično modulirajući uobičajene stanične aktivnosti MAML1 i povećavajući proliferativni kapacitet HPV-transformiranih stanica raka usmjeravajući ih prema održavanju transformiranog fenotipa. Sveobuhvatno, doktorska disertacija donosi nove uvide o funkcijama  $\alpha$ - i  $\beta$ -E6 onkoproteina i njihovoj ulozi u patogenezi izazvanoj HPV infekcijom.

**Ključne riječi:** HPV, E6, E6 varijante, rak vrata maternice, rak kože, E6AP, MAML1, onkogeneza, stabilnost proteina, proliferacija, migracija

## CONTENTS

|   |    |
|---|----|
| 1. INTRODUCTION.....  | 1  |
| 1.1. Human papillomavirus (HPV) .....                                       | 1  |
| 1.2. Classification of HPVs.....  | 1  |
| 1.2.1. Alpha papillomaviruses .....   | 3  |
| 1.2.2. Beta papillomaviruses.....   | 4  |
| 1.3. Epidemiology of HPV infection.....                                     | 5  |
| 1.3.1. Incidence, prevalence and persistence of HPV infection.....          | 6  |
| 1.4. Malignancies associated with HPV infection.....                        | 7  |
| 1.4.1. Nomenclature and classifications of malignancies .....               | 7  |
| 1.5. Virus structure and genome organization.....                           | 9  |
| 1.6. HPV life cycle .....   | 13 |
| 1.7. Molecular mechanisms of HPV-induced carcinogenesis.....                | 17 |
| 1.7.1. HPV E7 oncoprotein.....  | 20 |
| 1.7.2. HPV E6 oncoprotein.....  | 22 |
| 1.7.3. HPV E6 oncoprotein and the ubiquitin proteasome system .....         | 27 |
| 1.7.4. HPV E6 oncoprotein and interference with p53 tumor suppressor .....  | 30 |
| 1.7.5. HPV E6 oncoprotein and apoptosis .....                               | 32 |
| 1.7.6. HPV E6 oncoprotein and PDZ-domain containing proteins.....           | 37 |
| 1.7.7. HPV E6 oncoprotein and exploiting the host DNA damage response ..... | 43 |
| 1.7.8. HPV E6 oncoprotein and centrosomal abnormalities.....                | 45 |
| 1.7.9. HPV E6 oncoprotein and DNA replication .....                         | 45 |
| 1.8. HPV E6 oncoprotein and Notch signaling pathway.....                    | 49 |
| 1.8.1. Canonical Notch signaling pathway .....                              | 49 |
| 1.8.2. HPV E6 inhibition of Notch signaling pathway .....                   | 50 |
| 2. AIMS OF THE STUDY.....   | 58 |
| 3. MATERIALS AND METHODS.....   | 60 |
| 3.1. Materials.....   | 60 |

|        |   |    |
|--------|---|----|
| 3.1.1. | Buffers and solutions .....   | 60 |
| 3.1.2. | Chemicals, detergents and antibiotics.....                              | 61 |
| 3.1.3. | Commercial kits and reagents.....                                       | 62 |
| 3.1.4. | Enzymes and corresponding buffers.....                                  | 64 |
| 3.1.5. | Antibodies.....   | 64 |
| 3.1.6. | DNA and protein markers.....  | 65 |
| 3.1.7. | Protein inhibitors.....   | 65 |
| 3.1.8. | Media for maintaining cell and bacterial cultures.....                  | 66 |
| 3.1.9. | Instruments and programs.....   | 67 |
| 3.2.   | Molecular methods.....  | 69 |
| 3.2.1. | Site-directed mutagenesis .....   | 69 |
| 3.2.2. | Preparation of chemocompetent <i>DH5<math>\alpha</math></i> cells ..... | 70 |
| 3.2.3. | <i>DH5<math>\alpha</math></i> transformation .....                      | 71 |
| 3.2.4. | Isolation of plasmid DNA.....   | 71 |
| 3.2.5. | Horizontal gel electrophoresis .....                                    | 73 |
| 3.3.   | Cell culture .....  | 73 |
| 3.3.1. | Cell lines .....  | 73 |
| 3.3.2. | Maintenance of cell lines .....   | 74 |
| 3.3.3. | Cell counting.....  | 74 |
| 3.3.4. | Freezing and thawing cells.....   | 75 |
| 3.4.   | Cell biology .....  | 75 |
| 3.4.1. | Transient transfection.....   | 75 |
| 3.4.2. | siRNA silencing.....  | 77 |
| 3.4.3. | Cell migration assay.....   | 78 |
| 3.4.4. | Cell proliferation assay .....  | 78 |
| 3.4.5. | Apoptosis assay.....  | 79 |
| 3.5.   | Protein analysis .....  | 80 |
| 3.5.1. | Western blot analysis .....   | 80 |
| 3.5.2. | Half-life experiments .....   | 81 |
| 3.5.3. | Immunoprecipitation.....  | 82 |



|        |  |     |
|--------|--|-----|
| 3.5.4. | GST pull-down.....   | 84  |
| 3.5.5. | Cell fractionation assays .....  | 85  |
| 3.5.6. | <i>In vitro</i> degradation assay .....  | 86  |
| 3.6.   | Confocal microscopy.....   | 87  |
| 3.7.   | Statistical analysis .....   | 88  |
| 4.     | <b>RESULTS</b> .....   | 90  |
|        | PART I Oncogenic potential of naturally occurring HPV-16 E6 variants.....  | 90  |
| 4.1.   | Generation of HPV-16 E6 mutants using site-directed mutagenesis .....  | 90  |
| 4.2.   | HPV-16 E6 D25N L83V variant exhibits increased capacity to interact with E6AP ....   | 91  |
| 4.3.   | The interaction between HPV-16 E6 D25N L83V and E6AP leads to an increase in E6AP degradation .....                                | 93  |
| 4.4.   | HPV-16 E6 D25N L83V is rapidly turned over at the proteasome .....   | 95  |
| 4.5.   | HPV-16 E6 and the corresponding mutants efficiently degrade p53 and PDZ-domain containing substrates <i>in vitro</i> .....         | 99  |
| 4.6.   | HPV-16 E6 and the corresponding mutants efficiently degrade p53 in cultured cells  | 105 |
| 4.7.   | HPV-16 E6 and the corresponding mutants efficiently target PDZ-domain containing substrates MAGI-1 and DLG1 in cultured cells..... | 107 |
|        | PART II MAML1-induced HPV E6 oncoprotein stability is required for cellular proliferation and migration.....                       | 111 |
| 4.8.   | HPV E6 oncoproteins from $\alpha$ and $\beta$ types interact with MAML1 .....  | 111 |
| 4.9.   | Protein amount of $\alpha$ - and $\beta$ -HPV E6 oncoproteins is MAML1-dependent .....   | 114 |
| 4.10.  | An LXXLL motif of MAML1 is required for HPV E6 protein level regulation .....  | 118 |
| 4.11.  | The stability of HPV E6 protein pool in HeLa, CaSki and HT1080 HPV-8 E6 cells is MAML1-mediated .....                              | 122 |
| 4.12.  | MAML1 stabilizes a distinctive cellular pool of HPV-18 E6 and an exclusive single cellular pool of HPV-8 E6.....                   | 125 |

|       |   |     |
|-------|---|-----|
| 4.13. | p53 and DLG1 degradation is not E6/MAML1 complex dependent .....  | 128 |
| 4.14. | HPV E6 protein turnover is regulated by MAML1 .....   | 131 |
| 4.15. | E6 cellular distribution is altered in presence of MAML1 .....  | 135 |
| 4.16. | Silencing MAML1 has no effect on apoptosis .....  | 137 |
| 4.17. | E6/MAML1 complex impacts cell proliferation synergistically with E6AP .....                                     | 140 |
| 4.18. | E6/MAML1 complex impacts cell migration.....  | 142 |
| 5.    | <i>DISCUSSION</i> .....   | 145 |
|       | PART I Oncogenic potential of naturally occurring HPV-16 E6 variants.....                                       | 145 |
|       | PART II MAML1-induced HPV E6 oncoprotein stability is required for cellular proliferation<br>and migration..... | 157 |
| 6.    | <i>CONCLUSIONS</i> .....  | 175 |
| 7.    | <i>REFERENCES</i> .....   | 177 |
| 8.    | <i>LIST OF TABLES AND FIGURES</i> .....   | 204 |
| 9.    | <i>SUPPLEMENTARY DATA</i> .....   | 208 |
| 10.   | <i>ABBREVIATIONS</i> .....  | 211 |
| 11.   | <i>CURRICULUM VITAE</i> .....   | 216 |

# 1. INTRODUCTION

## 1.1. Human papillomavirus (HPV)

*Papillomaviridae* is a diverse epitheliotropic family of small, non-enveloped, circular double-stranded DNA viruses, that infect all homoeothermic vertebrates (International Agency for Cancer Research 2012; King et al. 2005) with some interesting exceptions such as *Papillomaviridae* family presence in fish (López-Bueno et al. 2016). Among those different *Papillomaviridae* families, the most widely studied are human papillomaviruses (HPVs), that preferentially infect the basal layer of cutaneous and mucosal epithelial tissues at different anatomical locations, resulting in a variety of clinical symptoms ranging from benign warts to invasive cancers (Doorbar 2005a; H. zur Hausen 1996). Papillomaviruses (PVs) are ubiquitous viruses transmitted primarily by direct physical and sexual contacts, and the most of infections do not typically cause evident disease with severe clinical symptoms. The majority HPV types cause benign flat or protruding warts (papillomas), while only a few of them can induce advance cases of malignant transformation. In 1976, Professor Harald zur Hausen revealed that development of cervical cancer was associated with a specific type of HPV infection (zur Hausen 1976), for which he received a Nobel prize in medicine in 2008. His discovery led to decades of research on genital mucosal HPVs resulting in the discovery of a subset of HPV types with an oncogenic potential. In addition, the extensive epidemiological studies have classified those HPVs into oncogenic or ‘high-risk’ (HR) HPV types, which are responsible for approximately 4.5% of cancers cases worldwide (de Martel et al. 2020).

## 1.2. Classification of HPVs

To date, more than 440 different HPV genotypes have been identified (Van Doorslaer et al. 2017; McBride 2022), with different tissue tropism and potential to promote cell proliferation and malignant transformation (Burk et al. 2013). Thus, HPVs are divided into five large genera, which comprise alpha ( $\alpha$ ), beta ( $\beta$ ), gamma ( $\gamma$ ), mu ( $\mu$ ) and nu ( $\nu$ ) (De Villiers et al. 2010).

The HPV classification was established following strict criteria of the International Committee on the Taxonomy of Viruses (ICTV), by which PVs are classified based on sequence similarity and sequence overlapping of the major L1 structural protein (De Villiers et al. 2004; De

Villiers et al. 2010). The reason behind classification based upon sequence similarity of the HPV L1 gene is that it is highly conserved among all PVs. Different genera share less than 60% of nucleotide sequence similarity of the L1 gene, species share between 60% and 70% of nucleotide identity and overlap, and virus types share between 71% and 89% of identical nucleotides in sequence within the L1 gene (De Villiers et al. 2004; De Villiers et al. 2010).

Nowadays, the *Papillomaviridae* family contains 53 genera, each of which is further divided into several species (Van Doorslaer et al. 2017). Between those 53 genera only five of them include PVs that infect humans, and those are above mentioned  $\alpha$ ,  $\beta$ ,  $\gamma$ ,  $\mu$  and  $\nu$  genera. To be classified as a novel papillomavirus type, an individual PV type cannot share more than 90% of nucleotide similarity to any other known PV type (De Villiers et al. 2010; De Villiers et al. 2004). Individual HPV types are highly species and tissue specific, and besides humans, to date PVs have been also detected in fish (López-Bueno et al. 2016), reptiles (Lange et al. 2011), birds (K. Van Doorslaer et al. 2009) and mammals (Rector and Van Ranst 2013). The  $\gamma$ -genus includes the majority of the described HPV types, 99 different types, followed by the  $\alpha$ -genus with 65 types and the  $\beta$ -genus consisted of 54 types (Gheit et al. 2019). The genera  $\mu$  and  $\nu$  include only 3 and 1 known types, respectively.

According to the initial and basic classification of the PVs, whose tissue tropism-based nomenclature is in use in the past few decades, it is common to divide HPVs in two separate groups based on the anatomical origin of the infection, as either mucosal or cutaneous types. However, now it is revealed that within the  $\alpha$ -genera which comprises mostly mucosal types, there are some cutaneous HPV types (i.e. HPV-2, -3, -7 and -10 etc.) (Thomas et al. 2013b; De Villiers et al. 2004). Furthermore, recent studies have also detected  $\beta$ - and  $\gamma$ -HPVs at mucosal sites making classification even more complex (Bottalico et al. 2012; Hampras et al. 2017). With this knowledge, the division into mucosal and cutaneous types does not represent incontrovertible paradigm anymore and needs to be reconsidered, especially in the light of new discoveries that are yet to follow.  $\beta$ ,  $\gamma$ ,  $\mu$  and  $\nu$  genera contain HPV types that infect cutaneous epithelia of the skin (Van Doorslaer et al. 2017), causing common warts rarely associated with cancer development (De Villiers et al. 2010). However, general categorization of cutaneous HPVs as non-cancer-causing types is not applicable for all cutaneous HPVs. Some  $\beta$ -HPV types, like  $\beta$ -HPV-38, show similarities with mucosal HR HPV types, and were shown to be associated with cancer development (Caldeira et al. 2003a; Viariso et al. 2011).

In addition to this,  $\beta$ -HPV-5 and  $\beta$ -HPV-8 have also been detected in cutaneous lesions, as well as squamous cell carcinomas (SCCs) (Aldabagh et al. 2013; Mühr et al. 2015).

Given to the currently large and further growing number of newly discovered HPV types, in recent years a novel approach that clusters PVs was proposed (Brimer et al. 2017). Particularly, what is common to  $\alpha$ -HPV compared to all others HPV genera, is the preference of E6 oncoproteins for interacting with cellular ubiquitin ligase E6-associated protein (E6AP; also known as UBE3A, ubiquitin protein ligase E3A), while all others HPV genera show association with Notch transcriptional co-activator Mastermind like 1 (MAML1). A recent study revealed and established the hypothesis about an early evolutionary split among PV genera, between those viruses encoding for E6 oncoproteins that associate with MAML1 and those E6 oncoproteins which associate with E6AP (Brimer et al. 2017). This evolutionary divergence provides a basis for categorizing PVs into two major functional groups, into those that physically and functionally target MAML1, and those that physically and functionally target E6AP. Grouping of PVs into those that target Notch signaling via interaction with MAML1 protein, and those that target cellular substrates for proteasome-mediated degradation via association with E6AP, provides a novel factor and an unique feature for categorizing PV types in a simplified way compared to sequence difference within L1 capsid gene (Brimer et al. 2017).  $\alpha$ -HPV E6 oncoproteins associate with the cellular ubiquitin ligase E6AP, by binding to its LXXLL motif, thereby regulating its ubiquitin ligase activity.  $\beta$ ,  $\gamma$  and  $\mu$  genera of E6 proteins bind a similar LXXLL motif present on the cellular transcriptional co-activator MAML1, and with this interaction repress Notch signaling, which appears to be critical for their productive life cycle (Brimer et al. 2017; Brimer et al. 2012; Brimer et al. 2007; Zanier et al. 2013).

### **1.2.1. Alpha papillomaviruses**

*Alphapapillomavirus* types ( $\alpha$ -HPVs) preferentially infect genital, anal and oral mucosa (King et al. 2005), and are classified on the basis of extensive clinical, experimental and epidemiological evidences of their etiological role in the development of lesions that can progress to cervical, anogenital, and head-and-neck carcinomas (International Agency for Research on Cancer (IARC)). So far, fourteen  $\alpha$ -HPV types (16, 18, 31, 33, 35, 39, 45, 51, 52, 56, 58, 59, 68, 73) have been classified as high-risk (HR) HPV types causing mostly cervical cancer.

Of those HR HPVs, HPV-16 and HPV-18 together are associated with approximately 80% of cervical cancer cases globally, while the remaining 20% are linked to infection by other widespread HR HPVs (de Sanjose et al. 2010). HPV type 16 (HPV-16) is the most prevalent oncogenic HPV associated with 61% of all cervical cancer cases (de Sanjose et al. 2010), and can be further classified into four major variant lineages (A, B, C and D) (Burk et al. 2013). HPV-18 is widely accepted as the second most prevalent carcinogenic HPV type by its presence in 16% of cervical cancers worldwide (Chen et al. 2015). HPV-18 sequence variants were also identified and form three phylogenetic lineages (A, B, and C). On the other hand, low-risk (LR) types (the most common examples are HPV-6 and HPV-11) cause benign anogenital warts and are rarely found in squamous intraepithelial lesions, possibly as a part of multiple HPV infections (Boda et al. 2018; Bouvard et al. 2009).

HPV infections in the majority of cases are cleared by the host immune system, but the common period of infection lasts from a few months up to two years from the initial viral entry (C. A. Moody and Laimins 2010). However, the infection for certain reasons in some individuals cannot be neutralized by the host immune system, which then persists for long periods of time and can result in the development of different types of neoplasia (zur Hausen 2002). Thus, persistent infections with HR HPVs, most commonly with HPV-16 and HPV-18, has been recognized as the main causative agent of cervical cancer. The difference between HPV-16 and HPV-18 is reflected in the fact that, among cervical carcinoma cancer cases, HPV-18 is more associated with the development of adenocarcinomas (ADC), and accounts for 37% of cervical ADC worldwide, while HPV-16 mainly causes cervical squamous cell carcinomas (Chen et al. 2015). HPVs also cause different types of anogenital cancers including carcinomas of the vagina, vulvar, and penile cancers (Lont et al. 2006; Madsen et al. 2008, 30). Furthermore, it was shown that HR HPV infections, mostly with HPV-16, are associated with approximately 50% of head-and-neck cancers (HNC), particularly oropharyngeal cancer (Taberna et al. 2017).

### **1.2.2. Beta papillomaviruses**

Since 2018, there has been a huge expansion in the discovery of new *Betapapillomaviruses* ( $\beta$ -HPVs) types isolated from individuals with immunodeficiency (Tirosh et al. 2018).  $\beta$ -HPVs infect cutaneous tissue around hair follicles and can predispose the development of UV-mediated

skin cancer (Lambert et al. 2020). The *Betapapillomavirus* genus comprises 54 HPV types detected in normal, as well as precancerous tissue and in cancerous cutaneous tissue (King et al. 2005; Gheit 2019). Since the number of cutaneous HPVs has been increased over the last five years, there was a need for more precise classification of  $\beta$ -HPVs. Thus, currently  $\beta$ -HPVs are classified into five separated phylogenetic species. HPV-5 and HPV-8 together with 19 additional HPVs are classified as species 1. There are 22 members classified as species 2 including cancer-causing HPV-38, four are species 3, one belongs to species 4, three to species 5, and 4 have not yet been classified (Burk et al. 2013). A smaller portion of  $\beta$ -HPV types, including HPV-5, -8 and mentioned HPV-38, have oncogenic potential in hypersensitive organ transplant recipients who were under immunosuppressive treatment, and in patients with a rare hereditary disease named epidermodysplasia verruciformis (Orth et al. 1987; Orth et al. 1978). In those cases  $\beta$ -HPVs have been found in benign skin warts, actinic keratosis, keratoacanthoma, psoriasis and in cutaneous squamous cell carcinomas (CSCC) (Egawa and Doorbar 2017; Howley and Pfister 2015). Keratoacanthoma are low grade, rapidly growing skin tumors derived from the hair follicle cells. In addition, it has been established that  $\beta$ -HPV infection cannot promote tumors in the same manner as HR HPVs that cause tumors dependent on continued viral oncogene expression (Tommasino 2017). So,  $\beta$ -HPVs are characterized as co-factors in combination with ultraviolet (UV) irradiation that contribute to the development of non-melanoma skin cancers (NMSC) by inhibiting apoptosis of infected cells (Tommasino 2017; Jackson et al. 2000). However, an etiological role for  $\beta$ -HPV types in skin cancers remains mostly unclear and must be further investigated.

### **1.3. Epidemiology of HPV infection**

Worldwide, among  $\alpha$ -HPV-associated cancers about 90% are attributable to female cancers of which 91% is cervical cancer, in contrast to 10% male cancers (de Martel et al. 2020). Cervical cancer rates (age-standardized (W) rate per 100,000) vary greatly between geographical regions ranging from 40 in low and middle income countries (sub-Saharan Africa, Melanesia, South America, and South-Eastern Asia) to 4 in high income countries (Northern America, Australia/New Zealand, and Western Asia), with mortality rates varying up to 18 times (Sung et al. 2021). This huge variation is mostly due to the combined effect of HPV prevalence, the quality

of screening programs, vaccination and the public health conditions (Vaccarella et al. 2014). Besides cervical cancer, other HPV-attributable female cancers (9%) account for 11,000 cases of vulvar cancer worldwide per year, 14,000 vaginal cancers, 19,000 anal cancers and 11,100 HNC. In addition, HPV-attributable male cancers account for 41,500 cases of HNC worldwide per year, 18,000 penile cancer and 9,900 anal cancer (de Martel et al. 2020). The HPV-associated HNC represent 52,600 cases worldwide per year, 79% (41,500) in men and 21% (11,100) in women, of which 42,100 (80%) in both gender are oropharyngeal cancers, occurring mostly in high income countries (de Martel et al. 2020). According to the USA data, in the line with mentioned numbers of HNC, a significantly higher prevalence of oral HPV infection has been observed in infected men (10.1%), than in women (3.6%) (Senkomago et al. 2019).

### **1.3.1. Incidence, prevalence and persistence of HPV infection**

Genital HPV incidence rises intensely after average age of the first sexual intercourse (de Martel et al. 2020). HPV infections spread rapidly within sexually active both genders, as HPV is highly transmissible. An infected individual can obtain multiple infections of different HPV types, simultaneously or repeatedly, because the immune response to the infection is mostly weak and specific to a particular HPV type (de Martel et al. 2020). Cervical HPV infection incidence decreases with older age as a result of a lesser number of sexual contacts and owing to type-specific immunity developed after infections over the life span. However, the ratio of the viral re-activation increases with age, as the immunological response gets less effective (de Martel et al. 2020).

HPV prevalence is a function of both the incidence and the persistence of infection (Schiffman et al. 2007). Prevalence is highly variable due to different factors, including geographical region and the prevalence of different HPV variant types, sexual habits, age, host control and the immune response, the type of treatment and cervical screening. The persistence of virus more than 2 years is considered to be uncommon and in more than 90% of cases it is not detected within 5–7 years of the initial infection (Rodríguez et al. 2008).



## **1.4. Malignancies associated with HPV infection**

### **1.4.1. Nomenclature and classifications of malignancies**

To predict the risk of HPV-induced cancer development, several histological and cytological nomenclature systems have been developed. The most used and widespread cytological system for screening of precancerous cervical epithelial lesions and malignancies includes the Papanicolaou classification ('Pap' test), in which severity of the lesion is graded based on the abnormal mitotic changes in nuclear shape and size and percentage of cytoplasmic maturation lost in cervical cells (Schiffman et al. 2016). Histopathological classification used for cervical cancer diagnosis include the cervical intraepithelial neoplasia (CIN) scale, which differentiates tissue samples from mild dysplasia (CIN1), moderate dysplasia (CIN2), severe dysplasia (CIN3) and carcinoma *in situ*. The CIN scale is used as a marker of severity of the malignant transformation of the epithelial tissue (Schiffman et al. 2016).

#### ***1.4.1.1. Cervical cancer***

Cancer of the cervix uteri is the 4th most common cancer among women population worldwide, with 604,127 new cervical cancer cases diagnosed in 2020., and 341,831 recorded deaths (Sung et al. 2021). With those data and statistics cervical cancer turns out to be the second most frequent female cancer in women aged between 15 and 44 years on the global level (International Agency for Research on Cancer (IARC)). Persistent HPV infection mainly results in the development of squamous cell carcinoma, but HPV infection with HR HPV types, although much less frequent, can drive the development of endocervical adenocarcinomas. Thankfully, mortality rates of cervical cancer are substantially lower than its incidence (International Agency for Research on Cancer (IARC)), and it is important to emphasize that since most cervical cancers result from HPV infection they are therefore preventable through regular screening process and vaccination.

#### ***1.4.1.2. Anogenital cancers***

In addition to cervical cancer, HPV can cause anogenital benign warts and different types of anogenital squamous cell carcinomas (SCC), both in men and women, and these include penile, anal, vaginal and vulvar cancers (International Agency for Research on Cancer (IARC)).

HPV-related adenocarcinomas of the lower anogenital tract (vagina, vulva and anorectum area) are rare but morphologically very distinctive tumors that exhibit cytologic features similar to HPV-related endocervical adenocarcinoma. The primary vulvar adenocarcinomas are extremely rare with the existing literature limited to case reports, same as the primary anal canal adenocarcinomas (Voltaggio et al. 2020).

#### **1.4.1.3. *Head-and-neck cancers***

HPV can cause benign and malignant lesions of the mucosal tissue of the upper aerodigestive tract (Lechner et al. 2022). HPV oral infections in the last decade gained much clinical attention because of their involvement in the development of head-and-neck squamous cell carcinoma (HNSCC), a group name that refers to SCC, originating from the oral cavity, lips, larynx and pharynx. Oropharyngeal squamous cell carcinoma (OPSCC) is the most common cancer type of HNCs, and comprises tumors located in the posterior pharyngeal wall, the soft palate, uvula, the tonsillar complex and the base of the tongue (Lechner et al. 2022). The reason behind this statistics is that tonsillar crypts and the base of the tongue are immunoprivileged microenvironment which facilitates HPV infection and its persistence (Egawa et al. 2015). HPV-positive (HPV+) and HPV-negative (HPV-) HNSCCs are defined as separate tumor entities, with distinct molecular profiles and molecular background for the malignant transformation, disease biology, tumor characteristics and outcomes (Craig et al. 2019). In 2021 HPV accounted for 71% of all OPSCCs cases in the USA and for 51.8% cases in UK (Senkomago et al. 2019; Schache et al. 2016), emphasizing the importance of this current public health problem. Of these, 85–96% of OPSCC are caused by HPV-16 (Schache et al. 2016), although both mucosal and cutaneous HPVs can be detected in the oral cavity (Gheit et al. 2020).

### 1.5. Virus structure and genome organization

The structure of papillomavirus is characterized by a non-enveloped icosahedral shape, with a diameter ranging from 50 to 60 nm (Moody and Laimins 2010; Van Doorslaer et al. 2017). HPV genome is in the form of a double-stranded episome of approximately 8 000 base pairs (bp), and contains eight, or even nine (depending on the type of PV) open reading frames (ORFs) (Egawa et al. 2015). Furthermore, to stay preserved and to prevent tangling and damaging HPV genome is assembled and packaged into chromatin with a help of host cell histones. Icosahedral viral protein capsid is assembled of 360 copies of the L1 gene product, with a smaller number of L2 proteins linking the viral capsid to its viral genome (Buck et al. 2008). Viral gene expression is controlled by different promoters and with a process of mRNA splicing that enables viral gene products to be expressed at different stages during the viral life cycle (Doorbar 2006).

The HPV genome is organized into three major regions (**Figure 1**) (Graham and Faizo 2017). A long control region (LCR), also called the upstream regulatory region (URR), located between the L1 and E6 ORFs, is a non-coding region of the genome that contains the origin of replication, as well as post-transcriptional control sequences that control viral gene expression. Hence, LCR contains the early promoter and other regulatory elements involved in viral DNA replication and transcription including SP1, AP1, NF1, TEF1, OCT1, YY1, BRN-3a, NF-kB, NF-IL6, KRF-1, GATA3, FOXA1, GATA3, binding sites for the E1 and E2 viral gene products and the TATA box (Bernard 2013). The early region encodes the early (E), well-conserved core genes E1, E2, E4, E5, E6 and E7 involved in viral gene expression, regulation of transcription, replication, proliferation and survival (C. Moody 2017). The late region (L) encodes two structural proteins, large capsid protein L1 and minor capsid protein L2 (**Figure 1 and 2**). ‘E’ states for ‘early’, whereas ‘L’ indicates ‘late’ and their names reflect the period in the viral life cycle when transcription occurs.

HR HPV genomes contain the early and late promoters that are active during different stages of the viral life cycle (Geisen and Kahn 1996). In undifferentiated cells, viral gene expression is regulated by the early promoter, which is located upstream of the E6 ORF in the LCR. For HPV-16 and HPV-31 the early promoter is termed as p97 (**Figure 1 and 2**), and p105 for HPV18 (Braunstein et al. 1999; Geisen and Kahn 1996; Ozbun and Meyers 1998). The early promoter directs the expression of E1 and E2, which are necessary for viral replication. The late promoter is located in the E7 ORF and is activated during cell differentiation. Late promoter for

HPV16 is p670 (Figure 1 and 2), p742 for HPV31 and p811 for HPV18 (Grassmann et al. 1996). The late promoter drives expression of E1, E2, E1<sup>^</sup>E4 and E5 to facilitate productive viral replication. In addition, the L1 and L2 ORFs are also expressed from the late promoter in the suprabasal layers as a result of changes in splicing (Grassmann et al. 1996; Hummel et al. 1992).

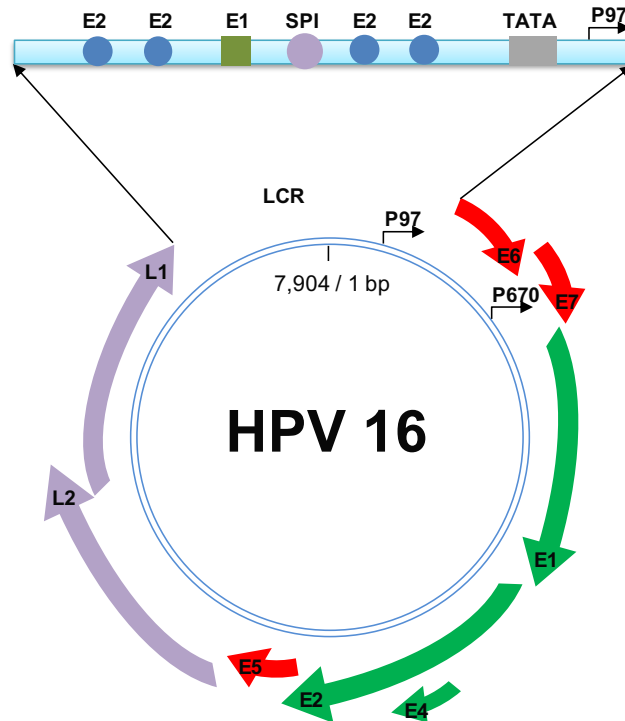


**Figure 1. Schematic representation of HPV-16 genomic organization.** The HPV genome contains three main regions: the early and late regions, based on the timing of viral gene expression, and the long control region (LCR). The early region encodes for regulatory proteins that are essential for viral transcription and replication and cell cycle control. The late region encodes two structural proteins, L1 and L2, required for capsid formation. The LCR contains most of the regulatory DNA sequences needed for replication and expression of the viral genes, including the ORFs, enhancer and promoter regions. Adapted from (Schiffman et al. 2016).

The core proteins (E1, E2, L1 and L2) are directly involved in viral genome replication (E1 and E2) and viral assembly (L1 and L2), and are highly conserved among PVs (C. Moody 2017). They are necessary for completion of the viral life cycle, enabling the undisturbed viral replication and shedding of the virions (Van Doorslaer and McBride 2016). The accessory proteins (E4, E5, E6 and E7) exhibit greater variability considering the timing of their expression and a greater variability of their functional characteristics.

E1 encodes a virus-specific enzyme ATP-dependent DNA helicase, obligatory for viral genome replication and amplification as it recruits cellular replication factors to viral ORFs, and it specifically binds and unwinds the ORF (Bergvall et al. 2013). E2 is a sequence-specific DNA binding protein that interacts with different cellular gene products and modifies their roles to benefit the virus (McBride 2013). Thus, the most important role of E2 is to act as an auxiliary replication factor that binds the E1 helicase in the ORF to form the replication initiation complex, and it recruits the cellular DNA replication machinery (Stubenrauch et al. 1998). Furthermore, E2 is a transcriptional regulator that can activate or repress viral transcription (Graham 2016). Besides the key role in viral genome replication and transcription, E2 is also involved in arrangement and maintenance of viral episomes during replication by interacting with chromatin adapter proteins and by tethering viral genomes to host mitotic chromosomes. Furthermore, in dividing cells, the low viral genome copy number is maintained by the complementary regulation of E1 and E2 proteins, while E2 retains the genomes in the nucleus and distributes them to daughter cells during replication (McBride et al. 2019). E2 binds to the promoter of E6 and E7 genes to retain their low expression levels and to block the access of transcription factors in undifferentiated cells (McBride 2017). Some HPV types express the spliced transcript which is a fusion of E8 and the C-terminal part of the E2 ORF, termed as E8<sup>E2</sup> that encodes for a protein that includes an E8 domain fused to the hinge and DNA-binding domains of E2 (Dreer et al. 2017). E8<sup>E2</sup> functions to limit the viral replication and transcription in undifferentiated cells in the basal layer and differentiated cells in the suprabasal layers of stratified epithelium.

The early accessory genes (E4, E5, E6 and E7) exhibit certain diversity between types, and are also in some literature termed as the regulatory genes because they have roles in the regulation of virus shedding, cell cycle re-entry, avoiding apoptosis and immune escape (Egawa et al. 2017; Fehrmann et al. 2003; Vande Pol and Klingelutz 2013; McLaughlin and Münger 2010). E4 has different roles associated with viral genome amplification, virion assembly, shedding and transmission of packed virions (Doorbar 2013). The E4 ORF is positioned in the middle of the E2 ORF (**Figures 1 and 2**) (Wilson et al. 2005). Specifically, it is located within the region that encodes the flexible hinge domain of E2. This overlap results in the primary E4 gene product, as well as the major spliced transcript known as E1<sup>E4</sup>, being translated from the spliced mRNA (Wilson et al. 2005). E1<sup>E4</sup> fuses the first five amino acids of the E1 ORF with E4. The role of

E1<sup>E4</sup> is to cause G2 cell cycle arrest in differentiated cells, to enhance viral replication and release of virions (Doorbar 2013).

Only  $\alpha$ -HPVs in their sequence contain an additional coding sequence, located between the early and late region that encodes for E5 gene (**Figures 1 and 2**) (C. Moody 2017). Individual  $\alpha$ -HPV type encodes one of four different types of E5 protein (E5 $\alpha$ , E5 $\beta$ , E5 $\gamma$  and E5 $\delta$ ). E5 is a transmembrane protein that localizes in the endoplasmic reticulum of the host cell and promotes proliferation by activating different cellular signaling pathways such as, for the epithelial tissue important epidermal growth factor receptor (EGFR) signaling (C. Moody 2017). With a function of promoting proliferation and facilitating efficient productive replication in differentiating cells E5 is considered to be the minor oncoprotein as it is unable to cause cellular transformation, but has a supportive pro-carcinogenic roles (Gutierrez-Xicotencatl et al. 2021; Liao et al. 2013). Through the actions of E5, HPV can evade adaptive and innate immune systems, by not presenting viral antigens on the major histocompatibility complex (MHC) molecules (C. A. Moody and Laimins 2010a).

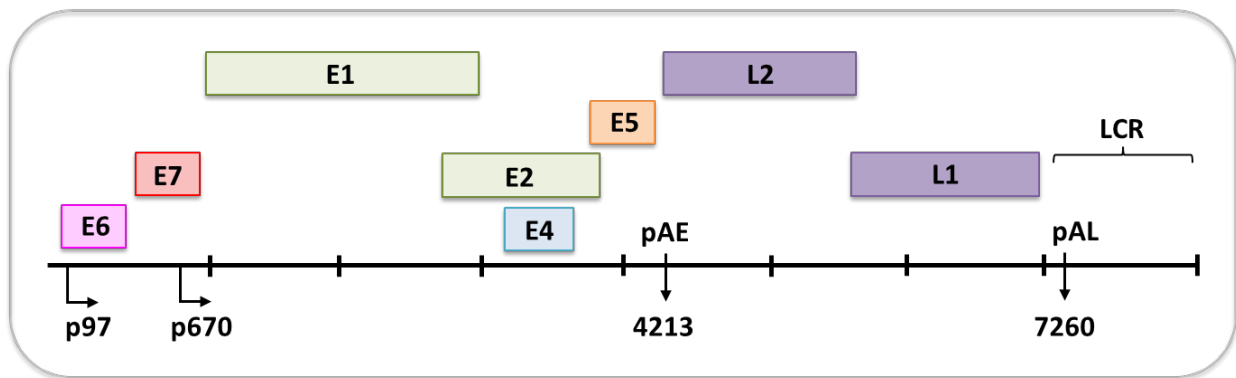


**Figure 2. Linear representation of the HPV-16 genome.** Different ORF are indicated as a block. The early promoter is located upstream of the E6 ORF (p97) and the late promoter is located in the E7 ORF (p670). The early polyadenylation site (pAE) is located at the 3' end of the E5 ORF (pAE) and the late polyadenylation site (pAL) located in the LCR. The origin of replication and E1 and E2 binding sites are also located in the LCR. Adapted from (C. Moody 2017).

E6 and E7 are viral oncogenes and are regulated at the transcriptional level by E2, allowing genome amplification in the middle layers of the epithelium (Graham 2016). An essential function of E6 and E7 in the viral life cycle is to increase viral fitness and virion production by driving cell cycle re-entry, genome amplification in the differentiating suprabasal layers, avoiding apoptosis

and inducing cell proliferation (C. A. Moody and Laimins 2010a). The oncogenic  $\alpha$ -PVs are also unique for the reason that E6 and E7 proteins are transcribed from a polycistronic, alternatively spliced mRNA (Rosenberger et al. 2010). Splicing of the oncogenic polycistronic E6/E7 transcript also gives rise to a novel protein, termed as E6\*s, and their numbers can vary depending the virus type (Pim et al.1997).

The virus capsid contains 360 molecules of L1 protein arranged into 72 capsomeres structured of five L1 molecules (DiGiuseppe et al. 2017). Approximately 72 molecules of minor L2 protein per capsid are arranged as one L2 copy per capsomere, meaning that major L1 protein encapsidates the viral minichromosome, as well as minor L2 proteins to form the icosahedral-shaped virion. L1 almost completely covers surface of the mature virion and is required for the initial attachment to the host cell (DiGiuseppe et al. 2017). The ability of L1 to spontaneously form virion like particles (VLPs) created the basis for the development of vaccines against HPVs (Kirnbauer et al. 1992). During viral entry, a conformational change of the capsid results in protrusion of specific L2 sequences onto the surface of the virion to allow the endosomal transport of the viral particles inside the cell cytoplasm (Xie et al. 2020; Campos 2017). L2 is expressed again in later stages to assist in packaging of viral minichromosomes into progeny virions which are released without cell lysis from, as the epithelial cells are shed from the uppermost layers of the cornified epithelium (Scarth et al. 2021). L2 is highly conserved among HPV types and has been used as an alternative target antigen to develop HPV vaccine, since immunization with isolated L2 induce low-titer cross-neutralizing antibodies to a broad range of HPV genotypes (Yadav et al. 2019).

## **1.6. HPV life cycle**

HPV infects proliferating stem cells located in the basal layer of stratified squamous epithelia, as a result of small abrasions, micro-wounds or other epithelial trauma (Doorbar 2005b; C. A. Moody and Laimins 2010a). HPV via microabrasions has easier and direct passage towards basal cells in the transformation zone of the cervix which is particularly susceptible to the HPV infection (Day and Schelhaas 2014). As a consequence of microabrasions heparan sulfate chains of proteoglycans (HSPG) are exposed on the surface of the cells in the basal membrane (J. N. Roberts et al. 2007). Binding of the virus to heparin sulfate induces a conformational change in

the viral capsid, which in turn enables the association with cellular receptors exposed on the surface of the epithelial cells and keratinocytes in skin epidermis, which are target cells of HPV (Day and Schelhaas 2014). After binding to the cell surface, the virion is internalized by the process of cellular endocytosis, using the cellular retromer complex for retrograde transport to the trans-Golgi compartment (Xie et al. 2020).

Stratified squamous epithelium consists of five different layers which exhibit differences in the morphology and differ in their proliferative potential capacity (**Figure 3**). Hence, epithelial cells in the basal layer are in continuous proliferation, while the suprabasal layers embody differentiating cells that have exited the cell cycle and became terminally differentiated. HPV life cycle is strictly linked to the modulations in the differentiation status of the host epithelial cells and keratinocytes (Longworth and Laimins 2004; McBride 2017). After the infection HPV initiates transient replication producing approximately 50 up to 100 viral genomes per cell, implying that at this stages HPV genomes are present in the form of extrachromosomal elements or episomes. Viral episomes are maintained in the undifferentiated, proliferating basal cells, where they replicate with the host cell chromosomes (Longworth and Laimins 2004; McBride 2017). The beginning of the active cell division that occurs during wound healing process, which aims to repair epithelial traumas, is a crucial step for viral entry into the nucleus and consequent maintenance of the viral episomes (Pyeon et al. 2009). After cell division, one infected daughter cell migrates away from the basal layer and undergoes differentiation (C. A. Moody and Laimins 2010b). Simultaneously with the differentiation of epithelial cells and their migration towards the suprabasal layers, the productive phase of the viral life cycle is activated. This leads to the amplification of viral genomes from hundreds to thousands of copies per cell, which occurs in the microenvironment of terminally differentiated cells in the suprabasal layers (C. A. Moody and Laimins 2010b). Productive infection, termed as a productive because of virion production, involves E6/E7 low expression levels and does not require extensive cell cycle re-entry in the basal and parabasal cell layers (Schiffman et al. 2016) (**Figure 3**). E6 and E7 expression is required for genome amplification in the middle epithelial layers and initial virus assembly. The transition to the late stage of HPV infection is followed by the expression of late genes L1 and L2, virion assembly, release of virions from the surface of the epithelial tissue and disintegration of dead superficial epithelial cells into the surrounding microenvironment (Morgan et al. 2018; Doorbar 2005b) (**Figure 3**).



Regulation of the viral life cycle in this manner allows HPV to avoid detection by the immune system, because high-level viral gene expression and virion production are restricted to the upper layers of the epithelium which are not under immune surveillance (Stanley 2010).

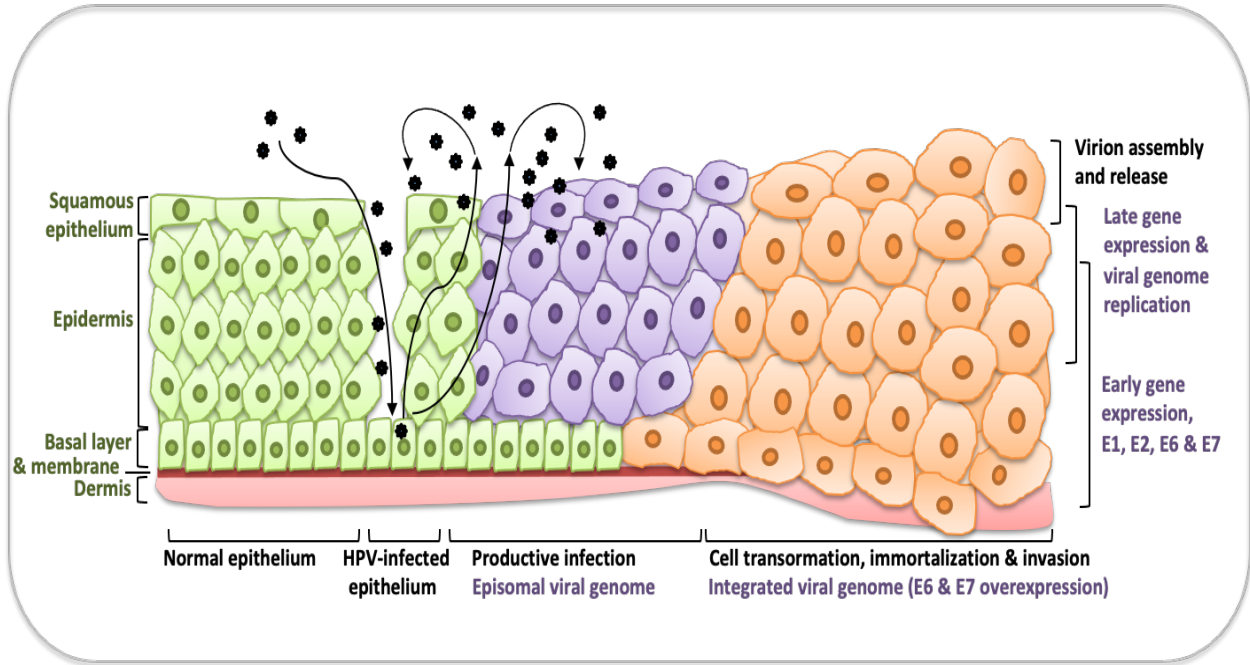


**Figure 3. HPV life cycle and development of malignancy.** Through microtraumas and fissures in epithelial tissue HPV infects epithelial cells in the basal layer. Uninfected epithelium is depicted on the left side, while infected epithelium is indicated on the right. Upon entry, the virus traffics through the endosome using the cellular retromer complex, becoming uncoated. Once in the nucleus the viral genomes are preserved as low copy episomes and early viral genes (E1, E2, E6, E7) are expressed. After cell division, one infected daughter cell migrates away from the basal layer and undergoes differentiation. Process of differentiation of HPV-infected cells induce the productive phase of the viral life cycle, which requires cellular DNA replication machinery. The expression of E6 and E7 disrupts cell cycle control, pushing differentiating cells into S phase, allowing viral genome amplification in cells that would normally exit the cell cycle. In the late-phase L1 and L2 proteins encapsidate synthesized viral genomes and progeny virions are shed from the topmost layers of the epithelium in viral-loaded squamous. Adapted from (Schiffman et al. 2016).

Described HPV strategy with establishing low-level, but continuous and persistent infection in mucosal and skin epithelia and restricting the productive infection to terminally differentiated cells in upper layers without inducing cell lysis, is highly effective for the viral fitness and promotes long-term persistent infection and immune evasion. Thus, HPV knowingly

manipulates the balance of cellular proliferation and differentiation, to provide both persistent infection in the basal cells and productive infection in differentiated cells (Stanley 2010).

Furthermore, HPV episomes do not encode polymerases or any other enzyme required for viral replication (McBride 2017). Since it depends on the host DNA replication machinery to replicate its DNA, HPVs use different mechanisms to perturb cellular regulatory pathways that regulate cell replication, maintaining differentiating cells in the state of active cell cycle. Epithelial differentiation in healthy, uninfected tissue results in an exit from the cell cycle, limiting replication capacity of terminally differentiated cells (McBride 2017). In the case of HPV infection, HPV keeps activated cellular genes necessary for the late gene expression, which are important for the amplification of viral DNA. On the contrary to the initial phases of HPV infection and viral genome maintenance in the proliferating basal cells, the productive phase of the viral life cycle, including replication, late gene expression and virion production, occur upon epithelial differentiation, in cells that in normal conditions, without being infected, would exit the cell cycle (McBride 2017). Although, in most of the cases, HPV infection is asymptomatic and neutralized by the immune system, in some individuals a certain parts of the viral genome become integrated into the host DNA, due to still not completely defined circumstances. This process results in the lost of the majority of the viral genes, except of E6 and E7 (C. Moody 2017). Viral DNA integration is not a part of the normal viral life cycle, since it results in termination of the productive life cycle due to the loss of genes needed to complete the synthesis of new virions. Once HPV DNA is integrated, the infection becomes abortive and no more virions are produced and released (Graham and Faizo 2017). With the integration, the expression of E6 and E7 falls under the control of cellular promoters as E2 gene is lost (C. Moody 2017). In the context of this, high-throughput methods for the analyses of the viral integration identified 3667 breakpoints for the integration of HPV genome in cervical lesions and a frequent integration site is a MYC oncogene, relevant for the oncogenic process, what is important in terms of HPV-induced malignancies (Hu et al. 2015).

### **1.7. Molecular mechanisms of HPV-induced carcinogenesis**

The viral integration of HR HPV types to the host genome is the key event in the process of malignant transformation and the maintenance of the transformed phenotype. The consequences of the viral integration and the mechanisms involved in the initiation of the malignant transformation will be discussed further in the sections below. Viral DNA integration in the host genome, leads to loss of the most parts of the viral genome and upregulated expression of the early oncogenes E6 and E7, which drives uncontrolled proliferation of the infected cell (Tomaić 2016a; Snijders et al. 2006; Steben and Duarte-Franco 2007). Hence, the oncogenicity of HPV is strictly dependent on the joint effects of E6 and E7 oncoproteins (Doorbar 2005a). As a proof of this it was shown by various analyses that abolition of expression, or inhibition of E6 and E7 functions in cells derived from cervical tumors results in a disruption of the transformed cell growth and induction of either senescence or apoptosis (Butz et al. 1996; Butz et al. 2003). The oncogenic activities of E6 and E7 are manifested by their targeting of diverse cellular signaling pathways involved in the regulation of cell-cycle entry, apoptosis, cell polarity networks and immortalization (Doorbar 2005a). The main cellular substrates targeted by E6 and E7 oncoproteins are tumor suppressor p53 (Scheffner et al. 1990a) and the retinoblastoma tumor suppressor protein pRb (Dyson et al. 1989), which are inactivated by the cellular proteasome machinery in presence of the viral oncoproteins. It is important to explain that the primary reason which drives HR E6 proteins to block p53 tumor suppressor functions is to facilitate the productive viral replication, since p53-mediated functions would negatively regulate viral genome amplification (Kho et al. 2013), and only subsequently, the consequences of inactivating p53 contribute to tumor development. Hence, the viral aims regarding p53 inactivation are not tumor development, since the virus would lose its replicative capacity, but rather facilitation and achievement of undisturbed viral fitness. The formation of the tumor is likely to occur during a long-term persistent HPV infection, which leads to the continual abrogation of p53 functions, resulting in the accumulation of genetic mutations and DNA damage, which are a prerequisite for viral pathogenesis.

Furthermore, it was shown that E6 mutants deficient for degradation of p53 can still immortalize cells, indicating that additional p53-independent targets play important parts in the process of the malignant transformation and that other cellular factors are necessary for cancer development (Wang et al. 2001; Liu et al. 1999). Transgenic mouse models have been used extensively to dissect the role of E6 and E7 in the development of malignancy. Studies have shown

that conditional deletion of pRb in epithelia of mouse animal model did not abolish completely the effects of E7 activities, showing the importance of an additional number of E7 cellular targets and their ability to mediate carcinogenic process (Strati and Lambert 2007a). In addition, pRb binding-deficient mutant of E7 can immortalize primary human keratinocytes if coordinates with E6 oncoprotein (Jewers et al. 1992). It was shown that chronic estrogen treatment together with continuous oncogene expression of HPV-16 E6 and E7 promotes the development of cervical cancer (Riley et al. 2003; Song et al. 1999). Although E6-expressing mouse models develop tumors, E7 is more efficient in initiating tumor formation, while E6 most likely plays a major role in the later stages of tumor progression (Riley et al. 2003).

Several studies that included transgenic mouse models demonstrated an important contribution of the conserved E6's binding motif, named PDZ-binding motif (PBM) since via this binding motif HR E6s interact with cellular PDZ domain-containing proteins, towards the development of malignancy. Mouse models expressing HPV-16 E6 in the epidermis develop epithelial hyperplasia, but transgenic mice that were expressing an E6  $\Delta$ PBM mutant failed to develop hyperplasia, which implies that the ability to cause hyperplasia progressing towards to a transformed SCC phenotype is dependent on the presence of an intact PBM (Nguyen et al. 2003). A significant reduction in the tumor size and multiplicity was noticed in mouse animal model expressing the E6  $\Delta$ PBM mutant in co-operation with wild type E7, compared with mouse models expressing wild type E6 and E7 (Shai et al. 2007), suggesting that E6 PBM plays a critical role in the maintenance of the transformed phenotype of HPV-infected cells.

Studies with transgenic mouse models of HNC differ from those of the skin and cervix, with respect to the role of E6 PBM in the development of these cancers (Jabbar et al. 2010). In the case of HNC, the E6 and E7 oncoproteins co-operate in the induction of SCC, with E7 being the more potent oncogene (Jabbar et al. 2010; Strati and Lambert 2007b). The studies performed on transgenic mouse models that expressed E6  $\Delta$ PBM, showed that E6 co-operating with E7 to cause HNSCC surprisingly does not require an intact E6 PBM (Jabbar et al. 2010). Results indicated that although E6 and E7 synergize to induce HNSCC in transgenic mice, currently unknown mechanism, independent of the E6 PDZ binding potential also takes a part in that process. Moreover, transgenic mouse models showed that actions of E6 cause altered centrosome copy number and centrosomal abnormalities (Riley et al. 2003). The roles of HR E6 in the activation of hTERT and telomerase, as well as in telomeric DNA regulation are multiple and

complex (Liu et al. 2009). Activated telomerase is found in HPV-positive cervical carcinoma cells and neoplastic lesions leading to continued and uncontrolled cell division. Furthermore, in response to aberrant proliferation HPV-infected cell accumulates mutations. As an example, HPV-positive lesions frequently harbor somatic mutations, like those of apolipoprotein B mRNA editing catalytic polypeptide-like (APOBEC) gene (Chen et al. 2015). APOBEC family of proteins is a group of cellular enzymes that catalyze the deamination in single-stranded DNA and have antiviral role in the innate immune system, so it is not surprising that the levels of the expression of APOBEC3A protein were found to be decreased in cervical cancer tissues.

Interestingly, in transgenic mouse models, high expression of HPV-16 E5 in the epidermis induced epithelial hyperproliferation that results in tumor formation (Maufort et al. 2007). It was shown that the expression of E5 is increased upon initiating the process of cell differentiation to promote proliferation of differentiated cells and productive viral replication. In estrogen-treated mice models, expression of E5 by itself induced cervical cancers, suggesting that E5 in some cases functions as a viral oncogene (Maufort et al. 2010).

On the contrary,  $\beta$ -HPV types infect the basal layer of the squamous epithelium of the skin and hair follicle region, but the exact mechanism of infection so far remains unknown (Boxman et al. 1997; Feltkamp et al. 2008). Interestingly, the viral integration is not the case with  $\beta$ -HPVs and there is no continuous oncoprotein expression allowing the persistence of the transformed phenotype during CSCC (Quint et al. 2015). By this, it seems that  $\beta$ -HPVs possibly contribute to the initial steps of tumor formation, but are not necessary for its maintenance (Tommasino 2017; Egawa and Doorbar 2017; Meyers and Munger 2014). So far it is known that  $\beta$ -HPVs can contribute to the appearance of multiple cellular mutations that can drive tumorigenesis, without continued viral gene expression required for tumor maintenance. This suggests that  $\beta$ -HPV infections have a more pronounced impact on the cellular microenvironment than on malignant transformation (Tommasino 2017; Egawa and Doorbar 2017; Meyers and Munger 2014). In addition,  $\beta$ -HPV-38 was shown to promote tumorigenesis in transgenic mice models by cooperative actions of E6 and E7 oncoproteins together with the ultraviolet light, resulting in the development of actinic keratosis-like lesions and SCC (Viarisio et al. 2011). *Mus musculus* papillomavirus 1 (MmuPV1) is an excellent animal model for dissecting the key aspects of the viral life cycle and pathogenesis of cutaneous HPV infection. MmuPV1 replicate and form skin warts and cancers in experimentally infected laboratory mouse strains, while MmuPV1 E6 shares

the capacity to inhibit NOTCH signaling with the skin cancer-associated HPV-8 E6. Importantly, it was shown that MmuPV1 E6 expression and the ability to bind MAML1 and inhibit NOTCH signaling are necessary for wart formation in mice (Meyers et al. 2017b). Currently, additional proteomic studies have started to shed some light on a novel cellular pathways that may be targeted by the various cutaneous  $\beta$ -HPVs (White et al. 2012).

### 1.7.1. HPV E7 oncoprotein

HPV E7 oncoprotein is a small acidic protein consisted of 98 amino acids and a zinc-binding domain at the C-terminus, whose structural integrity is necessary for molecular activities of E7 (Gammoh et al. 2006). Structurally, E7 is built of three main domains: the amino-terminal conserved domain 1 (CD1), the conserved domain 2 (CD2) containing an LXCXE binding motif and the CKII phosphorylation site, and the conserved domain 3 (CD3) containing zinc finger motif (**Figure 4**) (Prathapam et al. 2001). A part of N-terminal CD1 and CD2 corresponds to small parts of conserved regions 1 and 2 of adenovirus E1A (Cole and Danos 1987), while CD3 has sequences that overlap to those of simian vacuolating virus 40 large tumor antigen (SV40 LT) (Phelps et al. 1988; 1992; McLaughlin and Münger 2010; Roman and Munger 2013). The CD3 domain is formed by two CXXC domains that function as a dimerization domains (**Figure 4**) (Clemens et al. 1995).

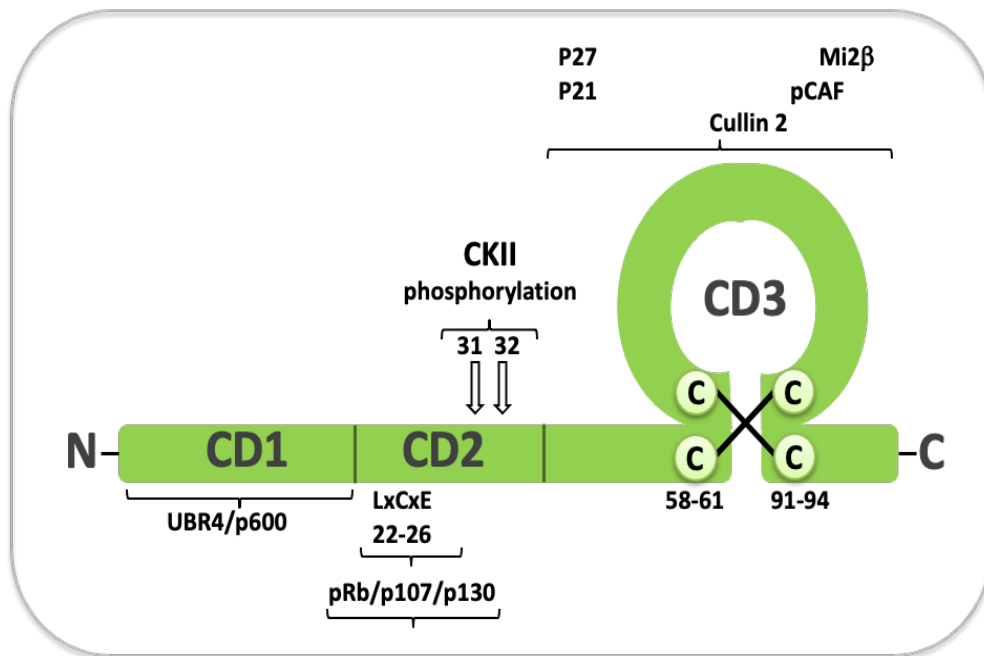


**Figure 4. Schematic representation of HR E7 protein structure.** CD1, CD2 and CD3 are structural regions of E7 necessary for maintenance of the molecular functions of E7 oncoprotein. C-terminal zinc finger domain, CXXC dimerization domains, LXCXE binding motif involved in pRb binding as well as two serine residues (31 and 32) important for casein kinase II (CKII) phosphorylation as a part of CD2 structure are indicated, along with other important E7's binding partners. Adapted from (Tomaić 2016a).

The overall structural integrity of the protein is critical for E7 interactions with its cellular targets, although most of the functions of E7 have been attributed to the CD2 and CD3 domains (Patrick et al. 1994). The main functions of HR E7 are to create a supportive environment within the differentiating epithelium that will be permissive for viral genome amplification, and to play a part in a modification of the cell cycle re-entry through the associations with the key regulators of the cell cycle control machinery (Tomaić 2016). Regarding to this, HR E7 oncoprotein functions to maintain the differentiating cell in a DNA synthesis-competent state, mostly by targeting pRb for proteasome-mediated degradation (**Figure 4**) (Dyson et al. 1989). Tumor suppressor pRb is a crucial cellular regulator of cell cycle progression, which controls the G1 to S-phase transition in cell cycle control (Smotkin and Wettstein 1986). Utilizing those activities E7 plays an important part in promoting tumor initiation in the early stages of HPV-driven malignancy as well as in and the process of malignant transformation, as the HPV-infected cell with accumulated mutations go through successive round of replication (Parkin and Bray 2006). Nevertheless, the proliferation of HPV-infected cells stimulated by E7 also does not correlate entirely with the ability of E7 to degrade pRb (Caldeira et al. 2000). Hence, casein kinase II (CKII) phosphorylation at the N-terminus of E7 is also critical for its transformation activity (**Figure 4**) (Barbosa et al. 1990). CKII phospho-acceptor site is part of the CD2, and besides the importance for E7's transforming capacity it has a role in driving S-phase progression (Firzloff et al. 1991; Chien et al. 2000).

E7 binds to the pRb-associated members of the pocket protein family that include p107 and p130, with a role in driving the cell cycle progression of differentiating epithelial cell into continuous S-phase state (**Figure 4**). This continuous S-phase-like state creates environment in the suprabasal layer suitable for replication of the viral genome (Morris and Dyson 2001). An important difference between HR and LR E7 oncoproteins is their diverse ability to interact with pRb and more specifically, also the ability of HR E7 to bind and degrade p107, which controls cell cycle entry in the basal layer, as well as p130, which is involved in cell cycle re-entry in the upper epithelial layers (Morris and Dyson 2001; Klingelutz and Roman 2012).

In order to complete these activities, E7 forms interactions with ubiquitin ligases, and the main one is cullin 2 (CUL2), a core component of the cullin-RING-ECS (Elongin BC–Cullin 5–SOCS-box) E3 ubiquitin ligase complex (**Figure 4**) (Huh et al. 2007). E7 also targets many other cell cycle regulators and transcription factors, and these interactions are important for the stability of E7 and additional modulation of different cellular processes related to the carcinogenic progression (Gammoh et al. 2006; Vats et al. 2022). Hence, the CD1 domain has a part in cellular transformation since E7 through this domain binds and deactivates UBR4/p600 whose loss of activity induces anchorage independent growth (DeMasi et al. 2005; Huh et al. 2005). Ubiquitin ligase UBR4/p600 is required for E7 proteasome-mediated PTPN14 degradation, correlating with pRb-independent transforming activities of HR E7 (Szalmás et al. 2017). E7 oncoprotein also retains S-phase competent state in differentiating keratinocytes abrogating CDK inhibitors p21 and p27 to maintain the activity of cyclin-dependent kinase 2 (CDK2)/cyclin A complex (**Figure 4**) (Helt et al. 2002). In addition, E7 oncoprotein has a direct effect on centrosome duplication and occurrence of aberrant centrosome number (Duensing et al. 2000) as a result of E7 interaction with p53 but independently of pRb degradation (Duensing and Münger 2003), as well as an outcome of stimulating CDK2/cyclin activity involved in the abnormal centrosome duplication (Duensing et al. 2004).

### 1.7.2. HPV E6 oncoprotein

The HPV E6 oncoprotein contains 150 amino acids and has two zinc finger domains created by four CXXC motifs (**Figure 5**) (Cole and Danos 1987; Martinez-Zapien et al. 2016). The structural integrity of these motifs is crucial for E6 oncoprotein activities and are highly conserved across all HPV types (Kanda et al. 1991; Sherman and Schlegel 1996). The crystal structure of the intact E6 oncoproteins was characterized (Nominé et al. 2006a; Zanier et al. 2013; Martinez-Zapien et al. 2016). and it includes HPV-16 E6 and the specific domains of HPV-18 E6, HPV-51 E6 and Bovine Papillomavirus 1 (BPV-1) E6 oncoproteins (Nominé et al. 2006a; Zanier et al. 2013; Zhang et al. 2007). HPV E6 forms interactions with many cellular substrates through different conserved binding motifs. PBM is exclusively present on the C-terminus of HR HPV E6 oncoproteins and mediates the interaction with numerous cellular PDZ domain-containing proteins (**Figure 5**) (Thomas et al. 2008a; Bennett Saidu et al. 2019). Another conserved binding motif of E6 is the LXXLL binding motif. Via this binding motif E6 oncoprotein interacts with E3 ubiquitin-



protein ligase E6AP, the preferred interacting partner of  $\alpha$ -HPV E6 oncoproteins (**Figure 7**) (Huibregtse et al. 1993d; Elston et al. 1998; White et al. 2012).

Hence, as already being emphasized, the main oncogenic activity of HR E6 oncoproteins is the ability to interact with the p53 tumor suppressor (**Figure 7**) (Scheffner et al. 1990a). LR E6 oncoproteins also bind to p53, but the interaction is rather weak (Pietsch and Murphy 2008; Oh et al. 2004). Only the interaction between HR E6 and p53 drives p53 degradation via the ubiquitin proteasome pathway (Scheffner et al. 1990b).

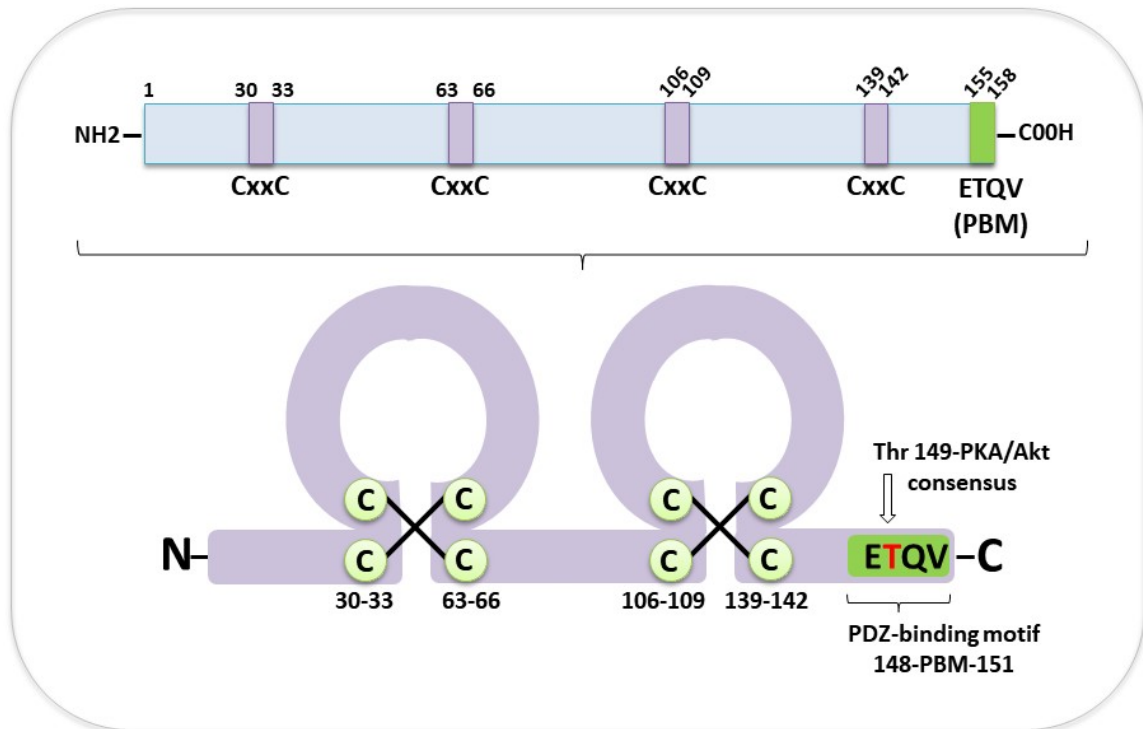


**Figure 5. Schematic representation of HR HPV E6 oncoprotein structure.** Schematic diagrams of E6 structure both as a linear (upper panel) and 2D representations (lower panel) show two zinc finger domains created by four CXXC motifs. The C-terminal E6 PDZ binding motif (ETQV) and the overlapping site of PKA phosphorylation are arrowed. Adopted from (Tomać 2016c).

Consequently, the described ability of HR E6 to degrade p53 has major implications for the overcoming of p53 tumor suppressor activities, yet E6 can also act as potent inhibitor of p53 transcriptional activity through the interaction with histone acetyltransferases to prevention even p53 acetylation (Zimmermann et al. 1999). Furthermore, E6 inhibits apoptotic signaling through the degradation of proapoptotic factors BAX and BAK (Garnett and Duerksen-Hughes 2006a) and

activates enzyme telomerase reverse transcriptase (hTERT) and enzyme telomerase for the preventing telomere shortening in response to successive rounds of replication and persistent proliferation which subsequently induces immortalization of HPV-infected cell (**Figure 10**) (Howie et al. 2009). E6-mediated degradation of PDZ domain containing proteins leads to loss of cell polarity and induction of hyperplasia because cellular targets that are bound by E6 oncoprotein through the PBM motif are important regulators of the cell adhesion, cell contacts and cell polarity networks (Thomas et al. 2008b). Through these interactions HR E6 oncoproteins act as a major contributor in maintaining the transformed phenotype (Doorbar 2005a). More about those processes will be discussed in detail at the following sections.

#### ***1.7.2.1. Naturally occurring HPV E6 variants***

Different HPV types are defined upon the established divergence between HPV nucleotide sequences which is 10% or more, for phylogenetically close genomes that share a mutual ancestor (Bernard et al. 1994). PV genes that differ no more than 2% in the coding regions and 5% in the non-coding regions of the genome, with respect to the prototype isolates for the same strain are defined as intra-type variants (also defined as subtypes or lineages) (Burk et al. 2013a). Studies in which sequencing analyses on E6 gene and the LCR region were performed have revealed the existence of numerous natural variant forms of HR HPV types (Zhang et al. 2015; Burk et al. 2013b). HPV-16 E6 naturally occurring variants were most extensively researched because of their epidemiological prevalence (Burk et al. 2013a). These HPV-16 E6 variants were divided into four major phylogenetic clusters according to the geographic distribution and origin: A (European-Asian, EAS), B (African1, AF1), C (African 2, AF2), and D (North American/Asian American, NA/AA) (Burk, Harari, and Chen 2013a). Next, the four lineages have been subdivided into eleven sublineages that are: (1) A1, A2, A3 (European, E), A4 (Asian, As); (2) B1 (Afr1a), B2 (Afr1b); (3) C1 (Afr2a), C2 (Afr2b); and (4) D1 (North American, NA), D2 (Asian American 1, AA1), and D3 (Asian American 2, AA2), and the sublineages have also been stratified into classes and subclasses.

Nowadays, a broad spectrum of intratype variants of HPV-16 E6 is known, accompanied with high levels of diversity, biological behavior, global geographic distribution and different levels of risk to cause cancer progression (Burk et al. 2013a). A number of studies has shown that the

intratype variants of 16 E6 from the European branch (for example E-G350, E-A176/G350 and E-C188/G350) and Asian-American variants (for example AAa and AAc), have differential expression of multiple genes involved in the development of cervical and anogenital cancers, in comparison to HPV-16 E6 European-Prototype (Zacapala-Gómez et al. 2016). Thus, their gene expression profiles show differential regulation of the host genes involved in cell adhesion, angiogenesis, apoptosis, differentiation, cell cycle control, proliferation, transcription and protein translation. More interestingly, for a specific nucleotide substitutions studies were shown to be linked with increased oncogenic activity and a potential to induce cancer (Sichero et al. 2012; Pillai et al. 2009; Shang et al. 2011; Pande et al. 2008).

The most representative examples are clinical and experimental studies which analyzed the presence of T350G nucleotide substitution, which was shown to correlate with an increased risk of cervical neoplasia development, pointing out to T350G nucleotide variation as an additional risk factor for persistent infection and high-grade lesion progression (Sichero et al. 2012). Furthermore, functional studies demonstrate that 16 E6 T350G variant (hereinafter E6 L83V) with an amino acid substitution at the position 83 from leucine to valine, has biological advantages and increased oncogenic activity over the European-Prototype (hereinafter 16 E6 wild type). These include increased levels of p53 degradation, ability to abolish keratinocyte differentiation (Stöppler et al. 1996; Asadurian et al. 2007a), immortalization and transformation abilities (Richard et al. 2010), regulation of tumorigenesis by the NOTCH signaling pathways (Chakrabarti et al. 2004), degradation of proapoptotic BAX and increased interaction with E6BP (Lichtig et al. 2006a). Another important HPV-16 E6 variant of the European branch is E-A176/G350 (hereinafter E6 D25N L83V), which contains an extra amino acid change at the D25N residue, with the amino acid substitution from aspartic acid to asparagine, that is the most closely related with the development of cervical cancer in South-American region (Ortiz-Ortiz et al. 2015). Furthermore, analyses have revealed that cells transfected with E6 D25N L83V variant express higher protein levels regarding the other evaluated 16 E6 variants, despite of having similar mRNA levels (Zacapala-Gómez et al. 2016). Furthermore, E6 D25N L83V-transfected cells demonstrated differences in gene expression profile in comparison with cells transfected with wild-type (wt) 16 E6. Besides those findings, the majority of additional molecular mechanisms responsible for an increased cancer risk of those HPV-16 naturally-occurring variants are still poorly defined and underlying mechanisms remain unrevealed.

Sequence mutations that result with an amino acid change are non-synonymous, while mutations that do not change an amino acid are synonymous. Non-synonymous mutations can be detrimental, beneficial or neutral to viral fitness and can be accompanied by subtle changes at the protein structural level, as well as with changes in protein activity. Recently, an extensive study demonstrated the 3D protein structures of several intra-type variants with non-synonymous mutations (Rodríguez-Ruiz et al. 2019). It was of a great importance to generate those 3D protein structures representing the intra-type E6 variants using the crystallized structure of HPV-16 E6 European-Prototype as a template, to predict the potential structural disorders and perform molecular dynamics simulations (**Figure 6**) (Rodríguez-Ruiz et al. 2019).

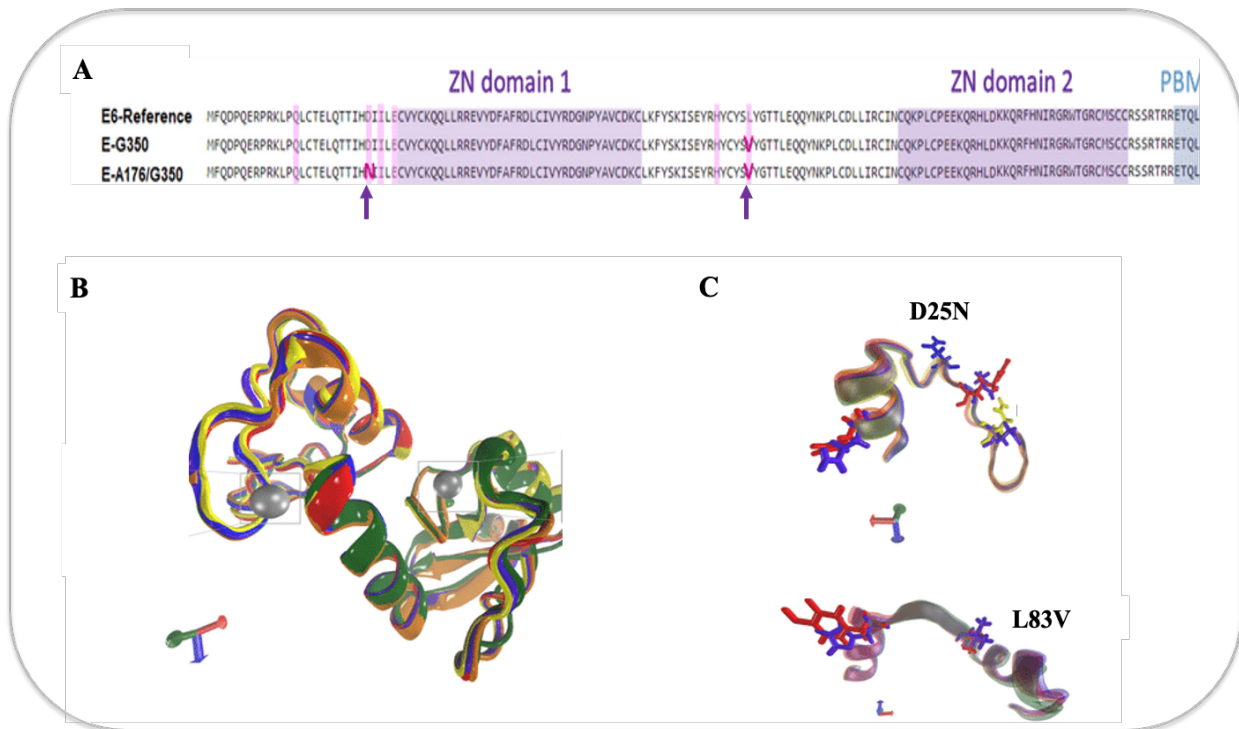


**Figure 6. The sequence alignment and 3D structure of HPV-16 E6 European-Prototype with indicated L83V and D25N/L83V mutations.** (A) Alignment of HPV-16 E6 sequence with the sequences of E-G350 and E-A176/G350 variants. Zinc finger domains are indicated as purple area in the sequence, PBM is indicated in blue and the mutation positions are highlighted with bolded nucleotides and arrows. (B) 3D structural representation of HPV-16 E6 European-Prototype. The protein orientation is indicated by the corresponding axes. (C) Precise visualization of the amino acid changes D25N and L83V. Adapted from (Araujo-Arcos et al. 2022).

The results showed that 16 E6 L83V and D25N/L83V with non-synonymous mutations do not significantly alter their 3D structures. Molecular dynamics simulations of the variants showed

minimal changes in structure, but broad changes in physicochemical parameters, which can presumably be involved in the differential patterns of interactions with cellular protein targets (**Figure 6**) (Rodríguez-Ruiz et al. 2019).

### **1.7.3. HPV E6 oncoprotein and the ubiquitin proteasome system**

As mentioned earlier in the text, a common feature of HR E6 and E7 oncoproteins is the ability to direct many of their cellular substrates for proteasome-mediated degradation (C. A. Moody and Laimins 2010a; Lou and Wang 2014), and to achieve that, HPVs have developed different strategies to make the use of the ubiquitin-proteasome system (UPS) to support and benefit viral fitness and the life cycle (Lou and Wang 2014; Tomaić, Pim, and Banks 2009a). The UPS is a regulatory pathway responsible for the most of intracellular protein degradation in eukaryotic cells. It controls the degradation of short-lived, regulatory damaged and misfolded proteins, in order to protect and maintain complex cellular functions, as well as cellular homeostasis (Hershko and Ciechanover 1997). Regulatory and signaling pathways that are essential for the cell functioning are regulated by ubiquitination and they include: cell cycle control, cell proliferation, DNA transcription and repair, apoptosis, cellular metabolism, protein quality control, membrane and intracellular trafficking, as well as the immune response to foreign antigens (Ciechanover 2005; Rousseau and Bertolotti 2018). Process of the ubiquitination is a cascade activity consisted of several steps in which the ubiquitin molecule is transferred to the target protein. First, ubiquitin molecule is activated and bound by an E1 ubiquitin-activating enzyme, then transferred to an E2 ubiquitin-conjugating enzyme and, finally, transferred to lysine residues on the target protein by E3 ubiquitin-protein ligase (Finley 2009). The proteasome recognizes and binds to the polyubiquitinated protein, following by its unfolding and degradation into small peptides.

The best characterized ubiquitin ligases utilized by E6 and E7 oncoproteins are E6AP and the cullin-2 ubiquitin ligase, respectively (White et al. 2012; Huibregtse et al. 1993d; Scheffner et al. 1993). E6AP ubiquitin ligase complexes with E6 and it is involved in targeting p53 and many other cellular targets, while E7 uses the cullin-2 ubiquitin ligase complex to target pRb (Huibregtse et al. 1993d; Huh et al. 2007). E6AP is the principal HECT domain-containing E3 ubiquitin ligase that associates with  $\alpha$ -HPV E6 proteins. The interaction occurs via LXXLL motif, which is a part

of the structure of E6 oncoprotein, (Huibregtse et al. 1993). After the interaction occurs, a stable complex E6/E6AP is formed, which enables E6 to modulate various cellular pathways to optimize cellular environment to be permissive for the productive viral life cycle, but it also plays major roles in the process of carcinogenesis (**Figure 10**) (Scheffner et al. 1993; Huibregtse et al. 1993). Furthermore, transcriptional effects of E6 are also mostly dependent on the presence of E6AP (Kelley et al. 2005) which is directly linked with the stability of  $\alpha$ -HPV E6 oncoproteins, since it was demonstrated that E6 protein turnover is dependent on the presence of E6AP (Tomaić, Pim, and Banks 2009a). In addition, it was shown that the vast majority of HPV types are dependent on E6AP for the maintenance of appropriate E6 protein levels within the cell (Thomas et al. 2013b).

Since E6AP was initially identified through its interaction with HR HPV-16 and HPV-18 E6 proteins, it was originally thought that this association was exclusive to HR mucosotropic HPV types (Scheffner et al. 1993; Huibregtse et al. 1993b), but later studies have showed that LR HPV type 11 E6 could also complex with E6AP (Brimer et al. 2007a). In addition, *in vitro* proteomic analyses of cutaneous HPVs have shown that E6AP was also a protein interacting partner of E6 oncoproteins from cutaneous types HPV-10 ( $\alpha$ -HPV) and HPV-24 ( $\beta$ -HPV) (Thomas et al. 2013b). Furthermore,  $\beta$ -HPV types 38 and 8 E6 were also shown to form a complex with E6AP (White et al. 2012; Brimer et al. 2017c; Thomas et al. 2013b) but as a result of this interaction  $\beta$ -E6s activates telomerase (Bedard et al. 2008).

Even though E6AP is essential for the stability of the  $\alpha$ -HPV E6 oncoproteins, as a consequence of E6/E6AP interaction E6AP goes through the process of self-ubiquitination which leads to its degradation at the proteasome (Kao et al. 2000). On the one hand, E6/E6AP interaction and binding to the LXXLL motif triggers E6AP ubiquitin ligase activation and a formation of ternary complex with E6 and cellular target proteins, while stimulation of E6AP self-ubiquitination is triggered separately, independent to the binding via LXXLL. As a confirmation of E6AP self-ubiquitination, it was shown that E6AP is stabilized in HPV-positive cancer cells when expression of E6 was repressed (Kao et al. 2000).

There are also additional ubiquitin ligases and other components of the UPS which are hijacked by E6 and used for its degradatory activities. These are not only critical for successful viral replication, but also necessary for maintenance of the transformed phenotype (Lou and Wang 2014; Đukić et al. 2020). HR and LR  $\alpha$ -HPVs, as well as  $\beta$ -HPVs interact with HERC2, another putative HECT domain-containing E3 ubiquitin ligase (White et al. 2012; Vos et al. 2009). E6AP

mediates interaction of HPV-16 E6 and HERC2, which subsequently modulates the ubiquitin ligase activity of E6AP (Martínez-Noël et al. 2012). The role of HERC2 in the HPV life cycle, and the process of HPV-induced malignancy has yet to be elucidated. UBR5/EDD is a HECT domain-containing E3 ubiquitin ligase linked to carcinogenesis (Clancy et al. 2003). Studies have showed that EDD strongly interacts with HPV-18 E6, but only weakly with HPV-16 and HPV-11 E6 (Tomaic et al. 2011). EDD regulates E6AP levels in a way that reduction in EDD levels results in increased proteolytic activity of E6/E6AP, which in HeLa cells leads to the enhanced cell resistance to apoptosis and growth arrest (Tomaic et al. 2011). This suggests that changes in EDD expression profile during viral life cycle could have a profound effect upon the ability of E6 to target substrates for proteolytic degradation and thereby directly influence the development of HPV-induced malignancy. Another E3 ubiquitin ligase that has been shown to interact with HPV E6 is TRIM25, involved in the immune regulation (Hayman et al. 2019). Different HPV E6s were shown to interact with TRIM25, including HR HPVs (HPV-16, -18 and -33 E6), LR HPVs (HPV-6 and -11 E6) and cutaneous  $\beta$ -HPVs (HPV-5 and -8 E6), suggesting that HPV involvement in the modulation of the immune surveillance is conserved between different HPV types (Chiang et al. 2018). In addition, E3 ubiquitin-protein ligase UBR4/p600 was shown to be an interacting partner of  $\beta$ -HPV-38 E6 confirmed by *in vitro* assays (Thomas et al. 2013c). The interaction between  $\beta$ -HPV-38 E6 and UBR/p600 was a surprise, since UBR/p600 had been previously reported to a binding partner of multiple E7 oncoproteins (Huh et al. 2005; DeMasi et al. 2005).

Apart from ubiquitin ligases, other elements of the UPS, such as deubiquitinating enzymes (DUBs) have been also shown to interact with E6 oncoproteins from both  $\alpha$ - and  $\beta$ -HPV types. Furthermore, ubiquitin-specific protease (USP) enzymes USP15 was shown to be bound by  $\alpha$ -HPV-16, -18, -33 and -6 E6, as well with and  $\beta$ -HPV types 8 and 38 E6 (Chiang et al. 2018). USP15 was also demonstrated to be involved in the regulation of HPV-16 E6 protein stability. Moreover, HPV E6 oncoproteins from  $\alpha$ - and  $\beta$ -types were also shown to bind directly to the proteasome, with different affinities of binding to various proteasomal subunits (White et al. 2012; Đukić et al. 2020). All of this indicates a complex interplay between E6 oncoproteins and various components of the UPS, which is important for the viral productive life cycle and malignant transformation.

#### 1.7.4. HPV E6 oncoprotein and interference with p53 tumor suppressor

HR E6 oncoproteins have evolved to target p53, thereby preventing and overcoming cellular growth inhibition stimuli, which is the process that occurs both in undifferentiated and differentiated epithelial cells (C. A. Moody and Laimins 2010a). In HPV-positive background, the process of p53 perturbation is rather complex, since HR E6 oncoproteins have developed several molecular mechanisms to interfere with p53 functions.

Firstly, HR HPV E6s promote p53 ubiquitination and proteasome-dependent degradation through the interaction with E6AP by the formation of a ternary complex (**Figure 7 and 10**) (Scheffner et al. 1990a; Huibregtse et al. 1991). The formation of E6/E6AP/p53 complex requires the ability of E6 to multimerize via self-association at the amino-terminal domain (Zanier et al. 2013) to initiate the transfer of ubiquitin from the HECT domain of E6AP to p53 (Scheffner et al. 1993). Marking p53 with ubiquitin molecules results in its degradation at the proteasome, ultimately leading to a notable reduction in cellular p53 protein levels. Even though the remaining p53 in the cell is activated in a response to occurring DNA damage and replication stressors, but the checkpoint controls, as well as p53-induced apoptosis are blocked (C. A. Moody and Laimins 2010a). By degrading p53, HR E6s prevent cells from undergoing p53-driven apoptosis or growth arrest, which are the end results of E7-mediated cell cycle re-entry in the suprabasal epithelial layers as a consequence of pRb degradation (Wang et al. 2001). There are two more cellular mechanisms utilized by E6 to inactivate p53. First one involves the interference with p53 function as a direct binding of E6 oncoproteins which can block p53 transcriptional activation by intruding with its DNA-binding activity (**Figure 10**) (Lechner and Laimins 1994).

The second one requires E6 binding to the histone acetyltransferases p300 and CREB-binding protein (CBP) (**Figure 7**) (Patel et al. 1999; Zimmermann et al. 1999), as well as histone acetyltransferase ADA3 (Kumar et al. 2002), and by this interaction E6 contributes to the additional interference with p53 function by blocking the ability of these factors to acetylate p53 and therefore increase its stability (**Figure 10**) (Thomas and Chiang 2005). By the formation of p53/E6/p300 complex E6 represses p53-targeted genes activation and acts as a molecular switch that converts p53/p300 activating complex to a repressor complex, independently of E6AP-mediated degradation. Interestingly, in contrast to the p300 and CBP, E6 inactivates ADA3 by targeting it for proteasomal degradation (Kumar et al. 2002). ADA3 has been also shown to interact with p53 and enhance its transcriptional activity, making it a coactivator of p53.



As mentioned in the previous chapter, interestingly, LR E6 oncoproteins can also associate with E6AP (Brimer et al. 2007b), but the consequence of this interaction is not p53 degradation (Crook et al. 1991; Lechner and Laimins 1994; Li and Coffino 1996). Instead of p53 degradation, LR HPV E6 can block p53-induced transcription through the direct binding at the site of DNA-binding domain, which is a predominant mechanism by which LR HPVs act to abolish the growth-suppressive effects of p53 (Lechner and Laimins 1994; Crook et al. 1991). This mechanism of LR E6 oncoproteins used for manipulating with p53 functions is likely to be important for viral propagation but has a low oncogenic capacity in inducing malignancy.

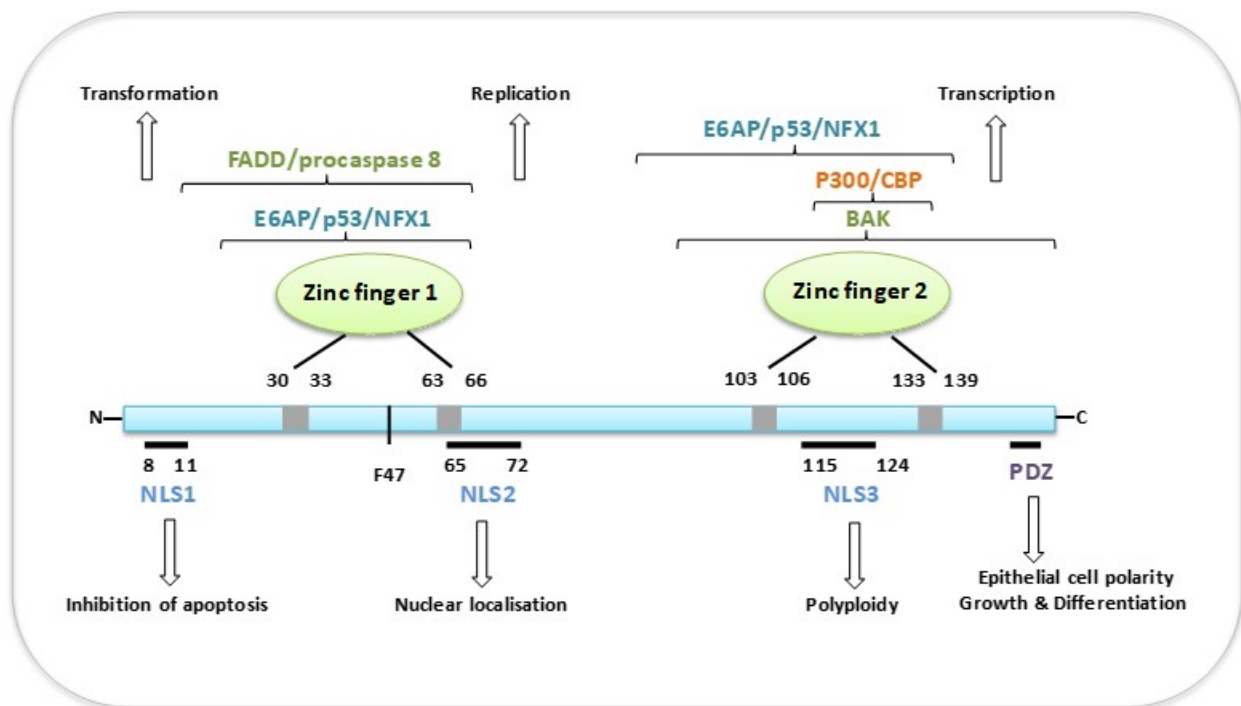


**Figure 7. Schematic representation of HR HPV-16 E6 protein structure, including the binding sites involved in interactions with its cellular targets and the corresponding functions of E6.** Four zinc-binding motifs are indicated as grey boxes. The two zinc fingers are shown together with regions that are involved in interaction with some of its cellular target proteins. E6 contains PDZ domain-binding motif at its C-terminal. Functions associated with proteins in different regions are indicated by arrows. Adapted from (Tomaić 2016a).

Research in the past ten years pointed out that, unlike HR  $\alpha$ -HPVs,  $\beta$ -HPV E6s are unable to target p53 for a proteasome mediated degradation (Cooper et al. 2003; Caldeira et al. 2003b; Cornet et al. 2012). Yet, instead of this,  $\beta$ -HPV E6 inhibits p53 stabilization in response to viral replication and genome-destabilizing events, allowing the accumulation of DNA damage and

mutations (Wallace et al. 2014a). However, recent studies have yielded some new discoveries about the effects of  $\beta$ -HPVs on p53, which are not uniform, as it was found that the expression of HPV-38 E6 and E7 in human keratinocytes induces stabilization of p53 (Tommasino 2017; Viarisio et al. 2018; Accardi et al. 2006), illustrating a diverse impact on p53 function mediated by  $\beta$ -HPV types and showing a role of HPV-38 in epithelial carcinogenesis. Interestingly, several more recent studies have also showed that HPV-49, HPV-17a and HPV-92 E6s could also bind and stabilize p53 (White et al. 2014a), reopening a question of the link between  $\beta$ -HPV E6 and p53. In the case of p53 transcription levels, it was shown that some  $\beta$ -HPV E6 types can block p53-induced transcription (Giampieri et al. 2004; White et al. 2014a). Furthermore,  $\beta$ -HPV E6s can also abolish p53-dependent and -independent apoptosis induced in cutaneous tissue in response to DNA damage caused by UV treatment (Jackson et al. 2000b; Giampieri et al. 2004). In the context of all those latest findings, it is important also to emphasize that  $\beta$ -HPV-17a, -38 and -92 E6s can block the ability of p53 to transactivate downstream genes following DNA damage, in particular to inhibit the induction of p21 (White et al. 2014a).  $\beta$ -types, same as  $\alpha$ -types, also interfere with the expression of downstream p53-regulated genes by associating with the transcriptional co-activators CBP and p300 (Wallace et al. 2012; Muench et al. 2010). HPV-38 and -8 E6 interaction with p300 and its destabilization blocks p53 acetylation, inducing inhibition of its transcriptional functions and attenuating p53 signaling (Muench et al. 2010).

#### **1.7.5. HPV E6 oncoprotein and apoptosis**

HPV E6 oncoproteins affect the proliferative capacity of infected cells by blocking apoptosis. Normal uninfected cells undergo apoptotic cell death upon extrinsic (death receptor and ligand interaction) or intrinsic signals (cellular stressors as radiation, UV lightning, toxic reagents, hypoxia, proapoptotic signaling cytokines). Apoptosis is one of the major cellular homeostatic programs to prevent aberrant cell growth and further division of cells with accumulated DNA damages and mutations. As explained earlier in the text, HPVs have evolved mechanisms to avoid and resist apoptotic cell death by targeting various apoptotic pathways, which would otherwise eliminate HPV-infected cells.

In addition to the inactivation of the p53-dependent cellular apoptotic response,  $\alpha$ - and  $\beta$ -HPV E6 oncoproteins can further abolish apoptotic signaling by interacting with the Bcl2 family

member proapoptotic protein Bak and degrade it in E6AP-dependent manner (Thomas and Banks 1998a; Underbrink et al. 2016; Jackson et al. 2000a), interfering with the intrinsic apoptotic pathway (**Figure 8** and **10**). Bak is an apoptogenic mitochondrial factor activated by an apoptotic stimulus, which undergoes a conformational change that leads to pore formation in the mitochondrial membrane that releases apoptotic factors (Simmonds and Storey 2008). Up until recently it was unknown whether LR E6s abrogate apoptosis. For both LR HPV-6 and -11 E6 oncoproteins it was shown to degrade Bak which is activated following UV treatment (Underbrink et al. 2016).  $\beta$ -HPV types also interfere with intrinsic apoptotic pathways.  $\beta$ -E6s can inhibit Bak and drive its proteasomal degradation in E6AP-dependent manner, which gives cells the ability to survive UV damage (Underbrink et al. 2008a). HPV-5, -8, -20, -22, -38, -76, -92, and -96 E6 degrade Bak, or inhibit its accumulation in keratinocytes treated with UV lightening, resulting in apoptosis evasion and blockade of the intrinsic apoptotic pathway. HERC1 ubiquitin ligase is required for HPV-5 E6-mediated Bak degradation (Holloway et al. 2015). Formation of ternary complex  $\beta$ -E6/HERC1/Bak is a unique mechanism used by the HPV-5 E6 to target Bak. Furthermore, it was shown that Bak protein levels are undetectable in HPV-positive skin cancers, in contrast to HPV-negative cancers (Underbrink et al. 2008b). Thus, Bak is one of the few highly conserved targets of both  $\alpha$ - and  $\beta$ -HPV E6 proteins.

Bax, same as his counterpart Bak, is another proapoptotic Bcl2 family member that is degraded through the actions of E6 (**Figures 8** and **10**) (Alfandari et al. 1999). Bax is a death effector which perforates the mitochondrial outer membrane, triggering the proteolytic cascade. Inhibition of E6 results in p53-dependent transcriptional activation of the PUMA promoter, leading to the activation and translocation of Bax to the mitochondrial membrane, causing cytochrome c release into the cytosol and the activation of caspase 3 (**Figure 8**) (Vogt et al. 2006). Perturbation of the p53/PUMA/Bax cascade is an important anti-apoptotic function of E6 in HPV-positive cancer cells.

In response to viral entry, the immune system of the host produces inflammatory cytokine named tumor necrosis factor  $\alpha$  (TNF- $\alpha$ ), a potent inhibitor of keratinocyte proliferation (Basile et al. 2001), which activates the extrinsic apoptotic pathway through the signaling via transmembrane cell surface death receptors of the TNF receptor superfamily. Those receptors include TNF receptor 1 (TNFR1), FAS (CD95) and the TNF-related apoptosis-inducing ligand receptors 1 and 2 (TRAIL-R1 and TRAIL-R2) (Raudenská et al. 2021). When death ligands TNF $\alpha$ , CD95L and

TRAIL are bound to death receptors, the extrinsic apoptotic pathway is activated upon receptor trimerization (**Figure 8**). Receptor rearrangement leads to the recruitment of adaptor proteins, such as FAS-associated death domain (FADD) and TNF receptor (TNFR)-associated death domain (TRADD), as well as procaspase 8 to the death-inducing signaling complex called DISC. Initiator caspases (e.g. caspase 8) are activated by the cleavage at the DISC and in turn activate executioner caspases (caspases 3 and 7) driving cell apoptosis (**Figure 8**) (Raudenská et al. 2021).

HR E6s block the apoptosis induced by TNF $\alpha$  and extrinsic signaling through the direct binding with TNFR1, which inhibits the formation of DISC and further transduction of apoptotic signals into the cell (Filippova et al. 2004a). E6 also interacts with the adaptor proteins FADD and caspase 8 (**Figure 8** and **10**) resulting in their degradation and block of the extrinsic apoptotic signaling mediated by FAS and TRAIL-R1 receptors (Garnett and Duerksen-Hughes 2006a; Filippova et al. 2004b). Furthermore, E6 suppresses activation of both caspase 3 and caspase 8, as a part of mitochondrial pathway (Raudenská et al. 2021). In response to viral entry, the immune system of the host produces inflammatory cytokine named tumor necrosis factor  $\alpha$  (TNF- $\alpha$ ), a potent inhibitor of keratinocyte proliferation (Basile et al. 2001), which activates the extrinsic apoptotic pathway through the signaling via transmembrane cell surface death receptors of the TNF receptor superfamily. Those receptors include TNF receptor 1 (TNFR1), FAS (CD95) and the TNF-related apoptosis-inducing ligand receptors 1 and 2 (TRAIL-R1 and TRAIL-R2) (Raudenská et al. 2021). When death ligands TNF $\alpha$ , CD95L and TRAIL are bound to death receptors, the extrinsic apoptotic pathway is activated upon receptor trimerization (**Figure 8**). Receptor rearrangement leads to the recruitment of adaptor proteins, such as FAS-associated death domain (FADD) and TNF receptor (TNFR)-associated death domain (TRADD), as well as procaspase 8 to the death-inducing signaling complex called DISC. Initiator caspases (e.g. caspase 8) are activated by the cleavage at the DISC and in turn activate executioner caspases (caspases 3 and 7) driving cell apoptosis (**Figure 8**) (Raudenská et al. 2021). HR E6s block the apoptosis induced by TNF $\alpha$  and extrinsic signaling through the direct binding with TNFR1, which inhibits the formation of DISC and further transduction of apoptotic signals into the cell (Filippova et al. 2004a). E6 also interacts with the adaptor proteins FADD and caspase 8 (**Figure 8** and **10**) resulting in their degradation and block of the extrinsic apoptotic signaling mediated by FAS and TRAIL-R1 receptors (Garnett and Duerksen-Hughes 2006a; Filippova et al. 2004b).

Morover, E6 suppresses activation of both caspase 3 and caspase 8, as a part of mitochondrial pathway (Raudenská et al. 2021).

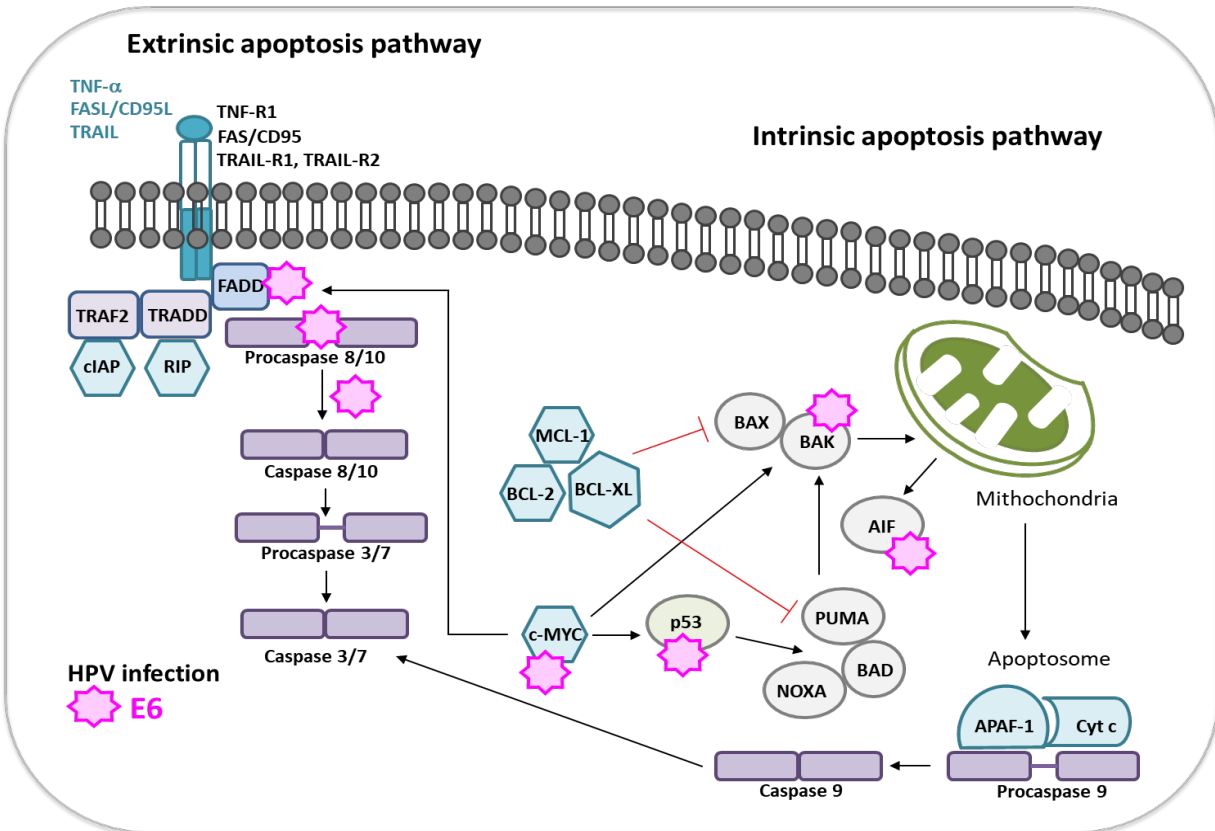


**Figure 8. HPV E6 oncoproteins interfere with apoptosis through a variety of mechanisms.** In addition to E6-mediated proteasomal inactivation of p53, E6 also degrades the proapoptotic cellular proteins Bak and Bax as a part of the inhibition of intrinsic apoptotic pathway. Extrinsic apoptotic pathway mediated by FAS, TRAIL and TNF receptors is abrogated via association of E6 with FADD and caspase 8, and through the interaction with TNF receptor. E6 also blocks procaspase activation to stop the downstream signaling in extrinsic apoptotic pathway, which is another way of interfering with cellular apoptosis. Adapted from (Skelin et al. 2022).

Furthermore, HPV16 E6 stimulates degradation of the c-Myc oncoprotein (**Figure 8**) (Gross-Mesilaty et al. 1998). c-Myc promotes oncogene-induced senescence (OIS) which is a tumor-suppressor mechanism which contributes to the prevention of cell transformation. Downregulation of c-Myc is beneficial for HPV infection because it leads to a reduction of the senescent cell phenotype. HR E6s can also act in a manner to activate pro-survival pathways inducing the upregulation of proapoptotic factors which include the members of inhibitors of

apoptosis protein (IAP) family. IAP family members are inhibitors of apoptosis protein 2 (IAP2, known as BIRC2) and survivin (also known as BIRC5) (Garnett and Duerksen-Hughes 2006a). HR E6s transactivate the survivin promoter, thereby increasing the cell's resistance to apoptosis. Considering IAP2, indirect activation of NF- $\kappa$ B signaling pathway by HR E6 leads to upregulation of cIAP2, thereby helping to create a resistance to different DNA damaging agents in the host cell (James et al. 2006). Furthermore, E6 oncoprotein activates signal transducer and activator of transcription 3 (STAT3) transcription factor by inducing the expression of the proinflammatory cytokine interleukin-6 (IL-6) via the NF- $\kappa$ B pathway (Morgan et al. 2018). The activation of STAT3 determines the sensitivity to extrinsic TRAIL-mediated apoptosis.

Another major apoptotic pathway targeted by HPV E6 oncoproteins is anoikis, associated with anchorage-independent growth (Chiarugi and Giannoni 2008). Anoikis is a form of apoptosis that is triggered in normal cells when they attempt to proliferate in the absence of an extracellular matrix (ECM). Integrins located on the cell surface interact with the components of ECM and regulate the signal transduction into the cell at the site of focal adhesion through the focal adhesion kinase (FAK), that works as an integrin-associated tyrosine kinase. Autophosphorylation and activation of FAK and its downstream substrate paxillin (PXN), a cellular adaptor protein, leads to cytoskeletal reorganization and formation of focal adhesions site. It was shown that HPV-positive cells express high levels of FAK, as well as increased levels of phosphorylated paxillin (McCormack et al. 1997). HPV-16 E6 binds to paxillin (S. B. Vande Pol, Brown, and Turner 1998a) through LXXLL motif and represents an essential component for FAK phosphorylation (**Figure 10**) (Tong and Howley 1997). As such, paxillin and FAK together initiate a signaling cascade that results in FAK phosphorylation and the recruitment of Src family of nonreceptor tyrosine kinases and Rho/Ras family of G proteins (Brimer et al. 2014). These interactions promote resistance to anoikis and allow HPV-infected cells to proliferate in the absence of the adherence to the ECM. E6 also interacts with calcium-binding protein E6BP (E6-binding-protein, also known as ERC-55) (Chen et al. 1995) and zyxin, a focal adhesion molecule with a role of a messenger from sites of cell adhesion to the nucleus (Degenhardt and Silverstein 2001).

### **1.7.6. HPV E6 oncoprotein and PDZ domain-containing proteins**

Epithelial tissues have a characteristic polarized cellular architecture and specialized cell-cell junctions, including desmosomes, tight and adherens junctions (Thomas et al. 2008b). There is a number of signaling and polarity complexes that are involved in the recruitment of proteins to the side of cellular junctions and establishment of cell polarity. Cellular polarity has a crucial role in the organization of signaling pathways, allowing the interpretation and transduction of the signals from the surrounding microenvironment, enabling the control of the proliferation, apoptosis, differentiation and motility of the cell (Ganti et al. 2015a). For the organization and control of cell polarity, it is crucial to maintain undisturbed spatial and temporal regulation of the cell polarity regulators.

One of the primary characteristics of the transition from the normal cell to benign neoplasm and a malignant cellular phenotype is a major disorganization of cellular architecture, including a loss of cell-cell contact junctions and apical-basolateral polarity (Dongre and Weinberg 2019). This process can occur through the degradation, interruption or mislocalization of the cellular components that regulate cell polarity. The impact of losing cellular polarity is reflected in the perturbation and changes of protein intracellular trafficking from the apical and basolateral sides of the epithelial cell, causing aberrant signaling due to mislocalization of receptors or adhesion molecules, that can ultimately promote cellular epithelial-mesenchymal transition (EMT) (Dongre and Weinberg 2019).

#### ***1.7.6.1. PDZ domain-containing proteins and cellular polarity***

PDZ (PSD95/DLG/ZO-1) domains are an important part of the structure of proteins involved in the regulation of cellular polarity. A PDZ domain consists of 80–90 amino acids in length and firstly was described from the three cellular proteins, the Post Synaptic Density 95 (PSD95), the Discs Large (DLG) and the Zona Occludens 1 (ZO-1) proteins (Ganti et al. 2015a). PDZ domains function as protein interaction domains able to bind to other PDZ domains and being bound by PDZ-binding motifs (Saras and Heldin 1996). PDZ-domain containing proteins usually have multiple PDZ domains and perform important roles in the cell, referring to the involvement in the assembly of signaling complexes associated with the regulation of polarity, cell growth, adhesion and motility. Furthermore, PDZ-domain containing proteins are involved in signal

transduction pathways important for cellular differentiation, proliferation, apoptosis, migration and intracellular trafficking (Ganti et al. 2015a). So far, over 20 different PDZ domain-containing proteins have been identified as targets of HR E6 proteins (ames and Roberts 2016) and among them some of the most well characterized include Discs large 1 (DLG1) tumor suppressor (Kiyono et al. 1997a), Scribble tumor suppressor (Scrib) (Nakagawa and Huibregtse 2000) and Membrane-associated guanylate kinase inverted 1 (MAGI-1) (Dobrosotskaya et al. 1997).

Cell polarity is maintained by an intricate interplay between the conserved groups of proteins that form distinct complexes which are: The Crumbs, Par and Scribble complexes (**Figure 9**). Apical polarity is controlled by the Crumbs complex, which is consist of Crumbs3, Pals1 and PatJ (Laprise 2011). The Par complex consists of Par3, Cdc42, Par6 and atypical protein kinase C (aPKC), and it is a dynamic complex that interacts with the Crumbs complex to maintain apical polarity (**Figure 9**) (Pim et al. 2012). The Scribble complex consists of the scaffolding proteins Scribble, DLG and Hugl, which participate in maintaining cellular basolateral polarity (**Figure 9**) (Thomas et al. 2005). The whole Scribble complex is linked to the mitogen-activated protein kinase (MAPK) signaling, following exposure to osmotic stress (Sabio et al. 2005). All above mentioned complexes interact through a series of mutually antagonistic interactions ensuring their correct spatial distribution in the cell (**Figure 9**). The Par and Scribble complexes are dependent on one to another for their correct localization in the cell, in the way that the Scribble complex restricts the Par complex to the apical membrane, whereas the Par and Crumbs complexes together exclude the Scrib complex from the apical membrane (Bilder et al. 2003). Those actions restrict the Scribble complex to the basolateral cellular membranes, together with the basolateral targeting of Scribble protein (Legouis et al. 2003). Even minimal alteration in the balances between each protein of the Scribble, Par and Crumbs complex can have effects on the precise functioning of the whole polarity supercomplex that comprises them all (Thomas et al. 2008a). Furthermore, this polarity supercomplex coordinates the transmission of intracellular and extracellular polarity-related signaling to cellular effectors, such as the cytoskeletal network and protein-trafficking pathways.

The tumor suppressors Scribble and DLG1, originally were discovered in the fruit fly *Drosophila melanogaster*, but the interest in studying those proteins has raised with the first discoveries of their potential roles in human tumorigenesis (Elsum et al. 2012). Those tumor suppressors regulate apicobasal cell polarity and play important roles in the control of cell



proliferation, survival, differentiation, migration, as well as cell invasion. Moreover, Scribble and DLG1 are involved in the regulation of different signaling pathways, vesicle trafficking and actin-myosin cytoskeleton organization (Thomas et al. 2005). The MAGI-1, MAGI-2 and MAGI-3 proteins are part MAGUK protein family with inverted structure, having guanylate kinase homology domains at the amino terminal end of the polypeptide and at least five PDZ domains (Dobrosotskaya et al. 1997). MAGUK family of proteins is crucial for maintaining junctional stability (Glaunsinger et al. 2000). Human MAGI-1 is implicated into the protein complex assembly at cell-cell contacts and tight-junction integrity (Kranjec and Banks 2011).

#### ***1.7.6.2. PDZ domain-binding motif (PBM) of HPV-E6***

The PDZ domain-binding motif (PBM) located at the extreme C-terminus of E6 proteins, with the canonical sequence X-S/T-X-V/L\_COOH, is found exclusively as a part of the structure of HR E6 proteins (**Figure 5**) (Lee and Laimins 2004; Kiyono et al. 1997b). The PBM motif is encoded by a small insert on the 3' end of the E6 ORF (Auslander et al. 2019). Through this PBM oncogenic E6 oncoproteins bind and degrade cellular PDZ domain-containing proteins, or in some cases alter their cellular localization, disrupting cell polarity network and the balance of symmetrical and asymmetrical cell division to regulate and support viral DNA replication (M. Thomas et al. 2008a), making cellular proteins containing PDZ domains important targets for the research of tumorigenicity caused by HR HPV E6 oncoproteins (Lee and Laimins 2004; Kiyono et al. 1997b; Javier 2008; Culp et al. 2006). The PBM on E6 has been shown to play essential roles in viral genome amplification because it was shown in differentiating epithelium of organotypic raft cultures that disruption of the E6 PBM caused defective HPV-18 genome amplification, loss of productive viral replication and downregulation of the late genes and obstruction of S-phase re-entry (Delury et al. 2013). However, interestingly, some LR  $\alpha$ -HPVs replicate efficiently without a PBM, such as LR HPV-40 of the  $\alpha$ -HPV group 3 that replicates well even with an ancestral and non-canonical structure of the PBM (Doorslaer et al. 2015). Taken together, E6 PBM plays an essential role in the virus life cycle, being required for expansion of replication-competent suprabasal cells (Lee et al. 2007).

Furthermore, PDZ-binding activity of E6 also regulates episomal maintenance and protects the mitotic integrity (Thomas et al. 2008b), while deletion of the PBM domain leads to mitotic abnormalities and prevents proliferation of suprabasal cells (Marsh et al. 2017).

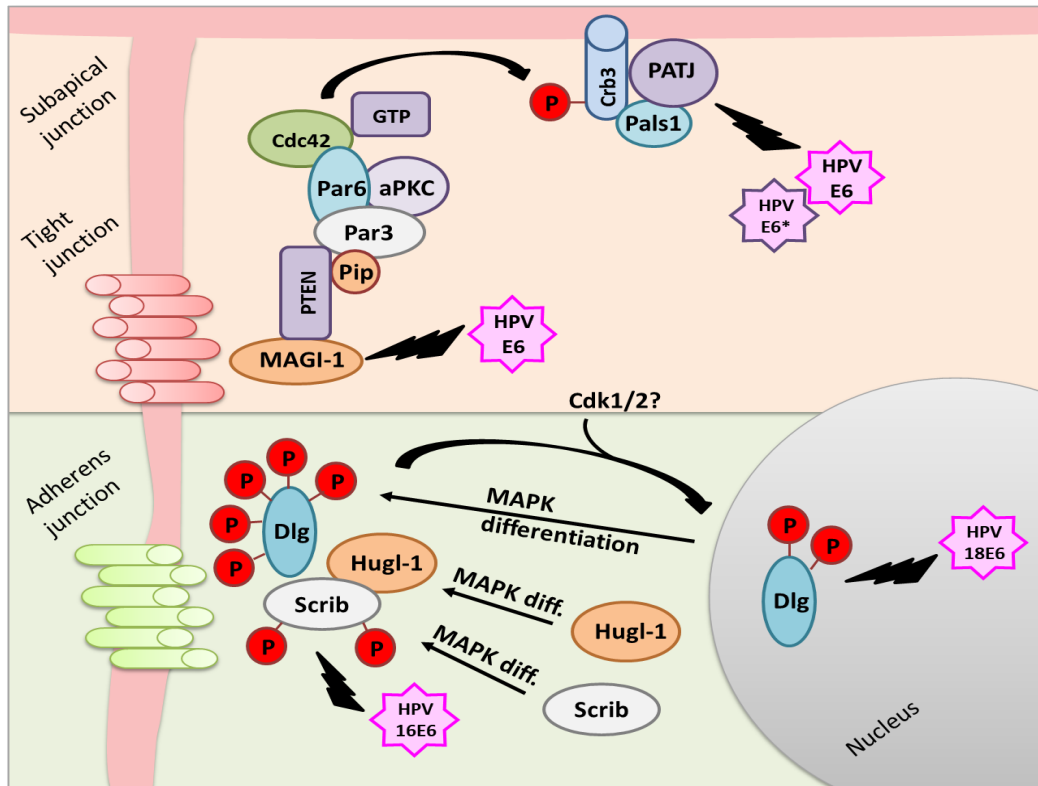


**Figure 9. HPV E6 oncoprotein regulation of cell polarity complexes.** Various PDZ domain-containing proteins are comprised into three major complexes that regulate cell polarity: apical polarity defined by the Crumbs complex, subapical by the Par complex and basolateral polarity by the Scrib complex. These complexes interact through a series of mutually antagonistic interactions ensuring correct spatial distribution and levels of expression. HR HPVs coordinately disturb cell polarity regulators. HPV-16 E6 preferentially targets Scribble, whereas HPV-18E6 preferentially targets DLG. MAGI-1 is also highly susceptible to HPV E6 degradation. PATJ is a substrate of both E6 and the alternatively spliced isoform E6\*. Post-translational modifications result in enhanced phosphorylation and relocalization of PDZ cellular substrates, with MAPK signaling driving an accumulation of the Scrib complex at the sites of cell–cell contact. Adapted from (Thomas et al. 2008b).

Different HPV E6 oncoproteins have different sequences of their PBMs that results in diverse target profiles (Thomas et al. 2005). HPV-18 E6's PBM motif has a perfect consensus sequence (ETQV) that enables greater specificity for its PDZ domain-containing targets, while

HPV-16 E6 PBM differs in one amino acid (ETQL) (**Figure 5**). hScrib/DLG apico-basal complex is differentially targeted by HPV-16 and HPV-18 E6, with HPV-16 E6 inducing hScrib degradation more efficiently than HPV-18 E6, while the reverse case is with DLG1, which is preferentially targeted by HPV-18 E6, over HPV-16 E6 (**Figure 9**) (Thomas et al. 2005). hDLG is bound by different E6 PBMs, including HPV-40 E6, which has an ancestral PBM, indicating an evolutionarily conserved interaction between E6 PBMs and DLG1 (Thomas et al. 2016). MAGI-1 is the major degradation target of both HPV-16 and HPV-18 E6 oncoproteins, in comparison to hDLG, hScrib, PTPN3, TIP2, FAP1, and PSD95 (Kranjec and Banks 2011). One of the direct consequences of MAGI-1 degradation is loss of tight-junction integrity, followed by mislocalization of the tight-junction protein ZO-1.

$\beta$ -HPV E6 proteins lack PBMs, yet as LR mucosal HPVs they also successfully complete their productive life cycle (Doorslaer et al. 2015). Ultimately, novel research supports the model in which the potential of E6 to degrade PDZ-domain containing proteins was acquired before their oncogenic ability, with evidence that the ancestor of both oncogenic and non-oncogenic HPVs acquired the potential to degrade human PDZ-containing proteins. PDZ/PBM interactions represent evolutionarily essential interactions that originally evolved to allow HPVs to colonize a new cellular niche, such as the transformation zone of cervix, since is unlikely for a virus to become oncogenic without first acquiring the ability to degrade PDZ proteins (Doorslaer et al. 2015).

#### **1.7.6.3. Phospho-regulation of the HPV E6 PDZ-binding motif**

The PBM motif of HR E6 oncoproteins can be post-translationally regulated through a process of phosphorylation, since it contains a protein kinase A (PKA) phospho-acceptor site (**Figure 5**) (Boon and Banks 2013). Phosphorylation of the key serine/threonine residue within the phospho-acceptor site of the PBM inhibits PDZ domain binding activity (Zhang et al. 2007; Kühne et al. 2000), so mechanistically, the process of phosphorylation regulates binding of E6s to PDZ domain-containing proteins (Boon and Banks 2013; Kühne et al. 2000, 6). Phosphorylation by either PKA or the serine/threonine kinase AKT, also known as protein kinase B (PKB), blocks binding of cellular PDZ-domain containing proteins and creates modulated binding site to allow direct interaction of E6 with another important protein, that is 14-3-3 $\zeta$ . As a member of 14-3-3 family of

highly conserved phospho-threonine/serine-interacting acidic proteins, 14-3-3 $\zeta$  is involved in the regulation of different cellular processes associated with cancer development, with frequently observed overexpression during various stages of malignant progression (Neal and Yu 2010; Muslin et al. 1996). There are seven known isoforms of 14-3-3 which are present in mammals, encoded by seven genes. 14-3-3 proteins function as adaptor proteins and through phospho-regulated binding they interact with a number of cellular proteins involved in cell signaling networks, apoptosis, metabolism, cytoskeletal maintenance and tumor suppression (Pozuelo Rubio et al. 2004; Jin et al. 2004). The intact PBM is necessary for interactions of E6 with 14-3-3 $\zeta$ , and it was shown that the switch between E6 binding to PDZ-domain containing cellular proteins and 14-3-3 $\zeta$  depends upon preferences of HPV types to either PKA or AKT phosphorylation. Phospho-regulation of the PBM and the PKA/AKT consensus recognition sequence were shown to be highly conserved between HR HPV types, but it is absent in all LR mucosal  $\alpha$ -HPV and cutaneous  $\beta$ -HPV E6 oncoproteins (Boon et al. 2015; Ganti et al. 2015b). Despite the highly conserved recognition sequence between HR HPVs, there are some differences. HPV-18 E6 PBM is a substrate for phosphorylation by PKA, HPV-16 E6 PBM can be phosphorylated by both PKA and AKT, while HPV-31 E6 is phosphorylated by AKT, but can be also recognized by PKA at the residues lying outside the PBM.

14-3-3 proteins are involved in the regulation of cell cycle, so it is possible that the interaction of E6 with 14-3-3 aims to maintain an environment favorable for viral genome amplification, active during the G2/M phase of the cell cycle. Recognition of 14-3-3 is less dependent upon the precise sequence of the PBM, in contrast to PDZ domain recognition for which sequence variations have a major impact. Changes in E6 phospho-status during the life cycle and malignant progression modulate the levels of PDZ domain-containing and 14-3-3 proteins and their interaction with E6, so future studies involving the role of phospho-E6 and its effects on 14-3-3 activity during the viral life cycle and tumorigenesis, should bring some novel insights regarding HPV-induced malignancy (Vats et al. 2023).

### **1.7.7. HPV E6 oncoprotein and exploiting the host DNA damage response**

The host DNA damage response (DDR) system is a complex network of signaling pathways that repair DNA damage which occur in the cell as a result of continuous DNA replication and metabolism, as well as from exogenous disruptors, including UV exposure, ionizing radiation, viral and bacterial infections (Ciccia and Elledge 2010). The stimulation of the major components of the DDR signaling network, ataxia telangiectasia mutated (ATM) and ataxia telangiectasia and Rad3-related protein (ATR) kinases, induces a cascade of phosphorylation events which activate the downstream effector proteins to stop cell cycle progression at the cell cycle checkpoint control. Cells with disrupted DNA damage recognition and DNA repair system accumulate mutations and damage that can ultimately lead to the malignant transformation (Lilley et al. 2007). HPVs have evolved mechanisms to disturb the host DDRs and manipulate with those pathways in their favor. Thus, HPVs function to activate ATM-related and ATR-related DDR factors and recruit them to the viral DNA replication foci, promoting viral DNA replication (Gillespie et al. 2012; C. A. Moody and Laimins 2010a). As a result of persistent presence of DDR factors and active replicative state, infected cell transits in the state of genomic instability (Weitzman and Weitzman 2014). Genetic instability implies depletion of the host factors that are responsible for maintaining genome integrity and increased rate of DNA breaks. The disruption of the DNA repair machinery induces mutations that overcome tumor suppressors' barriers leading to the oncogenic progression, which is a reason why genomic instability is frequently observed in HPV-associated cervical neoplasia (Lilley et al. 2007). E6 and E7 oncoproteins induce DNA damage and centrosome-related mitotic defects to destabilize the host genome (Wallace et al. 2014a). By reducing genomic stability as cells divide, these viral oncoproteins increase the acquisition of additional genetic changes that contribute to HPV-associated carcinogenesis genome.

More recent studies showed that after the induction of DNA damage or exposure of cells to the oxidative stress, the levels of E6 phosphorylation increase (Thatte et al. 2018). Depending on the stimuli, this type of phosphorylation of E6 can involve the ATM/ATR pathway, primarily through checkpoint kinase 1 (Chk1), and indirectly through checkpoint kinase 2 (Chk2), and activation of PKA (Thatte et al. 2018). The checkpoint effector kinases Chk1 and Chk2 are the key components of the DDR, and contain highly conserved kinase domains, although they are structurally and functionally distinct (Stracker et al. 2009). Chk1 activation is downstream of ATR,

and it is triggered in response to the replication stress that includes disruption of the replication forks, DNA crosslinks and UV damage, resulting in a single-strand DNA break. Chk2 is activated primarily by the ATM in response to double-strand breaks in DNA (DSBs) and it promotes DNA repair through homologous recombination or non-homologous end joining (NHEJ) (Stracker et al. 2009). DDR is linked to the regulation of E6 PBM functions and the inhibition of p53 tumor suppressor activity. The mechanism of action works in a way that DDR pathways directly sends signals to E6 PBM containing phospho-acceptor site, and it also initiates Chk1- and Chk2-driven phosphorylation (Thatte et al. 2018), resulting in enhanced ability of E6 to inhibit p53 transcriptional activity in phospho-dependent manner, independently of E6AP and the proteasome. This type of E6 PBM regulation via DDR pathways represents a mechanistic link between the function of the PBM and additional obstruction of p53 activities (Thatte et al. 2018). Intact E6 phospho-acceptor site plays an essential role in this process of E6-mediated inhibition of p53 transcriptional activity, thus blocking a subset of p53-responsive promoters, completely independent of the ability of E6 to induce p53 degradation.

Moreover, E6s from  $\beta$ -HPV-5, -8 and -38 all interact with p300, whilst for HPV-8 E6 was also shown to induce p300 degradation (Wallace et al. 2012). This process significantly reduces the levels of ATR protein in the cell, which plays a critical role in UV-induced DNA-damage signaling that is affected through the actions of  $\beta$ -HPV E6. This results in an increase in thymidine dimer mutations upon the exposure of the skin to UV irradiation (Wallace et al. 2012).  $\beta$ -HPV-5 and 8 E6 further disrupt the repair of DSBs (Wallace et al. 2015). On the other hand, via binding and destabilizing p300  $\beta$ -HPV-5 and -8 E6 interfere with the transcriptional factor at the promoter site of BRCA1 and BRCA2 genes. These two genes have an important role in a homology-dependent repair of DSBs. The resulting lower BRCA1/2 transcription levels reduce the ability of BRCA proteins to form repair foci at DSBs, thereby weakening DNA-damage signaling in the infected cell (Wallace et al. 2015).

### **1.7.8. HPV E6 oncoprotein and centrosomal abnormalities**

Centrosomes are the major organizing units of the microtubule network, consisted of a pair of centrioles (Sluder and Nordberg 2004). During G1 cell cycle phase, the centrosomes function as a template for synthesizing daughter centrioles. Furthermore, the main role of the centrosomes is the proper chromosome separation during cell division (Sluder and Nordberg 2004). To prevent multipolar mitoses or chromosomal aberrations, cell undergoes through one round of centriole duplication per division (Tsou and Stearns 2006). On the contrary, tumor cells have aberrant centrosome numbers as a result of disruption of the centriole duplication and a collapse in the mitotic spindle (Lingle et al. 1998). The expression of HR E6 induces numerous mitotic defects, including multipolar mitoses, chromosomal alterations, aneuploidy and anaphase bridges (A. Duensing et al. 2009). Bypassing of mitotic checkpoints is important for undisturbed viral replication, but this leads to malignant progression of HPV-infected cells.

Abnormal centrosome numbers result from an abnormal multipolar mitosis which is a characteristic feature of HPV lesions. Multiple cooperative actions of E6 and E7 consequently can induce centrosome abnormalities, which can further lead to chromosomal abnormalities and the development of aneuploidy (Duensing et al. 2000). In E6-expressing cells, aberrant centrosome numbers occur with the nuclear atypia, and it is thought that aberrant centrosome duplication is an early event that drives chromosomal instability. Under the normal conditions, cells with abnormal mitoses are targeted for apoptosis, but in infected cells actions of E6 and E7 allow accumulation of cells with abnormal centrosomes, in this way overcoming the G2–M checkpoint and inhibiting the apoptotic signaling, as explained earlier in the text (Patel et al. 2004). Furthermore, the actions of E6 and E7 independently can lead to avoiding of the mitotic checkpoints, resulting in the accumulation of polyploid and aneuploid cells (Thomas and Laimins 1998).

### **1.7.9. HPV E6 oncoprotein and DNA replication**

Normal cells have a limited lifespan and can only divide for a limited number of times, which is known as the Hayflick limit (Shay and Wright 2005). Human somatic cells end their period of existence by entering senescence, as a result of progressive shortening of DNA telomere, which occurs after successive rounds of replication and leads to inhibition of telomerase activity (Artandi et al. 2010; Shay and Wright 2005). Telomerase is an enzyme with a role in replication

of DNA sequences at the ends of chromosomes. HR E6s through different mechanisms cause telomerase activation and inhibition of the telomeres shortening, leading to continued and uncontrolled cell division (Snijders et al. 1998). The exact molecular mechanism by which HPV-16 E6 induces telomerase activity in epithelial cells has been revealed. The mechanism of action works via the transcriptional transactivation of the telomerase reverse transcriptase (TERT) catalytic subunit (Oh et al. 2001; Veldman et al. 2001), which along with pRb inactivation by E7, is the main step in the process of immortalization (Howie et al. 2009; Wise-Draper and Wells 2008). E6 hTERT activation is a critical step required for cellular immortalization, which is a prior condition to HPV-driven malignant transformation. E6 activates TERT and telomerase by the means of E6AP and interaction with c-Myc, whereas binding to hTERT promoter requires an intact E box (**Figure 10**) (Veldman et al. 2001; Veldman et al. 2003; Gewin and Galloway 2001). However, formation of E6/E6AP/c-Myc tertiary complex and binding to hTERT promoter is not unique among all HPV types. A good example of this is 16 E6, which for hTERT activation requires binding to c-Myc (Gewin and Galloway 2001; Liu et al. 2005), but not to E6AP (Sekaric, Cherry, and Androphy 2008a). Furthermore, HR E6 was found to bind hTERT, but also to repetitive sequences of telomeric DNA (Liu et al. 2009).

In somatic epithelial cells the hTERT gene is constitutively repressed through the repression of the hTERT promoter (Katzenellenbogen 2017). This promoter consists of 1100 nucleotides in length, with its core promoter comprising of 200-300 nucleotides. Transcriptional repressors of the hTERT are bound to *cis* elements to block transcription, and those *cis* elements are E-boxes, GC-rich sites, and X-boxes (Katzenellenbogen 2017). Two E-box *cis* elements are placed at the position of the transcriptional start of the hTERT gene and are normally bound by c-Myc in a form of heterodimer with Max or Mad. c-Myc/Max or c-Myc/Mad heterodimers are important for hTERT transcriptional activation or repression (R. Katzenellenbogen 2017). E6 oncoprotein via binding to the repressors and activators of the hTERT promoter modulates their activities. Targeted repressors are the upstream stimulating factors 1 and 2 (USF1 and USF2) and nuclear transcription factor, X-box binding protein (NFX1-91), while the activators are c-Myc/Max, SP1 and histone acetyltransferases (Howie et al. 2009). Furthermore, there are five GC-rich *cis* elements in the hTERT promoter (Katzenellenbogen 2017). SP1 activator binds to these elements and transcriptionally activates hTERT expression. Deletion of GC-rich *cis* elements leads to loss of the hTERT transcriptional activation (Katzenellenbogen 2017), but E6 overcomes this



by acting through SP1 transcriptional factor to activate hTERT transcription (**Figure 10**) (Oh, et al. 2001).

Finally, there are two X-boxes in the hTERT promoter. NFX1-91, the shorter splice variant of the NFX1 gene, which acts as a repressor of the hTERT transcription, is bound constitutively to the hTERT promoter downstream of the X-box (Katzenellenbogen 2017). E6 targets NFX1-91 in an E6AP-dependent manner, causing the mSin3A/HDAC repressor complex to dissociate from the hTERT promoter, leading to the activation of the hTERT transcription (Xu et al. 2008). HR E6 through a direct association with the cellular X box-binding protein NFX1-123, the longer splice variant of the NFX1 gene, upregulates TERT levels through the transcriptional and post-transcriptional mechanisms (**Figure 10**) (Katzenellenbogen et al. 2007). Overexpression of NFX1-123 leads to increased hTERT activity in the presence of HR E6, while abolishing of NFX1-123 reduces the ability of HR E6 to increase hTERT and telomerase activities (Katzenellenbogen et al. 2007). The mechanism by which NFX1-123 augments hTERT expression is the stabilization of the hTERT mRNA.

Concerning  $\beta$ -HPV types, several  $\beta$ -E6s drive hTERT activation and telomerase activity.  $\beta$ -HPV-5, -8, -20, -22 and -38 E6 activate hTERT in E6AP-dependent manner even though this association is much lower than association with HPV-16 E6 (Bedard et al. 2008). The intensity of telomerase activation is in proportion with the association between E6 and E6AP or NFX1-91 repressor, for each type of  $\beta$ -E6. Decreased E6AP protein levels lead to a reduced  $\beta$ -E6 ability to activate telomerase, suggesting the dependence of E6AP presence for the hTERT activation and formation of an E6/E6AP/NFX1-91 complex as a critical step in mediating telomerase activation (Bedard et al. 2008).

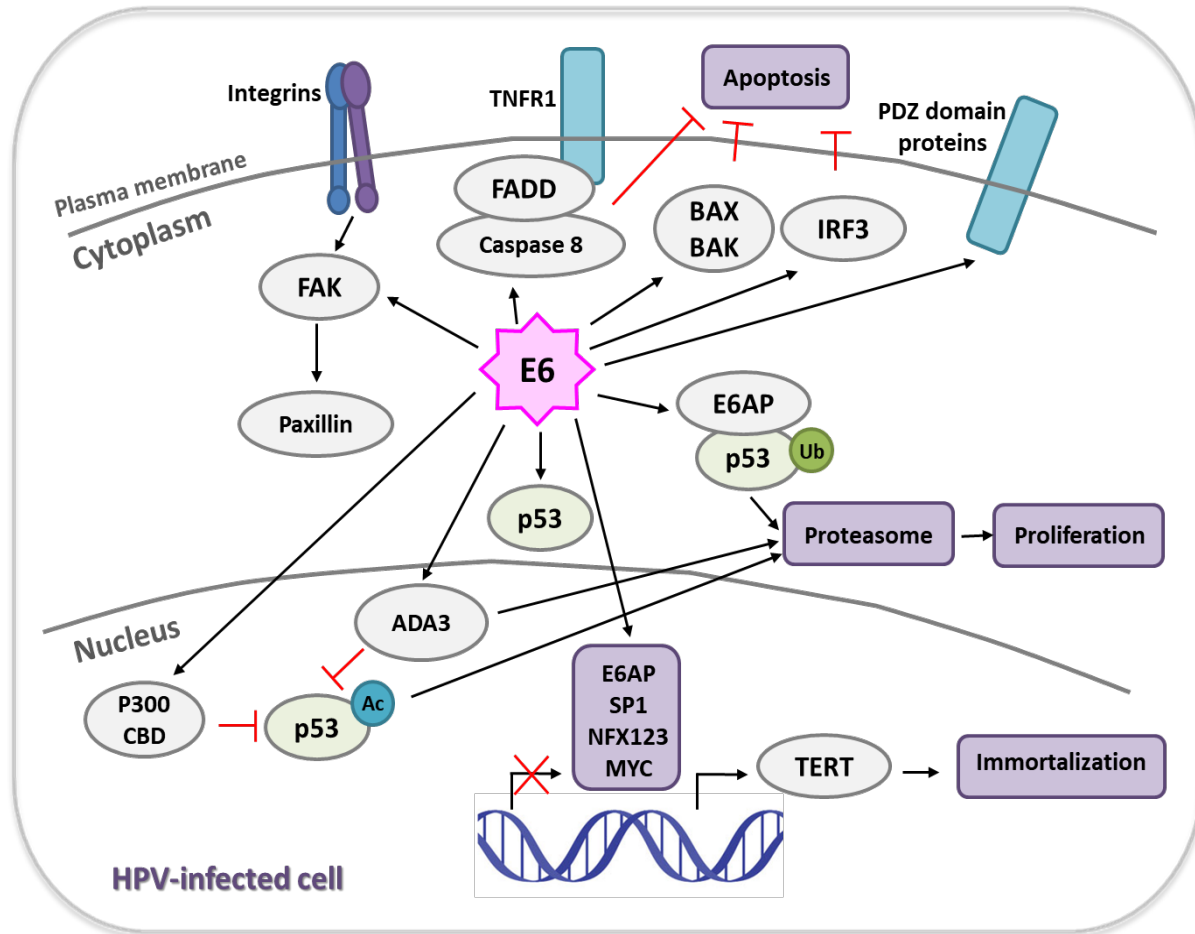


**Figure 10. Schematic representation of the cellular protein targets and signaling pathways affected by HR E6 oncoproteins.** HR E6 oncoproteins inhibit p53-dependent growth arrest and apoptosis in response to aberrant proliferation through several mechanisms, resulting in the induction of genomic instability, centrosomal abnormalities and accumulation of mutations. Formation of an E6/E6AP/p53 trimeric complex results in p53 degradation, while interactions of E6 with the histone acetyltransferases p300, CBP and ADA3 prevent p53 acetylation, in this way inhibiting the transcription of p53-responsive genes. E6 also inhibits apoptotic signaling through the degradation of pro-apoptotic BAX and BAK and by binding to the TNF- $\alpha$  receptor TNFR1, FADD and caspase 8. The interaction of E6 with SP1, MYC, NFX123 mediated by E6AP activates hTERT and telomerase, thus preventing telomere shortening concerning the successive proliferation and promotes immortalization. E6-mediated degradation of PDZ-domain containing proteins leads to the loss of cell polarity and induces hyperplasia. The interaction of E6 with the focal adhesion protein paxillin prevents anoikis and allows cellular growth in the absence of attachment to the ECM. Adapted from (C. A. Moody and Laimins 2010).

## 1.8. HPV E6 oncoprotein and Notch signaling pathway

### 1.8.1. Canonical Notch signaling pathway

The Notch phenotype was identified in 1917 by Thomas Hunt Morgan and nowadays this cellular pathway is recognized as being indispensable for cell proliferation, differentiation, and maintenance of stem cell properties. Albeit, it is also involved in development of many different human diseases, even malignant ones, where it can function either as an oncogene, or as a tumor suppressor (Lobry et al. 2011; Neumüller and Knoblich 2009; Bray 2016).

In humans there are four NOTCH receptors (NOTCH1–4), which are modulated by a number of similar and overlapping functions (Kojika and Griffin 2001). The NOTCH receptors and membrane anchored ligands Jagged-1 and 2 (JAG1-2) and Delta-like 1, 3, and 4 (DLL1-3-4), are located at the cell membrane surface (Bray 2016) (**Figure 11**, left panel). Upon the canonical Notch signaling activation, the ligand and receptor association cause conformational changes in the NOTCH receptor, which generate two consecutive, proteolytic cleavages of NOTCH. The first one is under the control of ADAM (a disintegrin and metalloprotease), while the second one is modulated by the  $\gamma$ -secretase enzymatic complex. The end result of this process is a release of the NOTCH intracellular domain (NICD) (Borggreffe and Liefke 2012). Upon cleavage, NICD is translocated to the cell nucleus, where it interacts with the DNA-binding protein named Recombination Signal Binding Protein for Immunoglobulin Kappa J Region (RBP-J $\kappa$ ; also known as CBF-1 or CSL), which is bound to a specific DNA nucleotide sequence (**Figure 11**, left panel). Binding of NICD to the RBP-J $\kappa$  results in a formation of NOTCH/RBPJ $\kappa$  transcriptional complex (NTC) (Borggreffe and Liefke 2012). This binding displaces a repressor-histone-deacetylase complex from RBP-J $\kappa$  and recruits MAML1 co-activator and acetyltransferases p300 or CBP (Contreras-Cornejo et al. 2016; Lobry et al. 2011). MAML1 is a core component of the transcriptional activation complex that mediates the effects of the canonical Notch signaling pathway by recruiting additional co-activators (Demarest et al. 2008). Upon the formation of the NTC in the nucleus, transcription of Notch target genes becomes dependent on a switch of the transcription complex from an “off transcription” to an “on transcription” state. (Borggreffe and Liefke 2012) This occurs through conversion of the RBP-J $\kappa$  from a transcriptional repressor to an activator and assembly of the activating complex (**Figure 11**, left panel) (Bray 2016; Borggreffe and Liefke 2012). The primary downstream targets and effectors of the activated NOTCH/RBP-J $\kappa$ /MAML1 complex are a set of the basic helix-loop-helix (b-HLH) transcriptional repressors,

including the Hairy and Enhancer of Split (HES) gene family and the HEY (Hairy Ears, Y-Linked) subfamily (Artavanis-Tsakonas and Muskavitch 2010; Borggreffe and Liefke 2012).

Cellular context is the determinant for the outcome of Notch signaling (Lobry et al. 2011). Hence, in a mouse animal model it was shown that Notch can function both as an oncogene or as a tumor suppressor, and this discrepancy depends on the cell and tissue context (Radtke and Raj 2003a; Lobry et al. 2011). Some of the Notch targets are common to many cell types, but appear to be tissue specific (Wang et al. 2012). Furthermore, RBP-J $\kappa$  recruits activation or repression complexes depending upon the cell context (Contreras-Cornejo et al. 2016). Notch signaling functions as an oncogenic driver in a number of human tumors, particularly in hematopoietic (Demarest, Ratti, and Capobianco 2008), breast cancer (Zhang, et al. 2015), nonsmall cell lung carcinoma (Wu, et al. 2015), as well as in gastric cancer (Du et al. 2014). In contrast, the suppressor effects of Notch have been documented in skin, as Notch acts as an important driver of keratinocyte differentiation, and perturbations of this pathway are highly associated with CSCC (South et al. 2014; Wang et al. 2011). The tumor suppressive effects of Notch in keratinocytes are largely thought to be due to an inhibition of cell proliferation during the process of differentiation (Aster et al. 2017; M. Zhang et al. 2016). Furthermore, it was found that Notch induces growth arrest and differentiation in keratinocytes through p21 and the markers of early differentiation (Rangarajan et al. 2001a). Overall, dual behavior of the Notch pathway, being able to function both as an oncogene or a tumor suppressor, is an interesting field with many open questions in cancer biology.

### **1.8.2. HPV E6 inhibition of Notch signaling pathway**

As described earlier, HPV life cycle is highly linked to the differentiation status of epithelial cells (C. A. Moody and Laimins 2010a). Notch tumor suppressor pathway in cutaneous tissues is a critical determinant of keratinocyte differentiation and acts by coordinating cell-cycle arrest and shifting keratinocytes towards terminal differentiation and ultimately cell death (Rangarajan et al. 2001a; Lowell et al. 2000a), making the differentiation program of the keratinocytes a perfect target for the viral perturbation.

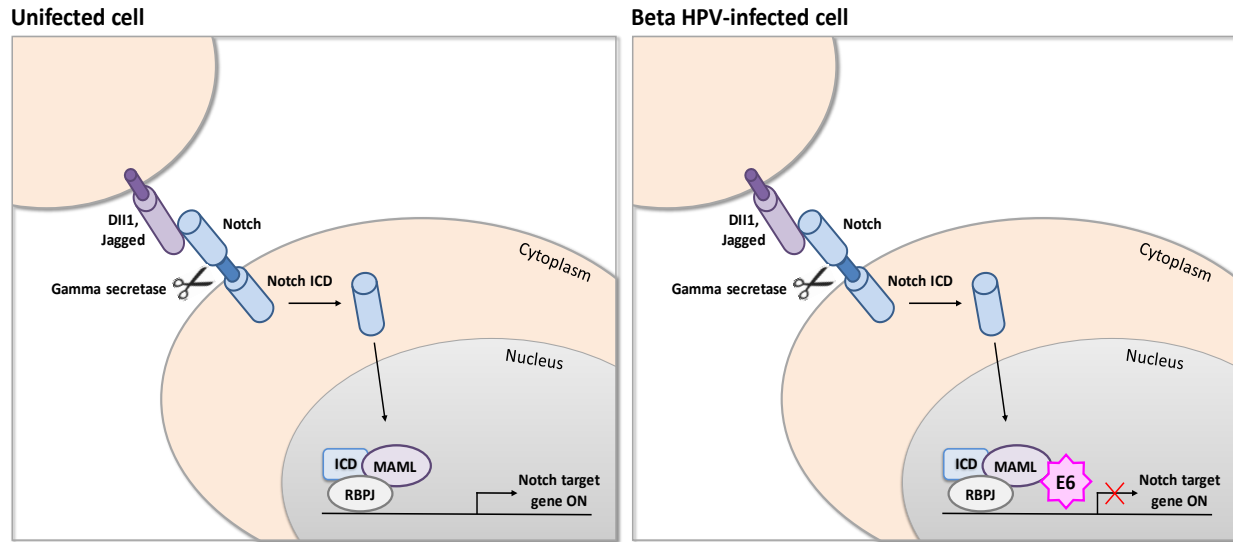


**Figure 11. Canonical Notch signaling pathway vs. Notch signaling in HPV-infected cells.** Interaction between NOTCH receptor (NOTCH1-4) and ligands JAG1-2 and DLL1-3-4 leads to the conformational change in NOTCH and enables cleavages by ADAM and  $\gamma$ -secretase. The cleavage releases Notch intracellular domain (NICD) which is translocated to the nucleus where it induces transactivation of Notch target genes. Transactivation occurs through the binding of NICD with DNA-bound RBP-J $\kappa$  and co-activator MAML,1 leading to the formation of the NOTCH/RBPJ $\kappa$  transcriptional complex (NTC) (left panel). Upon infection with  $\beta$ -HPV, E6 disrupts Notch activation by inhibiting RBPJ $\kappa$ /MAML1 transcriptional activator complex to be bound to Notch-targeted gene sequences. E6 binds to MAML1 directly, and subsequently and indirectly to RBPJ $\kappa$  and NICD (right panel). Adapted from (White 2019)

Even though molecular activities and pathways of cutaneous HPVs are not extensively studied, research in the past years found the connection between Notch signaling and  $\beta$ -HPVs (Rozenblatt-Rosen et al. 2012a; White et al. 2012; Tan et al. 2012a; Brimer et al. 2012b). Identification of MAML1 as a conserved interactor of  $\beta$ -E6s has raised interest for investigation of its potential in respect of the biological properties of cutaneous HPVs and their contribution to malignant development in cutaneous tissue utilizing Notch signaling pathway, which will be discussed in the following sections.

The effects of  $\alpha$ -HPV E6 on Notch signaling and molecular mechanisms in the background of that process is even less well established than for  $\beta$ -HPV E6. Like  $\beta$ -HPV E6s, HPV-16 E6 has an impact in altering Notch signaling, but so far it is known that the underlying mechanism is different from  $\beta$ -HPV E6s. It has been proposed that HPV-16 E6 inhibits Notch signaling through a mechanism which implies p53 degradation (Lefort et al. 2007; Dotto 2009; Yugawa et al. 2007). It was shown that HPV-16 E6 via a combined inactivation of p53 and NOTCH1 prevents fidelity

of keratinocytes towards differentiation and promotes keratinocyte proliferation (Kranjec et al. 2017). HPV-16 E6 inhibits NOTCH1 cleavage and decreases Notch-responsive genes transcription through p53 degradation, although the complete mechanism remains to be elucidated. The inactivation of Notch signaling in the basal layer provides an insight into the possible mechanism that HR  $\alpha$ -HPV E6 oncoproteins can utilize to contribute to the basal cell sustainability and proliferation (Kranjec et al. 2017). Simultaneously, HPVs must ensure adequate cell differentiation to support viral genome amplification. In stratified epithelia, the lower layers are subjected to epidermal growth factor stimulation and expression of the EGFR. Signal transduction from growth factor receptors plays a critical role in modulating HPV-16 E6 function by restricting E6 expression to a growth factor-rich environment (Kranjec et al. 2017).

Interestingly, MAML1 was identified as binding partner of HPV-16 E6 (N. Brimer et al. 2012b), even though 16 E6/MAML1 interaction was not observed in all proteomic analyses that were including 16 E6 (White et al. 2012; Rozenblatt-Rosen et al. 2012a).

#### ***1.8.2.1. Beta-HPV E6 associate with MAML1***

MAML1, as a member of the Notch transcription complex, has been identified as a cellular interacting protein of E6 proteins of some  $\beta$ -HPV E6s, HR- $\alpha$  HPV-16 E6 and of bovine papillomavirus type 1 (BPV-1) E6, associated with cutaneous fibropapillomas (Brimer et al. 2012c; Meyers, Spangle, and Munger 2013a; Tan et al. 2012a; Rozenblatt-Rosen et al. 2012b). Considering  $\beta$ -HPVs, it was reported that HPV-8 E6 forms a complex with MAML1 (N. Brimer et al. 2012b). Furthermore, it was shown that a number of  $\beta$ -HPV E6s repress Notch transcriptional activation of Notch-responsive genes and this repression is dependent upon the interaction with MAML1 (**Figure 11**, right panel). Hence, binding of E6 to MAML1 coactivator is required for the inhibition of Notch signaling in keratinocytes, that is a common feature of  $\beta$ -HPV E6 oncoproteins, which is not shared with  $\alpha$ -HPV E6 oncoproteins (Brimer et al. 2012b). This finding for the first time elucidated a mechanism of the viral antagonism linked to Notch signaling, suggesting Notch signaling to be an important epithelial cell signaling pathway targeted by  $\beta$ -HPVs (Brimer et al. 2012b).

The N-terminus of MAML1 contains a basic domain that interacts with the ankyrin repeats of NICD and the DNA-binding RBP-J $\kappa$  (Nam et al. 2006; Wu et al. 2000), and two acidic domains

(N- and C-termini). The N-terminal acidic domain interacts with p300 (Ribeiro et al. 2007) (**Figure 12**). MAML1 also contains two transactivation domains (TADs) that recruit additional cellular factors necessary for Notch transcriptional activation of the target genes (Nam et al. 2006). The interaction of  $\beta$ -HPV E6 with MAML1 was mapped to already mentioned and well described LXXLL (LDDLL) motif at the C-terminal acidic domain of MAML1 located at the position 1009-1013 amino acids, within the transactivation domain 2 (TAD2) (Tan et al. 2012a). (**Figure 12**).

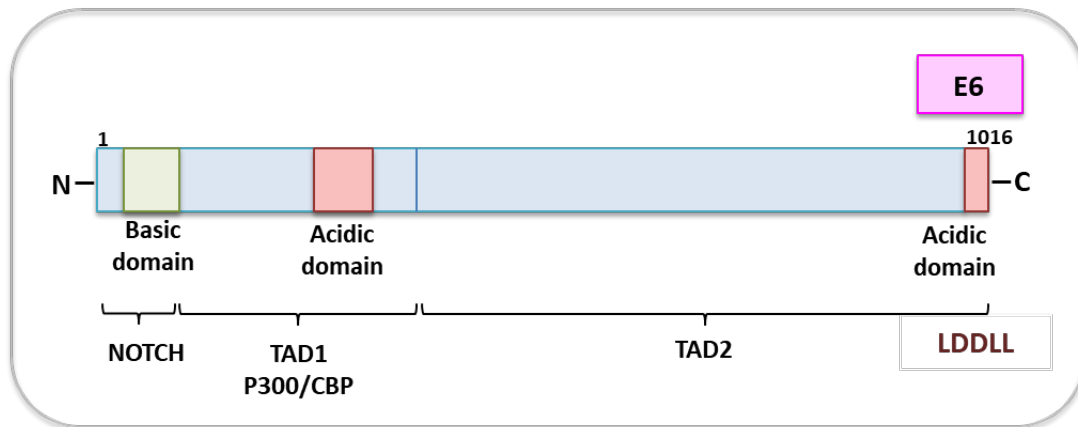


**Figure 12. Schematic representation of human Mastermind-like transcriptional coactivator 1 (MAML1) protein structure.** MAML1 contains an N-terminal basic domain and two acidic domains (N- and C-terminal). The N-terminal basic domain is responsible for interactions with the ankyrin domain of the NOTCH receptors. The sequences after the basic domain, referred as transcriptional activation domains (TADs), exhibit transcriptional activity. In MAML1 structure there are two TADs, TAD1 which contains the CBP/p300-binding site and TAD2, whose activities are required for Notch signaling. LXXLL motif is a part of TAD2, located on the extreme C-terminus of the acidic domain of MAML1 (aa 1009-1013) and it is required for HPV E6 binding. Adapted from (McElhinny et al. 2008)

The Leu-Xaa- Xaa-Leu-Leu (LXXLL) motif was originally observed in co-activator and co-repressor proteins that interact with hormone-activated nuclear receptors (Savkur and Burrell 2004; Plevin et al. 2005). Examples of LXXLL motifs in human cell have also been documented in proteins that do not directly interact with nuclear hormone receptors, including several transcription factors (Heery et al. 1997; Parker et al. 1999) and histone acetyltransferases CBP and p300 (Torchia et al. 1997). Furthermore, so far it was confirmed that  $\alpha$ - and  $\beta$ -HPV E6 oncoproteins recognize some of their target proteins, including E6AP (Huibregtse et al. 1993e), Interferon Regulatory Factor IRF-3 (Ronco et al. 1998), E6BP (Chen et al. 1995) and MAML1

(Brimer et al. 2012b; Rozenblatt-Rosen et al. 2012c; Tan et al. 2012b) through the described acidic leucine (L)-rich motif containing the LXXLL consensus sequence (X indicates any amino acid) (Chen et al. 1998; Zanier et al. 2013). BPV-1 E6 recognizes a subclass of acidic LXXLL sequence termed as LD motif and via this motif interacts with the focal adhesion protein paxillin (Wade et al. 2008; Tong and Howley 1997; Vande Pol 1998b). Interestingly, the LXXLL motifs that associate with nuclear hormone receptors in human cell are typically basic, while the E6-associated LXXLL motifs are acidic (Heery et al. 1997). The interaction between nuclear hormone receptors and their LXXLL peptide ligands typically involves 6 amino acid peptide motifs, while E6 oncoproteins interact with a longer sequence of 10-20 amino acids that contains a central LXXLL motif.

HPV-8 E6 inhibition of the Notch tumor suppressor pathways in cutaneous tissues is followed by delayed differentiation and sustained proliferation of differentiating keratinocytes (Meyers et al. 2017b). Forms of MAML1 deficient for acidic C-terminal domain act as dominant negative proteins, and expression of those truncated forms of MAML1 in mouse animal models resulted in appearance of CSCC (Proweller et al. 2006; Reichrath and Reichrath 2012), revealing an important role of Notch/RBPJ $\kappa$ /MAML1 complex in suppression of epithelial squamous carcinogenesis. Furthermore, different studies have demonstrated that all components of the Notch transcription effector complex act as tumor suppressors in normal mouse squamous epithelium (Rangarajan et al. 2001a; Nicolas et al. 2003). In those studies cell differentiation was lost under different conditions that involved disruption of Notch signaling in the squamous epithelium of transgenic mice by either tissue-specific NOTCH deletion (Rangarajan et al. 2001a; Nicolas et al. 2003),  $\gamma$ -secretase deletion to block the cleavage of NOTCH (Pan et al. 2004), deletion of the RBP-J $\kappa$ -binding subunit (Yamamoto et al. 2003; Blanpain et al. 2006) and expression of a dominant negative MAML1 (Proweller et al. 2006; Reichrath and Reichrath 2012). All those different disrupting conditions resulted in squamous cell carcinomas. Mentioned studies indicate the importance of the association between cutaneous E6s and MAML1 in disturbing Notch signaling and why it is biologically meaningful in the terms of altering the keratinocyte differentiation program and preparation of cellular environment for viral replication, and productive HPV life cycle. In the context of biological significance it is also speculated that it would be plausible for HPV fitness that E6 does not simply ablate Notch signaling, which would result in loss of epithelial integrity, but rather modulates its activation during the viral life cycle



and early replication, to restore or enhance Notch signaling in the suprabasal layers (Brimer et al. 2012b).

The mechanism by which HPV-8 E6 functions to impair Notch signaling is only partly elucidated because the inhibition of Notch signaling by HPV-8 E6 via binding MAML1 is different from the global inhibition of Notch activation at the level of NOTCH receptor processing (Meyers et al. 2013a). For  $\beta$ -HPV types, so far established working model is that HPV-8 E6 disrupts Notch activation during keratinocyte differentiation by blocking the recruitment of additional co-activators required for the transcriptional activation of RBPJ $\kappa$ /MAML1/NICD activator complex bound to Notch-responsive promoter within Notch-targeted gene sequences, instead of inhibiting transcriptional activator complex to be bound Notch-targeted gene sequences (**Figure 13**). MAML1 binding to RBPJ $\kappa$  requires a composite NICD/RBPJ $\kappa$  binding groove, and thus MAML1 cannot bind one factor independently of the other (Portal et al. 2011). It has been reported that HPV-8 E6 binds to MAML1 directly, and subsequently and indirectly to RBPJ $\kappa$  and NICD (Tan et al. 2012a).

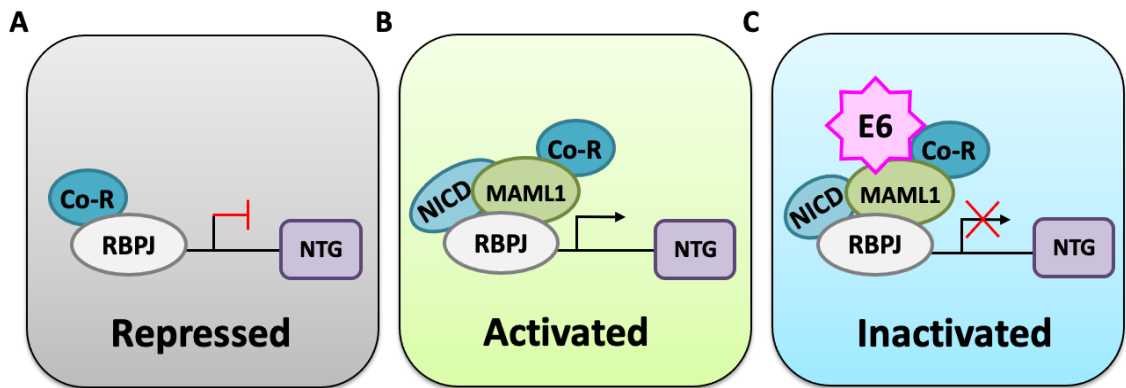


**Figure 13. Schematic representation of a model mechanism by which HPV-8 E6 gets access to the regulatory regions of Notch target genes.** (A) In the repressed state, NOTCH-targeted genes (NTG) are repressed because of presence of co-repressors (Co-R) that are bound to the DNA-binding RBPJ $\kappa$ . (B) In the active state, Notch intracellular domain (NICD) is bound to RBPJ $\kappa$ , MAML1 and other Co-As such as p300/CBP. (C) Association of HPV-8 E6 with MAML1 may prevent formation of the activator RBPJ $\kappa$ /MAML1/p300 complex and thereby preserve the repressor complex, or HPV-8 E6 may bind to the activator complex and interfere with its transcriptional activation. Adopted from (Meyers et al. 2013a).

Acetyltransferase p300 also has a role in this process as a co-activator of Notch signaling (Bray 2016). Hence, E6 can inhibit the binding of p300 necessary for MAML1 co-activator activity to inhibit formation, or inactivate DNA-bound RBPJ/MAML1/p300 transcriptional activator complex (**Figure 13**) (Meyers et al. 2013a). p300 has three LXXLL motifs and possesses the capacity to recognize LXXLL motifs, but associates with MAML1 via MAML1's TAD1 domain (**Figure 12**) (Ribeiro et al. 2007), whereas, as explained above, 8 E6 associates with LXXLL motif on MAML1 as a part of TAD2, hence does not directly compete with p300 binding to TAD1. p300 binding with HPV-8 E6 is not mediated via MAML1, although HPV-8 E6 binding to TAD2 can prevent p300 binding to TAD1 (Ribeiro et al. 2007). Many of HPV-8 E6 mutants that were not able to bind p300/CBP, were also found to be MAML1-binding defective, thus further complicating the interpretation of the studies investigating consequences of the p300 interactions with HPV-5 and HPV-8 E6 oncoproteins (Meyers et al. 2017b). The potential mechanism could be that E6 binding to TAD2 of MAML1 may inhibit expression of Notch transcriptional target genes by interfering with recruitment, or displacing p300 from MAML1's TAD1.

MAML1 has an additional novel function as a co-activator, which is independent of its function as a part of Notch signaling pathway, via exhibiting the co-activator function for p53 (Zhao et al. 2007). Findings that MAML1 recruits p300 to Notch transcriptional complex (Avantaggiati et al. 1997), raised a possibility that MAML1 may also function as a p53 co-activator. MAML1/p53 interaction involves the N-terminus of MAML1 and the DNA-binding domain of p53. With this, MAML1 becomes a part of the activator complex that binds to the p53-response elements within the promoter of the p53 target genes (Avantaggiati et al. 1997). So, MAML1 interacts directly with p53, associates with p53 transcriptional complexes and enhances p53-mediated gene transcription. This MAML1 co-activator function is an evolutionarily conserved role in p53-mediated transactivation (Avantaggiati et al. 1997). Even though MAML1 function as p53 co-activator is separated from Notch co-activator function, it would be interesting to speculate that those two functions could be a possible link between MAML1's role in  $\alpha$ - and  $\beta$ -HPV E6-induced oncogenic activities related to Notch signaling. Activation of Notch signaling was shown to inhibit p53-mediated apoptosis, suggesting an antagonism of Notch and p53 in their regulation (Nair et al. 2003a). Since  $\beta$ -HPV E6 inhibits Notch signaling via binding to MAML1 and  $\alpha$ -HPV-16 E6 inhibits Notch signaling via abrogating NOTCH1 cleavage and decreasing

Notch-responsive gene transcription mediated by p53 degradation, their mechanism of actions presumably can be cross-connected.

Moreover, since Notch signaling has a central role in keratinocyte differentiation, one can assume that other HPV types, besides BPV-1,  $\beta$ -types HPV-1 and HPV-8 E6 and  $\alpha$ -type HPV-16, can also modulate Notch, directly or indirectly. The direct way would be by the described inactivation of Notch signaling through the association with MAML1 in order to delay keratinocyte differentiation (Brimer et al. 2012b). On the other hand, the repression of Notch signaling can occur through an indirect interaction with p53 (Nair et al. 2003a).

## 2. AIMS OF THE STUDY

The process by which HPV initiates tumor formation and fosters tumor progression represents a suitable model for better understanding the development of many other human malignancies and allows identification of additional signaling pathways altered during oncogenesis. HPV E6 oncoprotein is one of two main viral oncoproteins and is directly responsible for development of a number of HPV-induced human malignancies, with cervical cancer being the principal disease. The overall aim of this thesis is to get a better understanding of E6 oncoprotein functions through interactions with cellular substrates and how this reflects upon its roles in inducing pathogenesis.

Only limited data are available about the molecular differences between the wild-type HPV-16 E6 oncoprotein and its variants, which provides only a partial insight into the mosaic of understanding their respective abilities to contribute towards cell transformation. Thus, revealing the molecular mechanisms in the background of their changed biological properties remains an important open question. The hypothesis of Part I of the thesis was that changes in the amino acid composition of HPV-16 E6 variant oncoproteins may affect their binding strength with well-characterized cellular substrates.

Part I of this doctoral thesis aims to:

- Biologically characterize three intra-type genetic variants (HPV-16 E6 D25N, E6 L83V and E6 D25N L83V) to determine if they exhibit functional differences which might cause alterations in their various biological properties and the ability to cause malignant transformation
- Investigate the capacity of HPV-16 E6 variants to form interaction with E6AP ubiquitin ligase, utilize the proteasomal machinery and subsequently induce E6AP self-ubiquitination and proteasomal degradation
- Analyse HPV-16 E6 variants' protein levels and their protein half-life
- Investigate if naturally occurring amino acid mutations in HPV-16 E6 variants might have an impact on their abilities to target well-characterized cellular substrates including p53 tumor suppressor and PDZ domain-containing substrates MAGI-1, DLG1 and Scrib by using both *in vitro* and overexpression assays in cultured cells
- Monitor cellular localization of HPV-16 E6 variants

The Part II of this doctoral thesis rises an important question whether there is a common underlying biological reason for the interaction of E6 oncoproteins via LXXLL motif with both E6AP and MAML1. Hence, E6 oncoproteins contain an LXXLL motif that is crucial for their interactions with several cellular proteins. The most important interactor of HR E6 oncoproteins, to which they bind via this motif, was shown to be E6AP, whilst cutaneous E6 oncoproteins were demonstrated to preferentially complex through the same motif with MAML1. Previously has been reported that the binding of  $\alpha$ - and some  $\beta$ -HPVs to E6AP via LXXLL motif leads to upregulation in E6 oncoprotein stability. Unlike the well-described E6 stabilization by E6AP, no detailed research has been done on the potential effects of HR mucosal E6s complexing with MAML1 via LXXLL motif, on E6 protein stability and function.

The focus of the Part II of doctoral thesis was to:

- Investigate if HPV E6 oncoproteins from  $\alpha$ -HPV types interact with transcriptional activator MAML1
- Elucidate if the binding of both  $\alpha$ - and  $\beta$ -HPV E6s to MAML1 results in E6 oncoprotein stabilization
- Analyse whether the ability of HR mucosal E6 to target p53 and the PDZ-domain containing substrate DLG1 for proteasome-mediated degradation is MAML1-dependent
- Monitor the rate of  $\alpha$ - and  $\beta$ -HPV E6 protein turnover in the absence of MAML1 and E6AP
- Evaluate changes in cellular localization and distribution of  $\alpha$ - and  $\beta$ -HPV E6s in the presence or absence of MAML1
- Investigate if E6 oncoprotein stabilization might influence E6 molecular activities and the biological processes in the cell, including the impact of MAML1 on cell proliferation, migration and apoptosis in HPV-positive background

### 3. MATERIALS AND METHODS

#### 3.1. Materials

##### 3.1.1. Buffers and solutions

The list of buffers and solutions used in this doctoral thesis are listed in **Table 1**.

**Table 1. Buffers and solutions**

| <b>Buffers and solutions</b>  | <b>Components</b>  |
|---|--|
| Acrylamide stock for the preparation of polyacrylamide gels                   | 29.2% (w/v) acrylamide, 0.8% (w/v) bisacrylamide   |
| Ammonium persulfate (APS) solution for the preparation of polyacrylamide gels | 10% (w/v) APS  |
| Coomassie Brilliant Blue for membrane staining                                | 3 g/L Coomassie Brilliant Blue R250, 10% (v/v) glacial acetic acid, 45% (v/v) methanol   |
| E1A lysis buffer, immunoprecipitation buffer                                  | 50 mM HEPES, 250mM NaCl, 0.5M EDTA, 0.1% (v/v) NP-40   |
| Flow cytometry staining buffer (FCSB)   | 5% (v/v) FBS, 0.5 mM EDTA, 2 mM NaN <sub>3</sub>   |
| Freezing medium for cells   | 10% (v/v) DMSO in FBS  |
| HEPES-buffered saline (2 x HBS)   | 50 mM HEPES, 280 mM NaCl, 1.5 mM Na <sub>2</sub> HPO <sub>4</sub>  |
| Membrane destain buffer   | 40% (v/v) methanol, 7% (v/v) acetic acid   |
| Milk solution for membrane blocking   | 10% (w/v) milk powder in PBS (or TBS)  |
| Modified E1A lysis buffer, immunoprecipitation buffer                         | 50 mM HEPES (pH 7.4), 150 mM NaCl, 1 mM EDTA, 0.25% (v/v) NP-40  |
| Phosphate Buffered Saline (PBS)Tween-20 (PBST), buffer for washing membranes  | 0.20% (v/v) Tween-20 in PBS, pH 7,4  |
| Paraformaldehyde (PFA) solution for cell fixation                             | 4.7% (v/v) formaldehyde in PBS   |
| Phosphate Buffered Saline (PBS)   | 137 mM NaCl, 2,7 mM KCl, 1.4 mM KH <sub>2</sub> PO <sub>4</sub> , 4.3 mM Na <sub>2</sub> HPO <sub>4</sub> ×7H <sub>2</sub> O, pH 7.4 |
| Ponceau-S for membrane staining   | 0,10% (v/v) Ponceau-S, 5% (v/v) acetic acid  |
| Running Buffer (RB), buffer for SDS-PAGE                                      | 190 mM glycine, 25 mM Tris, 0,10% (v/v) SDS  |
| Laemmli 2x buffer, gel loading buffer for protein samples                     | 100 mM Tris-HCl, pH 6.8, 200 mM DTT; 4% (v/v) SDS; 20% (v/v) glycerol; 0.001% (w/v) bromphenol blue                                  |
| Low salt dilution buffer (LSDB), immunoprecipitation buffer                   | 50 mM Tris-HCl pH 8.0, 20% (v/v) glycerol, 100 mM KCl, 0.1% (v/v) NP-40, 1 mM DTT, 50 mM NaF, 1 mM orthovanadate, 1 mM PMS           |
| SDS solution for the preparation of polyacrylamide gel and running buffer     | 10% (w/v) SDS  |
| Solution for the preparation of chemocompetent DH5α cells                     | 25 mL 0.1 M CaCl <sub>2</sub> , 20 mL H <sub>2</sub> O, 5 mL glycerol  |
| Stripping buffer for removing antibodies from the membrane                    | 0.2 M NaOH in PBS  |
| TAE, agarose gel electrophoresis buffer                                       | 40 mM Tris, 20 mM acetic acid, 1 mM EDTA   |

|   |  |
|---|--|
| TE, buffer for calcium phosphate transfection and DNA dilution                        | 10 mM Tris, 1mM EDTA                               |
| Transfer Buffer (TB), buffer for transferring proteins to nitrocellulose membranes    | 25 mM Tris-HCl, 190 mM glycine, 20% (v/v) methanol |
| Tris buffered saline (TBS)  | 0.5M Tris-HCl, 1.5 M NaCl, pH 7.4                  |
| Tris buffered saline Tween-20 (TBST), buffer for washing membranes                    | 0.10% (v/v) Tween-20 in TBS, pH 7.4                |
| Tris buffer for the preparation of polyacrylamide separation gel                      | 1.5 M Tris, pH 8,8                                 |
| Tris buffer for the preparation of polyacrylamide stacking gel                        | 1.5 M Tris, pH 6,8                                 |
| Triton X-100 solution for cell permeabilization and production of GST-fusion proteins | 0.1% (v/v) Triton X-100 in PBS                     |

### 3.1.2. Chemicals, detergents and antibiotics

All chemicals, detergents and antibiotics which were used for the preparation of buffers and solutions for the conduction of various experiments and treatment of cells and bacteria are listed in a **Table 2**, **Table 3** and **Table 4**.

**Table 2. Chemicals for various experiments and cell treatment**

| <b>Product</b>                        | <b>Manufacturer</b>           | <b>Cat. Number</b> |
|---------------------------------------|-------------------------------|--------------------|
| 2-mercaptoethanol                     | Sigma-Aldrich, USA            | 60242              |
| 2-isopropanol                         | Gram mol, Croatia             | P150501            |
| Acetic acid                           | Gram mol, Croatia             | P150501            |
| Acrylamide                            | Carl Roth GmbH & Co., Germany | 7871.2             |
| Agarose                               | Sigma-Aldrich, USA            | A9539              |
| Ammonium persulfate                   | Sigma-Aldrich, USA            | 09913-100          |
| Bromophenol blue R                    | Sigma-Aldrich, USA            | B-0149             |
| BSA, bovine serum albumin             | Sigma-Aldrich, USA            | 9048-46-8          |
| CaCl <sub>2</sub>                     | Kemika, Croatia               | 1146609            |
| Coomassie Brilliant Blue R250         | Thermo Fisher Scientific, USA | LC6060             |
| DAPI, (4',6-diamidino-2-phenylindole) | Sigma-Aldrich, USA            | D1306              |
| DMSO, dimethyl sulfoxide              | Sigma-Aldrich, USA            | 47230              |
| DTT, dithiothreitol                   | Sigma-Aldrich, USA            | 3483-12-3          |
| EDTA, ethylenediaminetetraacetic acid | Sigma-Aldrich, USA            | E-5134             |
| Ethanol, 96% and 75%                  | Kemika, Croatia               | 0505001            |
| FBS, fetal bovine serum               | Sigma-Aldrich, USA            | F9665              |
| Glycerol                              | Kemika, Croatia               | 0711901            |
| Glycine                               | Sigma-Aldrich, USA            | 33226              |
| HEPES                                 | Sigma-Aldrich, USA            | H4034              |

|   |                               |           |
|---|-------------------------------|-----------|
| KH <sub>2</sub> PO <sub>4</sub>             | Kemika, Croatia               | 1112408   |
| IPTG, isopropyl β-D-thiogalactoside         | Sigma-Aldrich, USA            | 367-93-1  |
| L-glutamine                                 | Sigma-Aldrich, USA            | G3126     |
| Methanol, 96%                               | Gram mol, Croatia             | P140500   |
| MgCl <sub>2</sub> , 25 mM                   | Promega, Wisconsin, USA       | A3511     |
| Midori Green                                | BioCat GmbH, Germany          | MG04-NP   |
| NaCl  | Gram mol, Croatia             | 7647-14-5 |
| NaHCO <sub>3</sub>                          | J.T. Baker, USA               | 3506-01   |
| NaHPO <sub>4</sub>                          | Gram mol, Croatia             | P146010   |
| NaOH  | J.T. Baker, USA               | 3722-01   |
| N, N'-Methylenebisacrylamid                 | Sigma-Aldrich, USA            | M7279     |
| Ponceau-S                                   | Sigma-Aldrich, USA            | P3504     |
| Sodium pyruvate                             | Thermo Fisher Scientific, USA | 11360-039 |
| TEMED, N, N, N', N'-tetramethylethyldiamine | Sigma-Aldrich, USA            | T9281     |
| Trypsin/EDTA                                | Thermo Fisher Scientific, USA | 15400-054 |
| Tris  | Merck KGa, Germany            | KB313482  |
| Tris-HCl                                    | Sigma-Aldrich, USA            | 1185-53-1 |

**Table 3. Detergents for preparation of buffers and solutions**

| <b>Product</b>              | <b>Manufacturer</b>           | <b>Cat. Number</b> |
|-----------------------------|-------------------------------|--------------------|
| NP-40                       | Thermo Fisher Scientific, USA | 28324              |
| SDS, sodium dodecyl sulfate | Sigma-Aldrich, USA            | L3771              |
| Triton X-100                | Sigma-Aldrich, USA            | 9036-19-5          |
| Tween-20                    | Sigma-Aldrich, USA            | P2287              |

**Table 4. Antibiotics used for cell and bacteria culture**

| <b>Product</b>            | <b>Manufacturer</b>           | <b>Cat. Number</b> |
|---------------------------|-------------------------------|--------------------|
| Ampicillin                | Sigma-Aldrich, USA            | A9518              |
| Penicillin / Streptomycin | Thermo Fisher Scientific, USA | 15140-122          |
| Puromycin                 | Sigma-Aldrich, USA            | 58-58-2            |
| Kanamycin                 | Sigma-Aldrich, USA            | K4000              |

### 3.1.3. Commercial kits and reagents

All commercially available kits and reagents, which were used for various experiments, from DNA isolation, plasmid purification, cell transfection and immunoprecipitation are listed in a **Table 5**.



**Table 5. Commercial kits and reagents**

| <b>Product</b>                                      | <b>Appliance</b>   | <b>Manufacturer</b>                  | <b>Cat. Number</b> |
|---|--|--------------------------------------|--------------------|
| Annexin V Apoptosis Detection Kit                   | Kit for apoptosis detection  | Santa Cruz Biotechnology, USA        | sc-4252 AK         |
| Dynabeads® Protein G                                | Paramagnetic beads for immunoprecipitation assay   | Thermo Fisher Scientific, USA        | 10007D             |
| EZview™ Red Anti-FLAG® M2 agarose beads             | Affinity purification of FLAG-tagged proteins for immunoprecipitation assays                   | Sigma-Aldrich, USA                   | F2426              |
| ECL Western Blotting Detection Reagent              | Chemiluminescent reagent for detection of signals on the membrane                              | Amersham, Cytiva, USA                | RPN2106            |
| EZview™ Red Anti-HA agarose beads                   | Affinity purification of HA-tagged proteins for immunoprecipitation assays                     | Sigma-Aldrich, USA                   | E5779              |
| Glutathion-S-transferase agarose beads              | Affinity purification of GST-tagged fusion proteins for GST pull-down assays                   | Sigma-Aldrich, USA                   | G4510              |
| Monarch DNA Gel Extraction Kit                      | Kit with columns for purification of PCR reaction products from agarose gels                   | New England Biolabs, USA             | T1020G             |
| Monarch PCR & DNA Cleanup Kit                       | Kit with columns for purification of PCR reaction products                                     | New England Biolabs, USA             | T1030G             |
| NucleoBond PC500 Maxi prep Kit                      | Kit with columns for isolation of plasmid DNA  | Macherey-Nagel GmbH, Germany         | 740574.50          |
| NucleoBond PC100 Midi prep Kit                      | Kit with columns for isolation of plasmid DNA  | Macherey-Nagel GmbH, Germany         | 740573             |
| Lipofectamine 2000                                  | Transfection reagent   | Invitrogen, USA                      | 11-668-019         |
| ON-TARGETplus siRNA                                 | siRNA for target gene silencing  | Dharmacon, USA                       |                    |
| UptiBlue Viable Cell Counting Kit                   | Kit to quantitatively measure the proliferation of various cells                               | Interchim, USA                       | NT-UP66941         |
| ProteoExtract® Subcellular Proteome Extraction Kit  | Kit for extraction of subcellular proteomes from adherent and suspension-grown mammalian cells | The Calbiochem by Merck KGa, Germany | 539790             |
| Protran™ Nitrocellulose Blotting Membrane, 0.22 µm  | Nitrocellulose blotting membrane for western blot analysis                                     | Amersham, Cytiva, USA                | 1060001            |
| SuperSignal™ West Pico PLUS                         | Chemiluminescent reagent for detection of signals on the membrane                              | Thermo Fisher Scientific, USA        | 34580              |
| TnT® Quick Coupled Transcription/Translation System | <i>In vitro</i> translation system for eukaryotic cell-free protein expression                 | Promega, USA                         | L1170              |

|  |  |                               |        |
|--|--|-------------------------------|--------|
| TurboFect™                                       | Transfection reagent                                       | Thermo Fisher Scientific, USA | R0531  |
| Qiagen Plasmid Maxi Kit                          | Kit with columns for isolation of plasmid DNA              | Qiagen, USA                   | 12163  |
| QuikChange Multi Site-Directed Mutagenesis Kit   | Kit for PCR mutagenesis                                    | Agilent Technologies, USA     | 200513 |
| Wizard Plus SV Minipreps DNA Purification System | Kit with columns for isolation of plasmid DNA              | Promega, USA                  | A1460  |
| Wizard SV Gel and PCR Clean-Up System            | Kit with columns for purification of PCR reaction products | Promega, USA                  | A9282  |

### 3.1.4. Enzymes and corresponding buffers

Enzymes and their corresponding buffers which were used for site-directed mutagenesis are listed in **Table 6**.

**Table 6. Enzymes and corresponding buffers**

| Enzyme and buffers  | Manufacturer             | Cat. Number |
|---|--------------------------|-------------|
| <i>Pfu</i> DNA Polymerase                                   | Promega, USA             | M774A       |
| <i>Pfu</i> DNA Polymerase 10X Buffer with MgSO <sub>4</sub> | Promega, Wisconsin, USA  | M776A       |
| DpnI  | New England Biolabs, USA | R0176S      |

### 3.1.5. Antibodies

Primary and secondary antibodies used for protein detection in western blot analysis, immunoprecipitation, as well as for cellular localization in confocal microscopy are listed in **Table 7** and **Table 8**.

**Table 7. Primary antibodies**

| Enzyme and buffers    | Manufacturer                   | Cat. Number |
|-----------------------|--------------------------------|-------------|
| Anti-c-MYC (9E10)     | Santa Cruz Biotechnology, USA  | sc-40       |
| Anti-FLAG (M2)        | Sigma-Aldrich, USA             | F3165       |
| Anti-FLAG (M5)        | Sigma-Aldrich, USA             | F F4042     |
| Anti-FLAG rabbit      | Sigma-Aldrich, USA             | F7426       |
| Anti-GAPDH (0411)     | Santa Cruz Biotechnology, USA  | sc-47724    |
| Anti-HA HRP (HA-7)    | Sigma-Aldrich, USA             | HH3663      |
| Anti-Histone H3 (1G1) | Santa Cruz Biotechnology, USA  | sc-517578   |
| Anti-HPV18 E6 (G-7)   | Santa Cruz Biotechnology, USA  | sc-365089   |
| Anti-MAML1 Rabbit     | Cell Signaling Technology, USA | 4608S       |
| Anti-MAML1 (D3E9)     | Cell Signaling Technology, USA | 11959S      |
| Anti-MAML1 (D3K7B)    | Cell Signaling Technology, USA | 12166S      |
| Anti-MCM7 (141.2)     | Santa Cruz Biotechnology, USA  | sc-9966     |

|                                  |                               |         |
|----------------------------------|-------------------------------|---------|
| Anti-p53 (DO-1)                  | Santa Cruz Biotechnology, USA | sc-126  |
| Anti-SAP 97 (2D11)               | Santa Cruz Biotechnology, USA | sc-9961 |
| Anti-UBE3A (13)                  | BD Biosciences, USA           | 611416  |
| Anti-Vimentin (V9)               | Santa Cruz Biotechnology, USA | sc-6260 |
| Anti- $\beta$ -Actin HRP (AC-15) | Sigma-Aldrich, USA            | A3854   |
| Anti- $\beta$ -Galactosidase     | Promega, USA                  | Z378A   |

**Table 8. Secondary antibodies**

| <b>Antibody</b>                              | <b>Manufacturer</b>                         | <b>Cat. Number</b> |
|--|---|--------------------|
| Rabbit Anti-Mouse HRP                        | Agilent Technologies, USA                   | P0161              |
| Swine Anti-Rabbit HRP                        | Agilent Technologies, USA                   | P0217              |
| Alexa Fluor 488 donkey anti-mouse IgG (H+L)  | Invitrogen by Thermo Fisher Scientific, USA | A21202             |
| Alexa Fluor 488 donkey anti-rabbit IgG (H+L) | Invitrogen by Thermo Fisher Scientific, USA | A21206             |
| Rhodamine Red-X Goat anti-mouse (H+L)        | Invitrogen by Thermo Fisher Scientific, USA | R6393              |
| GAPDH-Alexa Fluor 680 (G9)                   | Santa Cruz Biotechnology, USA               | sc-365062          |
| Goat anti-mouse IgG H&L (IRDye® 800CW)       | Abcam, UK                                   | ab216772           |

### 3.1.6. DNA and protein markers

In **Table 9** and **Table 10** are depicted all DNA ladders, and protein markers ranging from 10 to 250 kDa, respectively.

**Table 9. DNA markers for determining the molecular weight of nucleic acids**

| <b>DNA ladders</b>             | <b>Appliance</b>                      | <b>Manufacturer</b>                          | <b>Cat. Number</b> |
|--------------------------------|---------------------------------------|--|--------------------|
| 1 Kb Plus DNA Ladder           | DNA marker ranging from 0.1 to 15 kb  | Thermo Fisher Scientific, Massachusetts, USA | 10787018           |
| BenchTop 1kb DNA Ladder        | DNA marker ranging from 0.25 to 10 kb | Promega, Wisconsin, USA                      | G754A              |
| Quick-load Purple 1kb Plus DNA | DNA marker ranging from 0.1 to 10 kb  | New England Biolabs, Massachusetts, USA      | N0550S             |

### 3.1.7. Protein inhibitors

Inhibitors are listed in **Table 11**. The proteasome inhibitor bortezomib (BTZ) was used in for determining if the fluctuations in protein levels were proteasome dependent. Cycloheximide was used to block protein synthesis in half-life experiments. The inhibitors were dissolved in

dimethyl sulfoxide (DMSO) and used at the indicated concentrations. Cocktail set 1 of protease inhibitors were dissolved in water and used for the supplementation of lysis buffers for protein isolation at the concentration 1:100.

**Table 11. Protein inhibitors**

| <b>Inhibitor</b>                  | <b>Mechanism of action</b>                     | <b>Manufacturer</b>                  | <b>Cat. Number</b> |
|-----------------------------------|--|--------------------------------------|--------------------|
| Bortezomib (10 $\mu$ M)           | proteasome inhibitor                           | Sigma-Aldrich, USA                   | 179324-69-7        |
| Cycloheximide (50 $\mu$ M)        | protein synthesis blocking                     | Sigma-Aldrich, USA                   | 66-81-9            |
| Protease Inhibitor Cocktail set 1 | protease inhibitors used for protein isolation | The Calbiochem by Merck KGa, Germany | 539131             |
| RNAse Inhibitor                   | RNAse activity inhibition                      | Thermo Fisher Scientific, USA        | N8080119           |

### 3.1.8. Media for maintaining cell and bacterial cultures

The composition of liquid nutrient media for growing cells or bacteria is shown in **Table 12**. Briefly, bacterial cells used for plasmid production were grown in lysogeny broth (LB) and on agar plates. In LB medium and agar plates ampicillin or kanamycin antibiotic was added. HeLa, CaSki, HEK293, CRISPR/Cas9 gRNA-mediated E6AP-null HEK 293 cells (Thatte and Banks 2017), C33A, H1299 and HT1080 stably expressing HPV8 E6 (Hufbauer et al. 2015a) were grown in Dulbecco's modified Eagle's medium (DMEM) with 10% fetal bovine serum (FBS), penicillin/streptomycin, L-glutamine and sodium pyruvate at 37°C in a humidified air incubator containing 10% CO<sub>2</sub>.

**Table 12. Cell and bacterial growth media and corresponding supplements**

| <b>Media for</b>      | <b>Product</b>                           | <b>Manufacturer</b>           | <b>Cat, number</b> |
|-----------------------|--|-------------------------------|--------------------|
| Media for bacteria    | Agar                                     | Sigma-Aldrich, USA            | 05040              |
|                       | LB broth                                 |                               | L3022              |
|                       | Ampicillin (or kanamycin) sodium salt    |                               | A9518              |
| DMEM for cell culture | DMEM                                     | Thermo Fisher Scientific, USA | 31600-083          |
|                       | Sodium Pyruvate (100 mM)                 | Thermo Fisher Scientific, USA | 11360039           |
|                       | L-glutamine (300 $\mu$ g/ml)             | Sigma-Aldrich, USA            | G-3126             |
|                       | Penicillin-Streptomycin (100 $\mu$ g/ml) | Thermo Fisher Scientific, USA | 15140122           |
|                       | Fetal Bovine Serum (FBS), 10% (v/v)      | Thermo Fisher Scientific, USA | 26140079           |

### 3.1.9. Instruments and programs

Instruments (**Table 13**) used for cell culture, protein and DNA analysis are listed according to different type of procedures. Computer programs used for data analysis and visualization are listed in a **Table 14**.

**Table 13. Instruments**

|                        | <b>Product</b>  | <b>Description</b>  | <b>Manufacturer</b>                      |
|------------------------|---|---|--|
| Cell culture equipment | Laminar flow, fume hood KTV-S                           | Laminar flow for working under sterile conditions                                       | Klimaoprema d.d., Croatia                |
|                        | BB-16 D-63450 Incubator                                 | Incubator for growing cells   | Heraeus Group, Germany                   |
|                        | CellDrop FL Fluorescence Cell Counter                   | Spectrophotometer device for cell counting  | DeNovix Inc., Delaware, USA              |
|                        | Dino-Eye eyepiece (AM7023(R4))                          | Digital eyepiece camera   | Dino-Lite Europe, IDCP B.V., Netherlands |
|                        | OmniPET Pipette Filler                                  | Pipette Filler  | Cleaver Scientific Ltd, UK               |
|                        | Easypet® 4421 pipetting aid                             | Pipette Filler  | Eppendorf, Germany                       |
|                        | LABSONIC® M ultrasonic homogenizer                      | Ultrasonic sonicator and probe with a diameter of 0.5 and 1 mm                          | Montreal Biotech Inc., , Canada          |
|                        | NanoPhotometer® N60                                     | Spectrophotometer device for measuring DNA quantites                                    | Implen GmbH, Germany                     |
|                        | Labystems Multiskan MS 352                              | Multiwell plate reader  | Thermo Fischer Scientific, USA           |
| Microscopes            | FACSCalibur   | Flow cytometer  | BD Bioscience, USA                       |
|                        | Leica TCS SP8 X   | Laser scanning confocal microscope equipped with a HC PL APO CS2 63×/1.40 oil objective | Leica Microsystems, Germany              |
|                        | Olympus CK30  | Culture microscope  | Olympus Corporation, Japan               |
| Imaging systems        | Alliance 4.7 Fluorescence and Chemiluminescence Systems | Device for detecting chemiluminescence signals and UV signals from agarose gels         | Uvitec Ltd, UK                           |
|                        | Alliance Q9 Advanced Chemiluminescence Imager           | Device for detecting chemiluminescence signals  | Uvitec Ltd, UK                           |
|                        | LI-COR Odyssey Fc Imaging System                        | Device for detecting chemiluminescence signals  | LI-COR Bioscience, USA                   |
|                        | Cyclone Plus Storage Phosphor System                    | Phosphoimager for detecting signal on the radioactive gels                              | PerkinElmer, USA                         |
| Centrifuge             | 5403  | Centrifuge  | Eppendorf, Germany                       |
|                        | 5415 C  | Centrifuge  | Eppendorf, Germany                       |
|                        | 5415 R  | Centrifuge  | Eppendorf, Germany                       |

|                                      |  |                                       |   |
|--------------------------------------|--|---------------------------------------|---|
|                                      | Heraeus Multifuge 3S-R                                 | Centrifuge                            | Thermo Fisher Scientific, USA                     |
|                                      | Sorvall LYNX 4000                                      | Superspeed centrifuge                 | Thermo Fisher Scientific, , USA                   |
| Rotators                             | SARMIX® M2000  | Rotation mixer                        | Sarstedt AG & Co., KG, Germany                    |
|                                      | Multi Bio RS-24  | Programmable rotator                  | Biosan Laboratories, Inc., USA                    |
| Thermal cyclers                      | Applied Biosystems Veriti™ 96-Well Fast Thermal Cycler | PCR machine for PCR optimization      | Thermo Fisher Scientific, USA                     |
|                                      | 2720 Thermal Cycler                                    | PCR machine                           | Applied Biosystems, Thermo Fisher Scientific, USA |
| Electrophoresis and transfer systems | omniPAGE   | System for vertical electrophoresis   | Cleaver Scientific Ltd, UK                        |
|                                      | PowerPRO 300   | Power supply device                   | Cleaver Scientific Ltd, UK                        |
|                                      | Mini-Protean®  | System for vertical electrophoresis   | Bio-Rad Laboratories, USA                         |
|                                      | Trans-Blot® Turbo™                                     | Transfer system                       | Bio-Rad Laboratories, USA                         |
|                                      | PowerPac™ Basic  | Power supply device                   | Bio-Rad Laboratories, USA                         |
|                                      | Wide Mini-Sub Cell GT                                  | System for horizontal electrophoresis | Bio-Rad Laboratories, USA                         |
|                                      | Sub-Cell GT  | System for horizontal electrophoresis | Bio-Rad Laboratories, USA                         |

**Table 14. Programs for data analysis and visualization**

| <b>Product</b>                                | <b>Description</b>                                | <b>Manufacturer</b>                |
|---|---|------------------------------------|
| Ascent Software                               | Software for Thermo Scientific microplate readers | Thermo Fischer Scientific, USA     |
| BioEdit 7.2                                   | Software for sequence alignment                   | Bioedit Company, USA               |
| DinoCapture 2.0                               | Microscope imaging software                       | Dino-Lite Europe, Netherlands      |
| FCS 3 Express                                 | Flow cytometry software                           | De Novo Software, USA              |
| GraphPad Prism                                | Statistical analysis software                     | GraphPad Inc., USA                 |
| ImageJ Fiji                                   | Quantification of image data                      | National Institutes of Health, USA |
| Leica Application Suite X (LAS X) 3.3.0.16799 | Software for Leica confocal microscope            | Leica Microsystems, USA            |
| MedCalc                                       | Statistical analysis software                     | MedCalc Software Ltd, USA          |
| Microsoft Office Excel 2016                   | Statistical analysis software                     | Microsoft Corporation, USA         |
| OptiQuant™ 5.4                                | Quantification software                           | PerkinElmer, USA                   |
| SnapGene                                      | Sequence and primer design program                | GSL Biotech LLC, USA               |
| UVIBand                                       | Quantification software                           | UVItec Cambridge, UK               |

## 3.2. Molecular methods

### 3.2.1. Site-directed mutagenesis

Site-directed mutagenesis is a molecular method used to create specific, targeted changes in double stranded plasmid DNA by using custom designed oligonucleotide primers to confer a desired mutation (**Table 15**). The pCA16E6D25N, 16E6L83V, 16E6D25N-L83V and pGEX-2T16E6D25N, 16E6L83V, 16E6D25N-L83V vectors were constructed using pCA16E6 and pGEX-2T16E6 as a PCR templates. Plasmid pCA16E6 is a pCDNA3 mammalian expression vector that contains two HA and a FLAG-tag epitope, and gene sequence of wild type HPV-16 E6 gene created by inserting into the multiple cloning site of pCDNA3 plasmid. pCA has a CMV promoter, so it is designed for constitutive expression in a variety of mammalian cell lines and contains ampicillin resistance gene for bacterial selection. pGEX-2T vector is used for the expression of GST-tagged fusion proteins. The expression is under the control of the tac promoter, which is induced by the lactose analog isopropyl  $\beta$ -D-thiogalactoside (IPTG). pGEX vector contains internal lacIq gene that is a repressor protein that binds to the tac promoter, preventing expression until induced by IPTG, in this way maintaining the control over expression of the gene insert. Mutagenesis was done using a modified protocol of the PCR mutagenesis kit (QuickChange Site Directed Mutagenesis) according to the manufacturer's instructions. The process uses a dsDNA vector with insert (pCA16E6 and pGEX2-T16E6) and two synthetic oligo primers designed in overlapping orientation which in their sequence contain the point mutation of interest that will be incorporated in plasmid sequence. Incorporating oligo primers creates a re-circularized mutated plasmid with staggered nicks. The PCR protocol included usage of the *Pfu*<sup>®</sup> DNA Polymerase and *Pfu* DNA Polymerase 10x Reaction Buffer with MgSO<sub>4</sub>, nucleotides (dATP, dTTP, dGTP, dCTP) and primers designed in-house (Macrogen, Netherlands).

**Table 15. Specific primers for site-directed mutagenesis of pCA:16E6 and pGEX-2T:16 E6 vectors**

| Gene          | Primer         |   | Length | T <sub>m</sub> |
|---------------|----------------|---|--------|----------------|
| HPV16 E6 D25N | HPV16_E6D25N_F | 5' CAAACAAC TATACATAATATAATATTAGAATGTGTG 3' | 36 bp  | 53°C           |
|               | HPV16_E6D25N_R | 5' CACACATTCTAATATTATATTATGTATAGTTGTTG 3'   | 36 bp  | 53°C           |
| HPV16 E6 L83V | HPV16_E6L83V_F | 5'GACATTATTGTTATAGTGTGTATGGAACAACATTAG 3'   | 36 bp  | 58°C           |
|               | HPV16_E6L83V_R | 5'CTAATGTTGTTCCATACACACTATAACAATAATGTC 3'   | 36 bp  | 58°C           |

The mixture for each reaction was prepared by mixing 50  $\mu$ L of Master Mix, 1.25  $\mu$ L each of both primers (forward (F) and reverse (R)),  $c = 10 \mu\text{M}$ , 50 ng of plasmid template, 1  $\mu$ L dNTPs (10 mM) and supplemented with nuclease-free water up to the total volume of 50  $\mu$ L. The PCR reaction was done in a 2720 Thermal Cycler. The conditions for site-directed mutagenesis of pCA16E6 and pGEX-2T16 E6 vector are shown in **Table 16**.

**Table 16. PCR conditions for site-directed mutagenesis**

| Step                 | Temperature/ $^{\circ}\text{C}$ | Time/min | Number of cycles |
|----------------------|---------------------------------|----------|------------------|
| Initial denaturation | 95                              | 30       | 1                |
| Denaturation         | 95                              | 30       | 18               |
| Annealing*           | 55                              | 1        | 18               |
| Extension**          | 68                              | 5        | 18               |
| Final extension      | 68                              | 10       | 1                |
| End of reaction      | 4                               | $\infty$ | 1                |

\*The annealing temperature depends upon the sequence of the two primers, and was calculated as  $T_m - 5^{\circ}\text{C}$

\*\*Extension time depends on a PCR product size, approximately 2 min for every 1kb to be amplified

After temperature cycling the PCR product was treated with Dpn I enzyme for 2 h at  $37^{\circ}\text{C}$  using thermo mixer device. Dpn I was used to digest the parental DNA template to select mutation-containing synthesized DNA, and it was inactivated for 20 min at  $80^{\circ}\text{C}$ . All the constructs were verified by sequencing (Macrogen, Netherlands). The vector DNA containing the mutations was transformed into DH5 $\alpha$  competent cells.

### 3.2.2. Preparation of chemocompetent DH5 $\alpha$ cells

DH5 $\alpha$  cells are chemically competent *Escherichia coli* cells suitable for high efficiency transformation. For the preparation of the competent DH5 $\alpha$  cells, 5  $\mu$ L of bacteria glycerol stock stored at  $-20^{\circ}\text{C}$  was inoculated into 50 mL of liquid bacteria nutrient medium LB. A bacteria flask was agitated in the shaker at  $37^{\circ}\text{C}$ . Bacteria growth was carefully monitored and  $\text{OD}_{600}$  value was measured using spectrophotometer NanoPhotometer $^{\circledR}$  N60.  $\text{OD}_{600}$  is an arbitrary value that helps to determine the cell growth stage and is an abbreviation indicating the optical density of a sample measured at a wavelength of 600 nm. When  $\text{OD}_{600}$  value reached a range of 0.3-0.4, 25 mL of the bacterial culture were aliquoted and kept on ice for 20 min. This was followed by centrifugation at  $6000 \times g$  for 5 min. The supernatant was discarded, and the pellets were resuspended in 12.5 mL of 50 mM  $\text{CaCl}_2$  precooled to  $4^{\circ}\text{C}$ , and left on ice for the following 20 min. After 20 min cells



were centrifuged again for 5 min at  $6000 \times g$ . The supernatant was discarded, and the pellets were resuspended in 2.5 mL of solution for the preparation of chemocompetent cells and left on ice overnight. The following day, 200  $\mu\text{L}$  of the prepared bacteria were aliquoted into sterile tubes and stored in a freezer at  $-80\text{ }^{\circ}\text{C}$ .

### **3.2.3. DH5 $\alpha$ transformation**

The transformation of chemocompetent bacterial cells by heat shock was performed by adding approximately 100 ng of plasmid DNA to a 50  $\mu\text{L}$  aliquot of bacterial cells followed by incubation for at least 5 min on ice, which enabled DNA adsorption to the bacterial cell surface. After this step, a heat shock was induced for 2 min at  $42^{\circ}\text{C}$ , which caused the introduction of foreign DNA into bacterial cells. The bacteria and DNA mixture was put back on ice for additional 10 min. Next, 100  $\mu\text{L}$  of liquid nutrient LB medium without antibiotics was added in a sterile tube with transformed cells and incubated at  $37\text{ }^{\circ}\text{C}$  for 1 h with agitation. During the incubation time antibiotic resistant proteins encoded from the plasmid backbone were generated. The entire volume of the transformed bacterial mixture was plated on 10 cm LB agar plates with an antibiotic. LB agar plates that contained either ampicillin (for the transformation of the plasmids containing an ampicillin resistance gene sequence) or kanamycin (for the transformation of the plasmids containing a kanamycin resistance gene sequence) were used. After overnight incubation at  $37\text{ }^{\circ}\text{C}$  individual colonies were obtained. To isolate plasmid DNA, a few individual colonies were isolated and grown in liquid nutrient medium LB with a suitable antibiotic, placed in a shaker at  $37\text{ }^{\circ}\text{C}$  overnight with agitation for the promotion of bacterial growth. The following steps are described in chapter 3.2.4. After successful transformation, an aliquot of transformed bacterial cells was mixed with a 50% (v/v) aqueous solution of glycerol in a 1:1 ratio. In this way, the transformed bacteria were stored for a longer time at  $-20\text{ }^{\circ}\text{C}$ .

### **3.2.4. Isolation of plasmid DNA**

Plasmid DNA was isolated using commercial kits according to the manufacturer's instructions. After isolation, the concentration of plasmid DNA was determined, and sample was

verified on gel electrophoresis by comparison of the molecular weight of the isolated plasmid with the molecular weight of the original plasmid.

#### **3.2.4.1. DNA plasmid preparation**

For a large-scale plasmid production in DH5 $\alpha$  cells, cells were grown in 400 mL LB medium overnight at 37°C with agitation. Overnight bacterial culture was harvested by centrifuging at 6000 x g for 15 min at 4°C. Plasmid DNA was isolated using Qiagen Maxi prep or NucleoBond PC500 kit according to the manufacturer's instructions. Briefly, DH5 $\alpha$  which produced the plasmid of interest were resuspended, lysed, and neutralized using the appropriate buffers. Cell lysate was cleared by centrifugation at 12 000 x g and DNA was bound on QIAGEN or NucleoBand columns. The plasmid DNA was washed and eluted from the column using the provided elution buffer and precipitated using 2-isopropanol. Precipitated DNA was pelleted by centrifugation at 12 000 x g for 45 min at 4°C, and supernatant as removed. Precipitated DNA pellet was washed in sterile 70% ethanol, centrifugated for additional 10 min at 16 000 x g, after which ethanol was removed. Air-dry pellet of ultrapure DNA was diluted in a suitable amount of nuclease-free water or TE buffer (pH 8.0), depending on the storage length. To produce a smaller amount of plasmid DNA NucleoBond PC100 Midi prep kit and Wizard Plus SV Mini prep kit were used according to the manufacturer's instructions. Bacterial cells were grown in 100 mL (Midi prep) or 20 mL (Mini prep) LB medium overnight at 37°C with agitation.

#### **3.2.4.2. Measuring of DNA concentration**

The concentration of plasmid DNA was determined using a NanoPhotometer® N60 spectrophotometer. As a blank 1  $\mu$ L of DNA elution solution (nuclease-free water or TE elution buffer) was used, while 1  $\mu$ L of sample was used to determine the concentration of nucleic acids. The concentration was determined by measuring the absorbance at 260 nm, the wavelength at which nucleic acids absorb UV light. The purity of the sample was verified by measuring the absorbance ratio at 260 and 280 nm, and 260 and 230 nm ( $A_{260}/A_{280}$  and  $A_{260}/A_{230}$ ). The  $A_{260}/A_{280}$  value for pure DNA is about 1.8. If the  $A_{260}/A_{230}$  value is from 2.0 to 2.2, it is considered that the nucleic acids are sufficiently pure.

### 3.2.5. Horizontal gel electrophoresis

An agarose gel for separation of nucleic acids was prepared by dissolving agarose in TAE buffer by heating in a microwave oven. When agarose was completely dissolved in the buffer the nucleic acid detection dye Midori Green was added. Depending on the size of the plasmid or the PCR products that were subjected to a separation with electrophoresis, different density gels (1% - 2%) were used. Samples were prepared by mixing with 5x gel loading buffer. A DNA ladder marker was loaded to determine molecular weights of nucleic acids. Electrophoresis was performed in a Wide Mini-Sub Cell GT or Sub-Cell GT device, filled with 1x TAE buffer at a constant voltage 120 V.

### 3.3. Cell culture

All cell culture work was carried out in a HEPA-filtered laminar flow hood under sterile conditions. Surface was wiped clean with 70% ethanol, while the interior and contents were sterilized using UV lamp for 15 min prior and after work.

#### 3.3.1. Cell lines

All cell lines used for this doctoral thesis are indicated and listed in **Table 17**. All of them are adherent cell lines grown *in vitro* until complete confluence. Cell lines were grown in a humidified air at constant conditions of 37 °C and 5% CO<sub>2</sub> in a cell incubator.

**Table 17. Cell lines used for this doctoral study**

| Cell line         | ATCC®         | Properties   |
|-------------------|---------------|--|
| HEK-293           | CRL-1573™     | Adenovirus-immortalized human embryonic kidney cell line         |
| E6AP-null HEK-293 | /             | CRISPR/Cas9 gRNA-mediated E6AP-null HEK-293 cell line            |
| HeLa              | CCL-2™        | HPV-18 positive cervical adenocarcinoma cell line                |
| CaSki             | CRM-CRL-1550™ | HPV-16 positive advanced cervical carcinoma epidermoid cell line |
| C33A              | HTB-31™       | HPV-negative cervical carcinoma cell line                        |
| HT1080 8 E6       | /             | Fibrosarcoma epithelial cells stably expressing HPV-8 E6         |
| H1299             | CRL-5803™     | Metastasis of small lung cancer cells                            |

HEK293 cells and CRISPR/Cas9 gRNA-mediated E6AP-null HEK-293 cells were used in overexpression assays, immunoprecipitations, GST pull-down assays, protein fractionation assays, as well as cellular proliferation assays. CaSki, HeLa and HPV-8 E6 expressing HT1080 cells were used for siRNA silencing, half-life experiments, immunofluorescence and cellular migration assays. H1299 cell line was used in immunofluorescence experiments. C33A cells were used for the co-immunoprecipitation experiment.

### **3.3.2. Maintenance of cell lines**

For cells in culture, DMEM medium was changed every two to three days. Cells were passaged when they were  $\geq 80\%$  confluent using trypsinization. First, DMEM was removed by aspiration, and afterwards cells were washed with PBS. After PBS removal, 1mL/10 cm tissue culture dish of trypsin/EDTA solution was added and cells were incubated for 1-5 min at 37°C, which was sufficient for cells to be detached completely from the dish bottom. Trypsin/EDTA was inactivated by adding 5 mL of fresh DMEM complete media. Media was pipetted gently up and down to allow breakage of formed cell clusters. If cells were intended to be kept in culture, the appropriate volume of cells needed for 1:10 dilution was transferred into new tissue culture dish and supplement with a fresh DMEM medium. Transferred cells were distributed evenly by shaking the dish back and forth, and then placed in the incubator at 37 °C and 5% CO<sub>2</sub>. Cells were counted, if intended to be seeded for further experiments.

### **3.3.3. Cell counting**

A Neubauer chamber was used to count cells after the trypsinization. Trypsinized cells were resuspended in 5 mL of DMEM medium and 10  $\mu$ L of cell suspension was applied to the cell counting chamber below the cover slip. The cells were counted in a total of 4 quadrants. The total number of cells per milliliter was counted according to the formula:

$$\text{Cell number/mL} = \frac{\text{number of calculated cells} \times \text{dilution factor}}{\text{number of counted quadrants}} \times 10^4$$

Cells were also counted by using CellDrop FL, fluorescence cell counter. Ten  $\mu\text{L}$  of trypsinized cells previously resuspended in 5 mL of DMEM medium were pipetted into the counting chamber of a spectrophotometer device, where they were counted and analyzed.

#### **3.3.4. Freezing and thawing cells**

Prior to freezing, cells were washed twice with PBS and treated with trypsin. Trypsin was inactivated by adding 5 mL of DMEM complete medium in which cells were resuspended and transferred to a sterile 15 mL conical tube. Conical tubes with cells were centrifuged for 4 min at  $4^{\circ}\text{C}$  and  $300 \times g$ , after which residual medium was removed. The cell pellet was resuspended in 1 mL of cryoprotective nutrient medium for cell freezing (FBS with 10% (v/v) DMSO). The cells were transferred into cryoprotective tubes for freezing, placed in a freezing container and stored in a freezer on  $-80^{\circ}\text{C}$  for several hours. Usage of freezing container provides the critical  $1^{\circ}\text{C}/\text{min}$  cooling rate required for successful cryopreservation of cells. After few hour cells were stored in a freezer at  $-80^{\circ}\text{C}$  for a longer period (several months at the most). For a long-term storage, more than a few months, cells were stored in liquid nitrogen.

Freshly thawed cells from cryoprotective tubes were transferred into a sterile 15 mL conical tube with 5 mL of DMEM complete medium. The cells were centrifuged at  $4^{\circ}\text{C}$  and  $300 \times g$  for 4 min, the supernatant was poured off, and the cell pellet was resuspended in DMEM complete medium and transferred into a sterile dish. A sterile dish with thawed cells was supplemented with addition 5 mL of fresh DMEM medium and placed in an incubator.

### **3.4. Cell biology**

#### **3.4.1. Transient transfection**

In this doctoral research several different methods of transient transfections were used. This included calcium phosphate transfection, as well as commercially available reagents *Lipofectamine 200* and *TurboFect*.

#### **3.4.1.1. Calcium phosphate transient transfection**

A day prior to transfection  $3.5 \times 10^5$  cells/6 cm dishes were seeded in 3 mL DMEM complete medium so that, at the time of transfection the following day, cell would be about 20-30% confluent. The following day, cell media was aspirated and replaced with fresh DMEM complete media, and transfections were carried out in 1.5 mL tube as follows: 11  $\mu$ L of  $\text{CaCl}_2$  (2.5 M) was mixed with 95  $\mu$ L of TE buffer (pH 7.6), and the specific amount of DNA depending on the experiment and the plasmid size. The mixture was resuspended carefully and added dropwise in a previously prepared 100  $\mu$ L of 2x HBS in sterile 1.5 mL tubes. The final transfection mixture was incubated for 40-45 min at room temperature (RT) and then drop-wise added on cells. Dishes were gently mixed, after which were placed in the incubator. Approximately 24 h (in some experiments 48 or 72 h) post transfection cells were harvested for various experiments. For the transfection in 10 cm plates, a day prior to transfection,  $7 \times 10^5$  cells/10 cm were seeded in 5 mL DMEM complete media, and transfections were carried out in 1.5 mL tubes with a doubled the amount of reagents that were used for the transfections in 6 cm tissue culture dishes. The following steps were the same as for transfections in 6 cm plates.

#### **3.4.1.2. Lipofectamine 2000 transfection**

A day prior to transfection  $7 \times 10^5$  cells/10 cm were seeded in 5 mL DMEM complete media so that the following day cells would be about 70-90% confluent. For each sample, transfection complexes were prepared so that DNA/lipofectamine ratio would be 1:3. In this manner 4-5  $\mu$ g DNA were diluted in serum-free DMEM medium without added supplements to make 100  $\mu$ L in total in the first 1.5 mL sterile tube. In the other 1.5 mL sterile tube, 8  $\mu$ L of *Lipofectamine 2000* were diluted in 100  $\mu$ L of serum-free DMEM media without any supplements. Mixtures were incubated separately for 5 min at RT and after the incubation time they were combined and mixed gently by pipetting. The combined mixtures were then incubated for 20 min at RT and added dropwise on cells. The plates were mixed gently, after which were left in the incubator at 37°C and 5%  $\text{CO}_2$ . The media were changed 5-6 h later when formed complexes already entered the cells, so DMEM medium without supplements were replaced with DMEM complete medium.

### 3.4.1.3. *TurboFect* transfection

Twenty-four hours before transfection with *TurboFect* transfection reagent  $3.5 \times 10^5$  cells/6 cm were seeded in 3 mL DMEM complete medium. At the time of transfection, the confluence of cells was 70-90%. The transfection reagent was prepared immediately before the transfection by diluting 6  $\mu$ g of DNA in 600  $\mu$ L of serum-free DMEM. DNA mixture and serum-free DMEM were mixed gently by pipetting and 16  $\mu$ L of *TurboFect* transfection reagent were added to the diluted DNA and mixed immediately by pipetting, after which it was incubated for 15-20 min at RT. DNA/*TurboFect* mixture was added dropwise to each dish. The plates were mixed gently, and transfected cells were incubated at 37°C with 5% CO<sub>2</sub> atmosphere in the incubator.

### 3.4.2. siRNA silencing

Transient transfection of cells with small interfering RNA molecules (siRNA) was used to silence MAML1 and UBE3A genes with the method of direct silencing on adherent cells according to the manufacturer's instructions. A day prior to transfection  $3.5 \times 10^5$  cells were seeded on 6 cm dishes and transfected the following day with ON-TARGETplus human MAML1 siRNA-SMARTpool (siMAML1) and ON-TARGETplus human UBE3A siRNA-SMARTpool (siE6AP), final concentration of used siRNA was 20  $\mu$ M. Cells were collected 72 hours after transfection and silencing was verified by western blot analysis. siRNA against luciferase (siLuc) was used as control.

**Table 18. Small interfering RNA molecules (siRNA) used to silence MAML1 and UBE3A genes**

| siRNA   | Name   | Manufacturer   |
|---------|--|----------------|
| siMAML1 | ON-TARGETplus human MAML1 siRNA-SMARTpool (5 nmol)   | Dharmacon, USA |
| siE6AP  | ON-TARGETplus Human UBE3A siRNA – SMARTpool (5 nmol) | Dharmacon, USA |
| siLuc   | Luciferase Duple (20 nmol)                           | Dharmacon, USA |

### **3.4.3. Cell migration assay**

Simple method for monitoring cell migration is the "wound healing" assay (also known as the scratch assay), which is based on monitoring the dynamics by which cells cover the gap in the monolayer of the adherent cells. The migration of the cells towards the center is monitored until the wound is closed.

#### ***3.4.3.1. Wound healing/scratch assay***

HeLa cells were seeded on a 6-well plate ( $1.2 \times 10^5$ ) three days before the monolayer wound healing/scratch assay was performed, so that on the day of the experiment they were confluent, but still in one layer. On the day after the seeding cells, HeLa cells were transfected with a control siLuc, siMAML1 and siE6AP alone or in combination. After 48 h, a scratch wound was generated in the confluent cells with a sterile Artline p2 pipette tip (Thermo Fisher Scientific, USA) by making a line to remove cells from the dish bottom. The cells were washed in PBS three times to remove detached cells and new DMEM complete medium was added. The resulting gaps, or the wounds, were photographed under a microscope using a Dino-Eye digital eyepiece camera that was connected to a computer and DinoCapture 2.0 microscope imaging software. After an additional 18 h, the wounds were photographed again. The obtained images were processed to calculate the wound closure and gap areas. The cells were then harvested by scraping, centrifuged and pellets resuspended in 2x SDS buffer. MAML1, E6AP and E6 protein levels were further analyzed by western blotting to verify the silencing.

### **3.4.4. Cell proliferation assay**

UptiBlue reagent is a non-toxic aqueous dye used to assess cell viability and cell proliferation of various cell lines. The system incorporates an oxidation-reduction indicator that fluoresces and changes color in response to chemical reduction of growth medium resulting from cell growth (metabolic activity). HEK-293 cells were seeded on 6 cm dishes ( $1.2 \times 10^5$ ), incubated overnight at 37°C with 5% CO<sub>2</sub> atmosphere and transfected the following day. The cells were transfected with pCA plasmids expressing HPV-16 E6 and HPV-18 E6, alone or in combination with MAML1, E6AP or both. Twenty-four hours post transfection, the cells were detached, counted on CellDrop FL spectrophotometer device, and seeded at  $0.5 \times 10^4$  cells per well to a final



volume of 100  $\mu$ L in a 96-well plate and incubated for a further 48 h. Cell proliferation was monitored using Uptibblue reagent, so 10  $\mu$ L of Uptibblue reagent solution (5% (v/v) in PBS) was added to the culture medium 72 h after transfection and incubated for the next 5 h in the incubator. The absorbance was measured at 575 nm and 590 nm on a Labsystems Multiskan MS 352 multiwell plate reader with accompanying Ascent Software.

### **3.4.5. Apoptosis assay**

Apoptosis was detected by staining cells with Annexin V and propidium iodide (PI) followed by flow cytometry analysis on a FACSCalibur flow cytometer (BD). Normal cells express phosphatidylserine in the inner side of the cell membrane, when the cell starts the process of apoptosis, phosphatidylserine becomes exposed on the cell surface. While the exposed phosphatidylserine is detected by Annexin V, PI stains necrotic cells, which have leaky DNA content. The pattern of Annexin V and PI staining differentiates apoptotic and necrotic cells. HeLa cells and HT1080 HPV 8 E6 cells were seeded in the concentration of  $3.5 \times 10^5$  cell in 6 cm tissue culture dish and transfected the following day with siMAML1, siE6AP or their combination. siLuc was used as a control. Seventy-two hours after transfection, cells were harvested by collecting both the supernatant (floating apoptotic cells) and by trypsinizing the adherent cells by incubation for 5-7 min with 0,2% EDTA in PBS to detach the cells. Cells were washed twice with PBS + 2% FCSB and centrifuged at  $670 \times g$  for 5 min at 4°C. Each pellet was resuspended in 400  $\mu$ L of PBS+ 2% FCSB. 100  $\mu$ l of incubation buffer with 2  $\mu$ l of FITC conjugated Annexin V (1 mg/ml) and 2 $\mu$ l of propidium iodide (1 mg/ml) were added to the cell pellet, according to the manufacturer's instructions. Three groups of control cells were used: control 1 (unstained) (400  $\mu$ l of cells + 100  $\mu$ l of incubation buffer), control 2 (Annexin V only) 400  $\mu$ l of cells + 100  $\mu$ l of incubation buffer with 2  $\mu$ l of Annexin (1 mg/ml) and control 3 (PI only) (400  $\mu$ l of cells + 100  $\mu$ l of incubation buffer with 2  $\mu$ l of PI (1 mg/ml). Samples were examined on the FACSCalibur flow cytometer immediately after staining. The data were analyzed with FCS 3 Express Flow Cytometry Software.

### 3.5. Protein analysis

#### 3.5.1. Western blot analysis

##### 3.5.1.1. *Protein isolation for western blot analysis*

All steps of cell collection and protein isolation were performed on ice and in a centrifuge precooled to 4 °C. When fully confluent, cells for protein isolation were harvested by scrapping with a sterile scraper, collected and centrifuged for 4 min at 300 × g. The supernatant was discarded and proteins for western blot analysis were isolated from cell pellets with the addition of 2x SDS Laemmli protein buffer. The cell pellet from one tissue culture dish with a diameter of 10 cm was collected in 100 µL of SDS lysis buffer. To resuspend cell clusters the isolation procedure was performed on a sonicator using an ultrasonic probe with a diameter of 1 mm at an amplitude of 80 Hz. Cell pellets were sonicated for 5 s. Proteins were stored at -80 °C until used for western blot analysis.

##### 3.5.1.2. *SDS-polyacrylamide gel electrophoresis (SDS-PAGE)*

SDS-PAGE (sodium dodecyl sulfate - polyacrylamide gel electrophoresis) is the first step in protein analysis using the western blot method. Gels for electrophoresis were prepared as shown in **Table 19**. Preparation of gels was done in two steps. In the first step, the lower part of the gel, so-called the separating gel was poured between two glass slides. In the second step, the top portion of the gel, so-called the stacking gel was poured. The comb was placed to form wells during gel polymerization. The equal amounts of protein samples were loaded into wells of the SDS-PAGE gels (approximately 25-50 µg of the total proteins were loaded), along with molecular weight protein marker. Electrophoresis was carried out in an omniPAGE vertical electrophoresis system with SDS-PAGE running buffer. The samples migrated for approximately 30 min at a voltage of 100 V in the stacking gel after which the voltage was increased to 120 V.

**Table 19. Polyacrylamide gels composition**

| Separating gel        | 7.5%  | 10%  | Stacking gel        | 4%    |
|-----------------------|-------|------|---------------------|-------|
| dH <sub>2</sub> O     | 4.7   | 3.8  | dH <sub>2</sub> O   | 3.7   |
| 1.5 M Tris-HCl pH 6.8 | 3     | 3    | 1.5MTris-HCl pH 6.8 | 0.65  |
| 30% Acrylamide        | 2.6   | 3.5  | 30% Acrylamide      | 0.8   |
| 10% SDS               | 0.1   | 0.1  | 10% SDS             | 0.05  |
| 10% APS               | 0.15  | 0.07 | 10% APS             | 0.05  |
| TEMED                 | 0.003 |      | TEMED               | 0.005 |

### **3.5.1.3. Protein transfer to nitrocellulose membrane**

Nitrocellulose membrane with a pore size of 0.22  $\mu\text{m}$ , 3 mm Whatmann papers and sponges were soaked in 1x transfer buffer prior to assembly of the transfer cassette. After SDS-PAGE, gels were removed from the tank into the prepared transfer cassette. WB cassette was placed into a transfer tank and proteins were transferred to a membrane overnight at the constant voltage of 20 V in an omniPAGE transfer system.

### **3.5.1.4. Immunoblotting**

After the protein transfer, membranes were stained with Ponceau S solution for a few minutes to visualize protein bands as a confirmation that the protein transfer was successful. The Ponceau S-stained membranes were rinsed with several washes in distilled water until membrane became clear from the red Ponceau staining. Membranes were blocked in 10% dry milk in PBST or TBST, for 30 min at 37°C with constant agitation. After blocking membranes were incubated with the indicated primary antibodies diluted in 10% milk in PBST or TBST (for 2h at RT or overnight at 4°C) with gentle agitation so that antibody was evenly distributed over the membrane. Membranes were washed in PBST or TBST (3 x 10 min), each with gentle rocking and then incubated for 1h with HRP-linked secondary antibodies (anti-rabbit 1:1000 or anti-mouse 1:1000), after which antibodies were washed again in 1x PBST or TBST. The signals were developed either with SuperSignal™ West Pico PLUS Chemiluminiscent Substrate or Amersham ECL Western Blotting Detection Reagents and detected by Uvitec Alliance 4.7 or Uvitec Alliance Q9 Mini imaging systems. If required, antibodies were detached from membrane using with 0.2 M NaOH solution in PBS for 20 min after which membranes were blocked in 10% dry milk and re-probed.

## **3.5.2. Half-life experiments**

HeLa cells and HT1080 HPV-8 E6 expressing cells were transfected with siLuc - control, siMAML1 and siE6AP alone or in combination. Seventy-two hours later, prior to harvesting, cells were treated with cycloheximide which was added in fresh DMEM medium. The cells were harvested at different time points (0, 30, 60, 90, 120 min) and analyzed by western blot. Control cell were treated with DMSO.

### **3.5.3. Immunoprecipitation**

#### ***3.5.3.1. Protein isolation for the immunoprecipitation assay***

When fully confluent, cells were harvested by scrapping with a sterile scraper, collected in a sterile tube and centrifuged for 4 min at  $300 \times g$ . For the immunoprecipitation analysis using anti-FLAG and anti-HA agarose beads proteins were isolated from the cell pellet using a 300  $\mu$ L of precooled E1A lysis buffer with added protease inhibitors that enabled the preservation of the protein interactions. Protease inhibitor Cocktail Set I was added to the isolated proteins in 1:100 dilution. For the co-immunoprecipitation assay using magnetic beads, proteins were isolated from the cell pellet using a 300  $\mu$ L of a low salt dilution buffer (LSD).

Cell pellets were resuspended on ice and collected protein samples were subjected to sonification, using an ultrasonic probe with a diameter of 1 mm at an amplitude of 80 Hz for 1 sec. After the sonification, samples were left on ice for 20 min and protein isolation was obtained by centrifugation for 20 min at  $16,000 \times g$ . After the centrifugation proteins were isolated in the supernatant, which was then transferred to a new sterile tube and could be stored at  $-80^\circ\text{C}$  or used immediately for co-immunoprecipitation assay.

#### ***3.5.3.2. Immunoprecipitation using anti-FLAG and anti-HA agarose beads***

Some of the immunoprecipitation experiments were performed using anti-FLAG agarose beads, while in the other experiments anti-HA agarose beads were used. Twenty  $\mu$ L of resuspended agarose beads were washed three times with 1 mL of E1A buffer followed by a centrifugation for 4 min at  $300 \times g$  between each wash. This step is used to equilibrate the beads in the immunoprecipitation buffer, whereby the agarose resin remains as the precipitate, and the remaining supernatant was discarded by aspiration. Protein lysates isolated as described previously (chapter 3.5.3.1.) were mixed with prewashed anti-FLAG or anti-HA agarose beads. Ten percent (v/v) of protein lysates were collected as an input for each sample. Inputs were transferred to a new 1.5 mL tube, mixed with 30  $\mu$ L of 2x SDS Laemmli lysis buffer, boiled for 10 min at  $95^\circ\text{C}$  and stored in a freezer at  $-80^\circ\text{C}$  until the samples were used for SDS-PAGE and western blot analysis. Meanwhile, tubes with agarose beads mixed with protein lysates were incubated on a rotating wheel for 2h at RT or overnight at  $4^\circ\text{C}$ . This was followed by centrifugation for 4 min at  $300 \times g$  to pellet the beads. The precipitated immunocomplexes on beads were washed three times with 1 mL of E1A buffer, and centrifuged for 4 min at  $300 \times g$ , between each wash. After the third

wash, supernatant was completely discarded and 40  $\mu\text{L}$  2x SDS Laemmli lysis buffer was added to each sample, and gently pipetted to resuspend the agarose beads. The samples were heated for 10 min at 95  $^{\circ}\text{C}$  and separated on and SDS-page together with input samples.

### **3.5.3.3. Immunoprecipitation using magnetic beads**

C33A cells were transfected with pXJ41-FLAG or pXJ41:16E6-FLAG plasmid and harvested 48 h post transfection. Protein isolation was done as described in a chapter 3.5.3.1. For the co-immunoprecipitation using magnetic beads coupled to the antibody, the magnetic beads were first had to be bound to the anti-FLAG M5 antibody. Therefore, the beads were resuspended in LSD buffer by vortexing, after which 50  $\mu\text{L}$  of beads were transferred into a new sterile tube. The beads were separated from the LSD buffer on the magnetic stand and the supernatant was removed by aspiration. Two  $\mu\text{g}$  of anti-FLAG M5 antibody diluted in 200  $\mu\text{L}$  of PBS with 0.02% (v/v) Tween-20 was added to the beads and incubated on a shaker for 40 min at RT. Using a magnetic stand, the beads were separated, and the supernatant discarded by aspiration. The beads coupled with anti-FLAG M5 antibody were washed three times in 500  $\mu\text{L}$  of LSD buffer by gentle pipetting and the supernatant was separated again using the magnetic stand and aspiration between each wash. The samples of isolated proteins for each sample were added to magnetic beads coupled to the anti-FLAG M5 antibody and gently resuspended by pipetting. The samples were incubated for 2h at RT using rotating wheel. The beads were separated on a magnetic stand and the supernatant was removed to a new sterile tube as an input sample to determine the binding of protein of interest to the antibody. The magnetic beads were washed three times using 500  $\mu\text{L}$  of LSD buffer and separated on a magnetic stand between each wash. After the third wash, the supernatant was discarded, and the beads were resuspended in 100  $\mu\text{L}$  of LSD buffer and transferred to a new sterile tube to avoid co-elution of proteins attached to the tube wall. The magnetic beads from the new sterile tube were separated on a magnetic stand, supernatant was discarded and 20  $\mu\text{L}$  of elution buffer was added to the beads and heated for 10 min at 95  $^{\circ}\text{C}$ . Prepared samples were separated on SDS-polyacrylamide (SDS-PAGE) gel and co-precipitated cellular proteins were detected by western blotting with anti-MAML1 and anti-FLAG antibodies, as well as with anti-GAPDH-Alexa Fluor 680 which was used as a loading control. Immunoreactive proteins were visualized using IRDye-coupled secondary antibodies and a LICOR Odyssey Fc imaging system.

### 3.5.4. GST pull-down

#### 3.5.4.1. *GST fusion protein production and purification*

DH5 $\alpha$  *Escherichia coli* competent cells were transformed with GST-E6 constructs (GST-16 E6, -18 E6, -11 E6, -8 E6 and GST-16 E6L83V, -16 E6D25N, -16 E6D25N L83V) described in a chapter 3.2.1. To produce GST fusion proteins, 100  $\mu$ l of bacterial glycerol stock was used to inoculate 40 mL of LB medium with antibiotic (ampicillin antibiotic was used, depending on an antibiotic resistance gene in a plasmid sequence) and grown overnight at 37°C with constant shaking. The following day overnight the bacterial culture was transferred to a freshly prepared 400 mL of LB medium containing ampicillin at the final concentration of 75  $\mu$ g/mL and incubated at 37°C with shaking, until OD<sub>600</sub> was 0.5-0.6. OD<sub>600</sub> value was determined using a NanoPhotometer® N60 spectrophotometer. As a blank 1  $\mu$ L of LB medium was used, while 1  $\mu$ L of inoculated bacterial sample was used to determine OD<sub>600</sub>. At this point to the bacterial culture isopropyl- $\beta$ -D-thiogalactopyranoside (IPTG) was added to a final concentration of 1mM, and the suspension was further incubated on a shaker at 30°C (optimal temperature to produce E6-fusion proteins) for additional 3-5 h. The bacterial culture was harvested for 15 min at 7000 x g. The supernatant was discarded, while the bacterial pellet was resuspended in 10 mL of ice-cold PBS with 1% (v/v) Triton X-100 and transferred to a 30 mL conical tube. The bacteria were sonicated using an ultrasonic probe with a diameter of 1 mm at an amplitude of 80 Hz on ice, 2 x 30 s with at least 30 s pause between pulses and centrifuged for 15 min at 7 000 x g. The supernatant was transferred to a new 15 mL tube. Meanwhile, glutathione-S-transferase agarose beads were rehydrated in ice-cold PBS. Prepared 300-500  $\mu$ L of rehydrated beads were combined with bacterial supernatant and incubated overnight at 4°C on a rotating wheel. The following day, the beads were centrifuged at 4°C for 4 min at 825 x g and washed with ice-cold PBS with 1% (v/v) Triton X-100. The washing step was repeated three times. After the third wash, the supernatant was completely removed using a Hamilton needle and 20  $\mu$ L of 2x SDS Laemmli lysis buffer was added on GST bound agarose beads. Samples were incubated for 10 min at 95°C. Prepared samples were separated on SDS-PAGE to verify the purity, molecular size and the amount of produced protein. This was done by staining the polyacrylamide gel with Coomassie Brilliant Blue stain. The amount of produced GST fusion proteins for GST-pull-down assays were balanced depending

on the results of stained gels. The rest of GST-fusion protein beads were resuspended in 2-3 mL of cold PBS with 1% (v/v) Triton X-100 and 20% (v/v) glycerol, and stored at -80°C.

#### **3.5.4.2. GST pull-down assay**

The pre-cleared whole cell lysates of HEK-293 cells and E6AP-KO HEK293 cells (transfected a day before) were collected, and proteins were extracted in modified E1A buffer, as described in the chapter 3.5.1.2. From the prepared protein extracts, 10% (v/v) of each sample was transferred in a new 1.5 mL tube to serve as an input. After preparing the inputs, an equalized amount of GST bound agarose beads were prepared and washed three times with E1A buffer. Between each wash, samples were centrifuged for 4 min at 300 x g. After the last wash, using a Hamilton needle, the supernatant was removed from the beads, and the beads were incubated with protein lysates overnight at 4°C (or 2 hours at RT) on a rotating wheel. The following day beads were centrifuged for 4 min at 300 x g and washed three times with E1A buffer. Using Hamilton needle the supernatant was again removed from the beads, followed by addition of appropriate amount of 2x SDS Laemmli loading buffer. The beads were resuspended well and boiled for 10 min at 95 °C. The bound proteins were detected using SDS-PAGE and western blotting with appropriate antibodies.

#### **3.5.5. Cell fractionation assays**

For cell fractionation analyses, HEK-293 cells were seeded on 10 cm dishes at a density of  $7 \times 10^5$  prior to transfections. Twenty-four h post transfection the cells were collected by scraping and fractionated into 4 fractions: cytoplasmic (F1), membrane/organelle (F2), nuclear (F3) and cytoskeletal (F4) using the ProteoExtract Cell Fractionation Kit according to the manufacturer's instructions. Cells were collected and washed carefully with cold PBS, resuspended in 600  $\mu$ L of Wash buffer, transferred to a sterile tube, incubated 5 min on ice and centrifuged for 10 min at 300 x g at 4°C. Cell pellets were resuspended in 300  $\mu$ L of Extraction buffer I with 1.5  $\mu$ L Protease Inhibitor Cocktail set I and incubated for 10 min on ice. The suspensions were centrifuged for 10 min at 1000 x g at 4°C and supernatants (F1) were collected in new tubes. The remaining pellets were resuspended in 300  $\mu$ L of Extraction Buffer II with 1.5  $\mu$ L Protease inhibitor Cocktail Set I and incubated for 10 min on ice. The suspensions were centrifuged for 10 min at 6000 x g at 4°C

and supernatants (F2) were collected in new tubes. Cellular pellets were then resuspended in 150  $\mu$ L of the Extraction Buffer III with 1.5  $\mu$ L of Protease Inhibitor Cocktail Set I and incubated for 10 min on ice. These were again centrifuged for 10 min at 6800 x g and 4°C, and the supernatants (F3) were collected in new tubes. The remaining cell pellets were resuspended in 150  $\mu$ L Extraction Buffer IV with 1.5  $\mu$ L Protease Inhibitor Cocktail set I and stored as F4. The fractions were analyzed by SDS-PAGE followed by western blot analysis using anti-HA antibody, anti-MCM7 antibody (clone 141.2), anti-GAPDH antibody, anti-histone H3 antibody (clone D1H2) and anti-vimentin antibody (clone E5) with appropriate anti-mouse secondary antibody.

### 3.5.6. *In vitro* degradation assay

Target proteins were transcribed and translated *in vitro* in rabbit reticulocyte lysate using the TnT® Quick Coupled Transcription/Translation Systems according to the manufacturer's instructions. This system provides eukaryotic cell-free protein expression and *in vitro* translation combining RNA polymerase, nucleotides, amino acids and rabbit reticulocyte lysate solution. To use these cell-free protein expression system, 1  $\mu$ g of plasmid DNA containing a T7 promoter was added to an aliquot of RNA polymerase, nucleotides, amino acids and rabbit reticulocyte lysate mixture (TNT® T7 Master Mix) and incubated in a 50  $\mu$ L reaction volume for 90 minutes at 30°C.

**Table 20. Reaction components for *in vitro* protein transcription/translation**

| <b>Components</b>   | <b>Reaction</b>                 |
|---|---------------------------------|
| Rabbit reticulocyte lysate  | 25 $\mu$ L                      |
| TNT® Buffer   | 2 $\mu$ L                       |
| Amino acids (without methionine and cysteine)   | 1 $\mu$ L                       |
| RNA polymerase T7   | 1 $\mu$ L                       |
| RNAse inhibitor   | 1 $\mu$ L                       |
| [ <sup>35</sup> S] methionine (1,000Ci/mmol)/ or [ <sup>35</sup> S] cysteine (1,000Ci/mmol) | 1 $\mu$ L                       |
| Plasmid DNA   | 1 $\mu$ g                       |
| Nuclease-Free Water   | to a final volume of 50 $\mu$ l |

E6 translation, target protein translation (p53, DLG1, MAGI-1 and Scrib) and a control translation was set up. HPV-16 E6, -16E6D25N, -16E6L83V, -16E6D25N-L83V proteins were radiolabeled with [<sup>35</sup>S] cysteine, while their protein partners p53, DLG1, MAGI-1 and Scrib were



labeled with [<sup>35</sup>S] methionine. A control sample was translated using water-primed lysate (WTP) and radiolabeled with [<sup>35</sup>S] cysteine.

For the analysis of transcribed/translated proteins, 2 μL aliquots were analyzed by SDS-PAGE and autoradiography. Dried SDS-PAGE gels were quantitated by phosphorimager using the Cyclone Plus storage phosphor system and analyzed using the OptiQuant software.

After the successful cell-free expression, degradation assays were performed by setting up reaction tubes with the samples of mutant E6 proteins (HPV-16 E6, -16E6D25N, -16E6L83V, -16E6D25N-L83V), and combined with their target protein partners (p53, DLG1, MAGI-1 and Scrib). Based on the quantification, *in vitro* translated target proteins (p53, MAGI-1 and Scrib) were mixed at a ratio 1:3 with the wild type or mutant E6 proteins (in the case of DLG1 the ratio was 1:5 with E6s). All volumes were equalized with the water-primed lysate and incubated at 30°C. At the different time points (0, 30, 60 and 90 min) aliquots were collected and analyzed by SDS-PAGE and autoradiography. Dried SDS-PAGE gels were quantitated again by phosphorimager using the Cyclone Plus storage phosphor system and analyzed using the OptiQuant program.

### **3.6. Confocal microscopy**

For the immunofluorescence assay HeLa, HT1080 8 E6 and H1299 cells were seeded on sterile cover slips placed in 6-well plates and transfected the following day (siRNA silencing in the case of HeLa and HT1080 8 E6 cells). Seventy-two hours (for H122 cell 24 h) post transfection, the DMEM complete medium was removed, and cells were washed with PBS. Cells were then fixed by using 4.7% (v/v) paraformaldehyde (PFA) solution in PBS for 20 min at RT. After fixation cell were washed in PBS three times, and permeabilized with PBS solution containing 0.1% (v/v) Triton X-100 for 5 min at RT, which was again followed by washing with PBS. After permeabilization, cells were incubated in PBS solution with added 0.1 M glycine for 30 min at RT and washed again. Fixed cells were incubated with primary antibodies diluted in PBS (1:100 dilution) overnight at 4 °C in a humidified chamber. The next day, cells were gently washed with PBS three times, and incubated with fluorescently conjugated mouse or rabbit secondary antibodies (diluted 1:700 in PBS) for 30 min at 37°C. Final washing, after the incubation in secondary antibodies was done by using a distilled water, again repeating it for three times. Cover slips were mounted facing down on a glass slide. The mounting medium contained DAPI, a

fluorescent dye for the DNA labeling. Cell images were taken by Leica TCS SP8 X laser scanning confocal microscope equipped with an HC PL APO CS2 63×/1.40 objective with oil immersion, laser diode at 405 nm and a supercontinuous excitation laser with emission in the range 470-650 nm. Secondary antibodies conjugated with fluorophores included: Rhodamine Red and Alexa Fluor 488 for HeLa and HT1080 8 E6 cells, and fluorescein isothiocyanate (FITC) and Alexa Fluor 488 for H1299 cells. The excitation wavelengths and the detection wavelength range were: 490 nm and 500-550 nm for FITC, 540nm and 570-590 nm for Rhodamine Red, 490nm and 500-550nm for Alexa-488, 405 nm and 430-500 nm for DAPI.

### 3.7. Statistical analysis

All experiments were repeated at least three times and one representative result is shown in the figures. For the western blot experiments results were quantified by ImageJ program. E6 band intensity was first normalized with the image background after which it was divided with the value of normalized  $\beta$ -galactosidase (LacZ), which served as transfection control. The average normalized relative expression of E6 of at least three experiments where E6 was transfected alone, was taken as control. All normalized relative expressions of E6 (transfected alone or with MAML1 or E6AP) were expressed as fold changes in respect of the control E6. In some experiments, the LOG2 of these fold changes was calculated to better depict the increase or decrease in protein amounts. The same procedure was applied in experiments with p53, DLG1 and MAGI-1 overexpression. Data were analyzed by GraphPad Prism or MedCalc software.

For wound healing/scratch assay gap areas were measured using the MRI wound healing tool macro from ImageJ software (NIH, USA) ([http://dev.mri.cnrs.fr/projects/imagej-macros/wiki/Wound\\_Healing\\_Tool](http://dev.mri.cnrs.fr/projects/imagej-macros/wiki/Wound_Healing_Tool)). The results were presented as a percentage of the closed area using GraphPad Prism. For the cell proliferation assay the results were expressed as a percentage of the reduced Uptibblue reagent with the indicated standard error of the mean (SEM) using GraphPad Prism. *In vitro* degradation assays were quantitated using the Cyclone Plus storage phosphor system and analyzed using the Opti Quant program. The mean % degradation at the end of each assay was calculated, taking the target protein at the initial time point (0 min) to be 100% degradation, with the indicated standard deviation (SD).

The differences and their statistical significance between groups were determined by one-way ANOVA or Student's T-test. P values of under 0.05 were considered significant (\*), under 0.01 very significant (\*\*) and under 0.001 extremely statistically significant (\*\*\*), which is a standard way of presenting results in biology if statistical significance wants to be stratified. All values are averages of at least three independent experiments and the standard error of the mean is depicted as error bars. The number of stars associated with the p-value is shown in **Table 21**.

**Table 21. The significance of the number of stars on the displayed results**

| <b>Number of stars</b>                    | <b>P values</b> |
|---|-----------------|
| Significant (*)                           | <0.05           |
| Very significant (**)                     | <0.01           |
| Extremely statistically significant (***) | <0.001          |

## 4. RESULTS

### PART I Oncogenic potential of naturally occurring HPV-16 E6 variants

Many different HPV-16 E6 variants are isolated from the patients located at various geographical regions. Their main characteristics are reflected in the differences in their abilities to cause malignant transformation of the epithelial cells. Some of these variants are more frequently found in cancers, implying some likely very important differences in their oncogenic potentials to drive malignant progression. The molecular mechanisms responsible for increased cancer risk of a number of HPV-16 variants are however still poorly defined. The focus of the first part of this doctoral research was biochemical and mechanistic analyses of three intra-type genetic variants of HPV-16 E6, that included HPV-16 E6 D25N, E6 L83V and E6 D25N L83V, with a purpose of revealing how those two amino acid mutations might be involved in cancer development.

#### 4.1. Generation of HPV-16 E6 mutants using site-directed mutagenesis

To address various questions related to the functions and cellular pathways modulated by HPV-16 E6 mutants, the first step was to generate plasmids expressing HPV-16 E6 mutants using site-directed mutagenesis. To create desired targeted changes in double-stranded plasmid DNA, specifically designed oligonucleotide primers were utilized for this purpose. The pCA:16E6D25N, 16E6L83V, 16E6D25NL83V and pGEX-2T:16E6D25N, 16E6L83V, 16E6D25NL83V plasmids were constructed using pCA:16E6 and pGEX-2T:16E6 vectors as templates. pCA:16E6 plasmid is an expression vector with pCDNA3 backbone created by the insertion of two HA and a FLAG epitope into the multiple cloning site of a pcDNA3 plasmid, that contains gene sequence of the reference wild-type HPV-16 E6 gene. pGEX-2T vector is used for expression of GST-fusion proteins. The mutagenesis was done using a modified protocol of the PCR mutagenesis kit. The process involved using pcDNA3:16E6 and pGEX2-T:16E6 vectors and two primers designed in an overlapping orientation, so that their sequences contain a sequence of the desired point mutation which had to be incorporated in the plasmid sequence. All the constructs were verified by DNA sequencing and alignments are shown in **Figure 14**. The obtained results were analysed using BioEdit software to confirm if the specific nucleotide mutations occurred at the desirable locations in the gene sequence of pCA:16E6 and pGEX-2T:16E6 plasmids. In this way it was also verified that no other unspecific mutations have occurred during the mutagenesis process.

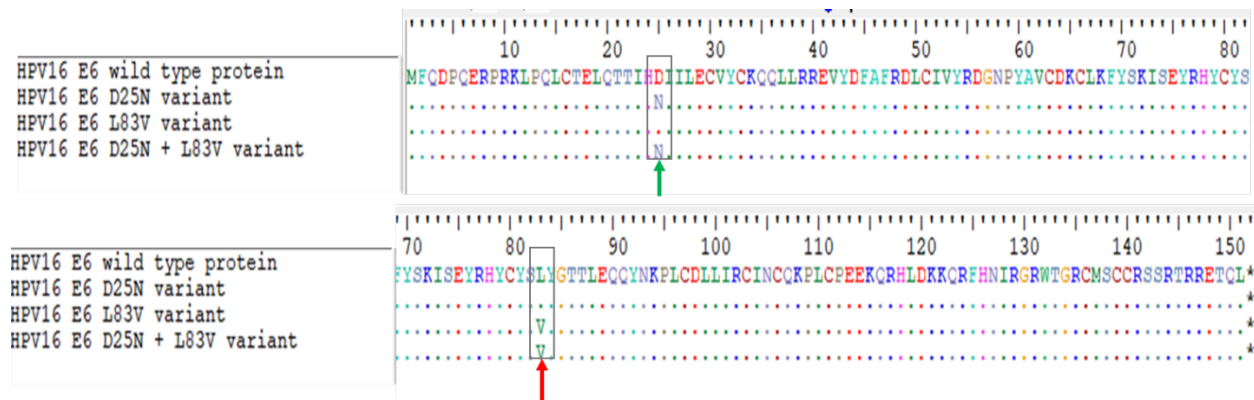


**Figure 14. DNA sequence alignment analysis after performing site directed mutagenesis using pCA:16E6 and pGEX-2T:16E6 plasmids as templates.** The expression vectors pCA:16E6L83V, pCA3:16E6D25N and pCA:16E6D25NL83V were generated through site directed mutagenesis using a pCA:16 E6 as a template. The pGEX-2T:16E6L83V, pGEX-2T:16E6D25N and pGEX-2T:16E6D25NL83V plasmids expressing GST-16E6 variant fusion proteins were constructed using pGEX-2T:16E6 as a template. The constructs were verified by DNA sequencing and analysed using BioEdit software to confirm the specific nucleotide changes in the gene sequences of pCA:16E6 and pGEX-2T:16E6 plasmids (alignment analysis is not depicted). The alignments of the three newly generated mutant gene sequences (HPV-16 E6 D25N, 16 E6 L83V and 16 E6 D25N L83V) from the pCA:16E6 plasmid are shown. Arrows point towards the sites of point mutations in 16 E6 gene sequence (D25N and L83V).

#### 4.2. HPV-16 E6 D25N L83V variant exhibits increased capacity to interact with E6AP

Previous studies have shown that E6AP ubiquitin ligase is a critical interacting partner of HPV E6 oncoproteins responsible for its protein stability and various degradatory activities (Tomaić, Pim, and Banks 2009a; M. Scheffner et al. 1993). Furthermore, it was also shown that the intensity of the interaction between various E6 oncoproteins and E6AP may vary (Huibregtse, Scheffner, and Howley 1993c). Therefore, the initial aim was to investigate the potential of newly generated HPV-16 E6 D25N, 16 E6 L83V and 16 E6 D25N L83V mutants to interact with E6AP. A method employed to investigate these interactions was a GST pull-down assay, which is a well-established technique for studying protein interactions. using GST-fusion proteins produced in DH5α *Escherichia coli* competent cells as described in Materials and Methods section. Briefly, confluent HEK-293 cells were lysed in E1A buffer to obtain the whole cell protein lysates that were then used for GST pull-down experiments with GST-fused 16 E6 oncoproteins. The GST

pull-down assay included GST:16E6, GST:16E6L83V, GST:16E6D25N, and GST:16E6D25NL83V, while GST alone was used as a control. The protein complexes were separated on SDS-PAGE, subjected to the western blot analysis and the levels of endogenous E6AP bound to GST-fusion proteins were detected using anti-E6AP antibody. As shown in **Figure 15A**, in this experimental setting, it was observed that all E6 mutant proteins were able to interact with endogenous E6AP. Interestingly, GST:16E6D25NL83V interaction with E6AP was decisively the strongest, followed by GST:16E6L83V, while GST:16E6D25N and GST:16 E6 exhibited weaker, but still evident interactions (**Figure 15A**).

HEK-293 cells that were used in the above-described GST pull-down assay endogenously express functional cellular E6AP. To undoubtedly confirm that the increased levels of the interaction between 16 E6 D25N L83V and E6AP observed in HEK-293 cells were indeed the consequence of E6/E6AP interaction, and not dependent on some other unspecific endogenous effects, it was necessary to include an additional cell line with impaired expression of E6AP. For this reason, CRISPR/Cas9 gRNA-mediated E6AP-null HEK 293 cells (E6AP knock-out; E6AP KO) (Thatte and Banks 2017) were included to verify the observed phenotype (**Figure 15B**). Hence, to investigate GST:16E6D25NL83V and E6AP interaction in more detail, an additional GST pull-down assay was performed by using HEK-293 E6AP KO cells transfected with FLAG-tagged E6AP plasmid. Again, GST:16E6, GST:16E6L83V, GST:16E6D25N and GST:16E6D25NL83V fusion proteins immobilized on glutathione agarose were incubated with HEK-293 E6AP KO cell lysates, while GST alone was used as a control. The proteins were separated on SDS-PAGE and the bound complexes were further analyzed by western blotting using anti-FLAG antibody to detect bound ectopically expressed E6AP. The results are shown in **Figure 15B**, and clearly demonstrate the same pattern of interactions as observed in **Figure 15A**. All analyzed 16 E6 mutants formed a complex with E6AP, yet the preferred interacting partner was again 16 E6 D25N L83V. All of this suggests that the observed effects were due to the interactions between the E6 oncoproteins and E6AP, rather than being mediated by other cellular factors. Furthermore, it also appears that these two mutations present in the same protein have an impact on the strength of interaction.

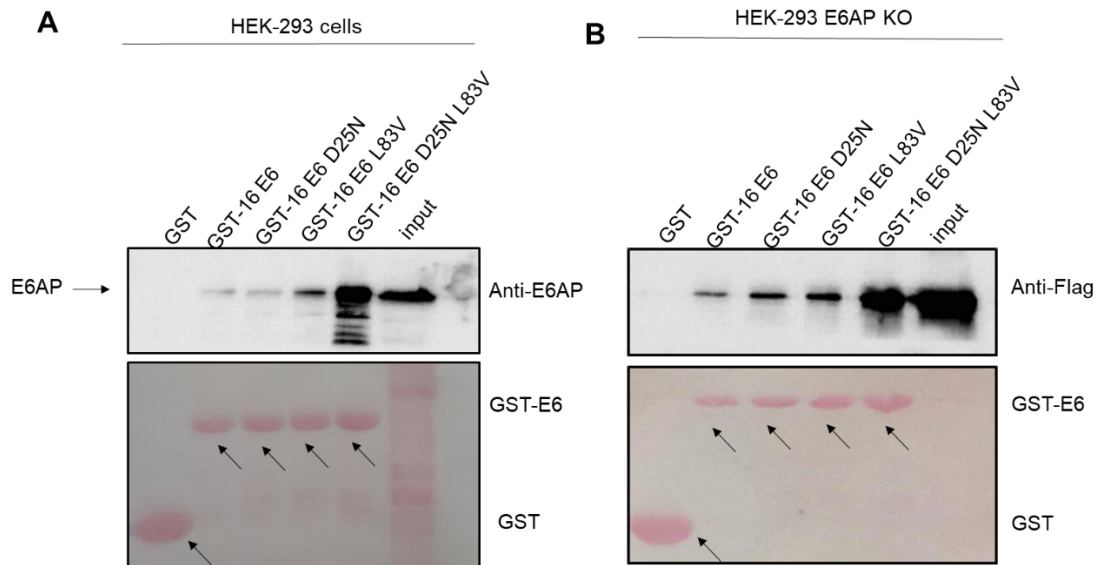


**Figure 15. HPV-16 E6 D25N L83V variant exhibits an increased capacity to interact with E6AP.** (A) GST pull-down assay was performed by incubating GST:16E6, GST:16E6L83V, GST:16E6D25N and GST:16E6D25NL83V fusion proteins immobilized on glutathione agarose with the whole cell lysates of HEK 293 cells. GST alone was included as a control. Bound complexes of E6AP and GST-fusion proteins were detected by western blot analysis using anti-E6AP antibody and compared to the amount of E6AP present in the input sample. (B) GST pull-down assay was performed by incubating GST:16E6, GST:16E6L83V, GST:16E6D25N and GST:16E6D25NL83V fusion proteins with the whole cell lysates of HEK 293 E6AP KO cells transfected with FLAG-tagged E6AP plasmid. GST alone was included as a control. Bound complexes of E6AP and GST-fusion proteins were detected by western blot analysis using anti-FLAG antibody and were compared to the amount of ectopically expressed FLAG-tagged E6AP present in the input sample. The lower membranes show the molecular weight and amounts of purified GST-fusion proteins visualized by Ponceau staining.

#### 4.3. The interaction between HPV-16 E6 D25N L83V and E6AP leads to an increase in E6AP degradation

Revealing of this novel interaction between 16 E6 D25N L83V and E6AP, and a confirming that 16 E6 D25N L83V is the preferred interacting partner provided a solid base to pursue this research further. As previously elaborated, the stability of E6 oncoproteins strictly depends on the presence of E6AP (Tomaić, Pim, and Banks 2009a), which is necessary for maintaining the optimal E6 proteins levels required for various E6 cellular activities (Miranda Thomas et al. 2013b). Interestingly, one of the consequences of this interaction is increased polyubiquitination of E6AP, which ultimately triggers its degradation.

After conducting the binding experiments and observing differences in the interaction capacity of the panel of 16 E6 mutants with E6AP, the next step was to perform a degradation assay to determine whether the stronger E6/E6AP interaction might also result in an increased capacity to change E6AP turnover and subsequent E6-mediated E6AP degradation. To address this, HEK-293 E6AP KO were co-transfected with FLAG-tagged E6AP and HA-tagged wild type 16 E6, as well as with HA-tagged 16 E6 D25N, 16 E6 L83V and 16 E6 D25N L83V mutants (**Figure 16**). To investigate whether the expression levels of E6AP protein turnover is dependent on the concentration of E6 oncoprotein, varying amounts of 16 E6 plasmids (3 and 5  $\mu\text{g}/\mu\text{L}$ ) were transfected into cells. After 24 hours the cells were harvested, and the cell lysates were analysed by SDS-PAGE and western blotting using anti-FLAG antibody to detect E6AP. As can be seen from **Figure 16**, the obtained result demonstrates that the highest capacity to change E6AP turnover of ectopically expressed FLAG-E6AP is observed in the presence of HPV-16 E6 D25N L83V variant, compared with either 16 E6 prototype or D25N and L83V E6 variants.

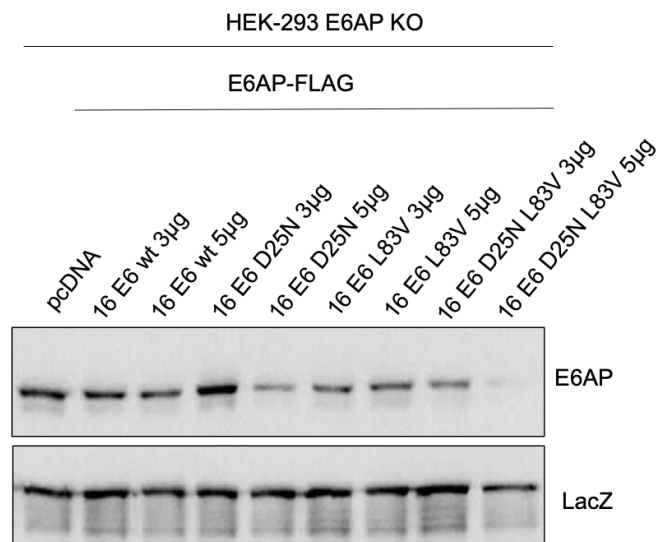


**Figure 16. HPV-16 E6 D25N L83V variant exhibits an increased capacity to induce E6AP degradation.** HEK-293 E6AP KO were transfected with FLAG-tagged E6AP alone or in combination with HA-tagged wild type 16 E6, HA-tagged 16 E6 D25N, 16 E6 L83V and 16 E6 D25N L83V (3 and 5  $\mu\text{g}/\mu\text{L}$  plasmid concentrations). After 24 hours the cells were harvested, proteins isolated and analysed by SDS-PAGE and western blotting. Anti-FLAG antibody was used to detect E6AP, while  $\beta$ -galactosidase (LacZ) was used as control to monitor transfection efficiency and loading.



Moreover, it was also found that the degree of E6AP degradation was dependent on the concentration of ectopically expressed E6 proteins. In all the samples, the increase in E6 concentration led to a more efficient degradation of E6AP. Interestingly, the highest degree of E6AP degradation was observed in cells co-transfected with E6AP and 5  $\mu\text{g}/\mu\text{L}$  of 16 E6 D25N L83V. This result is consistent with the results from the GST pull-down assays, clearly indicating that HPV-16 E6 D25N L83V variant exhibits the strongest interaction with E6AP, which is further reflected in the increased levels of E6AP degradation. Furthermore, the result also suggests that both D25N and L83V mutant induced E6AP degradation was somewhat less effective, possibly due to their decreased binding capacities observed from the GST pull-down assays.

#### **4.4. HPV-16 E6 D25N L83V is rapidly turned over at the proteasome**

Furthermore, after finding that 16 E6 D25N L83V mutant exhibits the strongest interaction with E6AP, in comparison with wild-type 16 E6 and the corresponding mutants, which consequently impacts the degree of E6AP protein turnover, the following step was to assess how this might reflect upon 16 E6 protein stability. To address this, HEK-293 cells were transfected with a plasmid expressing either HA-tagged wild type 16 E6 or HA-tagged 16 E6 D25N, E6 L83V and E6 D25N L83V mutants. After 24 hours cells were harvested, isolated proteins separated on SDS-PAGE and analyzed by western blotting. E6 protein levels were detected with HRP-conjugated anti-HA antibody, while anti- $\beta$ -galactosidase (LacZ) was used as a control to monitor transfection efficiency and loading. **Figure 17A** illustrates that the protein levels of 16 E6 D25N L83V were increased in comparison to both wild type 16 E6 and the other analyzed mutants. Interestingly, it was also noticed that the 16 E6 D25N mutant is less stable when overexpressed in HEK-293 cells, which suggests that possibly the L83V mutation in combination with D25N mutation might be responsible for the increased E6 protein stability.

The following step was to assess if the observed increased stability of D25N L83V mutant reflects its protein turnover. To assess this, cycloheximide chase assay was performed to examine the double mutant half-life. HEK-293 cells were transfected with plasmids expressing HA-tagged wild type 16 E6 or HA-tagged 16 E6 D25N L83V mutant. Twenty-four hours post transfection protein synthesis was blocked by the cycloheximide inhibitor to determine the rate of E6 protein turnover in a cellular condition when novel protein synthesis is abolished. The cells were collected

at different time points (0, 30, 60 and 90 min), isolated proteins were separated on SDS-PAGE and detected by western blot analysis using HRP-conjugated anti-HA antibody to detect wild-type 16 E6 and the mutant forms.

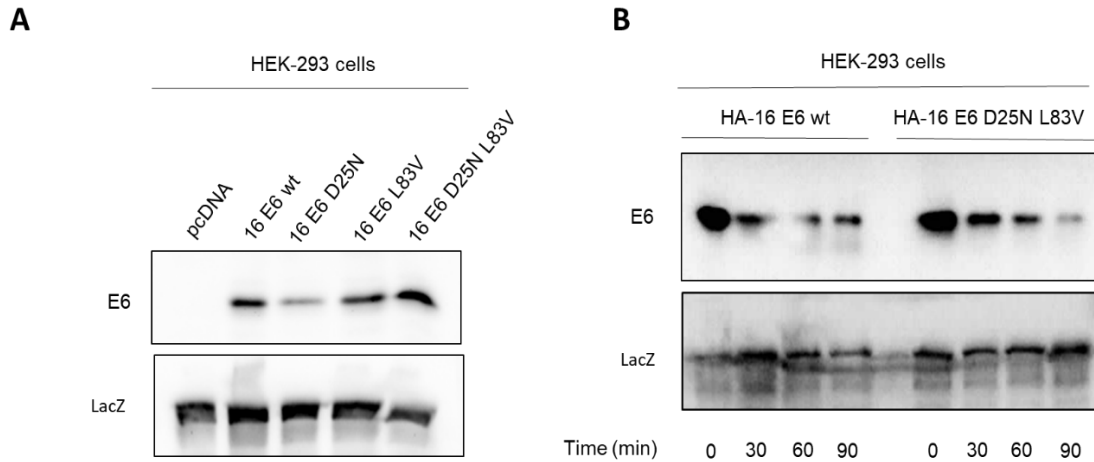


**Figure 17. HPV-16 E6 D25N L83V exhibits higher protein levels, but shorter protein half-life.** (A) HEK-293 cells were transfected with either HA-tagged wild type HPV-16 E6 or HA-tagged 16 E6 D25N, E6 L83V and E6 D25N L83V mutants. After 24 hours cells were harvested, proteins isolated and cell lysates separated on SDS-PAGE and analyzed by western blotting. E6 protein levels were detected with HRP-conjugated anti-HA antibody, while anti- $\beta$ -galactosidase (LacZ) was used as control to monitor transfection efficiency and loading. (B) HEK-293 cells were transfected with either HA-tagged wild-type 16 E6 or HA-tagged 16 E6 D25N L83V expression plasmids. Twenty-four hours post transfection cells were treated with cycloheximide inhibitor and harvested at indicated time points (0, 30, 60 and 90 min). Cell lysates were subjected to SDS-PAGE and western blot analysis. E6 expression levels were detected by HRP-conjugated anti-HA antibody, while  $\beta$ -galactosidase (LacZ) was used as control to monitor transfection efficiency and loading.

As indicated in **Figure 17B**, the half-life of wild-type 16 E6 started to decrease around 90 min time point, which is in agreement with previously reported results (Tomaić, Pim, and Banks 2009a; Androphy et al. 1987). Interestingly, under the same conditions 16 E6 D25N L83V exhibited a shorter half-life, with the protein levels of 16 E6 D25N L83V at 90 min time point being lower than the protein levels of wild-type 16 E6 (**Figure 17B**). From the presented experiment it can be concluded that although overall protein stability is likely to be higher for 16 E6 D25N L83V double mutant, its rate of protein turnover seems to be faster in the comparison to the wild-type 16 E6 oncoprotein. Hence, it seems that those observed changes in protein stability

and protein turnover between wild-type HPV-16 E6 and HPV-16 E6 D25N L83V are presumably linked to the two newly introduced mutations. Furthermore, possibilities that the mutations might also have an impact on E6 transcript levels or have an impact on E6 post-translational modifications cannot be excluded.

#### **4.5. D25N and L83V mutations in HPV-16 E6 do not affect its cellular localization**

Since protein interaction and degradation assays indicated that D25N and L83V mutations have an impact on 16 E6 association with E6AP, which subsequently affects their protein turnover, the following step was to determine if those mutations might also alter E6 oncoprotein cellular localization. In particular, the experiments included monitoring of the cellular localization of ectopically expressed wild-type HPV-16 E6 and the corresponding 16E6 mutants. H1299 cells were transfected with plasmids expressing either FLAG-tagged wild type 16 E6 or FLAG-tagged 16 E6 D25N, E6 L83V and E6 D25N L83V mutants. Twenty-four hours post transfection the cells were fixed and immunostained with primary anti-FLAG antibody and anti-mouse secondary antibody conjugated to Alexa Fluor 488 to detect E6s localization by using laser scanning confocal microscopy. As depicted in **Figure 18**, cellular localization of wild-type 16 E6, 16 E6 D25N, 16 E6 L83V and 16 E6 D25N L83V mutants showed similar distribution patterns, with predominant localization in the nucleus and a diffused distribution in the cytoplasm.

Since there are no available cell lines that endogenously express the corresponding 16 E6 mutants, an overexpression assay had to be conducted to determine cellular localization of the mutants. In this experimental setting there were no obvious differences in their cellular localization, suggesting that different oncogenic potential between the mutants is likely to be manifested through other mechanisms, independently of their cellular localization.

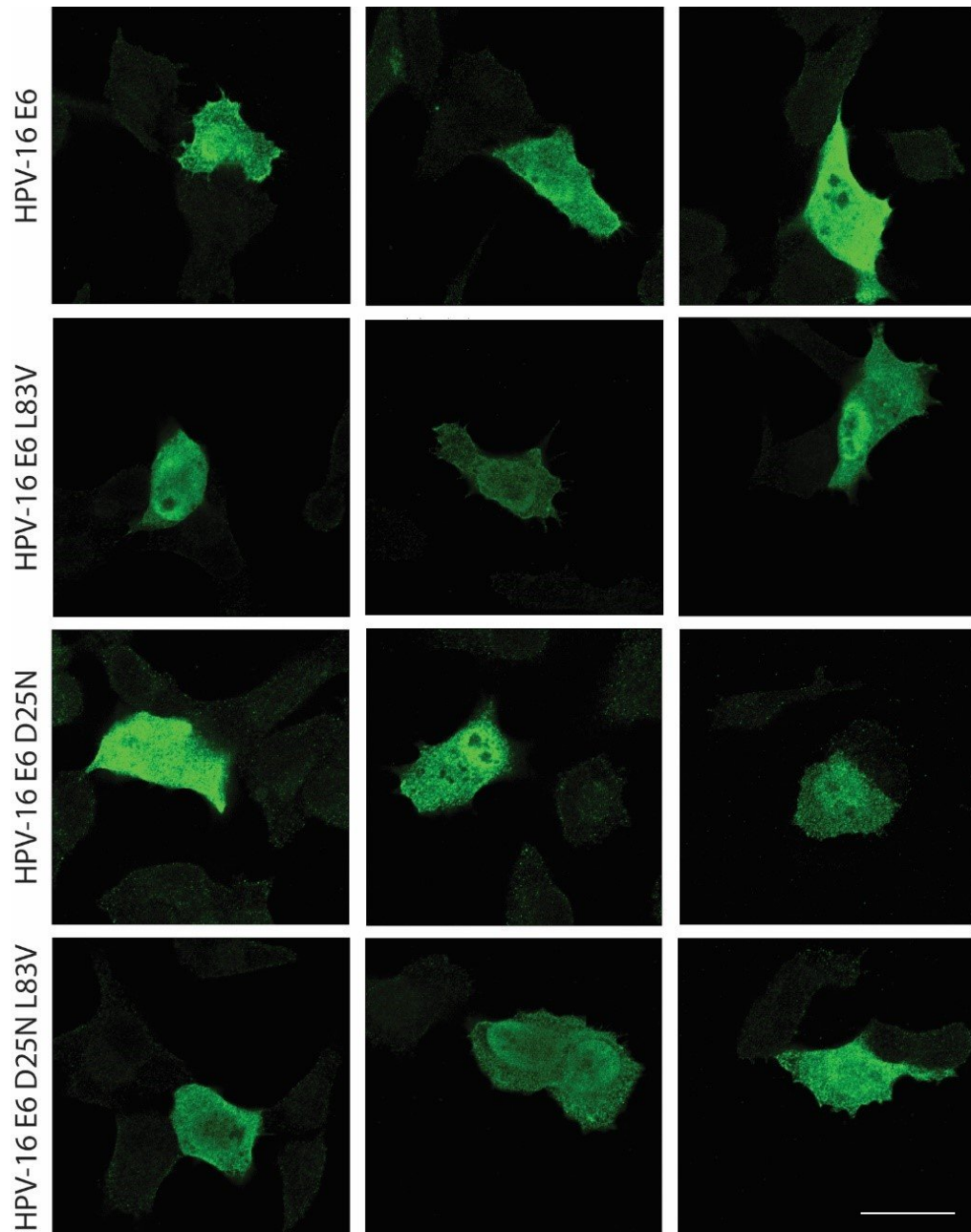


**Figure. 18. Cellular localization of ectopically expressed wild-type HPV-16 E6, 16 E6 L83V, D25N and D25N L83V oncoproteins.** H1299 cells were transfected with HA- and FLAG- tagged plasmids expressing either wild-type 16 E6 or E6 D25N, E6 L83V and E6 D25N L83V mutants. Twenty-four hours post transfection the cells were fixed and stained with anti-FLAG antibody and secondary anti-mouse antibody conjugated to Alexa Fluor 488 to visualize 16 E6 using laser scanning confocal microscopy. Three representative images for wild-type 16 E6 and each corresponding mutant are shown. Scale bars = 10  $\mu$ m.

#### 4.5. HPV-16 E6 and the corresponding mutants efficiently degrade p53 and PDZ-domain containing substrates *in vitro*

The focus of *in vitro* degradation assays was to assess the capacity of the 16 E6 mutants to target and degrade some of the main E6 cellular target proteins, that included p53 tumor suppressor and PDZ-domain containing substrates. Wild-type 16 E6 and the corresponding mutants were transcribed and translated *in vitro* as described in Materials and Methods section and incubated at 30°C for the indicated time points with *in vitro* translated p53, MAGI-1, DLG1 and Scrib proteins. For each of those analyzed target proteins, previous reports have shown to be degraded by 16 E6 under these *in vitro* conditions (Gardiol et al. 1999; M. Thomas et al. 2001; Miranda Thomas et al. 2005). Following *in vitro* translation/transcription, incubated proteins were separated on SDS-PAGE, after which the gel was dried and the remaining protein levels were assessed by autoradiography. The presented results of the quantifications represent the mean percentage of at least two assays per target protein, including p53, MAGI-1, DLG1 and Scrib.

The remaining levels of p53 were detected in the experimental conditions when p53 was translated alone and in the conditions when p53 was incubated with wild-type 16 E6 and the corresponding mutants. Previous research have shown that p53 starts to be degraded by E6 within 30 to 60 minutes of incubation (Tsvetkov et al. 2009), therefore, these time points were chosen for p53 degradation analysis in the presence of 16 E6s constructs (**Figure 19A**). The quantification analysis of the obtained blots determined that all included 16 E6s were efficient in degrading p53 with similar capacities. The percentage of p53 amount which remained after 60 min incubation with wild-type 16 E6 was 51.30%, with 16 E6 D25N 50.82%, 16 E6 L83V 36.48% and with 16 E6 D25N L83V 51.38% (**Figure 19B**). From the multiple experiments it is noticeable that 16 E6 D25N and 16 E6 D25N L83V were as efficient as wild type 16 E6 in inducing p53 degradation, while 16 E6 L83V mutant demonstrated a slightly increased capacity to target p53 for a proteasome mediated degradation. The quantification values of three independent experiments at the later degradation time point (60 min) were included in the statistical analysis performed by MedCalc software and depicted as a box and whisker plot (**Figure 19C**). Statistically significant increases in p53 degradation were observed when the amount of translated p53 alone was compared with the remaining amounts of p53 incubated with wild-type 16 E6 or E6 D25N, E6 L83V, and E6 D25N L83V mutants. However, there were no statistically significant differences between wild-type 16 E6 and 16 E6 mutants in their ability to induce p53 degradation. Hence, in the experimental

settings of *in vitro* assay, it appears that there were no marked changes between evaluated 16 E6 constructs and their abilities to target p53 for a proteasome mediated degradation, suggesting that the introduced mutations did not have an impact on 16 E6 function to target p53.

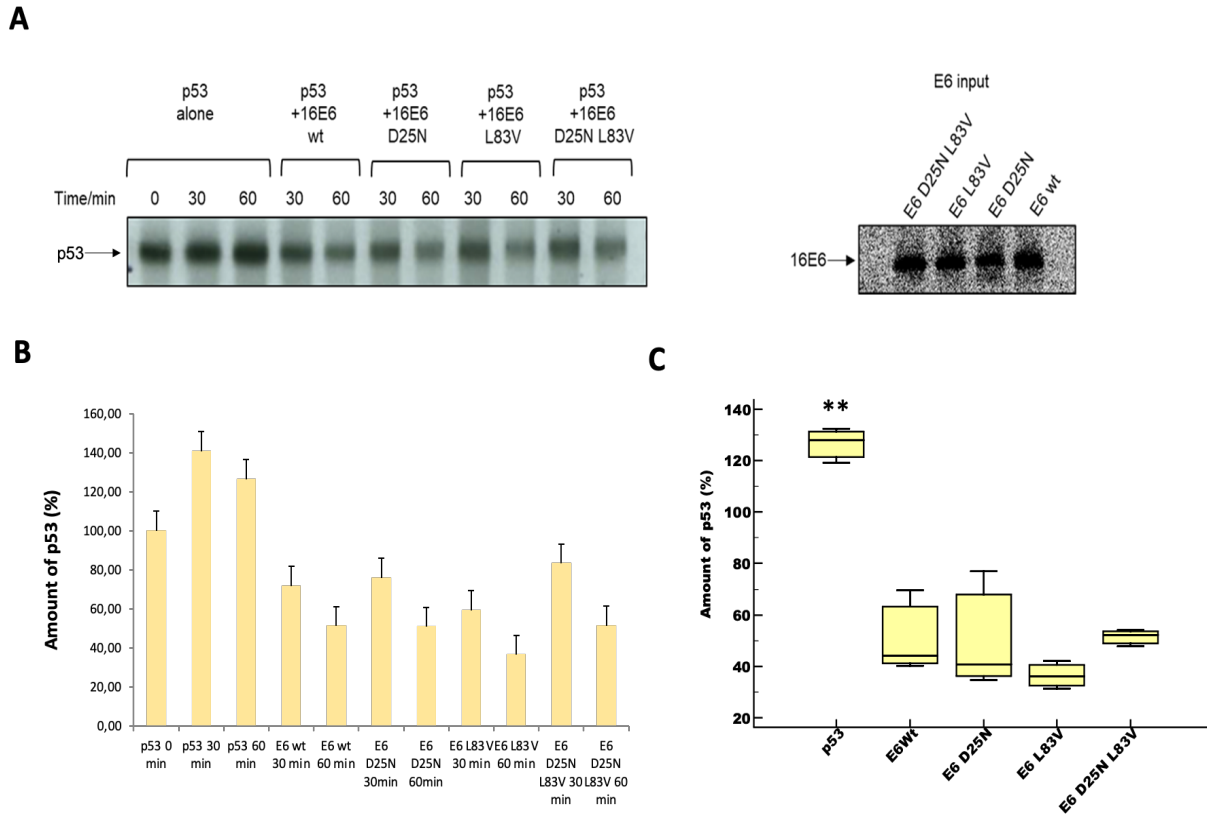


**Figure 19. HPV-16 E6 wild-type and the corresponding 16 E6 D25N, 16 E6 L83V and 16 E6 D25N L83V mutants efficiently degrade p53 *in vitro*.** (A) Equal amounts of *in vitro* translated p53 were mixed with 3x of the amount of wild-type 16 E6 and the corresponding 16 E6 D25N, 16 E6 L83V and 16 E6 D25N L83V mutants. E6 inputs are shown on the right panel. At the indicated time points (30 and 60 min) the samples were removed from the incubation at 30°C and analysed by SDS-PAGE and autoradiography. (B) The protein levels were quantitated by a phosphorimager and the mean percentage of p53 amount at the end of each assay was calculated, taking the sample with p53 at 0 min time point to be 100%. The results shown in a form of column graphs represent the mean percentage of p53 amount of at least 3 independent assays. (C) Statistical analysis performed by MedCalc software is depicted as a box and whisker plot, along with standard error indicated as a bar. Significance was determined performing ANOVA test including quantification values of three independent experiments at the later degradation time point (60 min) with  $p < 0.05$  taken as significant and  $p < 0.01$  taken as very significant (marked with \*\* above the bar).

The time points for evaluating MAGI-1 degradation in presence of 16 E6s were 15 and 30 min, due to previous research which showed the time period in which MAGI-1 gets efficiently degraded by E6 (M. Thomas et al. 2001; Miranda Thomas et al. 2005). Again, the levels of degradation were not detected in the experimental conditions when MAGI-1 was translated alone, but only in the samples in which wild-type 16 E6 and the corresponding mutants were introduced into the reaction mixture (**Figure 20A**). The obtained quantification analysis of MAGI-1 degradation revealed similar results as in the case with p53 degradation, where there was no major difference observed in the degradatory capacity of HPV-16 E6 D25N, 16 E6 L83V and 16 E6 D25N L83V mutants in comparison to wild-type 16 E6 (**Figure 20A and 20B**). The percentage of MAGI-1 amount which remained at 30 min time point with wild-type 16 E6 was 64.17%, with 16 E6 D25N 73.10%, with 16 E6 L83V 59.51% and with 16 E6 D25N L83V 67.77%, indicating that all evaluated 16 E6 constructs induced MAGI-1 degradation with similar capacities (**Figure 20A and 20B**). However, from the multiple experiment data it is noticeable that 16 E6 L83V mutant exhibited a slightly increased capacity to target MAGI-1 for a proteasome mediated degradation.

The quantification values of two independent experiments at the later degradation time point (30 min) was included in statistical analysis and depicted as a box and whisker plot (**Figure 20C**) and the significance was determined by ANOVA test. Comparing the levels of translated MAGI-1 at 30 min time point, with MAGI-1 degradation rates when incubated with either wild type 16 E6 or E6 D25N, E6 L83V and E6 D25N L83V mutants, showed a statistically significant increase in the degradation of MAGI-1. Yet, there was no statistically significant difference between the wild-type 16 E6 and 16 E6 mutants in their abilities to induce the degradation of MAGI-1. Overall, even though there were no statistically significant differences between the mutants in MAGI-1 degradation, 16 E6 L83V mutant appeared to be the most effective. This result correlates with the previous result of *in vitro* degradation of p53, where 16 E6 L83V was also the most efficient in the target degradation, suggesting the potential importance of this point mutation for E6 ability to target MAGI-1 (**Figure 19**). It is worth noting that the 16 E6 D25N mutant showed a slightly weaker ability to target MAGI-1 for proteasome-mediated degradation, similar to its effect on p53. This suggests that the D25N mutation in 16 E6 could be responsible for this effect.

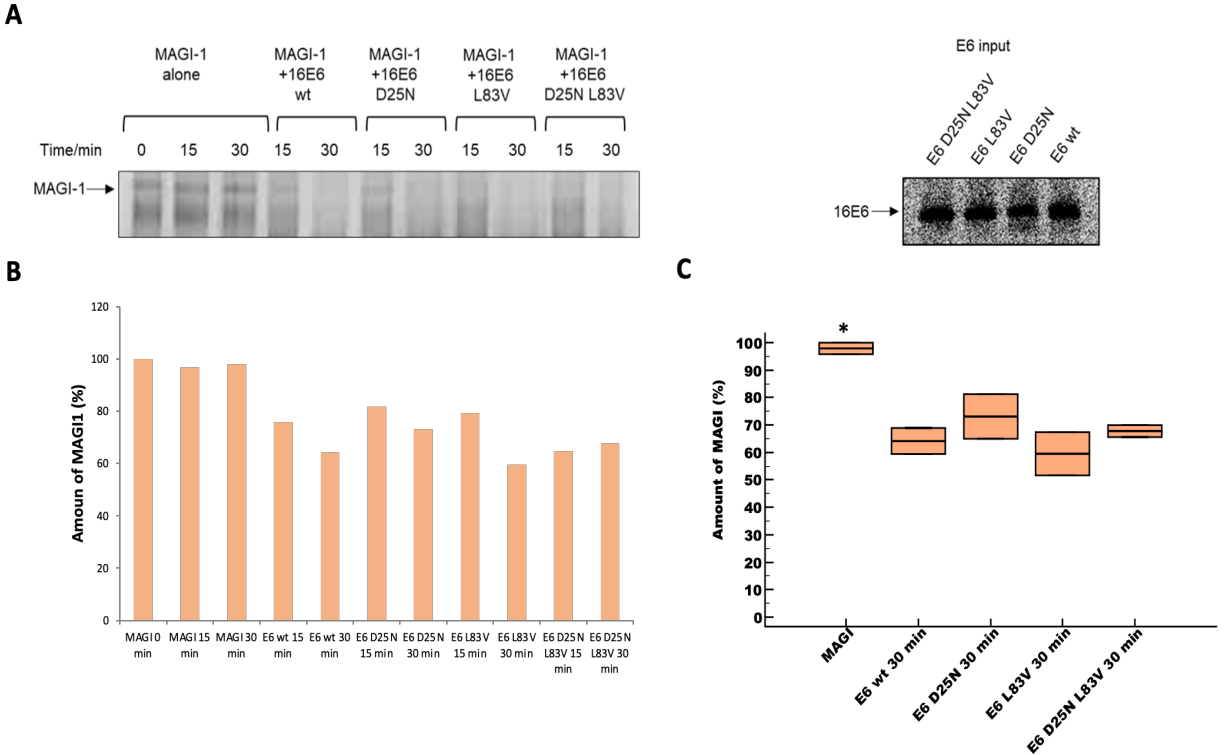


**Figure 20. HPV-16 E6 D25N, E6 L83V and E6 D25N L83V variants efficiently degrade MAGI-1 *in vitro*.** (A) Equal amounts of the *in vitro* translated MAGI-1 were mixed with 3x the amount of the wild-type or 16 E6 mutant oncoproteins. E6 inputs are shown on the right panel. At the time points of 15 and 30 min samples were removed from the incubation at 30°C and analysed by SDS-PAGE and autoradiography. (B) The SDS-PAGE gels were quantitated by phosphorimager analysis, and the mean percentage of MAGI-1 amount at the end of each assay was calculated, taking the sample with MAGI-1 at initial time point (0 min) to be 100% degradation. The result shown in a form of column graphs represent a mean percentage of two degradation assays. (C) Statistical analysis performed by MedCalc software is depicted as a box and whisker plot. The significance was determined by performing ANOVA test and includes quantification values of two independent experiments at the later degradation time point (30 min) with  $p < 0.05$  taken as significant (marked with \*).

In addition, an *in vitro* degradation assay was conducted also including DLG1. The time points selected for analyzing the degradation of DLG1 were 60 and 120 min, based on previous research which showed that DLG1 starts to be degraded during this time period (Gardiol et al. 1999). It can be seen from **Figure 21A** that neither one of the 16 E6 mutants was as efficient as the wild-type in inducing the degradation of DLG1. The percentage amount of DLG1 remaining after 120 min incubation with wild-type 16 E6 was 72.91%, with 16 E6 D25N 90.08%, with 16 E6 L83V 81.28% and with 16 E6 D25N L83V 91.39% (**Figure 21B**). Based on the statistical analysis (**Figure 21C**), all examined 16 E6 constructs induced DLG1 degradation with similar



intensities, but without statistically significant differences among them and even regarding to the percentage of DLG1 amount when DLG1 was translated alone. Interestingly, similar as for p53 and MAGI-1 degradation, it appears that the 16 E6 D25N mutant exhibited somewhat weaker capacity to target DLG1 for proteasome mediated degradation, which could be a consequence of this specific mutation.

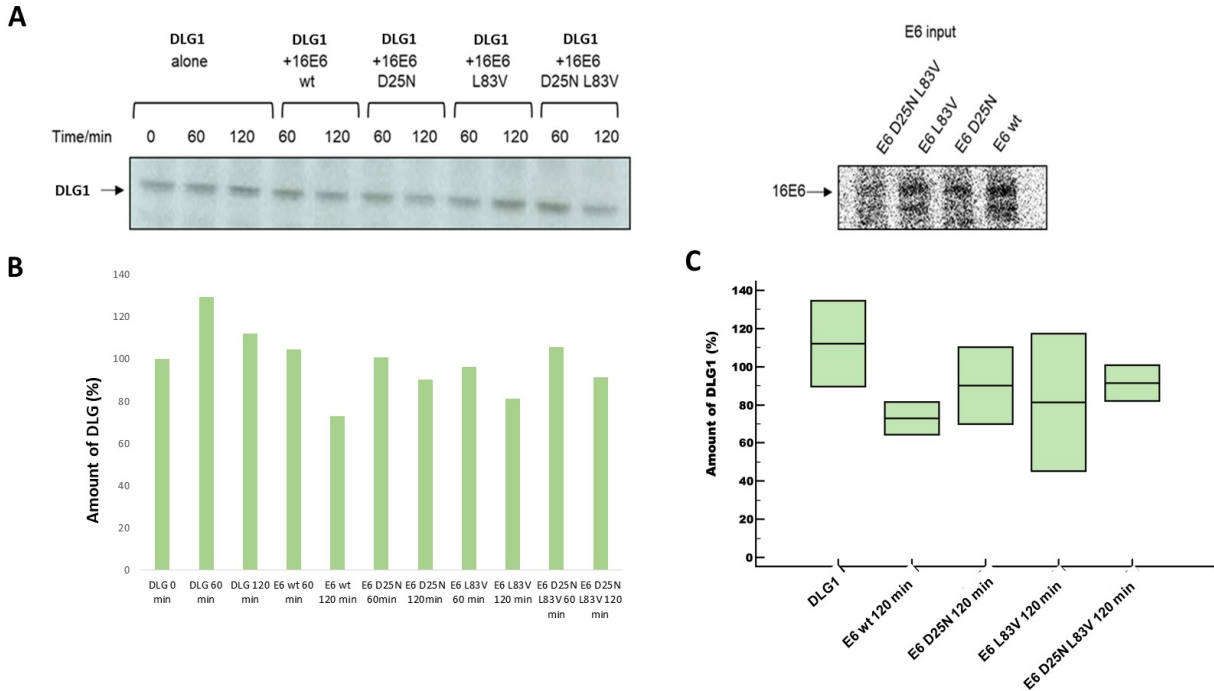


**Figure 21. HPV-16 E6 D25N, E6 L83V and E6 D25N L83V variants efficiently degrade DLG1 *in vitro*.** (A) Equal amounts of *in vitro* translated DLG1 were mixed with 5x the amount of the wild type or 16 E6 mutant oncoproteins. E6 inputs are shown on the right panel. At the time point of 60 and 120 min samples were removed from the incubation at 30°C and analysed by SDS-PAGE and autoradiography. (B) The SDS-PAGE gels were quantitated by phosphorimager analysis and the mean percentage of the amount of DLG1 at the end of each assay was calculated, taking the sample with DLG1 at the initial time point (0 min) to be 100%. The result shown in a form of column graphs represent a mean percentage of DLG1 amount of two degradation assays. (C) Statistical analysis performed by MedCalc software is depicted as a box and whisker plot. The significance was determined performing both ANOVA and Student's T-test and includes quantification values of two independent experiments at the later degradation time point (120 min).  $p < 0.05$  was taken as a significant.

Furthermore, Scrib susceptibility for 16 E6 and 16 E6 D25N L83V mediated degradation was also evaluated. The time points for analysing Scrib *in vitro* degradation were 60 and 120 min. The percentage of Scrib amount which remained after 120 min of incubation with the wild-type

16 E6 was 31%, while with 16 E6 D25N L83V mutant it was 55% (**Figures 22A and 22B**). Those quantification data clearly suggest that in this experimental setting wild-type 16 E6 showed greater efficiency in degrading Scrib. Statistically significant differences were observed when the degradation rate of Scrib translated alone at the 120 min time point was compared with the degradation rate of Scrib translated with either wild type 16 E6 or E6 D25N L83V mutant (**Figure 22C**). However, no significant difference was detected between the wild type 16 E6 and D25N L83V mutant. This pattern of Scrib degradation was similar to that observed with the other investigated PDZ-domain containing substrates, suggesting that in this experimental setting the double mutation did not significantly affect E6's ability to target Scrib.

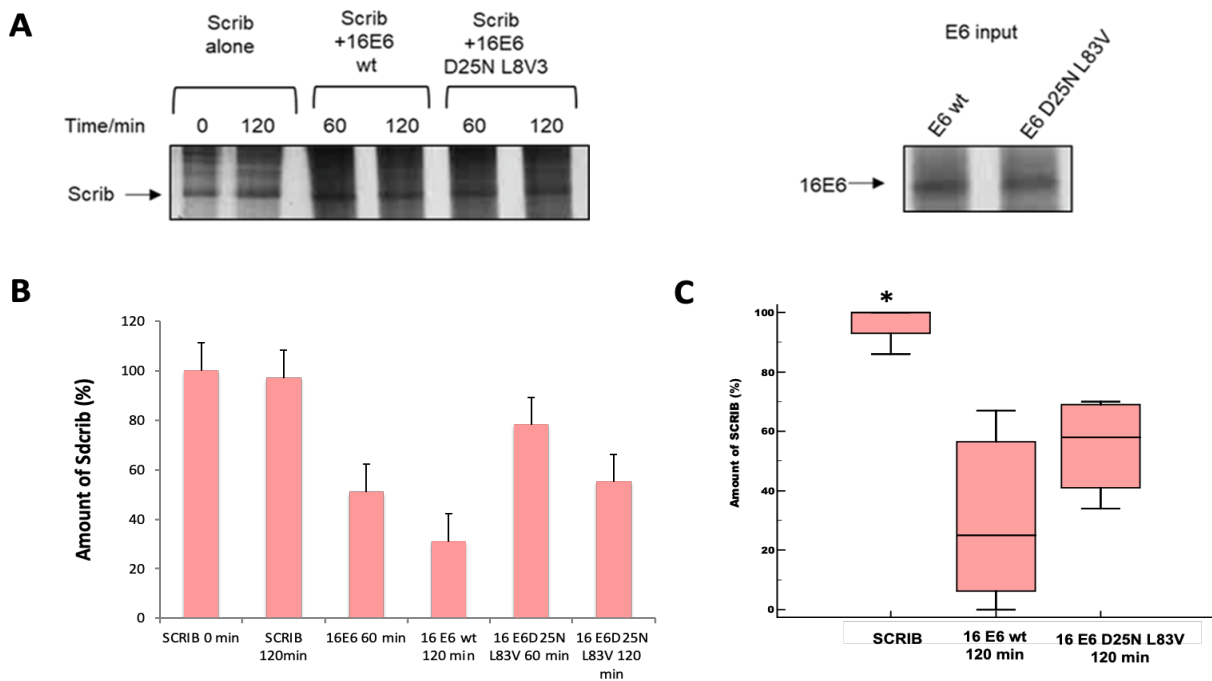
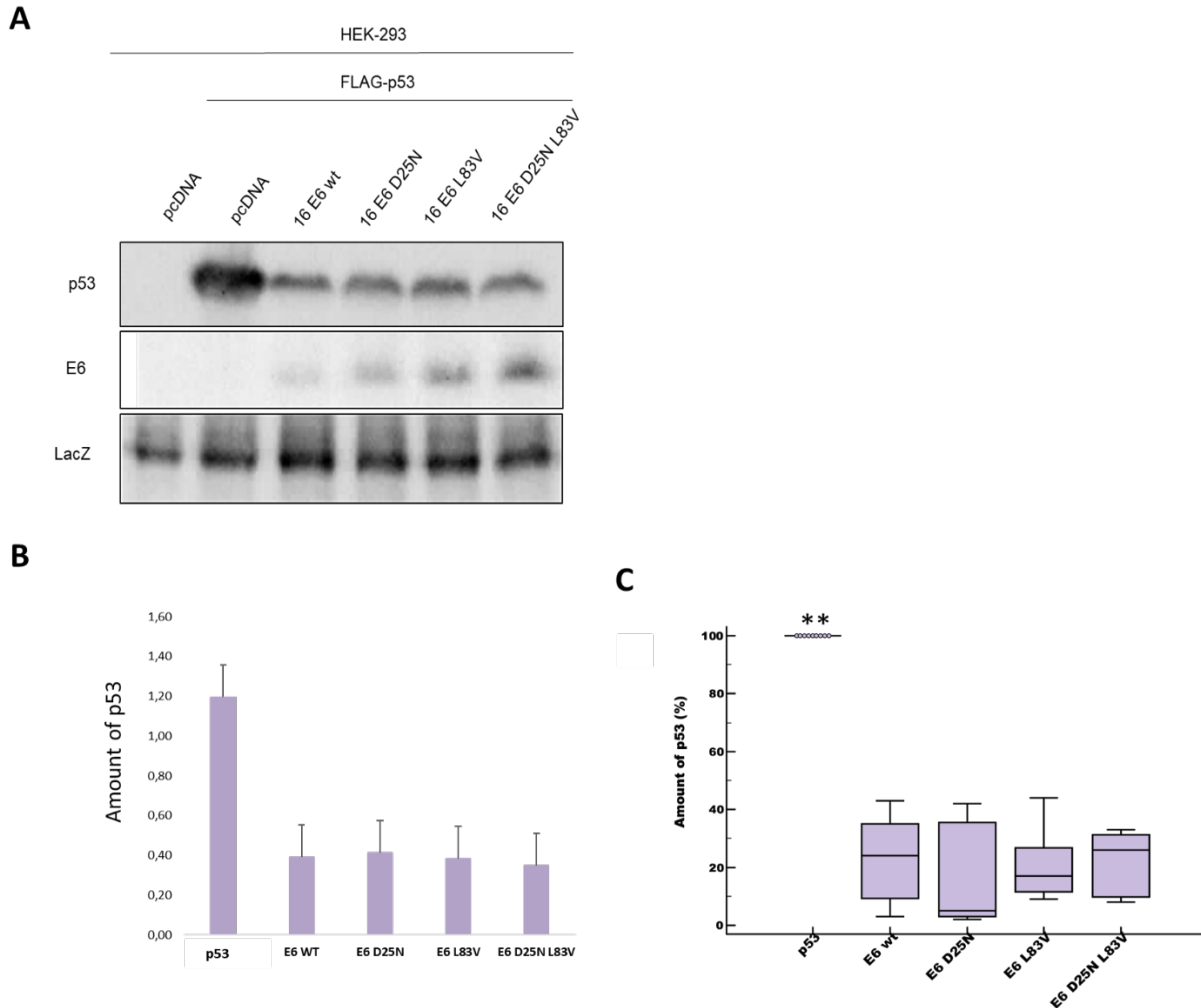


**Figure 22. HPV 16 E6 wild-type and E6 D25N L83V variant efficiently degrade Scrib *in vitro*.** (A) Equal amounts of *in vitro* translated Scrib were mixed with 3x the amount of the wild-type or 16 E6 D25N L83V. E6 inputs are shown on the right panel. At the time points of 60 and 120 min samples were removed from the incubation at 30°C and analysed by SDS-PAGE and autoradiography. (B) The SDS-PAGE gels were quantitated by phosphorimager analysis and the mean percentage of Scrib amount remaining at the end of each assay was calculated, taking the Scrib amount at the initial time point (0 min) to be 100%. The result shown in a form of column graph represent a mean percentage of Scrib amount of three degradation assays. (C) Statistical analysis performed by MedCalc software is depicted as a box and whisker plot. The significance was determined by ANOVA test and includes quantification values of three independent experiments at the later degradation time point (120 min) with  $p < 0.05$  taken as a significant (marked with \* above the bar).

Taking this together, the conclusion imposed after performing those *in vitro* degradation assays including p53, MAGI-1, DLG1 and Scrib as targets, is that no statistically significant difference among targets' degradation was seen for neither of the tested mutants. Even though there was no statistical significance, wild-type 16 E6 and E6 L83V mutant showed a trend of the increased capacity to target p53 and PDZ-domain containing substrates for the proteasomal degradation, while E6 D25N mutant degraded the target proteins with the lowest capacity. Therefore, the following step was to additionally verify these observations in cultured HEK-293 cell to establish potential differences regarding p53, MAGI-1 and DLG1 degradation under experimental settings of overexpression assay.

#### **4.6. HPV-16 E6 and the corresponding mutants efficiently degrade p53 in cultured cells**

After performing a panel of *in vitro* degradation assays which included the E6 constructs, p53 and PDZ-domain containing substrates, similar degradation assays were performed in cultured cells. HEK293 cells were co-transfected with FLAG-tagged p53 expression plasmid and plasmids expressing either the HA-tagged wild-type 16 E6 or HA-tagged 16 E6 D25N, E6 L83V and E6 D25N L83V mutants. After performing western blot analysis using anti-FLAG antibody to detect p53 and HRP-conjugated anti-HA antibody for detection of 16 E6 oncoprotein levels, the obtained results demonstrated degradation of ectopically expressed FLAG-p53 with both wild-type 16 E6 and the corresponding mutant forms (**Figure 23A**). Furthermore, all of the examined 16 E6s exhibited similar efficiency in targeting p53 for a proteasome-mediated degradation, with wild-type 16 E6, L83V and D25N L83V being equally efficient. This was confirmed in multiple experiments with a representative image of four independent experiments shown in **Figure 23A**. The results of the multiple experiments have been quantified, and a graphic representation of the densitometric analysis is presented as a column graph in **Figure 23B**. The quantification values of the performed multiple experiments were included in the statistical analysis to determine significance between the capacity of 16 E6 and the corresponding mutants to degrade p53. The significance was determined by performing ANOVA test, showing statistically very significant difference in degradation levels between p53 expressed alone in comparison with p53 co-expressed with 16 E6 and the corresponding mutants.

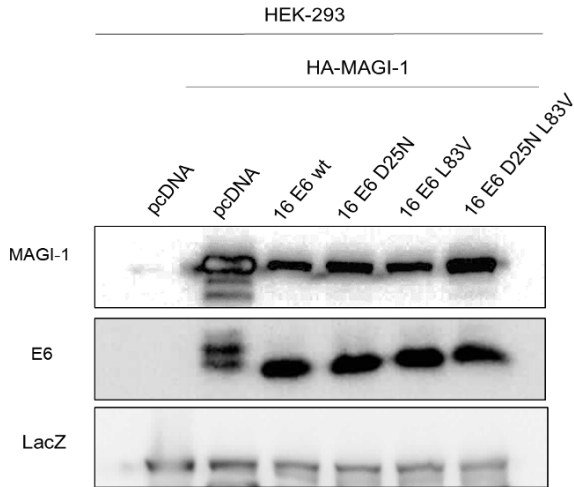
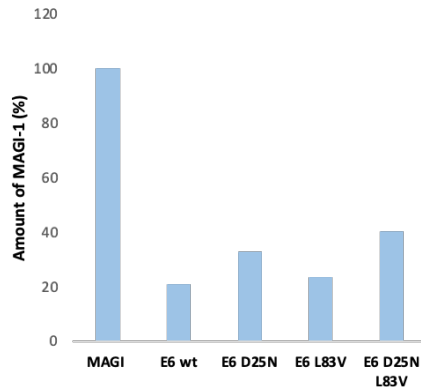
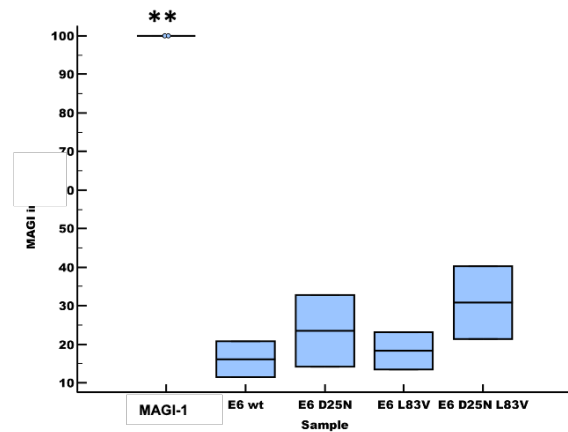


**Figure 23. D25N and L83V mutations in HPV-16 E6 do not affect E6 ability to target p53 for a proteasome mediated degradation.** (A) HEK-293 cells were co-transfected with FLAG-tagged p53 expression plasmid and plasmids expressing either the HA-tagged wild-type E6 or HA-tagged E6 D25N, E6 L83V and E6 D25N L83V mutants. After 24 hours the cells were harvested, isolated proteins separated on SDS-PAGE and analyzed by western blotting using anti-FLAG antibody to detect p53 and HRP-conjugated anti-HA antibody to detect 16 E6 protein levels.  $\beta$ -galactosidase (LacZ) was used as control to monitor transfection efficiency and loading. A representative image of four independent experiments is shown. (B) The graphic representation of the densitometric analysis was done in ImageJ software. Analysis was done by quantifying band densities for p53 protein levels expression normalized for background densities, after which relative expression was calculated by dividing p53 normalized density values with LacZ normalized density values. p53 average normalized relative expression was calculated for the control sample, and all normalized relative expressions were compared to that value. (C) The statistical analysis performed by MedCalc software is depicted as a box and whisker plot, along with the standard errors indicated as a bar. Significance was determined by ANOVA test and included quantification values of four independent experiments with  $p < 0.05$  taken as significant and  $p < 0.01$  taken as very significant (marked with \*\*).

However, there was no statistically significant difference between each of the 16 E6 mutants and the wild-type 16 E6, meaning that the mutations do not alter the ability of 16 E6 to target p53 for a proteasome mediated degradation (**Figure 23C**). Furthermore, this result is not in agreement with the *in vitro* degradation assays where 16 E6 L83V was the most efficient in degrading p53. The reason behind this discrepancy can be attributed to the differences in the experimental settings of the *in vitro* assays and overexpression assays performed in cultured cells, since *in vitro* assay cannot recapitulate entirely conditions in a living cell.

#### **4.7. HPV-16 E6 and the corresponding mutants efficiently target PDZ-domain containing substrates MAGI-1 and DLG1 in cultured cells**

In addition to the *in vitro* degradation assays, which included PDZ-domain containing substrates, the next step involved evaluation of the degradatory capacity of the E6 mutants to target MAGI-1 and DLG1 in cultured cells. To address this, HEK-293 cells were co-transfected with HA-tagged MAGI-1 expression plasmid (**Figure 24**) or HA-tagged DLG1 expression plasmid (**Figure 25**), and plasmids expressing either the HA-tagged wild-type 16 E6 or HA-tagged 16 E6 D25N, E6 L83V and E6 D25N L83V. A representative image of two independent experiments of MAGI-1 degradation is shown in **Figure 24A**. Interestingly, from these degradation assays it can be seen that 16 E6 L83V mutant exhibited similar potential to degrade MAGI-1 as the wild-type 16 E6. This result is in agreement with the *in vitro* degradation assay where 16 E6 L83V also appeared to be as efficient in degrading MAGI-1, as the wild-type 16 E6. On the contrary, D25N L83V and D25N mutants exhibited somewhat weaker degradatory activity towards MAGI-1. In **Figure 24B** a graphic representation of the densitometric analysis of multiple experiments performed in ImageJ software is shown. A quantification values of performed experiments were included in additional statistical analysis to calculate significance between the degradation rates of MAGI-1 co-transfected with either 16 E6 or 16 E6 D25N, E6 L83V and E6 D25N L83V mutants. The statistical significance was determined by performing ANOVA test, which showed a significant difference in the degradation levels of MAGI-1 expressed alone in respect to the degradation rate of MAGI-1 co-expressed with 16 E6 constructs.

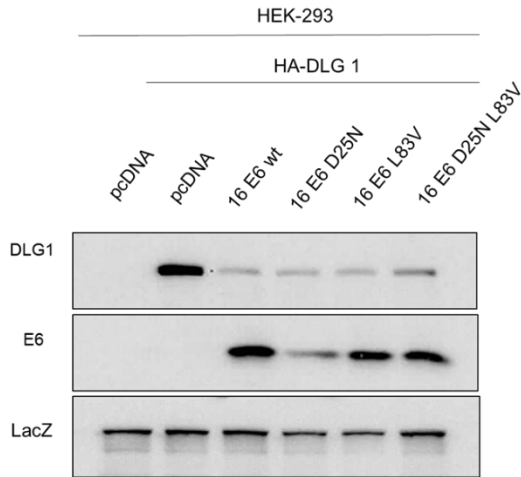
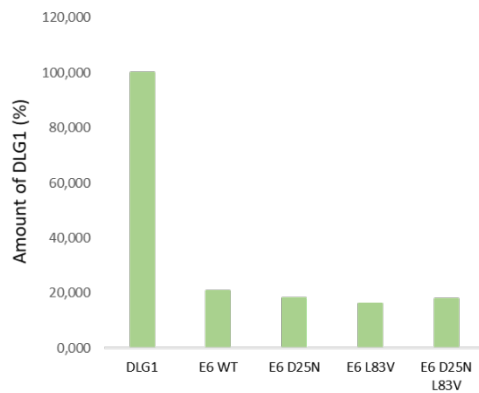
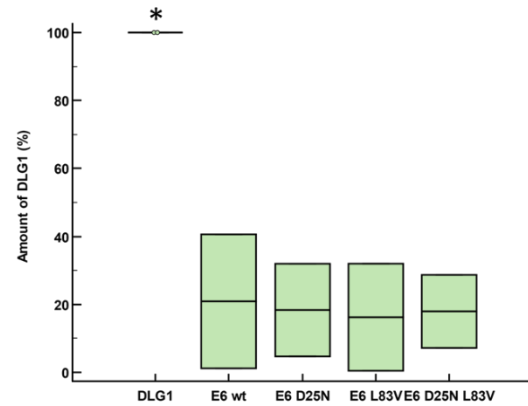
**A****B****C**

**Figure 24. HPV-16 E6 D25N L83V variant was least efficient in targeting MAGI-1 for proteasome-mediated degradation.** (A) HEK-293 cells were co-transfected with HA-tagged MAGI-1 expression plasmid either alone, or in combination with plasmids expressing either the HA-tagged wild-type E6, or HA-tagged E6 D25N, E6 L83V and E6 D25N L83V. After 24 hours the cells were harvested, and the cell lysates analysed by SDS-PAGE and western blotting using HRP-conjugated anti-HA antibody to detect MAGI-1 and 16 E6 protein levels.  $\beta$ -galactosidase (LacZ) was used as a control to monitor transfection efficiency and loading. (B) Densitometric analysis of multiple experiments was done in ImageJ software. The analysis was performed by quantifying band densities for MAGI-1 protein expression normalized for background densities, after which relative expression was calculated by dividing MAGI-1 normalized density values with LacZ normalized density values. MAGI-1 average normalized relative expression was calculated for control sample, and all normalized relative expressions were compared to that value. Each experiment was repeated two times and included in densitometric analysis. (C) The statistical analysis performed by MedCalc software is depicted as a box and whisker plot. Significance was determined by performing ANOVA test and included quantification values of two independent experiments.  $p < 0.01$  taken as very significant (marked with \*\*).

Despite that, there was no statistically significant differences between each of 16 E6 mutants and the wild-type 16 E6 in their ability to induce MAGI-1 degradation, suggesting that those 16 E6 mutations do not have an impact on this particular E6 degradatory activity (**Figure 24C**).

The same experimental settings were repeated to assess DLG1's degradation rates in HEK-293 cells. A representative image of two independent experiments is shown in **Figure 25A** and there was no observed difference between 16 E6 mutants and the wild-type 16 E6 in their ability to induce DLG1 degradation. Nevertheless, 16 E6 L83V showed somewhat more pronounced efficiency in degrading DLG1 in respect to wild-type 16 E6. **Figure 25B** shows graphic representation of a densitometric analysis performed in ImageJ software. An overexpression assay result for DLG1 degradation assay showed that DLG1 degradatory capacity was most pronounced with wild-type 16 E6, although 16 E6 L83V capacity for DLG1 degradation exhibited similar intensity. A quantification values derived from multiple experiments are included in an additional statistical analysis used for calculating significance of degradation rates between DLG1 transfected alone or co-transfected with 16 E6 or 16 E6 D25N, E6 L83V and E6 D25N L83V mutants. Significance was determined by performing ANOVA test, which showed statistically significant difference in the degradation levels of DLG1 alone in respect to the degradation rate of DLG1 in presence of 16 E6s. However, there was no statistically significant difference between 16 E6 mutants and the wild-type 16 E6 in their ability to induce DLG1 degradation (**Figure 25C**).

Taken together, from the obtained overexpression assay results it is noticeable that the most efficient degradation of ectopically expressed HA-MAGI-1 (**Figure 24**) and DLG1 (**Figure 25**) was driven by HPV-16 E6 L83V mutant. It is worth noting that 16 E6 D25N L83V mutant exhibited stronger interaction with E6AP than L83V, but on the contrary the lower target degradation efficiency towards PDZ-domain containing substrates, which can be explained by the established knowledge about an E6AP-independent degradation pathway of MAGI-1 and DLG1 (Grm and Banks 2004; Vats et al. 2022). Based on the results of both *in vitro* degradation and overexpression assays in HEK-293 cells, it can be concluded that there is no statistically significant difference in a degradation capacity between wild-type 16 E6 and corresponding mutants in targeting p53 and certain PDZ-domain containing substrates.

**A****B****C**

**Figure 25. D25N and L83V mutations in HPV-16 E6 do not affect E6 ability to target DLG1 for a proteasome mediated degradation.** (A) HEK-293 cells were co-transfected with HA-tagged DLG1 expression plasmid either alone, or in combination with plasmids expressing either the HA-tagged wild type E6, or HA-tagged E6 D25N, E6 L83V and E6 D25N L83V. After 24 hours the cells were harvested, the isolated proteins separated on SDS-PAGE and analysed by western blotting using HRP-conjugated anti-HA antibody to detect DLG1 and 16 E6 protein levels.  $\beta$ -galactosidase (LacZ) was used as a control to monitor transfection efficiency and loading. (B) Densitometric analysis of multiple experiments was done in ImageJ software. The analysis was performed by quantifying band densities for DLG1 protein expression normalized for background densities, after which relative expression was calculated by dividing DLG1 normalized density values with LacZ normalized density values. DLG1 average normalized relative expression was calculated for the control sample, and all normalized relative expressions were compared to that value. Each experiment was repeated two times and included in densitometric analysis. (C) The statistical analysis performed by MedCalc software is depicted as a box and whisker plot. Significance was determined performing ANOVA test and included quantification values of two independent experiments.  $p < 0.05$  was taken as a significant (marked with \*).



## **PART II MAML1-induced HPV E6 oncoprotein stability is required for cellular proliferation and migration**

### **4.8. HPV E6 oncoproteins from $\alpha$ and $\beta$ types interact with MAML1**

Previous proteomic analyses have revealed interactions between different cutaneous  $\beta$ -E6s and MAML1 through proteomic screens and interaction assays, and therefore it was believed that this interaction was mostly linked to cutaneous E6 oncoproteins (N. Brimer et al. 2012b; Tan et al. 2012b; Meyers, Spangle, and Munger 2013b; Meyers et al. 2017b). Only one of these studies in a panel of analysed HPV E6s also included monitoring of the association between MAML1 and HPV-16 E6 oncoprotein from  $\alpha$ -types (N. Brimer et al. 2012b). Surprisingly, that study for the first time demonstrated an interaction between HPV-16 E6 and MAML1, although the association was minimal in comparison to the associations of  $\beta$ -E6 oncoproteins with MAML1 (N. Brimer et al. 2012b). Most likely due to the low binding intensity of this potentially very important interaction between 16 E6 and MAML1, this line of research was not pursued extensively in the past. However, this intriguing finding has left many unanswered questions and raised an interest for further research and represented the basis for the analyses conducted in the second part of this doctoral thesis.

The initial experiments had an intention to corroborate if MAML1 is a binding partner of both  $\alpha$ - and  $\beta$ -HPV E6 oncoproteins. To tackle this question, a co-immunoprecipitation analysis was performed using HEK-293 cells transfected with plasmids expressing HA-tagged HPV-16 E6 and HPV-8 E6, alone or in combination with FLAG-tagged MAML1. Twenty-four hours post transfection the cells were harvested, resuspended in E1A lysis buffer and the cell extracts were incubated with anti-HA beads as described in a Materials and Methods section. Immunoprecipitated protein complexes were separated on SDS-PAGE and analysed by western blotting using HRP-conjugated anti-HA antibody to detect E6 oncoproteins, along with anti-FLAG antibody which detected MAML1. The results shown in **Figure 26A** demonstrate a clear interaction between HPV-8 E6 and MAML1, as it was expected based on the previous analyses, and a weaker, but an apparent interaction between HPV-16 E6 and MAML1.

The further extension of the protein interaction analysis was prompted by the confirmed HPV-16 E6/MAML1 interaction from the described co-immunoprecipitation assay, with the

intention to additionally verify the detected binding in a more natural setting. Hence, HPV-negative cervical tumor derived cell line C33A was used to recapitulate the microenvironment of the epithelial tissue. C33A cells were transfected with an empty plasmid containing a FLAG tag (pXJ41-FLAG) or the same plasmid with 16 E6 insertion (pXJ41:16E6-FLAG). Forty-eight hours post transfection, cell lysates were collected in LSD lysis buffer and isolated proteins incubated with anti-FLAG-antibody coupled to magnetic beads for the two hours at the RT. The immunoprecipitated complexes were further subjected to western blot analysis using anti-MAML1 and anti-FLAG antibodies, as well as GAPDH-Alexa Fluor 680 to detect GAPDH which was used as a loading control. As indicated in **Figure 26B**, in this experimental setting ectopically expressed FLAG-tagged HPV-16 E6 co-immunoprecipitated with endogenous MAML1, additionally supporting the initial observation of the complex formation between these two proteins. Furthermore, the presented results are in an agreement with previously published data and additionally support the important HPV-16 E6/MAML1 interaction.

The confirmation of 16 E6/MAML1 interaction opened a new direction for this doctoral research by further aiming to address if some other  $\alpha$ -HPV types could also interact with MAML1. Hence, having established an interaction between 16 E6 and MAML1 by performing co-immunoprecipitation analysis by two independent experimental approaches, the next step was to expand the analysis and investigate if multiple  $\alpha$ -HPV E6s can also complex with MAML1. In particular, to investigate whether MAML1 could complex with  $\alpha$ -types HPV-18 and -11 E6 oncoproteins, a GST pull-down assay was performed using GST-16 E6, GST-18 E6, GST-11 E6, GST-8 E6 fusion proteins, or GST alone as a control. GST-16 E6 and GST-18 E6 were included as representative types of HR  $\alpha$ -HPV E6s, while GST-11 E6 was a representative member of LR  $\alpha$ -HPV E6s. GST-8 E6, as a representative of  $\beta$ -E6s with an oncogenic potential and previously confirmed MAML1's binding partner, was included as a positive control for the comparison of the binding affinities. The corresponding purified GST-fusion proteins were incubated with cell lysates of HEK-293 cells previously transfected with FLAG-tagged MAML1. Bound protein complexes were separated on SDS-PAGE and analysed by western blotting using anti-FLAG antibody. From the results in **Figure 26C** it is noticeable that E6 oncoproteins from all analysed HPV types formed a complex with MAML1. HPV-8 E6 and MAML1 interaction was evidently the strongest, followed by 18 E6, the interaction with 16 E6 was somewhat weaker, while the interaction with 11 E6 was the weakest among all of them (**Figure 26C**).

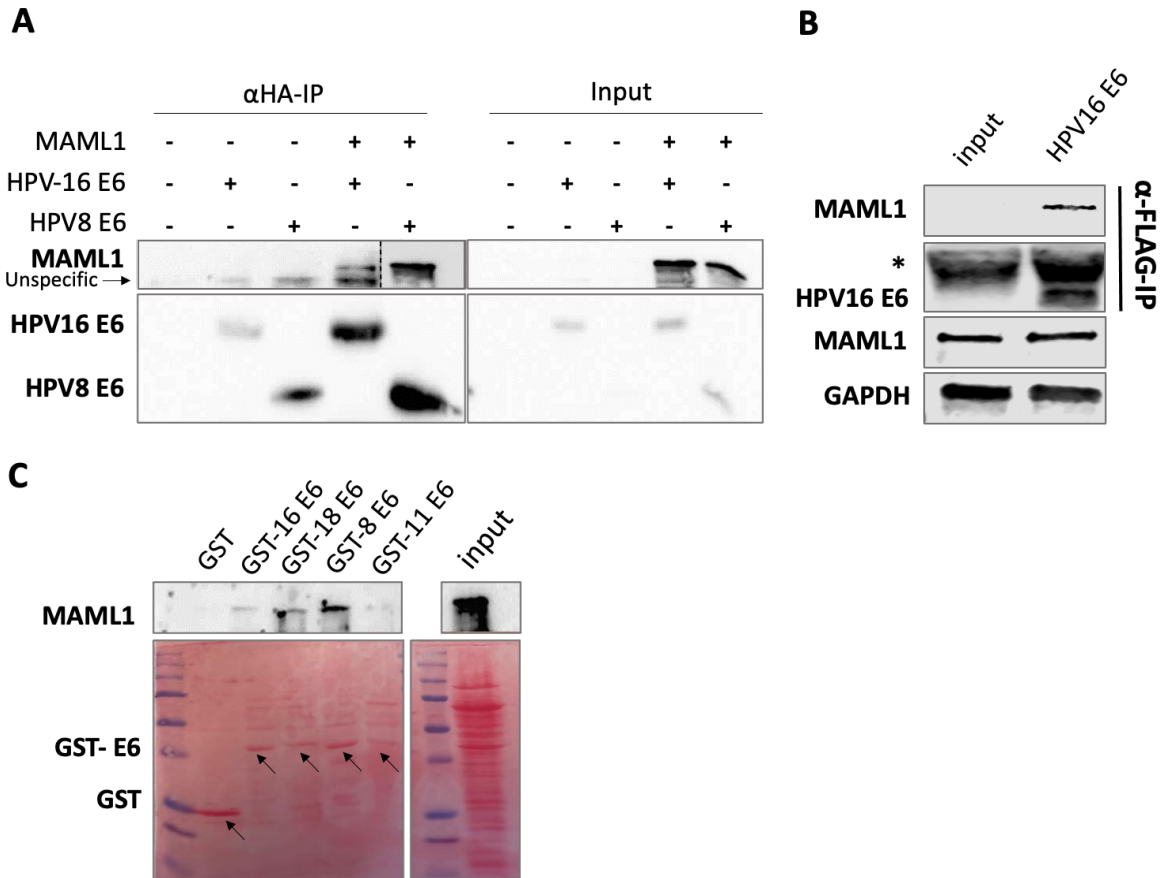


**Figure 26. Both  $\alpha$ - and  $\beta$ - HPV E6 oncoproteins bind to MAML1.** A) HEK-293 cells were transfected with HA-tagged HPV-16 E6 or HPV-8 E6, alone or in combination with FLAG-tagged MAML1. Cells were harvested in E1A lysis buffer and incubated with anti-HA beads on a rotating wheel 2 hours at RT. Co-immunoprecipitated complexes were subjected to SDS-PAGE and western blot analysis using HRP-conjugated anti-HA antibody to detect E6s and anti-FLAG antibody to detect MAML1. Detected FLAG-tagged MAML1 in co-precipitated MAML1/E6 complexes was compared with the amount of FLAG-tagged MAML1 present in a corresponding 10% of input sample. Dotted line separates different time exposures of the same membrane. B) C33A cells were transiently transfected with an empty vector or plasmid coding for FLAG-tagged HPV-16 E6. Forty-eight hours post transfection cells were harvested in LSD lysis buffer and incubated with anti-FLAG coupled magnetic beads. Co-immunoprecipitated complexes of MAML1 and HPV-16 E6 were separated on SDS-PAGE and subjected to western blot analysis with anti-MAML1 and anti-FLAG antibodies, together with 10% input. GAPDH was used as a loading control (\*stand for immunoglobulin light chain). C) HEK-293 cells were transfected with FLAG-tagged MAML1. After 24 hours, the cells were harvested, and the cell lysates were incubated with previously produced GST-16 E6, GST-18 E6, GST-8 E6 and GST-11 E6 fusion proteins. GST alone was included as a control. Bound complexes of MAML1 and GST-fusion proteins were detected by western blotting using anti-FLAG antibody and compared to the amount of FLAG-tagged MAML1 present in the input sample. The lower membrane shows the amounts of the purified GST-fusion proteins visualized by Ponceau staining.

Based on the presented results, it is evident that multiple  $\alpha$ -HPV E6 oncoproteins can form a complex with MAML1, albeit with varying intensities. Importantly, the results depicted in **Figure 26** indicate that while there is a clear preference of various  $\beta$ -HPV and  $\alpha$ -HPV types to associate with MAML1, it is not possible to exclusively classify HPV genera based on this interaction.

#### **4.9. Protein amount of $\alpha$ - and $\beta$ -HPV E6 oncoproteins is MAML1-dependent**

After confirming the efficient binding of multiple  $\alpha$ -E6s to MAML1, the next step was to investigate whether these validated interactions may affect the protein amount of E6 oncoproteins. Previous reports have established that the stability of  $\alpha$ -HPV E6 oncoproteins directly depends on the presence of E6AP, which shares the same LXXLL motif with MAML1 (Tomaić, Pim, and Banks 2009a). For LXXLL motif is known to facilitate the interaction between E6AP and HR E6 and therefore, it was intriguing to speculate that MAML1, which also contains the same motif, may influence the protein stability of the E6 oncoprotein.

To address the potential increase in the protein amounts of E6, HEK-293 cells were transfected with plasmids expressing HA-tagged E6 oncoproteins from different HPV types including HPV-8, -12, -14, -16, -18, -24, -33 and -38, either alone or in combination with FLAG- or Myc-tagged MAML1 or FLAG- or Myc-tagged E6AP. HPV-16, -18 and -33 E6 belong to HR mucosal  $\alpha$ -types, while HPV-12, -14, -24 are  $\beta$ -types, including HPV-8 and -38 E6 that are  $\beta$ -types with established oncogenic potential. Twenty-four hours post transfection the cells were harvested, proteins isolated and analysed by SDS-PAGE and western blotting, using anti-FLAG or anti-Myc antibodies for visualising MAML1 or E6AP, and HRP-conjugated anti-HA antibody for E6 detection. For the densitometric analysis, E6 protein band intensities from the samples transfected with the diverse E6s alone were compared with band intensities of those co-transfected with either MAML1 or E6AP. Based on this kind of analysis it was possible to establish potentially relevant changes in E6 protein amounts as a consequence of the interaction with MAML1 or E6AP. Furthermore, considering that the stabilizing effect of E6AP on HR mucosal and some cutaneous E6s, and the consequent increase in their protein levels, was previously reported (Tomaić, Pim, and Banks 2009a; Miranda Thomas et al. 2013b), allowed the assessment of potential impact of MAML1 on E6 protein amounts.

As shown in **Figure 27A**, surprisingly, E6 oncoproteins of all analysed HPV  $\alpha$ - and  $\beta$ -types were shown to exhibit increased protein levels as a consequence of the interaction with MAML1. This result additionally confirmed that HPV E6 proteins cannot be classified based on the association exclusively with either MAML1 or with E6AP. Moreover, what was even more important and relevant is that those results demonstrated a previously unknown and undefined role of MAML1 in regulating E6 protein levels increment and a potential novel role in HPV biology.

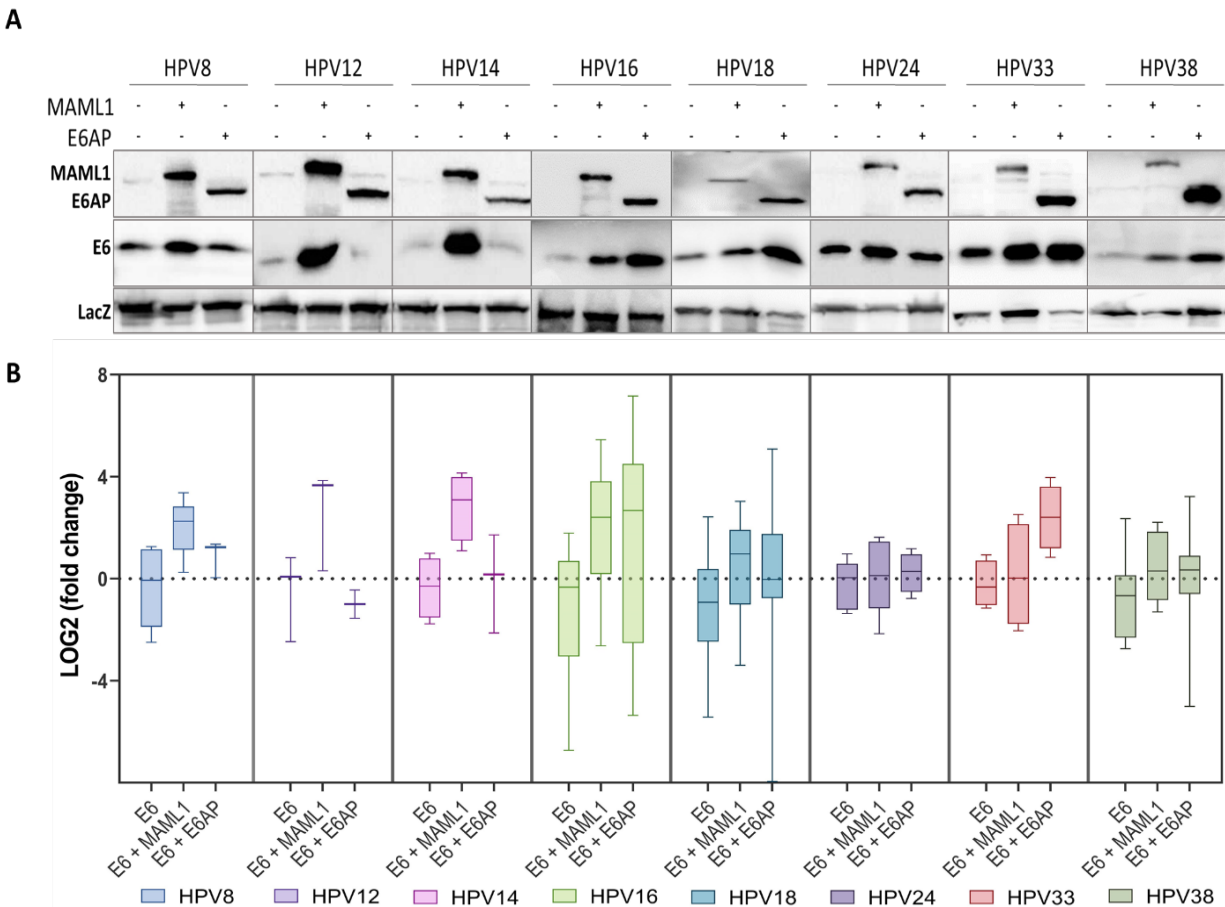


**Figure 27. MAML1 mediates the increase in E6 protein amounts from both  $\alpha$ - and  $\beta$ - HPV types.** A) HEK-293 cells were transfected with HA-tagged HPV-8, -12, -14, -16, -18, -24, -33 and -38 E6 alone or in combination with either FLAG- or Myc-tagged MAML1 or E6AP. After 24 hours cells were harvested and isolated proteins were separated on SDS-PAGE and analysed by western blotting. Proteins were detected by anti-FLAG or anti-Myc and anti-HA antibodies and visualized by chemiluminescence.  $\beta$ -galactosidase (LacZ) was used as a transfection and loading control. (B) Quantification analysis was performed with ImageJ software. The band density was measured and normalized with background density for each sample. After obtaining those measures, the relative expression was calculated by dividing normalized E6 density with LacZ density normalized with background.

Average relative expressions of E6s transfected alone (for each HPV type individually) were calculated and all relative E6 expressions were compared to those values in order to obtain E6 fold change. Each fold change in the samples where E6s were co-transfected with MAML1 or E6AP was calculated according to the corresponding values of E6 transfected alone from the same experiment. Graphical representation was done in a GraphPadPrism by showing LOG2 of fold changes as a box and whisker plot. Each experiment was repeated at least three times and all experiments were included in statistical analysis.

As expected, interaction with E6AP increased the protein levels of all examined  $\alpha$ -type HPV E6s, but what was rather surprising, E6AP also increased the protein levels of  $\beta$ -type HPV-38 E6, which was previously reported to bind E6AP (Miranda Thomas et al. 2013b). This indicates that although the majority of  $\beta$ -E6 oncoproteins preferentially interact with MAML1, which leads to an increase in their protein, there are some exceptions among  $\beta$ -E6s, which protein levels can also be impacted by E6AP (**Figure 27A**). Additionally, **Supplementary Figure 1** separately presents negative controls for **Figure 27A**. To undoubtedly confirm the effect of MAML1 and E6AP on E6 protein levels, both densitometric and statistical analysis were performed unifying multiple experiments (**Figure 27B**). LOG2 of fold changes is depicted as a box and whisker plot. This type of graphical statistic representation was chosen so that the increase in a band intensity is seen as a positive value and the decrease as a negative value.

HEK-293 cells that were used in above-described assays endogenously express functional cellular E6AP ubiquitin ligase. Therefore, to unquestionably confirm that the upregulatory effects on E6 protein levels observed in HEK-293 cells were indeed exclusively MAML1 dependent, and not depending on the effects of the endogenous levels of E6AP, it was necessary to include additional cell line with abolished expression of E6AP. For this reason, HEK-293 E6AP KO cells were transiently transfected with the same set of HA-tagged E6 expressing plasmids from HPV types -8, -12, -14, -16, -18, -24, -33 and -38 E6, either alone or together with MAML1 or E6AP, and analysed in the manner as described in **Figure 27**. Interestingly, all assessed E6 proteins from both  $\alpha$ - and  $\beta$ -HPVs again exhibited increased protein levels as a consequence of E6/MAML1 interaction, which was confirmed by multiple independent experiments (**Figure 28A**). This result additionally supported the initial observations and further confirmed that the effect on increased E6 proteins amounts is regulated by MAML1, independently of E6AP. Additionally, even in an E6AP-null background both MAML1 and E6AP expressions induced increasement in the protein levels of cutaneous HPV-24 and HPV-38 E6, as was also previously observed in HEK-293 cells. **Supplementary Figure 2** separately presents negative controls for **Figure 28A**.

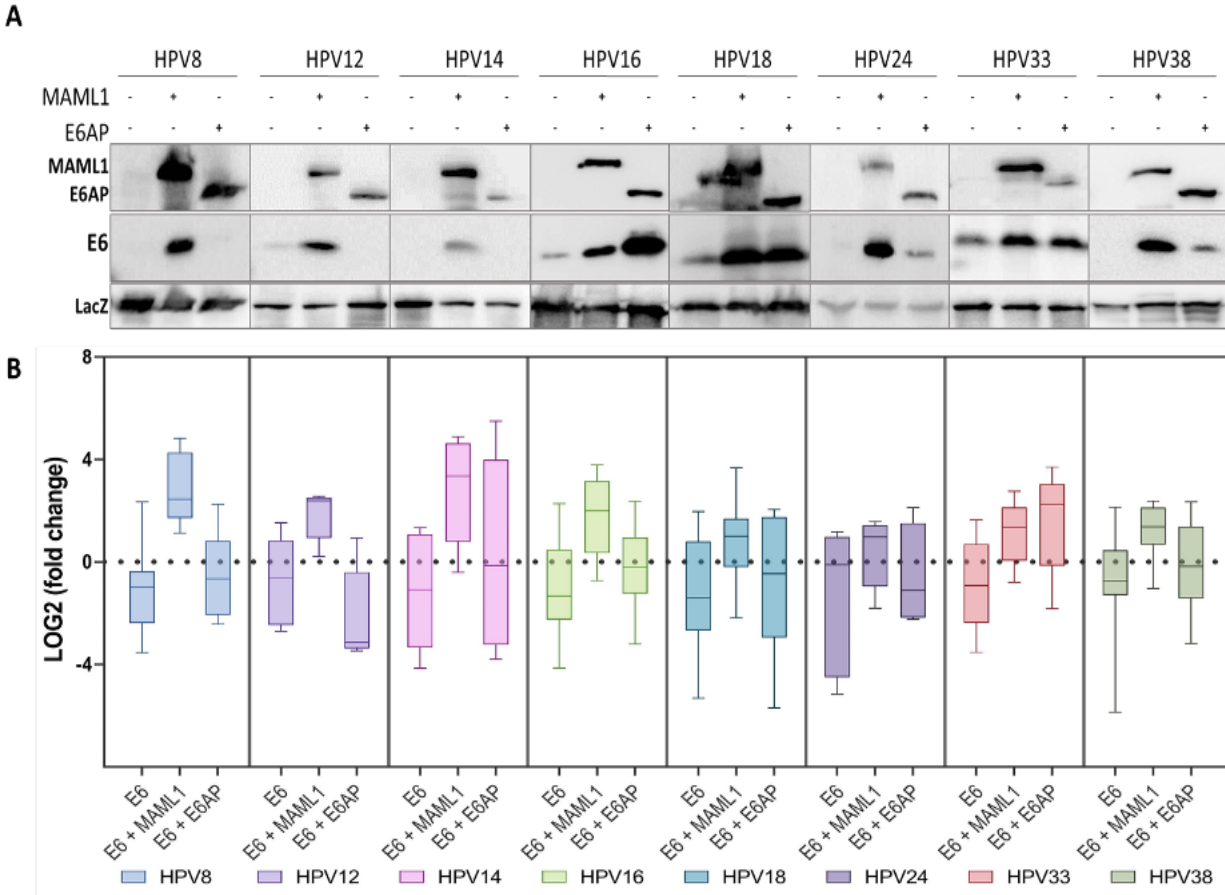


**Figure 28. MAML1-mediated upregulation of  $\alpha$ - and  $\beta$ -E6 protein levels are E6AP-independent.** (A) HEK-293 E6AP KO cells were transfected with HA-tagged HPV-8, -12, -14, -16, -18, -24, -33 and -38 E6 either alone or in combination with either FLAG- or Myc-tagged MAML1 or E6AP. After 24 hours the cells were harvested and isolated proteins separated on SDS-PAGE. Proteins were detected by western blot analysis using anti-FLAG or anti-Myc and anti-HA antibodies and visualized by chemiluminescence.  $\beta$ -galactosidase (LacZ) was used as a control to monitor transfection efficiency and loading. (B) Densitometric analysis was performed with ImageJ software. The band density was normalized with background density and relative expression was calculated. Average relative expressions of control E6s were calculated and all other relative E6 expressions were compared to those values, in order to obtain E6 fold change. Each fold change in the samples where E6s were co-transfected with MAML1 or E6AP was calculated according to the corresponding values of E6 transfected alone from the same experiment. Graphical representation was done in a GraphPadPrism by showing LOG2 of fold changes as a box and whisker plot. Each experiment was repeated at least three times and all experiments were included in statistical analysis.

To statistically confirm the effect of MAML1 and E6AP on E6 protein levels in HEK-293 E6AP KO cells, densitometric and statistical analysis were performed in the same manner as described for HEK-293 transfections, using same statistical method to assess the significance of

the results (**Figure 28B**). Altogether, from multiple experiments presented in **Figures 27** and **28** it is evident that the increase in E6 protein levels mediated by E6AP and MAML1 occurred in both cellular backgrounds. However, the proteins amounts varied among different types of E6, regardless of whether they were from  $\alpha$ - or  $\beta$ -HPVs. Those differences in increased protein levels can be attributed to the diverse strengths and intensities of the interactions between MAML1 and E6 proteins among distinct HPV types. This notion agrees with differences in the strength of interactions between MAML1 and E6s observed in GST pull-down assay (**Figure 26C**).

#### **4.10. An LXXLL motif of MAML1 is required for HPV E6 protein level regulation**

As it was described extensively in the introduction, both MAML1 and E6AP share an LXXLL motif, through which they interact with E6 oncoproteins (Nicole Brimer, Drews, and Vande Pol 2017c).  $\alpha$ -HPV E6s were demonstrated to associate with E6AP by binding to a conserved LXXLL motif on E6AP. This interaction is responsible for the stability of the E6 oncoprotein (Tomaić, Pim, and Banks 2009a), and also a prerequisite for the formation of a ternary complex with several cellular substrates. This results in ubiquitin molecules transfer from the ubiquitin ligase to these protein substrates, which are then subjected to proteasome-mediated degradation (Huibregtse, Scheffner, and Howley 1993d; M. Scheffner et al. 1993). The acidic domain located on the C-terminus of MAML1 also contains the LXXLL motif responsible for its association with HPV E6s (N. Brimer et al. 2012b; Tan et al. 2012b).

Based on aforementioned, the following aim was to determine whether an intact, wild-type LDDLL motif was necessary for MAML1 to induce increase in the E6 protein levels, as observed in the previous results (**Figures 27** and **28**). Therefore, in order to assess whether the LDDLL-binding motif is essential for the increase of E6s' protein amounts, the following experiments utilized a mutated form of MAML1. This MAML1 mutant used in the following experiments was created by inserting point mutations in two adjacent aspartate residues of the LDDLL motif, which were replaced by histidines, resulting in the LHHLL motif (**Figure 29**). This specific mutant was chosen based on previous research which demonstrated that the LHHLL mutation partially blocked  $\beta$ -E6 mediated inhibition of NOTCH signaling (Meyers et al. 2017b).



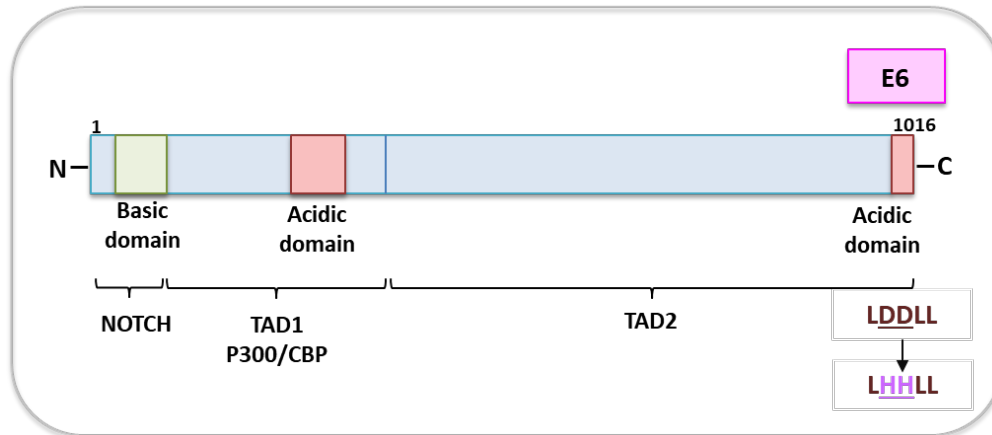


**Figure 29. Schematic representation of MAML1 protein structure with indicated point mutations in LXXLL motif.** MAML1 contains an N-terminal basic domain and two acidic domains (N- and C-terminal). In MAML1 structure there are two transcriptional activation domains (TADs), with TAD2 required for the involvement in Notch signaling. LXXLL motif is part of TAD2, located on the extreme C-terminus of the acidic domain of MAML1 (aa 1009-1013) and it is required for HPV E6 binding. Aspartate residues of the LDDLL motif were mutated to histidines (LHHLL) by inducing two point mutations in a nucleotide sequence of MAML1 gene. Adapted from (McElhinny, Li, and Wu 2008).

Hence, HEK-293 cells were transfected with plasmids expressing HPV-16, -18, and -8 E6, either alone or in combination with FLAG- or Myc-tagged MAML1 containing wild type LDDLL motif, or with the MAML1 mutant (MAML1 LHHLL). As can be seen from the results presented in **Figure 30A**, both wild-type MAML1 and MAML1 LHHLL mutant were found to increase HPV-8 and -18 E6 protein levels. However, differences in E6 protein level upregulation were observed between the mutant and wild type MAML1, which indicated that MAML LHHLL mutant exhibits a lower capacity to affect E6 protein levels in comparison with wild-type MAML1. This was the case for both HPV-8 and -18 E6. Interestingly, no discernible increase in HPV-16 E6 protein levels was observed as a result of its interaction with the LHHLL mutant. This implies to the differences in the interaction strength among different E6 oncoproteins and MAMIL1, even though they belong to the same genera and have similar oncogenic potential which is the case with HPV-16 and HPV-18 E6 (**Figure 30A**). This observation is also consistent with the differences in the strength of interactions between MAML1 and E6 previously observed in the GST pull-down assay, where HPV-16 E6 exhibited a lower affinity of binding to MAML1 in comparison to both HPV-18 and HPV-8 E6 (**Figure 26C**).

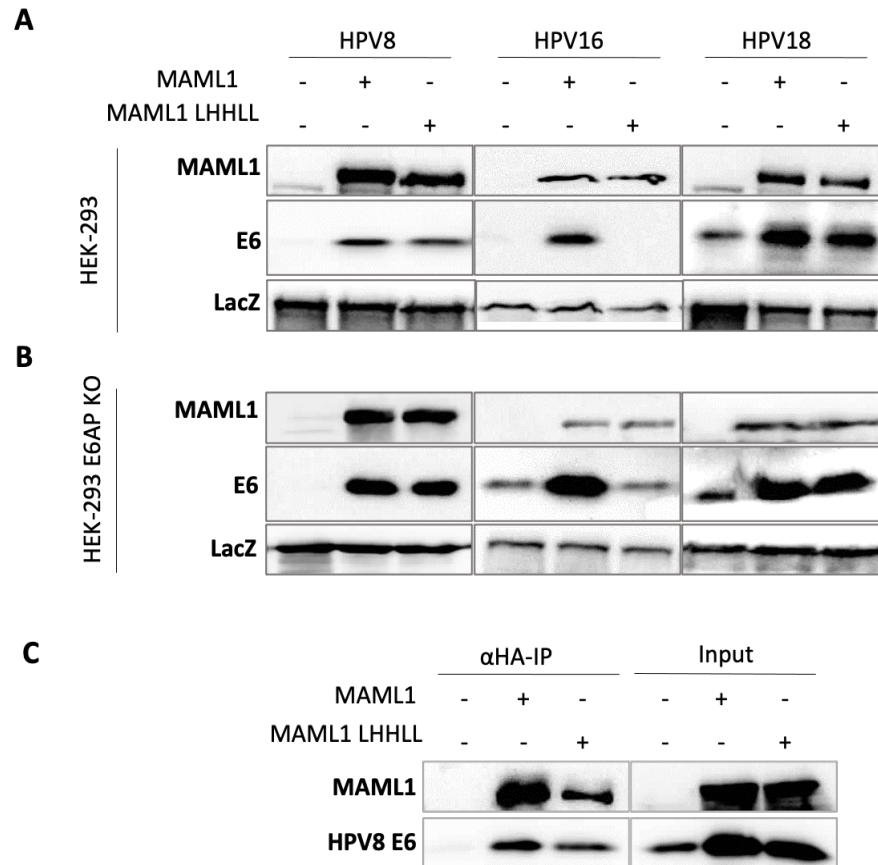


**Figure 30. MAML1 is involved in the regulation of E6 protein amounts via LXXLL motif.** (A) HEK-293 and (B) HEK-293 E6AP KO cells were transfected with either HA-tagged HPV-8, -16 and -18 E6 alone or in combination with FLAG-tagged MAML1 or FLAG-tagged MAML1 mutant (MAML1 LHHLL). After 24 hours cells were harvested, isolated proteins were separated on SDS-PAGE and analyzed by western blotting. MAML1 and MAML1 LHHLL were detected using anti-FLAG antibody, while E6s were detected with an anti-HA antibody.  $\beta$ -galactosidase (LacZ) was used as the control for the transfection efficiency and loading. (C) HEK-293 cells were transfected with HA-tagged HPV-8 E6 alone or in combination with FLAG-tagged MAML1 or FLAG-tagged MAML1 LHHLL. Transfected cells were harvested, lysed in E1A buffer and incubated with anti-HA beads on a rotating wheel at RT. The beads were extensively washed and co-immunoprecipitated complexes were subjected to western blot analysis with anti-FLAG and anti-HA antibodies to compare to the amount of transfected MAML1, MAML1 LHHLL or HPV-8 E6 present in 10% of the input.

Again, the findings were confirmed by repeating the same experiment in HEK-293 E6AP KO cells, to exclude any potential impact of endogenous E6AP. Cells were transfected with plasmids expressing HPV-16, -18, and -8 E6, either alone or in combination with FLAG- or Myc-tagged MAML1, or with FLAG- or Myc-tagged MAML1 LHHLL mutant (**Figure 30B**). The

proteins were isolated and subjected to western blot analysis in the same manner as described for **Figure 30A**. The results of this assay clearly demonstrated that both wild-type MAML1 and MAML1 LHHLL mutant increased HPV-8 and -18 E6 protein levels, although with different intensities. Since this observation was consistent in both cellular backgrounds, including HEK-293 and HEK-293 E6AP KO cells, it can be concluded that the increase of  $\alpha$ - and  $\beta$ -HPV E6 protein levels occurred regardless of the presence of the mutated LDDLL domain. **Supplementary Figure 3**, separately depicts negative controls for **Figures 30A** and **30B**.

After observing unique and noteworthy patterns in the interaction between MAML1 and both  $\alpha$ - and  $\beta$ -HPV E6 oncoproteins, as well as the significance of the LDDLL domain, the next step in the research was to delve deeper into these discoveries through the utilization of co-immunoprecipitation experiment. Performing this analysis was important to determine if the E6/MAML1 complex was formed exclusively through the LXXLL motif or if other parts of the interacting proteins were potentially involved. Hence, a co-immunoprecipitation analysis was performed using HEK-293 cells transfected with plasmid expressing HA-tagged HPV-8 E6, alone or in combination with FLAG-tagged MAML1 and MAML1 LHHLL (**Figure 30C**). Negative controls for **Figure 30C** are shown separately on **Supplementary Figure 4**. Twenty-four hours post transfection the cells were harvested, lysed using E1A immunoprecipitation buffer and the cell extracts were incubated with anti-HA beads. Immunoprecipitated protein complexes were separated on SDS-PAGE and analysed by western blotting using HRP-conjugated anti-HA antibody to detect E6 oncoproteins, along with anti-FLAG antibody which detected MAML1 and MAML1 LHHLL mutant. With this protein interaction analysis, it was shown that the mutated LDDLL motif in MAML1 did not fully abrogate the interaction with HPV-8 E6, since HPV-8 E6 still co-immunoprecipitated with MAML1 LHHLL. Although the degree of interaction between HPV-8 E6 with MAML1 LHHLL was lower in comparison with wild-type MAML1 which was reflected on the reduced binding capacity shown in **Figures 30A** and **30B**, the co-immunoprecipitation assay validated that the LXXLL binding motif is involved in facilitating the E6/MAML1 interaction.

Taken all of this together, it appears that all 5 amino acids which are a part of the intact LDDLL motif are involved in the association with E6s. Sterically this interaction can be extended even to other amino acids upstream or downstream of the LXXLL motif, since the mutant still interacted with HPV-8 E6, although to a lesser degree, which was accompanied by a reduction of

E6 protein levels (**Figure 30**). Based on these results, it is possible to speculate that mutating other amino acids in LDDLL motif may be necessary in order to further decrease or completely block the interaction between MAML1 and E6 oncoproteins. As such, future research could focus on identifying other critical amino acids and evaluating their impact on the interaction using the same techniques as site-directed mutagenesis and co-immunoprecipitation assays.

#### **4.11. The stability of HPV E6 protein pool in HeLa, CaSki and HT1080 HPV-8 E6 cells is MAML1-mediated**

Since the overexpression of MAML1 and E6 oncoproteins from different  $\alpha$ - and  $\beta$ -HPV types resulted in the increase of E6 protein levels in both HEK-293 cells and HEK-293 E6AP KO cells, this effect was further explored in HPV-positive cell lines with endogenous expression of E6. To investigate the effects of endogenous expression, HeLa (HPV-18 positive cervical adenocarcinoma cell line) and CaSki (HPV-16 positive advanced squamous cervical carcinoma cell line) cells were selected as the preferred experimental cell model due to their widespread availability and frequent use in research. In addition to HeLa and CaSki cells, the analysis also included HT1080 fibrosarcoma epithelial cell line, specifically an HT1080 cell line that stably expresses HA-tagged HPV-8 E6 (Hufbauer et al. 2015a). By incorporating these cells, it was sought to gain a more comprehensive understanding of the consequences of the interactions between MAML1 and HPV E6 oncoproteins across different cell types under endogenous experimental conditions. The effects on E6 protein levels in HPV-positive cell lines were explored in a reverse manner regarding to previous overexpression experiments, by abrogating endogenous levels of MAML1 and E6AP. All described cell lines were transiently transfected with siRNA to silence MAML1 (siMAML) and UBE3A/E6AP (siE6AP) genes, while siRNA against luciferase (siLuc) was used as control. To assess whether the process of stabilization and the increase of protein levels is proteasome dependent, cellular proteasome machinery was abrogated using the proteasome inhibitor bortezomib (BTZ). Cells were harvested and subjected to SDS-PAGE western blot analysis with anti-MAML1 and anti-E6AP antibodies to verify gene silencing. Having confirmed the successful ablation of MAML1 or E6AP, the following step was to assess the effect of silencing MAML1 and E6AP on E6 protein expression levels. In HeLa and HPV-8 FLAG

tagged-E6 expressing HT1080 cells this was assessed by using anti-HPV-18 E6 antibody for HeLa cells, and anti-FLAG antibody for HT1080 8 E6 cells.

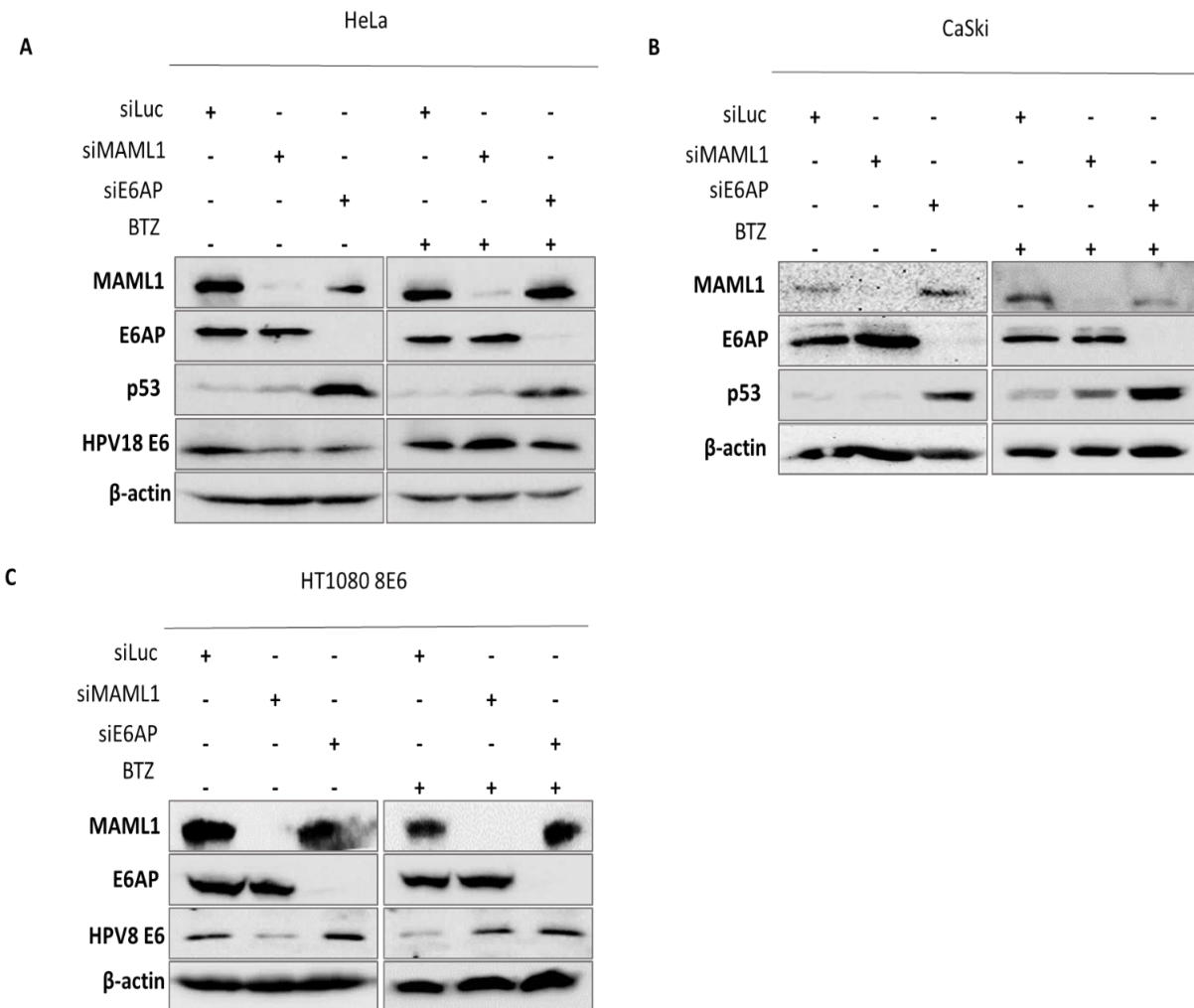


**Figure 31. MAML1 regulates endogenous E6 protein levels in HeLa, CaSki and HT1080 HPV-8 E6-expressing cells.** (A) HeLa cells were transfected with smartpools of the target siRNA, including siMAML1 or siE6AP, or siLuc as a control. Forty-eight hours after silencing, proteasome inhibitor bortezomib (BTZ; 10  $\mu$ M) was added. The cells were incubated for a further 24 hours after which were harvested, separated on SDS-PAGE and detected by western blot analysis with anti-MAML1, anti-E6AP, anti-HPV-18 E6, and anti-p53 antibodies.  $\beta$ -actin was used as a protein loading control. (B) CaSki were transfected with siMAML1 or siE6AP, or siLuc as a control. Forty-eight hours after silencing bortezomib was added. The cells were incubated for a further 24 hours after which were harvested, separated on SDS-PAGE and detected by western blot analysis with anti-MAML1, anti-E6AP and anti-p53 antibodies. (C) HT1080 HPV-8 E6 cells were transfected with either siMAML1 or siE6AP, or siLuc as a control. Forty-eight hours after silencing bortezomib was added. The cells were incubated for a further 24 hours after which were harvested, separated on SDS-PAGE and detected by western blot analysis with anti-MAML1, anti-E6AP and anti-FLAG (for detection of HPV-8 E6) antibodies.

The effect on the E6 protein levels in CaSki cells was evaluated in an indirect way, by using p53 as a surrogate marker and extrapolating HPV-16 E6 protein levels from the detected p53 protein levels using anti-p53 antibody, as p53 is degraded in the presence of HR E6 and E6AP (M. Scheffner et al. 1993; 1990b; Huibregtse, Scheffner, and Howley 1993c). The reason behind this approach is that commercially available anti-HPV-16 E6 antibodies were shown to be unsatisfactorily effective in the successful and precise detection of endogenous HPV-16 E6 levels.

As it can be seen from a **Figure 31A**, silencing MAML1 in HeLa cells induced a decrease in HPV-18 E6 protein levels. Inhibition of proteasomal degradation with BTZ annulled this effect, indicating that maintenance of HPV-18 E6 protein levels is associated with functional proteasome. Furthermore, it was surprising that silencing MAML1 and a subsequent decrease in the amount of E6 had no effect on p53 protein levels. It would have been expected that a decrease in the amount of E6 would lead to an increase in p53 protein levels as a result of a reduction of p53 degradation (M. Scheffner et al. 1993; Wynn H. Kao et al. 2000), but this effect was absent (**Figure 31A**). However, the effect on increased p53 protein levels was observed when E6 was downregulated as a result of E6AP silencing (**Figure 31A**), which in agreement with previously published results (Tomaić, Pim, and Banks 2009a). Silencing MAML1 and E6AP in CaSki cells resulted in a similar pattern of E6 protein expression levels as seen in HeLa cells, where silencing MAML1 also had no effect on p53 protein levels as can be seen from the expression profile of p53 that was similar to the one observed in HeLa cells (**Figure 31B**). Inhibition of the proteasomal degradation with BTZ resulted in an increase of p53 protein levels indicating that HPV-16 E6 protein levels and consequent p53 degradation were also associated with the proteasome machinery, same as in HeLa cells. Silencing E6AP resulted in the accumulation of p53 as a subsequent effect of E6 depletion (**Figure 31B**), again in agreement with previously published results (Tomaić, Pim, and Banks 2009a). Furthermore, silencing MAML1 in HPV-8 E6 expressing HT1080 cells also resulted in downregulation of HPV-8 E6. This effect was annulated when BTZ was added, suggesting that MAML1 is required for protein stabilization of  $\beta$ -HPV E6s, which is accomplished by confirming an involvement of the proteasome (**Figure 31C**). In the case of silencing E6AP, downregulation of E6AP had no effect on HPV-8 E6 levels, suggesting that E6AP is not indispensable for  $\beta$ -HPV-8 E6 protein stabilization, in contrast to  $\alpha$ -HPV E6s (**Figure 32C**). These results further support the phenotype presented in **Figures 27** and **28**, where overexpression of E6AP with HPV-8 E6 does not lead to its increased protein levels.

#### **4.12. MAML1 stabilizes a distinctive cellular pool of HPV-18 E6 and an exclusive single cellular pool of HPV-8 E6**

After confirming the interaction between both  $\alpha$ - and  $\beta$ -HPV E6s and MAML1, using protein interaction assays (immunoprecipitation and GST pull-down assay), and exploring the effects of these interactions on the protein levels and stability of  $\alpha$ - and  $\beta$ -HPV E6 oncoproteins using the ectopic expression and gene silencing assays in HPV-positive cell lines, the next objective was to assess cellular localization of p53 (used as a control for E6 expression in HeLa cells) and HPV-8 E6 oncoprotein. These experiments were carried out to investigate potential changes in subcellular localization of HPV E6s in presence and absence of endogenous MAML1.

The assessment of cellular localization of p53 and HPV-8 E6 was conducted by silencing MAML1 and E6AP expression levels in HeLa and HPV-8 E6-expressing HT1080 cells. Hence, cells were transfected with siMAML and siE6AP, or siLuc as a control. Seventy-two hours post transfection, cells were fixed and incubated with anti-MAML1, anti-E6AP and anti-FLAG (for detecting HPV-8 E6) antibodies, while monitoring of p53 localization was done by anti-p53 antibody, which served as a readout for HPV-18 E6 ablation in HeLa cells. The appropriate secondary antibodies conjugated with fluorophores were applied and changes in p53 and HPV-8 E6 cellular localization were monitored by laser scanning confocal microscopy. Ablation of E6AP in HeLa cells led to an increase in p53 protein recovery and consequent accumulation in the nucleus, due to the downregulation of 18 E6, whose stability was disrupted in the absence of E6AP (**Figure 32A**). On the contrary, ablation of MAML1 in HeLa cells did not have any effect on the nuclear accumulation of p53, in comparison to cells treated with siLuc (**Figure 32B**). This result is in an agreement with the result presented in **Figure 31A** where silencing MAML1 in HeLa cells and the subsequent decrease in detectable E6 levels had no effects on p53 protein levels. By contrast, silencing E6AP under the same experimental conditions in HT1080 HPV-8 E6 cells did not result in an evident effect on HPV-8 E6 protein levels (**Figure 33A**). This observation is also in agreement with the result of HPV-8 E6 protein levels from **Figure 31C**, which showed that downregulation of E6AP had no effect on HPV-8 E6 protein levels. Furthermore, MAML1 silencing in HPV-8 E6-expressing HT1080 cells resulted in the downregulation of nuclear HPV-8 E6 protein levels (**Figure 33B**).

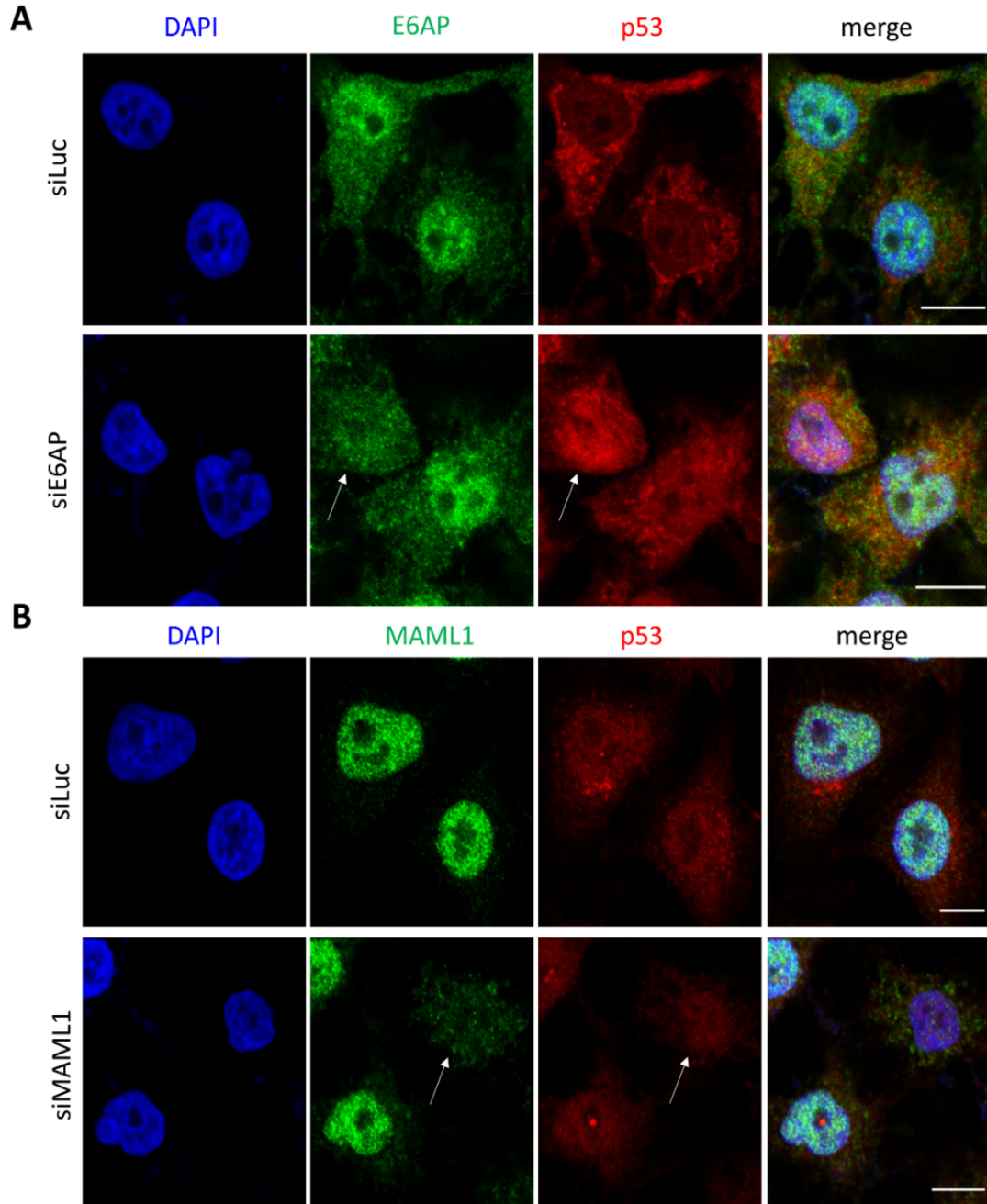


**Figure 32. MAML1 stabilizes distinctive cellular pools of HPV-18 E6.** HeLa cells were transfected with siLuc, (A) siE6AP and (B) siMAML1. Seventy-two hours post transfection the cells were fixed and stained with antibodies against MAML1 and E6AP to determine the silencing efficiency, and p53 as readout for HPV-18 E6 silencing detected with anti-p53 antibody. Anti-mouse and rabbit secondary antibodies conjugated to Alexa Fluor 488 or Rhodamine Red were used, and nuclei were visualized with DAPI. The excitation wavelengths and the detection wavelength range were 540 nm and 570-590 nm for Rhodamine Red, 490 nm and 500-550nm for Alexa-488 and 405 nm and 430-500 nm for DAPI. Scale bars are 10  $\mu$ m and arrows point towards cells of interest.



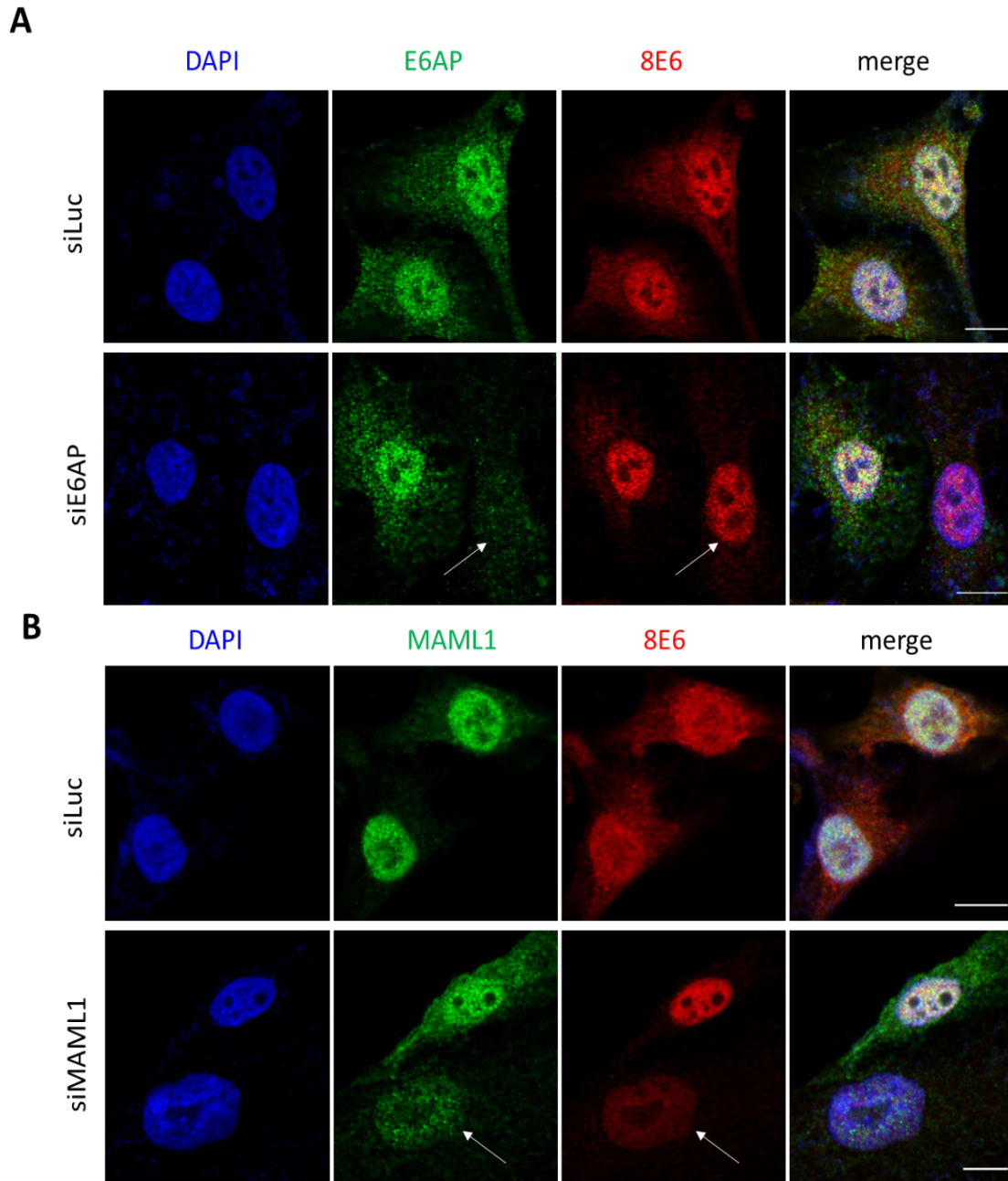


**Figure 33. MAML1 stabilizes an exclusive single cellular pool of HPV-8 E6.** HT1080 8 E6 cells were transfected with siLuc, (A) siE6AP and (B) siMAML1. Seventy-two hours post transfection the cells were fixed and stained with antibodies against MAML1 and E6AP to determine the silencing efficiency, and anti-FLAG to determine localization of HPV-8 E6. Anti-mouse and rabbit secondary antibodies conjugated to Alexa Fluor 488 or Rhodamine Red were used, and nuclei were visualized with DAPI. The excitation wavelengths and the detection wavelength range were 540 nm and 570-590 nm for Rhodamine Red, 490 nm and 500-550 nm for Alexa-488 and 405 nm and 430-500 nm for DAPI. Scale bars are 10  $\mu$ m and arrows point towards cells of interest.

These results are in line with the observations from the western blot analyses (**Figure 31**), revealing that silencing MAML1 does not have an effect on the cellular pool of HPV-18 E6 involved in p53 degradation. This further suggests that there are likely two or more cellular pools of HPV-18 E6 with distinct functions and interactions with different host proteins. Additionally, the lack of impact on HPV-8 E6 protein stability upon silencing of E6AP, consistent with the previous finding (**Figure 31C**), suggests the presence of a single cellular pool of HPV-8 E6 that exclusively interacts with MAML1.

#### **4.13. p53 and DLG1 degradation is not E6/MAML1 complex dependent**

To further monitor the recovery effects of endogenous p53 in HPV-18-positive HeLa cells, observed both in siRNA silencing experiments analysed by western blotting and confocal microscopy, additional experiments were conducted in cultured cells. Specifically, the aim was to explore the impact of MAML1 and E6AP coexpressed with HPV-16 E6 on p53 protein levels in the overexpression system. In order to determine whether the changes in p53 protein levels are specifically caused by the 16 E6/MAML1 interacting complex, rather than by the influence of endogenous E6AP, it was essential to include HEK-293 E6AP KO cells with impaired E6AP expression. This would allow to sequester the effects of 16E6/MAML1 complex on p53 expression without any interference from endogenous E6AP. Transfections were performed using FLAG-tagged MAML1, E6AP and p53, while 16 E6 was HA-tagged. As depicted in **Figure 34A**, MAML1 overexpression with HPV-16 E6 did not induce enhanced degradation of p53, even though increased E6 protein levels were detected, which agrees with all previously shown results (**Figures 28B** and **31B**). Furthermore, as it was expected, the overexpression of E6AP resulted in both higher protein levels of HPV-16 E6 and enhanced degradation of p53 (**Figure 34A**), as previously published (M. Scheffner et al. 1993; 1990b). **Figure 34B** shows a graphic representation of the statistical analysis done in a GraphPadPrism software, recapitulating the representative result presented on the blot, and demonstrating from the multiple experiments that the E6/MAML1 complex is not involved in p53 degradation.

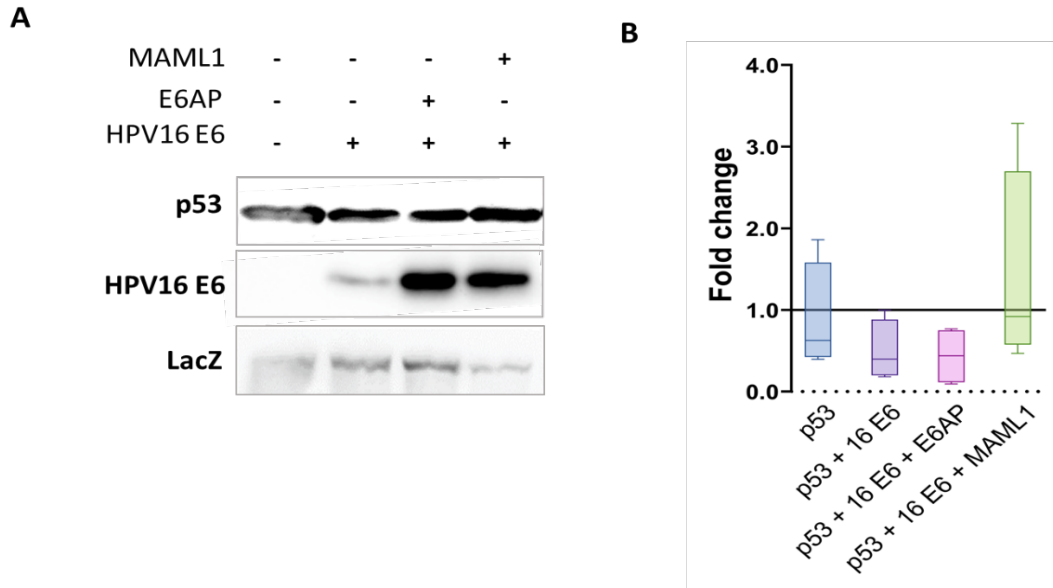


**Figure 34. 16 E6/MAML1 complex does not induce p53 degradation.** (A) HEK-293 E6AP KO cells were transfected with p53 expression plasmid in combination with HA-tagged 16 E6 alone or in combination with either FLAG-tagged MAML1 or E6AP. Twenty-four hours post transfection the cells were harvested, isolated proteins were separated on SDS-PAGE, subjected to western blot analysis and proteins were detected with anti-FLAG, anti-p53 and HRP-conjugated anti-HA antibodies.  $\beta$ -galactosidase (LacZ) was used as control to monitor transfection efficiency and loading. (B) Densitometric analysis was performed with ImageJ software by quantifying band densities for p53 protein expression normalized for background densities, after which relative expression was calculated by dividing p53 normalized density values with LacZ normalized density values. p53 average normalized relative expression was calculated for the control sample, and all normalized relative expressions were compared to that value. Statistical analysis was done in GraphPadPrism program. Fold change was calculated by dividing the relative expression of p53 in samples transfected with either MAML1 or E6AP with average relative expression of sample transfected with p53 alone. Each experiment was repeated at least four times.

Apart from p53, HR E6s also target PDZ-domain containing cellular proteins for proteasome-mediated degradation and this process is considered to play an essential role in later stages of HPV-induced malignancies (C. A. Moody and Laimins 2010a; M. Thomas et al. 2008a), as was extensively explained in the Introduction and the first part of Results section. The tumor suppressor DLG1 is a cellular polarity protein bound by a number of different HR E6s via their PBMs (Miranda Thomas et al. 2016), which is an important feature, since different HPV types have diverse sequences of their E6 PBMs, resulting in their diverse target profile (Miranda Thomas et al. 2005). Furthermore, it was previously shown that catalytically active E6AP is essential for the ability of E6 to degrade p53 (M. Scheffner et al. 1993), while DLG1 and the MAGI family

proteins were shown to be degraded by E6 quite effectively even without E6AP, indicating that E6 targets these cellular substrates in an E6AP-independent manner (Vats, Thatte, and Banks 2019). It is also the main reason why DLG1, as an E6AP-independent target, was along with p53, which is an E6AP-dependent target included in further analysis investigating the role of MAML1 in E6 degradatory activities. Therefore, the following experiment proceeded to investigate whether HR E6 stabilization by MAML1 might have an impact on targeting DLG1. Similar as in the experiment with p53 degradation, HEK-293 E6AP KO cells were transfected with a plasmid expressing HA-tagged DLG1 either in the presence or absence of 16 E6, and together with either FLAG-tagged E6AP or MAML1. Twenty-four hours post transfection, the isolated proteins were separated on SDS-PAGE, analysed by western blotting using HRP-conjugated anti-HA antibody to detect DLG1 and 16 E6, and anti-FLAG antibody to detect MAML1 and E6AP. From **Figure 35A** it can be seen that DLG1 was degraded very efficiently by HPV-16 E6 both in the presence or absence of E6AP, as it was expected from the previous research (Vats, Thatte, and Banks 2019; Massimi et al. 2008; S. S. Lee, Weiss, and Javier 1997). On the contrary, co-expression of MAML1 and HPV-16 E6 did not result in any additional degradation of DLG1, when compared to 16 E6 alone, although E6 protein level upregulation was evident in presence of MAML1. **Figure 35B** shows a graphic representation of calculated fold change using a GraphPadPrism software and from the multiple experiments it is evident that the E6/MAML1 complex is not involved in the degradation of DLG1.

Based on the results obtained thus far, it appears that while both E6AP and MAML1 are involved in stabilizing  $\alpha$ - and  $\beta$ -HPV E6s, they do not promote stability of the same cellular pools of E6. When MAML1 is silenced in the case of  $\alpha$ -HPV-16 and 18 E6, the remaining pool of E6 is still in complex with E6AP, and retains its catalytic activity, leading to the degradation of well-characterized cellular targets p53 and DLG1. On the other hand, when MAML1 is overexpressed together with HR E6, the stability of the E6 pool bound to MAML1 is increased, but it seems that this particular cellular pool of E6 is not catalytically active in targeting cellular targets such as p53 or DLG1. These findings suggested that E6/MAML1 complex may have a broader role in cellular processes beyond the degradation of specific substrates and highlighted the need for further investigation to better understand the full range of functions associated with this complex, which will be described in the following text.

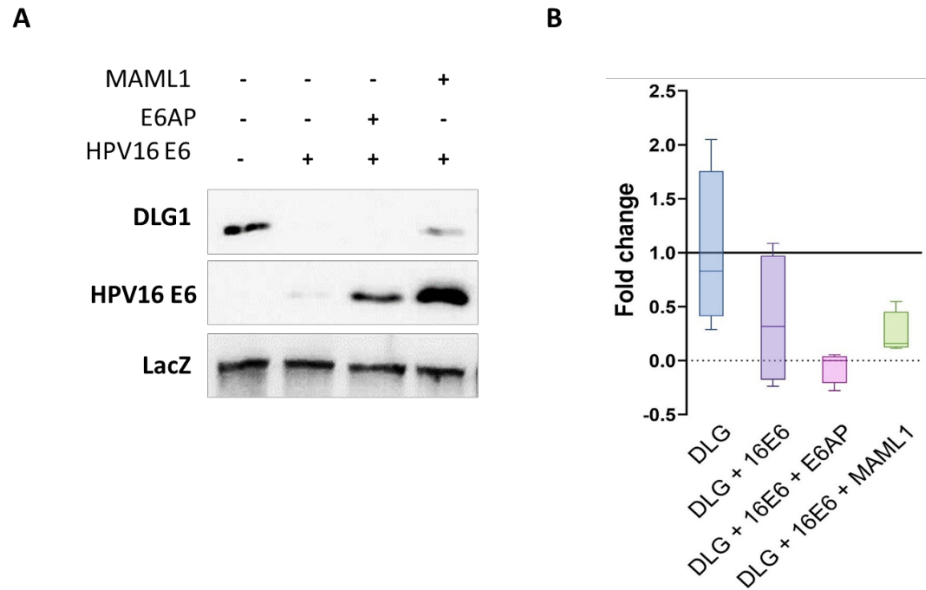


**Figure 35. E6/MAML1 complex does not induce DLG1 degradation.** (A) HEK-293 E6AP KO cells were transfected with HA-tagged DLG1 alone, in combination with HA-tagged 16 E6 or in combination with either FLAG-tagged MAML1 or E6AP. After 24 hours the cells were harvested and isolated proteins were separated on SDS-PAGE, detected by HRP-conjugated anti-HA and anti-FLAG antibodies with appropriate secondary antibodies, after which the proteins were visualized by chemiluminescence.  $\beta$ -galactosidase (LacZ) was used as control to monitor transfection efficiency and loading. (B) Densitometric analysis was performed with ImageJ software by measuring band densities for DLG1 protein expression that were normalized for background density, after which relative expression was calculated by dividing DLG1 normalized density values with LacZ normalized density values. DLG1 average normalized relative expression was calculated for control sample, and all normalized relative expressions of the co-transfected samples were compared to that value. Statistical analysis was done in GraphPadPrism calculating fold change by dividing the relative expression of DLG1 in samples transfected with either MAML1 or E6AP with average relative expression of sample transfected with DLG1 alone. Each experiment was repeated at least four times and all those experiments were included in statistical analysis.

#### 4.14. HPV E6 protein turnover is regulated by MAML1

After demonstrating that MAML1 silencing results in the downregulation of E6 protein levels (**Figure 31** and **Figure 33**), the subsequent inquiry was to determine how MAML1 affects the turnover rates of E6 protein of both  $\alpha$ - and  $\beta$ -HPV types. To investigate this, siRNA silencing was employed to abolish the expression of MAML1, E6AP, or both in HeLa and HPV-8 E6-expressing HT1080 cells, followed by a cycloheximide chase assay performed in these cellular

contexts. siLuc was used as a control. Seventy-two hours post silencing protein synthesis was blocked by a cycloheximide inhibitor in order to determine the rate of E6 protein turnover in a cellular condition when novel protein synthesis was blocked. After blocking the protein synthesis, the cells were collected and harvested at different time points (0, 30, 60, 90, 120 min), isolated proteins were separated on SDS-PAGE and detected by western blotting using anti-MAML1, anti-E6AP, anti-HPV-18 E6 antibodies and anti-FLAG antibody to detect HPV-8 E6 (**Figure 36**).  $\beta$ -actin was used as internal control for transfection efficiency.

Lower panel of **Figure 36** depicts the obtained densitometric analysis results presented in a form of the column graph. The initial band intensity of HPV-18 E6 at 0 min time point was taken as 100%, and the density at other time points were calculated as percentage of the decreased starting amount. Hence, after performing western blot and densitometric analyses it was observed that the half-life of HPV-18 E6 in control HeLa cells treated with siLuc was around 120 min (**Figure 36**), which is in agreement with previously reported results (Tomaić, Pim, and Banks 2009a; Androphy et al. 1987). Silencing either MAML1 or E6AP led to a shorter E6 half-life, with HPV-18 E6 half-life being around 90 min when MAML1 was silenced. Furthermore, silencing E6AP resulted in shortening of half-life even more, which was around 80 min. Silencing of both MAML1 and E6AP induced a further decrease in HPV-18 E6 half-life to approximately 60 min, indicating a synergistic effect of MAML1 and E6AP on HPV-18 E6 half-life, which was statistically confirmed (**Figure 36**).

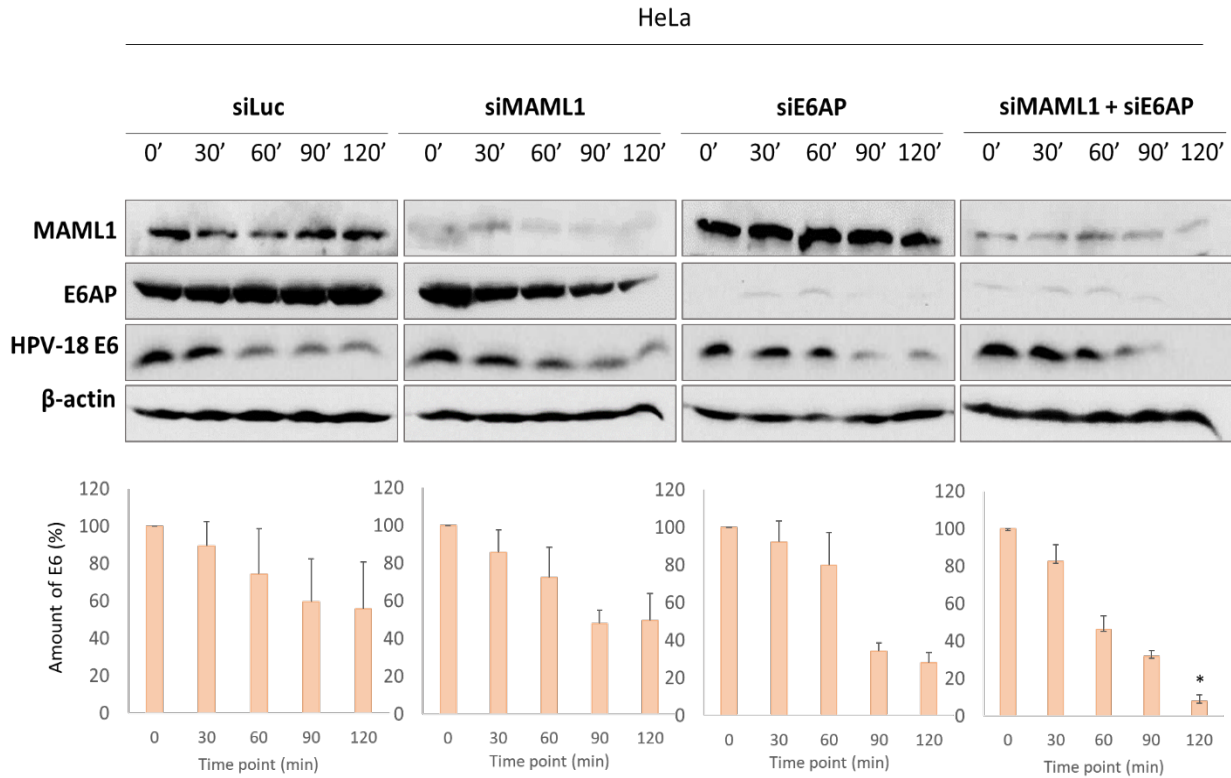


**Figure 36. MAML1 and E6AP exhibit a synergistic effect on HPV-18 E6 half-life.** HeLa cells were transfected with siRNAs siLuc, siMAML1 and siE6AP either alone or in combination. Seventy-two hours after silencing the cells were treated with cycloheximide inhibitor and harvested at indicated time points. E6 protein expression levels were analysed by SDS-PAGE and western blotting with anti-MAML1, anti-E6AP and anti-18 E6 antibodies.  $\beta$ -actin was used as internal control to monitor protein loading. Densitometric analysis was performed with ImageJ software. Band densities were first normalized for background density for each of the samples after which relative expression was calculated by dividing E6 normalized density with  $\beta$ -actin normalized density. The initial band intensity of 18 E6 at 0 min time point was taken as 100%, and the density at other time points were calculated as percentage of the decreased starting amount. The obtained statistical results are presented as column graphs with standard deviations (SD) indicated as a bar (lower panel). Each experiment was repeated at least three times. Significance was determined by ANOVA test using MedCalc, with  $p < 0.05$  taken as significant, and marked with \* above the bar.

The cyclohexamide chase assay was repeated under the same experimental settings in HT1080 HPV-8 E6 cells. As can be seen from the results at **Figure 37**, HPV-8 E6 had a half-life even longer than the 120 min. Interestingly, the half-life of HPV-8 E6 in cells with silenced MAML1 exhibited a decrease between 90 and 120 minutes. As expected, silencing E6AP had no effect on HPV-8 E6 half-life (**Figure 37**). Silencing both MAML1 and E6AP did not lead to any

further decrease of HPV-8 E6 half-life, in comparison to the decrease seen with silencing only MAML1, and no synergistic effect was seen as it was the case with HPV-18 E6.

Findings presented in **Figures 36** and **37** provide additional evidence, which support the direct involvement of MAML1 in the protein turnover of HPV E6 oncoprotein of both  $\alpha$ - and  $\beta$ -HPVs. Moreover, these analyses additionally support the fact that MAML1 exclusively regulates the turnover of HPV-8 E6 protein, whilst E6AP has no effect on the protein stability of HPV-8 E6.

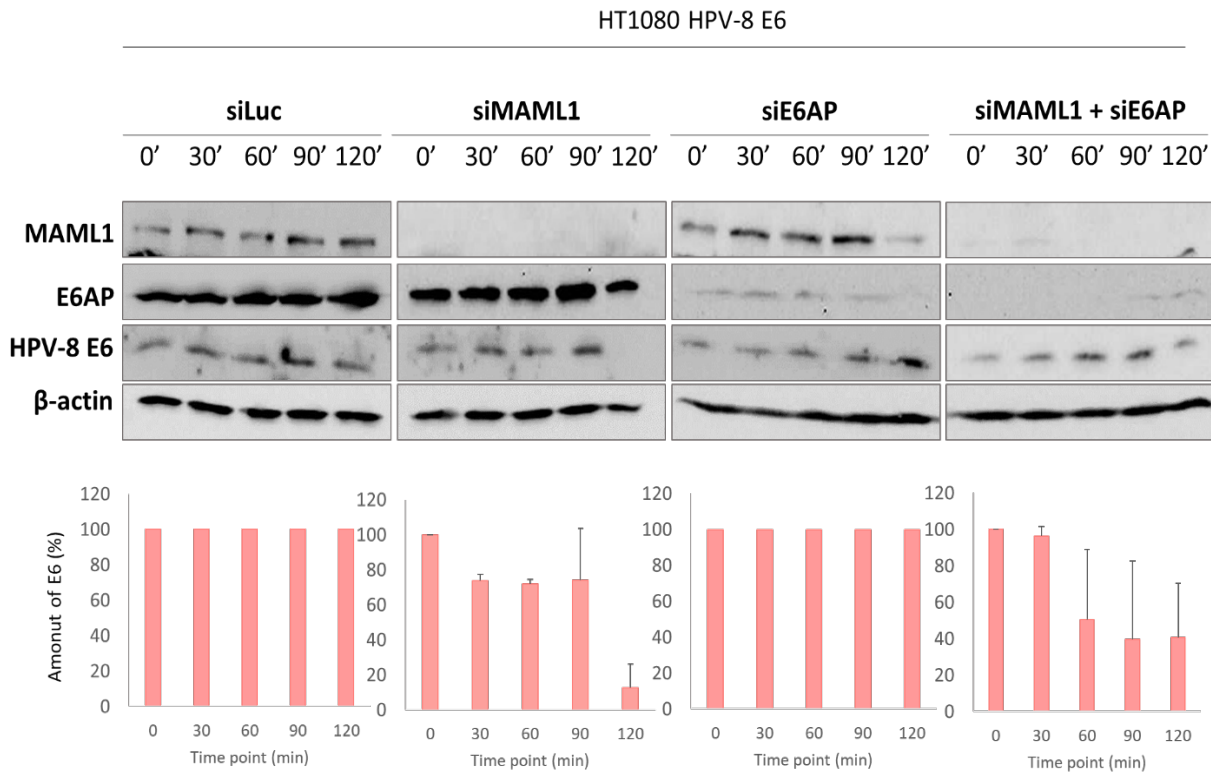


**Figure 37. HPV-8 E6 protein half-life is exclusively regulated by MAML1.** HT1080 HPV-8 E6 cells were transfected with siRNAs siLuc, siMAML1 and siE6AP either alone or in combination. Seventy-two hours after silencing the cells were treated with cycloheximide inhibitor added in cell culture medium. Cells were harvested at indicated time points. E6 protein expression levels were analysed by western blotting with anti-MAML1, anti-E6AP and anti-FLAG antibodies.  $\beta$ -actin was used as internal control to monitor protein loading. Densitometric analysis was performed with ImageJ software. Band densities were first normalized for background density for each of the samples after which relative expression was calculated by dividing E6 normalized density with  $\beta$ -actin normalized density. The initial band intensity of HPV-8 E6 at 0 min time point was taken as 100%, and the density at other time points were calculated as percentage of the decreased starting amount. The obtained statistical results are presented as column graphs with standard deviations (SD) indicated as a bar (lower panel). Each experiment was repeated at least three times.



#### 4.15. E6 cellular distribution is altered in presence of MAML1

Given that both MAML1 and E6AP stabilize  $\alpha$ - and  $\beta$ -HPV E6 proteins, an additional objective was to investigate whether these interactions affect the subcellular localization and distribution of E6 among different cellular compartments. To accomplish this, HEK-293 cells were transfected with either HA-tagged HPV-16 or -8 E6, either alone or in combination with FLAG-tagged MAML1 or E6AP. Cellular proteins were extracted using *ProteoExtract<sup>®</sup> Subcellular Proteome Extraction Kit* which enabled separation of cell lysates into cytosolic (C), membrane (M), nucleic (N) and microtubule (T) fractions. The fractionated proteins were separated on SDS-PAGE and detected via western blot analysis. The protein fraction purity was determined by incubation with specific antibodies that included anti-MCM7 for cytoplasm, anti-GAPDH for membrane, anti-histone H3 for nucleus and anti-vimentin for cytoskeleton.

As can be seen from the data presented on the top panel on **Figure 38**, HPV-16 E6 primarily localizes in the cytosolic fraction. Co-transfection with E6AP induces stabilization of cytosolic E6, but also increases 16 E6 protein levels in other three fractions. When 16 E6 was co-transfected with MAML1, these proportions have changed, and besides the signal detection in the cytosol, there was a notable increase in the amounts of E6 detected also in the nucleic and membrane fractions. MAML1 by itself localizes predominantly in the cytosolic fraction, with a smaller proportion in the microtubule fraction. By analysing protein levels of MAML1 in co-transfection with 16 E6, clear changes in a MAML1 distribution profile was visible, with a notable increase in the nucleic and membrane fractions, accompanied with 16 E6 accumulation in the same fractions (**Figure 38**, top panel). Co-transfection with 16 E6 also resulted in an increased accumulation of MAML1 in the cytoplasmic and microtubule fraction.

While examining the effect of MAML1 and E6AP on HPV-8 E6 distribution, a different pattern was observed. On the contrary to MAML1 and 8 E6 co-expression that caused an increase in the amount of 8 E6 in the cytosol, where MAML1 was predominantly detected, E6AP had no effects on HPV-8 E6 distribution (**Figure 38**, lower panel). The increase in the cytosolic 8 E6 when co-expressed with MAML1, as well as the stabilization of the nucleic E6, further confirmed the immunofluorescence results where MAML1 silencing in HPV-8 E6-expressing HT1080 cells resulted in the downregulation of nuclear HPV-8 E6 (**Figure 33B**).

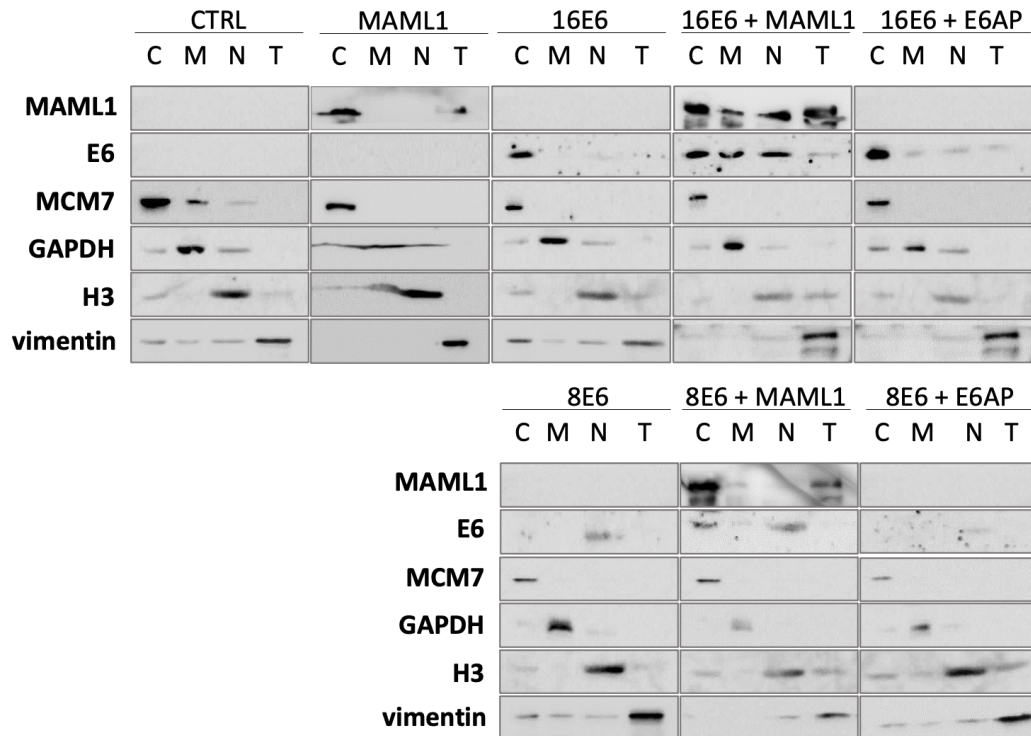


**Figure 38. MAML1 causes changes in HPV-16 E6 and HPV-8 E6 cellular accumulation.** HEK-293 cells were transfected with HA-tagged HPV-16 E6 or HPV-8 E6 alone or in combination with either FLAG-tagged MAML1 or E6AP. The cells were also transfected with an empty vector pcDNA3, used as a negative control and FLAG-tagged MAML1 alone. After 24 hours, the protein lysates were separated into the cytosolic (C), membrane (M), nucleic (N) and microtubule (T) cellular fractions. The fractionated proteins were separated on SDS-PAGE, 18 E6 and 8 E6 were detected by western blot analysis with HRP-linked anti-HA antibody, while MAML1 was detected with anti-FLAG antibody. The protein fraction purity was determined by incubation with anti-MCM7 for cytoplasm, anti-GAPDH for membrane, anti-histone H3 for nucleus and anti-vimentin for cytoskeleton (microtubules) antibodies.

Based on these results, along with the gene silencing experiments shown in **Figure 31C**, it was further confirmed that MAML1 and E6AP affect two different pools of HR HPV E6. This also suggests that the pool of E6 stabilized by MAML1 has unique functions and may interact with different cellular partners compared to the E6 stabilized by E6AP. As a result of these differences, the E6 stabilized by MAML1 may be present in different cellular compartments than E6 stabilized by E6AP. These findings highlight the importance of revealing the specific functions and interactions of different E6 pools to obtain a more comprehensive understanding of the complex role of E6 in HPV-driven oncogenesis.

#### 4.16. Silencing MAML1 has no effect on apoptosis

The experiments presented so far have provided solid evidence indicating that the ablation of MAML1 has a direct impact on the stability, distribution and E6 turnover of both  $\alpha$ - and  $\beta$ -HPVs. Thus, the following step was to assess whether these observed changes of E6 also impact the behaviour of the cell. This included investigating how E6 association with MAML1 might impact cellular apoptosis rate in comparison to its association with E6AP. The effect of HR E6 on inhibiting cellular apoptosis is well-characterized and extensively described in the introduction (Alfandari et al. 1999).

Cellular apoptosis was detected by staining the cells with Annexin V and propidium iodide (PI) followed by the flow cytometry analysis. HeLa cells and HT1080 cells stably expressing HPV-8 E6 were transfected with siMAML1 and siE6AP, alone or in combination, to ablate protein expression of MAML1 and E6AP, while siLuc was used as a control. Seventy-two hours post transfection the cells were collected and stained with FITC-conjugated Annexin V and PI. Three groups of control cells included the unstained cells, Annexin V-stained and PI-stained cells. The stained cells, including the experimental and control cells, were analyzed on the FACSCalibur flow cytometer. **Figures 39A** and **39B** depict the representative data in a form of dot plots for HeLa cells treated with different siRNAs and analysed using flow cytometry. The cells were gated against cell debris based on the size (FCS, forward scatter) and granularity (SSC, side scatter) (**Figures 39A** and **39B**, top left panel). The gated cells were then analysed based on Annexin V and PI, as depicted on the remaining four dot plots of **Figures 39A** and **39B**. Living cells negative for both Annexin V and PI staining are represented in the lower left quadrant, the upper left quadrant shows the cell population positive for PI staining (necrotic cells), the lower right quadrant depicts cells positive for Annexin V (early apoptosis), while the upper right quadrant (green population in the dot plots) represents cells that were positive for both Annexin V and PI (apoptotic cells). As evident from the presented dot plots, HeLa cells treated with either siLuc, siMAML1 or siE6AP show even grouping based on Annexin V-PI staining (**Figures 39A** and **39B**). Initially, quantification of double-positive cells stained with Annexin V and PI was conducted to determine the percentage of apoptotic cells. However, the observed percentage of these cells was very low, rendering it unsuitable for drawing meaningful conclusions. For this reason, a percentage of dead cells (including cells undergoing apoptosis) was calculated, which included necrotic cells, cells in early apoptosis, and apoptotic cells (**Figure 39E**).

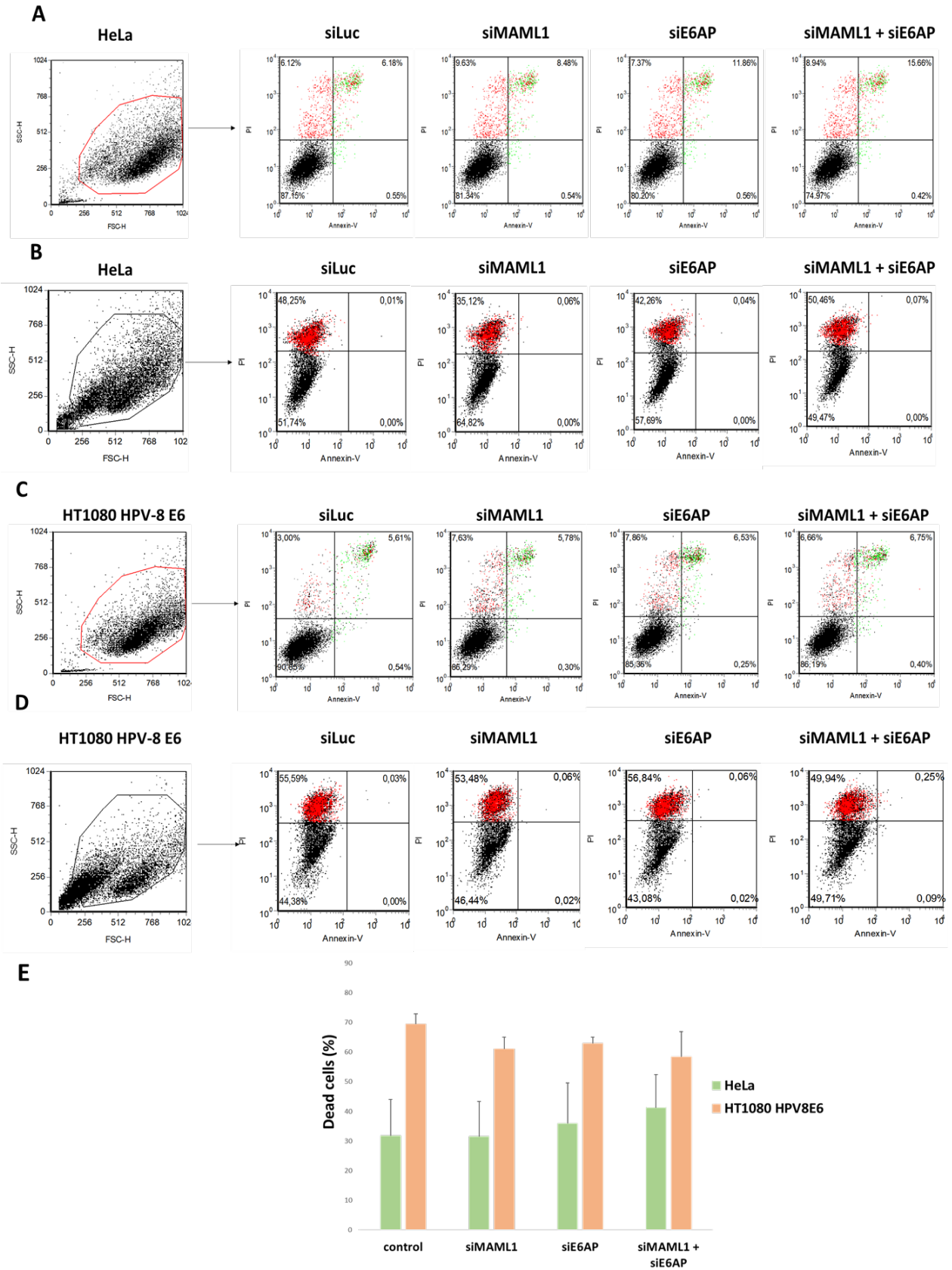


**Figure 39. Silencing MAML1 has no effect on cell apoptosis.** Flow cytometry analysis with Annexin V-PI staining was performed to evaluate the percentage of apoptotic cells. (A, B) HeLa cells and (C, D) HT1080 HPV 8 E6 cells were transfected with siMAML1, siE6AP, alone or in combination, while siLuc was used as a control. Seventy-two hours post transfection the cells were collected and stained with FITC-conjugated Annexin V and propidium iodide. Three groups of control cells were used in order to calibrate the instrument: unstained cells, Annexin V-stained and PI-stained. The data were analysed with FCS 3 Express Flow Cytometry Software. Representative dot plots from flow cytometry analysis for HeLa cells are shown. (E) A cell population positive for PI staining, as well as cells positive for Annexin V and double positive HeLa cells and HT1080 HPV 8 E6 cells stained with both Annexin V and PI, were quantified. These measurements were statistically presented as a percentage of dead cells in a column graph. Columns are means  $\pm$  SD percentage of dead cells of five independent experiments (bars represent SD).

While comparing the percentage of dead cells between four groups of the cells treated with different siRNAs, no significant difference was observed. Results of the flow cytometry analysis, therefore, indicate that silencing MAML1 or E6AP did not have an impact on cellular apoptosis, even though it would be expected that the decrease in E6 stability and protein levels, as a consequence of MAML1/E6AP silencing, would result in an increase of cellular apoptosis. A slight induction of apoptosis was seen in HeLa cells treated with both MAML1 and E6AP, possibly as a synergic effect of their silencing on HPV-18 E6 protein levels.

Representative data in a form of dot plots for the flow cytometry analysis of HT1080 HPV-8 E6 treated with siLuc, siE6AP and siMAML are depicted in **Figures 39C** and **39D**. The cells were processed and gated in the same manner as HeLa cells. HT1080 cells showed even grouping based on Annexin V-PI staining in both control and experimental groups (**Figures 39C** and **39D**). A percentage of dead cells was quantified and statistically presented in a form of graph (**Figure 39E**). Dead cells were calculated by incorporating a percentage of cell population positive for PI staining (necrotic cells), cells positive for Annexin V (early apoptosis) and cells that were positive for both Annexin V and PI (apoptotic cells). When comparing the percentage of dead cells among four groups of cells treated with different siRNAs, no significant difference was observed.

Finally, those results reflect the conclusion that silencing MAML1 or E6AP, or both in HeLa and HT1080 HPV 8 E6 cells does not have an effect on altering cellular apoptosis. Even though this result was not in agreement with the expected outcome based on the previous studies, the absence of the described effect could be possibly explained by the existence of additional cellular pathways and changes in cellular behaviour that can be influenced with silencing MAML1

and E6AP. It is possible that a longer duration of siRNA treatment may be required to observe the effects on cell apoptosis, exceeding the standard 72-hours treatment period.

Since there was no apparent change in the rate of apoptosis in the above elaborated experiment, the following steps were to evaluate some other possible biological changes, such as cellular proliferation and migration, which might occur in the absence of MAML1 in HPV-positive background.

#### **4.17. E6/MAML1 complex impacts cell proliferation synergistically with E6AP**

The fluctuations in E6 protein levels, which are dependent on the presence of MAML1 as observed in this doctoral thesis, raise an intriguing question about the potential impact on cell proliferation. E6 was shown to interact with different cellular proteins, and these interactions can modulate normal cellular processes such as cell cycle control and DNA repair. Therefore, it is possible that alterations in E6 protein levels as a consequence of the interaction with MAML1 could affect the cell's ability to proliferate and divide normally. Hence, the further aim was to investigate whether the two pools of HR E6s, one bound to E6AP and the other to MAML1, can independently have an impact on cellular proliferation. If it is assumed that the pool of E6 stabilized by MAML1 has distinct functions and interactions in comparison to the pool of E6 stabilized by E6AP, as suggested by the findings in this doctoral study, then it is possible that these complexes may have different effects on cell proliferation as well.

To test this, HA-tagged HPV-18 or -16 E6, together with either FLAG-tagged MAML1, E6AP or both were ectopically expressed in HEK-293 E6AP KO. Transfected cells were transferred from a tissue culture dishes to a 96 well plate in quadruplicates. Forty-eight hours after the cell transfer Uptiblue reagent was added in the log phase of the cell growth to measure cell proliferation. Five hours later the absorbance was measured on a multiwell plate reader and the percentage of Uptiblue reduction was quantified and calculated (**Figure 40**). Comparing the proliferation rate of the cells transfected with HPV-16 E6 alone, co-transfection with E6AP led to the statistically significant increase in the proliferation of E6AP KO cells, whereas co-transfection in combination with MAML1 did not change the proliferation in a statistically significant rate. In cells co-transfected with both MAML1 and E6AP proliferation rate was significantly elevated ( $p < 0.01$ , very significant), demonstrating a synergistic effect of MAML1 and E6AP on cell proliferation (**Figure 40**).

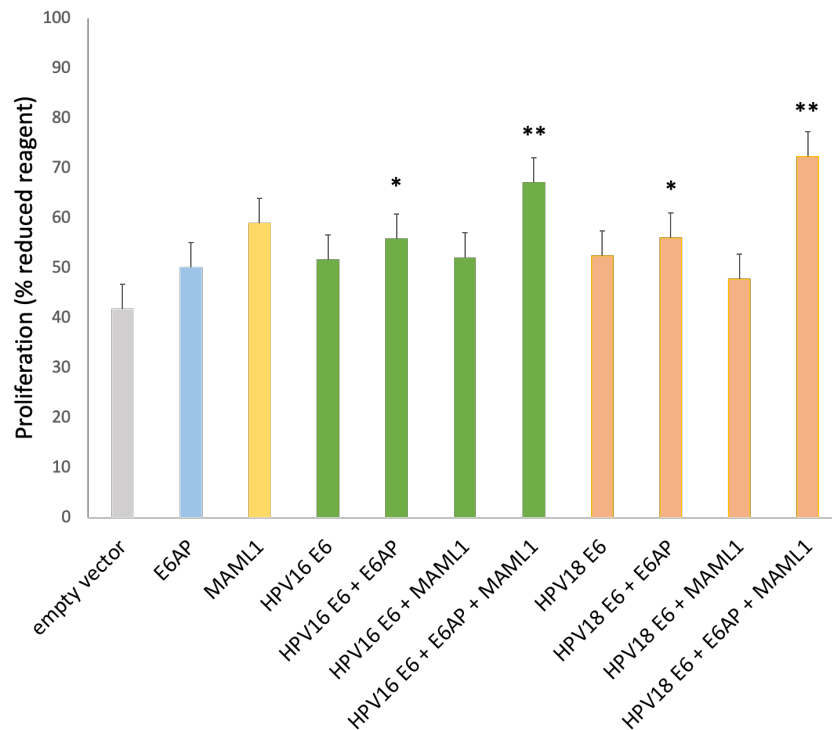


**Figure 40. MAML1 and E6AP cooperate in increasing E6-dependent cellular proliferation.** HEK-293 E6AP KO cells were transfected with HA-tagged HPV-16 E6 or HPV-18 E6, alone or in combination with FLAG-tagged MAML1, E6AP or both. The cells were also transfected with pCDNA3 empty vector, used as a negative control, and  $\beta$ -galactosidase (LacZ) as an internal standard to monitor transfection efficiency and loading. Twenty-four hrs after transfection, the cells were detached, counted and seeded in quadruplicates in a 96 well plate ( $5 \times 10^4$  cells per well), after which were grown for a further 48 hours. Uptiblue was then added to the wells and the absorbance at 570 nm and 595 nm was measured 5 hours later. The percentage of Uptiblue reduction was calculated to respond to the rate of proliferation. The average of at least three experiments is depicted on the graph, along with standard deviations. Significance was determined by Student's T-test using GraphPadPrim, with  $p < 0.05$  taken as significant, and marked with \* above the bar.  $p < 0.01$  taken as very significant and marked with \*\*.

As it was expected, HPV-18 E6 showed a similar trend on the proliferation rate of HEK-293 E6AP-KO cells, in comparison to the effects of HPV-16 E6. HPV-18 E6 alone induced an increase in cellular proliferation, which became even more pronounced with the co-transfection of E6AP. Again, it was confirmed that this increase is statistically significant. Co-transfection in combination with MAML1 did not positively affect the proliferation. Addition of both E6AP and MAML1 resulted in a further increase in proliferation rate (statistically very significant,  $p < 0.01$ ), showing strongly pronounced synergistic effect, despite MAML1 not having an individual impact

(**Figure 40**). E6 is known to promote cell proliferation through various mechanisms. However, its effects appear to be limited in the absence of E6AP, as suggested by the results shown in **Figure 40**, which highlights the importance and necessity of E6AP in promoting cellular proliferation. Transfecting cells with both E6 and E6AP resulted in the activation of viral oncoprotein's typical functions, including the degradation of p53 and PDZ-domain containing substrates, which consequently led to increased cell proliferation. On the other hand, E6/MAML1 complex induces the overall stability of this pool of E6, but apparently does not have the same proliferative effect. However, interestingly, in the situation when E6 cellular pools were stabilized by MAML1 and E6AP simultaneously, the rate of proliferation increased even more, suggesting that MAML1 and E6AP have a synergistic impact on E6, leading to increased cell proliferation, via yet undefined mechanisms.

#### **4.18. E6/MAML1 complex impacts cell migration**

It is well established that Notch cellular pathway is involved in the regulation of both cell proliferation and migration processes (Bray 2016). Despite the fact that the previous experiment showed no statistically significant effect of E6/MAML1 complex on cell proliferation, it cannot be excluded for this complex to impact cell behaviour through the effects on cell migration in HPV-positive background. A simple method for monitoring cell migration is the "wound healing" assay (also known as the scratch assay), which is based on a monitoring the dynamics of cell coverage as they fill a gap in the monolayer of adherent cells.

Thus, HeLa cells were transfected with either siMAML1, siE6AP or both, and siLuc was used as a control. Forty-eight hours after silencing the confluent cell monolayer was scratched with a pipette tip and the initial scratch was photographed (**Figure 41A**, left panel). The scratch in the cell monolayer was then photographed again after 18 hours to determine the potential differences (**Figure 41A**, right panel). The obtained images were quantified in a manner that edge of the gap (wound area) was marked with the MRI wound-healing tool macro, which is a part of ImageJ software, which measures the marked surface of a gap in the cell monolayer. With calculating surface area values, it was possible to observe changes in the migratory/proliferation potential of cells and distinguish the potential depending on the different silencing treatment.

Statistical analysis was graphically represented as a column graph using GraphPadPrism program (**Figure 41B**). Hence, silencing E6AP in HeLa cells led to a decrease in wound closure



from 73% (control cells transfected with siLuc) to 57%. This effect was expected in the context of the previously determined decreased 18 E6 protein stability as a consequence of silencing E6AP, so the down-regulated 18 E6 protein amount most likely led to the consequential reduced rate of E6-driven proliferation/migration.

Strikingly, silencing MAML1 decreased HeLa migratory/proliferation capacity to a similar degree as silencing E6AP, from 73% to 64% (**Figure 41B**) (even though statistical significance was lower in comparison to the control cells). This effect could be attributed to the decrease in the total amounts of E6 oncoprotein or potentially impaired Notch signaling. This was rather surprising considering that overexpressing MAML1 together with E6 did not have an impact on proliferation. However, in contrast to what was observed in the proliferation assay, in this experimental settings E6AP and MAML1 did not act synergistically, since the rate of migration remained the same as with the individually silenced E6AP and MAML1. The migratory capacity decreased from 73% in controls to 64% in cells treated with both siMAML1 and siE6AP, which was the same value as for cells treated with only siMAML1 (**Figure 41B**). Moreover, to confirm the efficiency of silencing, treated HeLa cells were harvested, proteins isolated and samples were analysed by SDS-PAGE and western blot using anti-MAML1 and anti-E6AP antibodies (**Figure 41C**).

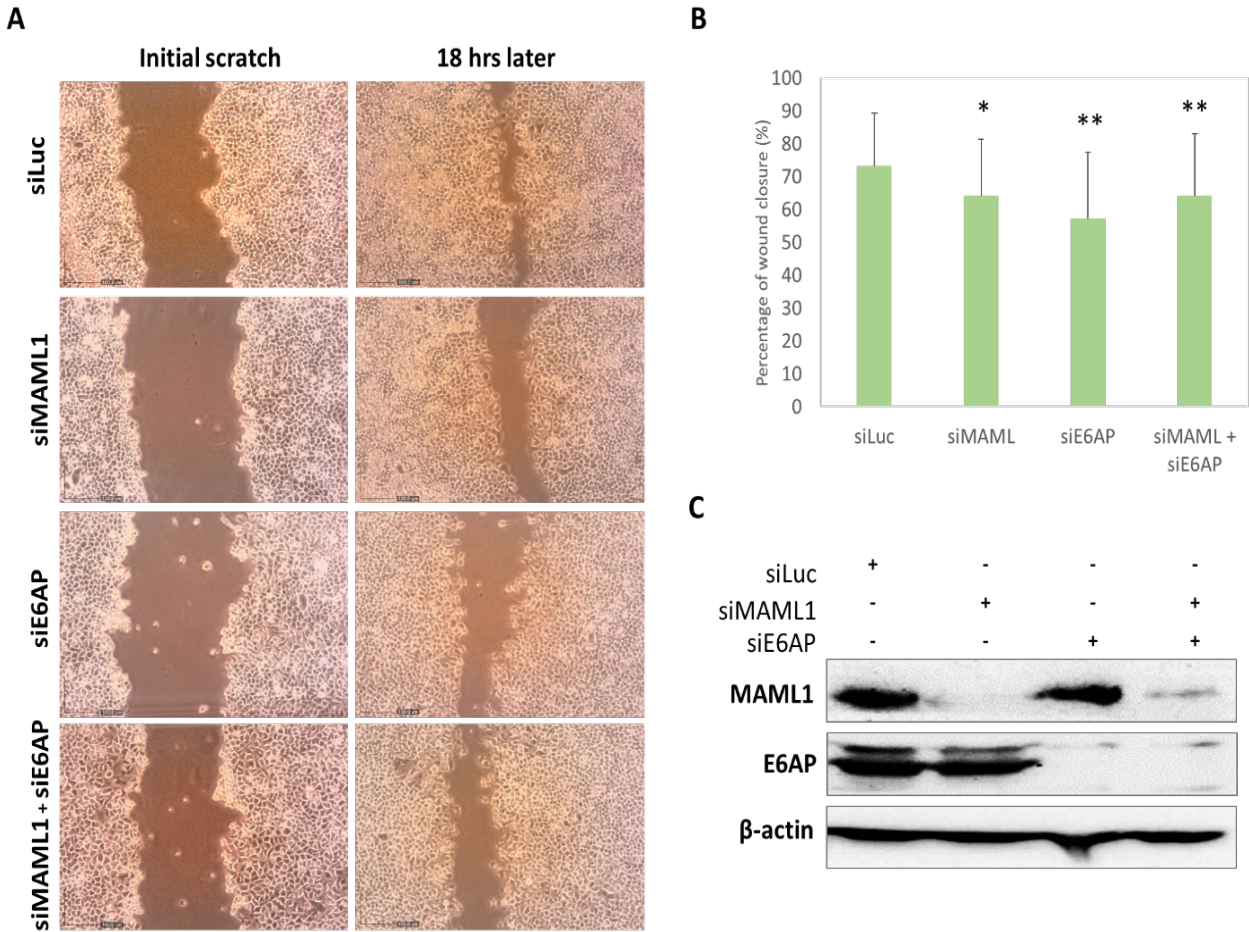


**Figure 41. Silencing MAML1 impacts cell migration in HPV-18 positive cells.** (A) HeLa cells were transfected with siLuc, siMAML1 or siE6AP. Forty-eight hours later, a wound scratch was made in the cell monolayer using pipette tip, the cells were washed and photographed. Eighteen hrs after initial scratching, the cells were photographed again. (B) Statistical analysis was graphically represented as a column graph using GraphPadPrism program. The surface area of the wounds was calculated with the MRI wound healing tool macro for ImageJ software, and the significance in the surface area difference between siRNA treatments was determined by Student's T-test, with  $p < 0.05$  taken as statistically significant and marked with \* ( $p < 0.01$  marked with \*\*). All experiments were repeated at least four times. (C) To confirm the efficiency of silencing, treated HeLa cells were harvested, protein isolated and samples analysed by SDS-PAGE and western blot using anti-MAML1 and anti-E6AP antibodies.  $\beta$ -actin was used as an internal control.

## 5. DISCUSSION

### **PART I Oncogenic potential of naturally occurring HPV-16 E6 variants**

Epidemiological studies have shown a remarkable association between the progression of high-grade cervical precursor lesions to invasive carcinomas with HPV-16 E6 intra-type variant forms, which differ in their abilities to modulate the carcinogenic HPV potential (Bernard et al. 2006; et al. 2013b). These numerous epidemiological studies have linked the changes in HPV-16 E6 nucleotide sequence with the altered biological functions and oncogenic potential of the virus (Hildesheim and Wang 2002; Stöppler et al. 1996; Burk et al. 2013b; Sichero et al. 2012; Asadurian et al. 2007a; Chakrabarti et al. 2004; Cochicho et al. 2021; Cornet et al. 2012; Lavezzo et al. 2016). However, due to the lack of mechanistic studies, the molecular background for those important epidemiological data has not been elucidated and the majority of molecular mechanisms responsible for an increased cancer risk of HPV-16 naturally occurring variants are still poorly defined. Since E6 oncoprotein primarily contributes to later stages of HPV-induced malignancy, it is assumed that the modifications in E6 may have a substantial impact on the progression of the disease towards a more malignant state. Exploring the carcinogenic potential of 16 E6 variants could explain the association of these amino acid changes with the increased risk of cervical neoplasia and highlight the importance for cervical cancer risk assessment. This doctoral thesis represents the first functional mechanistic study of three intra-type genetic variants of 16 E6, including 16 E6 D25N, E6 L83V and E6 D25N L83V, which evaluates their functions relevant to carcinogenesis.

HPV-16 E6 L83V intra-type variant has been clustered within the European variant branch and it is associated with an increased risk of cervical cancer progression and high frequency detection in the most of European regions (Grodzki et al. 2006; Bruni et al. 2010; Plummer et al. 2007; Kottaridi et al. 2022). Several functional analyses have revealed that HPV-16 E6 L83V variant exhibits enhanced capacity of p53 degradation and ability to abolish primary human foreskin keratinocyte (HFKs) differentiation induced by serum and calcium (Stöppler et al. 1996; Asadurian et al. 2007a; Zehbe et al. 2009), increased immortalization abilities of primary HFKs (Sichero et al. 2012; Togtema et al. 2015), established association with the regulation of tumorigenesis by the Notch signaling pathway (Chakrabarti et al. 2004), enhanced capacity of Bax

degradation (Asadurian et al. 2007b) and an increased interaction with E6BP over wild type HPV-16 E6 (Lichtig et al. 2006b). Furthermore, for this variant it has been shown to enhance E6-mediated MAPK signaling with increased expression of MAP2K1 and that it differentially regulates oncogenic Ras expression (Sichero et al. 2012; Chakrabarti et al. 2004). Furthermore, HPV-16 E6 L83V intra-type variant is more prone to undergo anoikis in human normal immortalized keratinocytes (NIKS) (Zehbe et al. 2009). The available epidemiological data highly suggests that the increased pathogenicity of HPV-16 E6 L83V mutant is likely to be attributed to other altered functions besides those that have been identified so far. HPV-16 E6 D25N L83V is an European variant form most closely linked with the development of cervical cancer in South-American region (Ortiz-Ortiz et al. 2015). In ectopic expression experiments, E6 D25N L83V variant exhibited higher protein levels in comparison to protein levels of other evaluated E6 variants (Zacapala-Gómez et al. 2016). In addition, E6 D25N L83V variant demonstrated differences in gene expression profiles, resulting in altered genetic expression in C33A cells. The observed differential expression involved host genes that play a role in the development of cervical cancer, and these included genes involved in adhesion, angiogenesis, apoptosis, differentiation, cell cycle regulation, proliferation, transcription, and protein translation (Zacapala-Gómez et al. 2016; Araujo-Arcos et al. 2022). Furthermore, currently, there is no experimental evidence to show whether HPV-16 E6 D25N variant additionally contributes to cancer progression opposed to wild-type HPV-16 E6, and therefore, more studies are needed to fully understand the significance of this variant. However, based on studies of the HPV-16 E6 D25N L83V variant, it is possible that D25N mutation may additionally increase the oncogenic potential of HPV-16 E6 protein and contribute to the progression of cervical cancer.

E6-mediated p53 degradation is considered as a hallmark function of HR HPV types (Scheffner et al. 1990b). The utilization of E6AP and the ubiquitin proteasome system for the degradation of p53 is an important factor contributing to the carcinogenic process, but there are also other oncogenic activities of HR E6s that play roles in this process. This implies also to degradation of PDZ-domain containing cellular substrates (Thomas et al. 2008c). The enhanced oncogenic potential of HPV-16 E6 variants has been attributed to their altered and advanced intrinsic biological properties, specifically their increased ability to engage in oncogenic activities. This implies that the higher prevalence of variant forms in cancer progression may be attributed to

their increased capability to interact with, utilize, and subsequently degrade well-established E6 cellular targets. In this doctoral thesis, it was observed that all evaluated HPV-16 E6 mutant oncoproteins exhibited an increased association with E6AP, albeit to varying degrees of intensity. HPV-16 E6 D25N L83V interaction with E6AP was decisively the strongest, followed by HPV-16 E6 D25N and HPV-16 E6 L83V, while the interaction with wild-type HPV-16 E6 was the weakest. To confirm that the increased levels of the interaction between 16 E6 D25N L83V and E6AP were indeed a consequence of E6/E6AP complex formation, and were not dependent on some unspecific endogenous effects, the experiment was repeated in E6AP KO cells and yielded a consistent result. There could be several possible reasons for the increased levels of interaction between 16 E6 D25N L83V mutant and E6AP. One possible explanation is that the D25N and L83V mutations alter the conformation of the E6 oncoprotein leading to a higher affinity for E6AP, even though the results of the *in silico* suggest that 16 E6 L83V and D25N L83V mutations do not significantly alter HPV-16 E6 3D structures (Rodríguez-Ruiz et al. 2019). Additionally, these mutations may potentially affect the accessibility of the LXXLL binding motif on E6, leading to increased availability for binding to E6AP. Molecular dynamics simulations of the variants showed minimal changes in the structure, but broad changes in physicochemical parameters, which can presumably be involved in the differential patterns of interactions with cellular protein targets (Rodríguez-Ruiz et al. 2019). Another possibility is that the mutations alter the surface charge distribution of the E6 oncoprotein, making it more favourable for interaction with E6AP.

E6AP is essential for  $\alpha$ -HPV E6 protein stability, as well as for maintenance of appropriate E6 levels within the cell (Tomaić, Pim, and Banks 2009a). However, it is also worth noting that E6AP itself undergoes self-ubiquitination, which ultimately leads to its degradation. This process is additionally amplified by the binding of E6 to E6AP (Kao et al. 2000). Based on the results of E6/E6AP binding experiments and the differences observed in the capacity of the mutants to interact with E6AP, the following step was to determine whether stronger E6/E6AP interaction also implies a higher degree of subsequent E6-mediated E6AP degradation. The obtained result indeed demonstrated higher degradation of E6AP in the presence of HPV-16 E6 D25N L83V variant, in comparison with either prototype 16 E6 or with the D25N and L83V E6 variants. This was in agreement with the results of the GST pull-down assays, which demonstrated that the HPV-16 E6 D25N L83V variant was the strongest in binding to E6AP, which has consequently reflected

on the levels of E6AP degradation. The increased E6-mediated degradation of E6AP by the HPV-16 E6 D25N L83V variant may be linked to changes in the conformation of E6AP induced by the interaction with the variant. This altered conformation may increase the accessibility of E6AP lysine residues to E6-mediated ubiquitination, thus further promoting its degradation (Kao et al. 2000). Moreover, the increased stability of HPV-16 E6 D25N L83V variant (Zacapala-Gómez et al. 2016), may also lead to a higher level of sustained interaction with E6AP, resulting in prolonged E6AP ubiquitination and subsequent degradation. E6AP is known to have a faster turnover rate than most other E3 ubiquitin ligases, meaning it is more rapidly degraded and replaced within the cell (Martin Scheffner and Kumar 2014). This fast turnover rate of E6AP allows rapid regulation of its target proteins and prevents accumulation of potentially harmful or misfolded proteins. Additionally, the turnover rate of E6AP can be regulated by other proteins and cellular factors, further affecting its dynamic role in protein modulation. In the case of E6/E6AP interaction, fast turnover rate could contribute to the need for continuous E6/E6AP binding required for maintaining the stability of E6 within the cell, which is favorable for the overall viral fitness. Therefore, the stronger interaction between HPV-16 E6 D25N L83V variant and E6AP, and subsequent higher degree of E6-mediated E6AP degradation, could be attributed to the joint effect of changes in E6AP conformation and ubiquitination of lysine residues, that alter the stability and turnover of E6AP.

Furthermore, after establishing that HPV-16 E6 L83V and D25N L83V mutants exhibit stronger interaction with E6AP, which was reflected in increased E6AP turnover in comparison to the wild-type 16 E6, an additional step was to assess if the strength of these interactions impacts the protein levels of HPV-16 E6 mutants. Hence, as already mentioned, the stability and protein levels of  $\alpha$ -HPV E6s depend on their association with E6AP (Tomaić, Pim, and Banks 2009a), so it was assumed that the stronger interaction between HPV-16 E6 D25N L83V and E6AP would lead to an upregulated HPV-16 E6 D25N L83V protein levels. Indeed, 16 E6 D25N L83V exhibited increased protein levels in comparison to the protein levels of wild-type HPV-16 E6 in the overexpression experimental settings. These results confirm and additionally support the findings of a previous study, which showed that C33A cells transfected with HPV-16 E6 D25N L83V, also exhibited upregulated E6 protein levels in comparison to the other investigated HPV-16 E6 variants (Zacapala-Gómez et al. 2016). The elevated protein levels of HPV-16 E6 L83V, in comparison to wild-type 16 E6, were consistent with its interaction profile and binding with E6AP.

This finding was also supported by a previous study where protein levels of HPV-16 E6 L83V in human keratinocytes were found to be comparable to, or even higher than the levels of wild-type HPV-16 E6 (Asadurian et al. 2007a). This result was also rather expected since several studies have reported HPV-16 E6 L83V enhanced capacity to target p53 for a proteasome mediated degradation (Stöppler et al. 1996; Asadurian et al. 2007a), increased transformation abilities (Sichero et al. 2012) and enhanced capacity of Bax degradation and E6BP interaction (Lichtig et al. 2006a), all mechanisms associated and dependent to the increased E6 stability and protein levels. Interestingly, it was also observed that the HPV-16 E6 D25N mutant showed a decreased protein levels when overexpressed in HEK-293 cells, which was quite surprising since its binding strength to E6AP was similar to the one of wild-type E6AP. Taking all of this together suggest that some other, yet undiffined and E6AP-independent cellular mechanisms, could be responsible for the decreased protein levels of this mutant.

The following analyses investigated if the two amino acid mutations had an impact on HPV-16 E6 protein turnover. It was observed that the half-life of wild-type HPV-16 E6 started to decrease around 90 minutes, which is an agreement with the previous reports (Tomaić, Pim, and Banks 2009a; Androphy et al. 1987). Interestingly, ectopic expression of HPV-16 E6 D25N L83V resulted in shorter half-life, with HPV-16 E6 D25N L83V half-life at the 90-minute time point being lower than the wild-type HPV-16 E6 half-life, implying to a more rapid protein turnover. These findings suggested that the HPV-16 E6 D25N L83V mutant is less stable than the wild-type protein, possibly due to mutation-dependent changes affecting its conformation or altering the surface charge distribution. Interestingly, this observation was in contrast to the ectopic expression levels of the double mutant, which were clearly upregulated in comparison to HPV-16 E6 and the other two mutants, suggesting a possibility that the stability of the double mutant could be also in part regulated on the mRNA level. Moreover, one needs to be aware that these experiments were performed in the overexpression systems, which were used primarily due to the lack of cancer cell lines isolated from patients infected with this particular variant. Therefore, this observation could be more complex *in vivo* and might not reflect entirely the results obtained in the overexpression assays.

The characterization of the mutants was investigated further in order to determine if their cellular localization was affected by the corresponding mutations. The latest research showed HPV-16 E6 mostly localize in the nucleus and ribosomal areas of the cytoplasm (Mesplede et al.

2012; Ganti et al. 2016). By investigating cellular localization of the ectopically expressed wild-type 16 E6 and its corresponding mutants, it was observed that all mutants exhibited distribution similar to the wild-type protein, with a predominant localization in the nucleus, while a diffused pattern of E6 signal was also detected in the cytoplasm. Hence, it seems that the mutations, whilst potentially inducing conformational changes of the oncoproteins' structure or altering the surface charge distribution, did not affect their localization. However, since these experiments involved overexpression of the E6 mutants, it was likely that potential minor changes in the protein localization could be masked in this experimental system. A solution in achieving a more accurate cellular localization results in future experiments would be to create cell lines stably expressing tagged forms of the E6 mutant proteins, possibly using CRISPR/Cas9 genome editing technology, or to generate patient-derived cells. These cells lines would resemble more natural settings of E6 expression levels and in this way possible changes in the oncoprotein localization could be detected more easily.

As already being emphasized, the main oncogenic activity of HR E6 oncoproteins is ability to interact with the p53 tumour suppressor (Scheffner et al. 1990a), which enables that virus evade apoptosis and overcome negative growth regulation, all of which are preceding stages of HPV-associated cancers. Interaction between HR E6/E6AP and p53 drives p53 degradation via the ubiquitin proteasome pathway, consequently having major implications for overcoming p53 tumor suppressive activities. Additionally, through their PBM's HR E6 oncoproteins bind and degrade a number cellular PDZ-domain containing proteins, which leads to their reduced tumor suppressors' activities and disruption of cell polarity networks. This E6's activity has been shown to be critical for later stages of HPV-induced malignancy (Thomas et al. 2008a), which was confirmed by many different experimental analyses (Kranjec and Banks 2011; Kranjec et al. 2014). Because of the importance of p53 and PDZ-domain containing proteins targeting for enhancing the progression of hyperplastic lesions into metastatic cancer during the process of HPV-mediated carcinogenesis, this doctoral study investigated 16 E6 mutants' capacity to degrade p53 as well as some of the well-characterized PDZ-domain containing E6's target proteins, such as MAGI-1, DLG1 and Scrib. One of the hypotheses in this doctoral thesis presumed that different 16 E6 mutant forms could differently target p53 and PDZ-domain containing proteins. This was based on the fact that the mutations may affect the surface charge distribution, changes in physicochemical parameters



and stability of the oncoprotein, which could impact its interactions with cellular targets, and also change the oncoprotein preference in targeting them. PDZ domain-containing proteins are particularly sensitive to this due to their large diversity in interacting with E6 oncoproteins and the specificity of binding (Thomas et al. 2008a). Thus, the capacity of the E6 mutant-mediated degradation of p53, MAGI-1, DLG1 and Scrib was explored using degradation assays, both in *in vitro* conditions and in cultured cells.

For the *in vitro* degradation assays, E6 proteins were *in vitro* transcribed and translated, and incubated with *in vitro* transcribed and translated substrates p53, MAGI-1, DLG1 and Scrib. Each of these cellular substrates has been shown previously to be targeted by E6 in these type of assays (Gardiol et al. 1999; Thomas et al. 2001; Thomas et al. 2005; Huibregtse et al. 1991). In the case of p53 degradation, between HPV-16 E6 and HPV-16 E6 mutants there was no statistically significant difference in their abilities to induce p53 degradation, but all examined 16 E6s induced p53 degradation with a similar intensity. The statistical data suggested that HPV-16 E6 D25N and HPV-16 E6 D25N L83V were as efficient as wild-type HPV-16 E6 in inducing the degradation of p53, while HPV-16 E6 L83V mutant degraded p53 in the most effective manner, which is in accordance with the previously published results (Stöppler et al. 1996; Asadurian et al. 2007a). There could be multiple reasons for the lack of differences observed in the *in vitro* assay between wild type 16 E6 and 16 E6 mutants in targeting p53. One possibility is that the experimental conditions used in these assays might not fully mimic the complex cellular environment where the interactions between E6 and p53 occur. For example, some important co-factors or post-translational modifications required for efficient E6-mediated degradation of p53 might be missing in the *in vitro* assay. Additionally, other cellular factors or competing interactions might be present in the cell that can modulate the efficiency of E6-mediated degradation of p53 *in vivo*, but are absent in the *in vitro* assay. Furthermore, the expression levels of E6 and p53 might differ between the *in vitro* assay and *in vivo* cellular conditions, which could have also affected the observed results.

Similar results were obtained in assays with MAGI-1 where there was no major difference observed in the degradatory capacity of the corresponding mutants. All examined HPV-16 E6s induced MAGI-1 degradation with a similar intensity and without statistically significant differences in comparison to wild-type HPV-16 E6. Although there was no statistically significant difference, HPV-16 E6 L83V mutant degraded MAGI-1 in the most effective manner.

Interestingly, this result is in agreement with the result of p53 *in vitro* degradation where 16 E6 L83V was also most efficient in degrading p53. On the contrary, it appears that the D25N mutant exhibited somewhat weaker capacity to target PDZ-domain containing protein MAGI-1 for proteasome mediated degradation. Hence, L83V mutation in the 16 E6 oncoprotein may lead to changes in physicochemical properties or surface charge that might impact its ability to target certain cellular proteins, including MAGI-1 and p53. On the other hand, the D25N mutation presumably has no advanced effect on the overall physicochemical properties of the 16 E6 protein, which led to a weaker degradation potential of MAGI-1 in comparison to the L83V mutant. The mutation D25N L83V in HPV-16 E6 did not affect its capacity for degrading MAGI-1 and showed a similar degradation effect as the wild-type 16 E6.

Furthermore, neither one of the 16 E6 mutants was as efficient as wild-type HPV-16 E6 in inducing the degradation of DLG1, even though all assessed HPV-16 E6s induced DLG1 degradation with a similar affinity, but without statistically significant difference. Similar as for MAGI-1 degradation, it appears that the D25N and D25N L83V mutants exhibited somewhat weaker capacity to target DLG1 for a proteasome mediated degradation. The observed weaker capacity of the D25N mutant for mediating degradation of both MAGI-1 and DLG1 may be explained due to its lower protein levels compared to the wild-type HPV-16 E6, L83V and D25N L83V mutants, as observed in the overexpression assays. This suggests that the stability of the D25N mutant is likely compromised, possibly due changes in the physicochemical properties, leading to decreased ability to target these PDZ domain-containing proteins for degradation. Although in the *in vitro* assays all E6 mutants were equally translated, the differences in protein levels seen in the overexpression assays may be an indicator for the *in vitro* assays that there are certain differences in the protein stability of the E6 mutants.

The degradation assay which involved Scrib was performed to evaluate HPV-16 E6 D25N L83V because of its increased interaction with E6AP. The result showed the same trend as for the rest of the evaluated PDZ-domain containing substrates, with wild-type 16 E6 being more efficient in degrading Scrib than the double mutant. It seems that D25N L83V mutation reduces variant's overall ability to degrade Scrib. It is possible that other cellular factors or post-translational modifications might play a role in E6 efficiency to target Scrib. Additionally, the increased interaction of the D25N L83V mutant with E6AP may be more relevant to its ability to degrade other PDZ-domain containing substrates or perform other cellular functions, rather than primarily

degrading Scrib (Thomas and Banks 2015). On the other hand, a possibility that HPV-16 E6 D25N L83V mutant can modulate Scrib activities by affecting its cellular localisation and thus blocking or abolishing its interaction with other cellular partners potentially leading to changes in downstream signaling pathways, cannot be excluded.

As *in vitro* results did not fully align with previously published findings (Stöppler et al. 1996; Asadurian et al. 2007a) or with the anticipated outcome regarding the initial observation of the increased association with E6AP, additional degradation experiments were conducted to investigate E6-dependent degradation of p53, MAGI-1, and DLG1. These were performed as overexpression assays in HEK-293 cells. Considering p53 degradation, all of the examined HPV-16 E6s exhibited similar efficiency in targeting p53 for a proteasome-mediated degradation, with wild-type HPV-16 E6, L83V and D25N L83V being equally efficient. This result was not in agreement with the *in vitro* degradation assay where HPV-16 E6 L83V was the most efficient in degrading p53. However, previous studies have also reported some inconsistencies regarding the ability of HPV-16 E6 L83V to target p53 for proteasomal destruction. Hence, while some studies have suggested that HPV-16 E6 L83V variant is more effective than the wild-type protein in targeting p53, other studies have reported similar levels of p53 degradation between wild-type HPV-16 E6 and HPV-16 L83V, without emphasizing the superiority of HPV-16 L83V (Sichero et al. 2012). These inconsistencies may be due to differences in experimental conditions, such as differences in cell lines used or E6 expression levels. From the initial protein interaction assay with E6AP, it would have been expected that HPV-16 E6 D25N L83V have a potential to degrade p53 more efficiently than wild-type 16 E6 and other two mutants, since the intensity of HPV-16 E6 mediated p53 ubiquitylation and proteasome-dependent degradation relies on the strength of interaction with E6AP (Scheffner et al. 1990a; Huibregtse et al. 1991). Yet, this research did not find a link between the stronger interaction of HPV-16 E6 D25N L83V with E6AP and capacity to degrade p53 or other evaluated cellular targets. This implies that E6AP-dependent upregulation of D25N L83V protein levels could be directed towards some other E6 cellular functions which do not involve protein target degradation. On the other hand, it could be speculated that the E6 mutants only degrade a certain amount of p53 to effectively carry out their p53-dependent functions, and that the observed levels of p53 degradation may be sufficient for adequate p53 reduction. Furthermore, these analyses did not examine phosphorylated forms of p53, which are

preferentially targeted for a proteasome mediated degradation by E6 (Bernard et al. 2011). A previously performed study which included HPV-16 E6 L83V and a similar 16 E6 D25E mutant, with an amino acid substitution on the same position as D25N, but instead of asparagine harbours glutamic acid (D25E), showed a uniform pattern of activity with minor differences among HPV-16 E6 L83V and 16 E6 D25E variants in p53 degradation activity (Yi et al. 2013). Taken together, these findings suggest that HPV-16 E6 can accommodate non-conservative changes between natural variants without changing its ability to degrade p53.

In addition, degradation assays conducted in cultured cells did not demonstrate an enhanced ability of the HPV-16 E6 mutants to target ectopically expressed MAGI-1 in comparison to prototype HPV-16 E6. However, the HPV-16 E6 L83V mutant induced MAGI-1 degradation with a similar affinity compared to wild-type HPV-16 E6. The enhanced capacity of HPV-16 E6 L83V for MAGI-1 degradation is in agreement with the *in vitro* degradation assay where 16 E6 L83V was the most efficient in degrading MAGI-1. However, it was surprising to observe the low affinity of the E6 D25N L83V mutant for MAGI-1 degradation in these experimental settings, suggesting that the D25N mutation does not play a role in targeting MAGI-1, or that it might be favouring other E6 functions over targeting MAGI-1. Considering the results of DLG1 degradation assays in the overexpression experiments, it was observed that the 16 E6 L83V mutant degraded DLG1 more efficiently than wild-type 16 E6. However, overall, there was no significant difference in the degradatory capacity of the 16 E6 mutants. Those results did not entirely reflect the *in vitro* assay results, where wild-type 16 E6 was more efficient in degrading DLG1, despite exhibiting similar degradation capacity as the 16 E6 L83V mutant in this experimental setting. A weaker capacity of 16 E6 D25N L83V mutant for MAGI-1 and DLG1 degradation can be explained in the context of E6AP-independent degradation of MAGI-1 and DLG1 mediated by HR E6s (Grm and Banks 2004). In this context, the initial observation that HPV-16 E6 D25N L83V exhibits an enhanced capacity to bind E6AP does not necessarily imply an enhanced capacity to degrade MAGI-1 and DLG1, further suggesting involvement of other ubiquitin ligases in this process (Vats et al. 2019). E6 degradation of Scrib was shown to be E6AP-dependent (Nakagawa and Huibregtse 2000), but *in vitro* results did not show that HPV-16 E6 D25N L83V has an advantage in respect to wild-type 16 E6 in targeting Scrib. This further implicates that the D25N mutation does not play a role in targeting PDZ-domain containing substrates, as well as that the experimental conditions

used in *in vitro* assay, do not fully mimic the complex cellular environment where the interactions between E6 and Scrib occur.

The discrepancy between the *in vitro* results and the results from the overexpression assays may suggest that HPV-16 E6 mutants are possibly subjected to post-translational modifications that change their interaction profile with cellular targets, but which do not occur in the reticulocyte lysate translation system. Post-translational modifications, such as phosphorylation or acetylation, can have a significant impact on protein interactions and stability, and these modifications may not be accurately replicated in the reticulocyte lysate translation system since it is a simplified *in vitro* system that lacks many of the complex cellular factors and conditions that exist *in vivo* (Khoury et al. 2011). Additionally, the overexpression assays in cells may also involve changes in protein folding that cannot be entirely recapitulated in the *in vitro* assays. Altogether, the differences in the abilities of 16 E6 mutants to degrade the main cellular targets that were examined in an overexpression assay may be due to a combination of factors, including changes in physicochemical properties or surface charge, potential changes in protein conformation, stability, and specific interactions with target proteins.

Based on the presented results it is also interesting to emphasize that E6 most likely does not induce the degradation of the entire cellular pools of Scrib and DLG1, but instead targets a specific subset of those proteins, which was also reported previously (Roberts et al. 2012; Anastas et al. 2012). In the case of HPV-18 E6, it was shown that only phosphorylated and nuclear fractions of DLG1 appear to be targeted for a proteasome mediated degradation (Thomas et al. 2005), suggesting that it is highly possible that in the case of 16 E6 mutants, minor alterations in their cellular localization may have occurred, which could have not been detected in the experimental settings of this study. This suggests that the 16 E6 mutants may not be able to degrade DLG1 or Scrib to the same extent as the wild-type 16 E6. Considering that these were overexpression assays, it is crucial to acknowledge the possibility of differences in the expression levels of mutant proteins within different cellular compartments, which could have affected the obtained results. Therefore, in order to accurately determine the effect of the mutants on protein degradation, it would be necessary to isolate cell lines from patients with these mutants and examine mutants' behaviour in their native cellular environment. Another possibility is that 16 E6 mutants act differently in diverse cellular compartments which can consequently alter to substrate degradation preference.

The same speculations that have been made for Scrib and DLG1 degradation may also be applied to the degradation of MAGI-1 with 16 E6 mutants.

*In silico* 3D model of HPV-16 E6 structure revealed L83V the position in the E6C zinc finger domain, in a region composed of completely buried residues surrounding the main hydrophobic core (Nominé et al. 2006b). Mutations within the buried residues are prone to structure destabilization and loss of function although this seems not to be the case for the L83V. A reduced degradatory activity of HPV-16 E6 D25N L83V that contains alterations in two residues, the L83V in the E6C domain and D25N alteration in an interface residue in the E6N domain, may be explained by a physicochemical change that interferes with E6N/E6C intramolecular bonds, together with E6 functions that depend on pseudodimeric arrangement of zinc finger domains (Asadurian et al. 2007b). The alteration from a charged acidic hydrophilic residue (aspartic acid D) to uncharged hydrophilic residue (asparagine N) could possibly alter the interaction with cellular HR E6 targets.

Altogether, these findings highlight the importance of the specific amino acid residues in the E6 oncoprotein for the modulation of certain cellular targets, as well as the potential impact of the mutations on the stability and E6 functions. The data presented in the first part of the thesis may navigate the way for future functional and mechanistic studies. It is likely that the naturally occurring variants may display also other biological differences than those described in this doctoral thesis, which could contribute to their pathogenicity. Further structural and biochemical analyses with E6 variants are warranted to improve understanding of their biological functions, epidemiology and how they modulate the progression of carcinogenesis. Overall, these analyses may partially help in better explaining the differences in the oncogenic potentials of the 16 E6 mutant forms and how these mutations could play roles in HPV-induced carcinogenesis.

## **PART II MAML1-induced HPV E6 oncoprotein stability is required for cellular proliferation and migration**

Notch signaling pathway is a key determinant in keratinocyte differentiation, which regulates cell cycle progression (Lowell et al. 2000b; Brimer et al. 2012a; Rangarajan et al. 2001b) and studies in the past years have found the connection between Notch signaling and  $\beta$ -genus HPVs (Rozenblatt-Rosen et al. 2012a; White et al. 2012; Tan et al. 2012a; Brimer et al. 2012b). Identification of MAML1, a co-activator of Notch signaling pathway, as a conserved interactor of  $\beta$ -genus E6s has raised a high interest for the investigation of its biological properties associated with the improvement of the viral fitness of cutaneous HPVs. So far, it has been well-described that binding of  $\beta$ -HPV E6s to MAML1 has an inhibitory effect on Notch signaling and keratinocyte differentiation, which was shown to be extremely important for the maintenance of a productive viral life cycle (Lowell et al. 2000b; Brimer et al. 2012a). Interestingly,  $\alpha$ -HPV-16 E6 was also found to bind to MAML1, but with much lower intensity (Brimer et al. 2017a). Confirming an interaction between a mucosal HPV E6 and MAML1 was rather surprising considering that MAML1 binding to E6 was thought to be exclusive for  $\beta$ -HPVs and the molecular basis of the interplay between HPV-16 E6 and MAML1 has not been explored in much detail. Although, HPV-16 E6 has been shown to affect Notch signaling, the mechanism underlying its impact is thought to be distinct from that of  $\beta$ -genus HPV E6s and does not involve MAML1 (Kranjec et al. 2017). It has been demonstrated that HPV-16 E6 also inhibits Notch signaling, albeit through a mechanism which implies the degradation of p53 (Lefort et al. 2007; Dotto 2009; Yugawa et al. 2007). HPV-16 E6 promotes proliferation of keratinocytes in the basal layer through the combined inactivation of p53 and NOTCH1; it inhibits NOTCH1 cleavage and decreases NOTCH transcription dependent upon p53 degradation, even though the full mechanism is still unknown (Kranjec et al. 2017).

The experiments conducted in this doctoral dissertation have validated the previously reported interaction between MAML1 and HPV-16 E6. However, this interaction appeared to be weaker than the interaction between HPV-8 E6 and MAML1, which was supported by the results of two large-scale proteomic analyses conducted prior to the discovery of the  $\alpha$ -HPV E6 interaction with MAML1. These studies failed to detect an interaction between HPV-16 E6 and MAML1 (Rozenblatt-Rosen et al. 2012c; White et al. 2012), which may explain the low intensity of

interaction observed in the presented analysis. Confirming an interaction between HPV-16 E6 and MAML1 encouraged this research to proceed in the way to further investigate if other  $\alpha$ -HPV E6s could also associate with MAML1. Using GST pull-down assay, it was demonstrated that besides HPV-16 and HPV-8 E6, -18 E6 and 11 E6 also interact with MAML1. As expected from the previous reports, as well as from the initial results of the second part of this thesis, HPV-8 E6 was found to be the strongest interactor of MAML1, followed by HPV-18 E6 and -16 E6, and finally HPV-11 E6 which had the weakest, but still evident interaction. Because of a very weak interaction between HPV-11 E6 and MAML1, and since HPV-11 is a LR type, it was decided not to pursue this avenue further. Taken together, the protein interaction assays, including immunoprecipitation and GST pull-down, showed that both HR and LR mucosal HPVs bind to MAML1. This finding is in contrast to the previously prevailing understanding that  $\alpha$ -HPV E6 oncoproteins do not interact with MAML1. However, this doctoral thesis supported the fact that although multiple mucosal E6 oncoproteins can complex with MAML1, its preferred interacting partners are E6 oncoproteins from cutaneous E6 types.

In the introduction section of this thesis, it was explained in detail that the main interacting partners of E6 are hijacked by HPVs to serve in adapting the cellular microenvironment for viral replication, productive viral life cycle and to improve viral fitness. The described *modus operandi* is irrespective of the genera the E6 oncoproteins belong to. Hence, HR E6s interact and form a stable complex with E6AP, resulting in E6 protein stabilization (Tomaić, Pim, and Banks 2009; Thomas et al. 2013). The E6/E6AP complex is subsequently directed by E6 towards a number of cellular targets important for maintaining the productive viral life cycle, ensuring their regulated turnover at the proteasome (Đukić et al. 2020; Kehmeier et al. 2002).  $\beta$ -PVs interact with MAML1 in order to repress Notch signaling, block cell differentiation and cell-cycle arrest as viral life cycle is highly dependent on the host cell differentiation status (Lowell et al. 2000b; Brimer et al. 2012a; Tan et al. 2012a). The previous phylogenetical clustering of E6 oncoproteins into two large supergenera based on their preferential interacting partners, the E6  $\alpha$ -supergenera which interacts with E6AP and the E6  $\beta$ -supergenera which interacts with MAML1 needs to be revised, since recent studies, including the one presented here, have confirmed that both  $\alpha$ - and  $\beta$ -HPV E6 proteins utilize the same LXXLL motif to bind both E6AP and MAML1, thus blurring the previous boundaries between the two supergenera (Tan et al. 2012a; Brimer et al. 2012b).



One of the aims of the second part of this doctoral thesis was to determine if  $\alpha$ - and  $\beta$ -HPV E6, by complexing with MAML1, can induce similar effects in increasing E6 protein levels and protein stability, as it was observed in the interactions between  $\alpha$ -HPV E6s and E6AP (Tomai c, Pim, and Banks 2009b). To investigate those potential effects on E6 protein levels, MAML1 was co-expressed together with the E6 oncoproteins from a panel of different  $\alpha$ - and  $\beta$ -HPVs (HPV - 8, -12, -14, -16, -18, -24, -33 and -38 E6), along with E6AP used as a control. Dramatically, in this experimental setting it was demonstrated that MAML1 has an upregulatory effect on E6 protein expression levels, for both  $\alpha$ - and  $\beta$ -HPV genera. Co-transfection of different HPV E6s with E6AP, as it was expected, had an upregulatory effect on the protein levels of all  $\alpha$ -HPV E6s included in the experiment, on the contrary to the  $\beta$ -PV E6s, where there were no effects detected on the protein levels of analyzed  $\beta$ -HPV E6s (HPV-8, 12, -14). However, exceptions to this were observed in the case of  $\beta$ -HPV-24 and -38 E6. Previous reports have noted that HPV-24 and HPV-38 (a cutaneous type with an oncogenic potential) interact with both MAML1 and E6AP (Thomas et al. 2013a; Tan et al. 2012b), indicating some potential similarities with HR E6 oncoproteins, such as having two distinct E6 cellular protein pools which might preferentially bind either MAML1 or E6AP.

Same overexpression assays were repeated in an E6AP-null background, which yielded similar results, allowing the conclusion that the observed effects of MAML1 in inducing increase of E6 protein levels were E6AP-independent. Notably, a more pronounced effect of MAML1 on E6 protein levels was observed for HPV-14 and -24 E6s, both of which are  $\beta$ -HPVs. This may be due to the fact that these HPV types possibly share higher similarities in their genetic makeup in respect to similar E6 protein sequences and motifs. These similarities may result in a stronger interaction between the E6 oncoproteins of these two HPV types and MAML1, leading to more efficient increase in protein expression levels of the E6 oncoproteins. Additionally, it is possible that other factors unique to these two HPV types, such as differences in their cellular localization or expression patterns, may contribute to their increased MAML1-dependent protein levels. Furthermore, the observed effect of MAML1 on  $\beta$ -HPV E6 oncoproteins is supported by its role in Notch inhibition achieved by  $\beta$ -HPV E6s, and a broader biological rationale in the background of this interaction. However, the reasons for increased  $\alpha$ -HPV E6 protein levels by MAML1 seem to be more complex. HR E6 oncoproteins could have presumably evolved to use the same conserved LXXLL binding motif to maintain strong interaction with E6AP and the weaker

secondary interaction with MAML1, to maximize their protein levels, enabling them to modulate a plethora of cellular functions. The increase of E6 protein levels is likely the result of its protected degradation in cells when it exists in complex with either MAML1 or E6AP.

In the absence of the target peptide such as LXXLL, E6 adopts a different structure and exhibits a tendency for self-association, because the few molecular bonds which connect the zinc finger domain E6N, linker helix and zinc finger domain E6C are insufficient to maintain the E6 architecture observed in the complex structures (Zanier et al. 2010). The tendency for self-association (Zanier et al. 2010) and the strong affinity for target motifs, (Sidi et al. 2011; Zanier et al. 2005; Sekaric et al. 2008b) suggest that most E6 molecules preferentially exist as target-bound complexes in infected cells (Zanier et al. et al. 2013). The absence of binding to a suitable LXXLL peptide rendered HPV-16 E6 and 18 E6 unstable, indicating that LXXLL peptide interactions play a dual role in both stabilizing and restructuring E6 (Ansari et al. 2012). Disrupting the binding of E6 to the LXXLL peptide leads to the inhibition of E6 downstream effects, showing that E6 docking to LXXLL peptides is essential for preserving E6 complete functions (Zanier et al. 2013). As a consequence of the increased protein levels, E6 can perform its numerous functions more efficiently, so it is likely that both of HR E6/E6AP and HR E6/MAML1 interacting complexes might be required for establishing an optimal cellular environment for the virus to complete its life cycle and successfully propagate virions. Furthermore, it would be also interesting to investigate the possibility of the existence of other ubiquitin ligases that might be involved in E6 degradation, when it is not bound to E6AP or MAML1. The absence of E6AP-mediated increase in the protein levels of  $\beta$ -HPV E6s is consistent with their limited involvement in the degradation of most well-established HPV cellular targets via proteasome machinery, with a few exceptions, such as proapoptotic Bak in the case of  $\beta$ -HPV-5 E6 (Wallace et al. 2014b; Underbrink et al. 2008a).

The discovery that cutaneous HPV E6 oncoproteins interact with the acidic LXXLL motif of MAML1 expanded the understanding of E6/MAML1 LXXLL-dependent interactions. Based on the high homology between E6AP's LQELL motif and MAML1's LHHLL motif (Vande Pol 2013b), this doctoral thesis raises an important question about whether there is a shared biological rationale for the interaction of E6 oncoproteins with the acidic LXXLL peptides of both MAML1 and E6AP. The results presented in this thesis highlight the similarity and the implications of E6 binding to the LQELL motif of E6AP and the LDDLL motif of MAML1. In particular, the ability

of E6 to bind to amino acid residues required for interaction with target proteins has some degree of flexibility (Zanier et al. 2013), which raises the question of whether the increased E6 protein levels as a result of an interaction with MAML1 is solely dependent on the LXXLL motif, or if it might require binding to accessory regions in MAML1's protein structure. Additionally, doctoral thesis also aimed to determine the extent of E6/MAML1 interaction dependence upon mutations in the LXXLL motif. Previous research has shown that mutating the aspartate residues of MAML1 LXXLL motif to histidines (LDDLL to LHHLL) decreased the capacity of HPV-8 E6 binding to MAML1 and partially block E6-mediated inhibition of Notch signaling (Meyers et al. 2017a). The same mutated form of MAML1 with LHHLL motif was used also in the analyses performed to determine whether MAML1-dependent increased E6 protein levels require an intact LXXLL binding motif. Interestingly, the results showed an upregulation of the protein expression levels of HPV-18 and -8 E6 in the presence of wild-type MAML1 and MAML1 LHHLL mutant. The interaction with mutant increased protein levels of both HPV-8 and HPV-18 E6 oncoproteins, but to a lesser degree than the wild-type MAML1. The same result was obtained in an overexpression assay and immunoprecipitation assays, which included MAML1 LHHLL. Hence, HPV-8 E6 and HPV-18 E6 retained the ability to achieve interaction with MAML1 LHHLL, indicating that binding to the LXXLL motif is required for the interaction with E6, but also suggests that broader peptide domains or specific adjacent amino acids can be included in achieving the complete interaction. Immunoprecipitation assays were used to evaluate whether the LHHLL mutant could contribute to the increased E6 protein levels despite its weaker binding with E6s. Residual binding was observed during immunoprecipitation analysis, indicating that the LXXLL motif is involved in the interaction and that the introduced mutations do not entirely block the interaction. It is possible that other amino acids within the motif are necessary for complete binding. To entirely eliminate the binding effect, the MAML1 ADDAA mutant, which is entirely ineffective in binding may be required (Tan et al. 2012b).

Interestingly, the protein levels of HPV-16 E6 were not increased when co-expressed with MAML1 LHHLL, possibly because of its weaker binding to MAML1 in the comparison with HPV-18 E6, as shown in GST pull-down assays, and thus mutating the aspartate residues in the LXXLL motif was sufficient to completely abrogate the binding. Therefore, it is possible that their binding is somewhat different, as it is the case with the two types of binding of different E6s with E6AP (Drews et al. 2020a). Namely, even though previous mutagenesis experiments performed

on E6AP showed that E6 interacts with a 20 amino acid peptide in E6AP structure that contains an LXXLL sequence (Huibregtse et al. 1993e), novel research concerning E6/E6AP interaction has established two different modes of interaction between E6 and E6AP (Drews et al. 2020b). Type I interactions imply that E6 interacts directly with the LXXLL peptide motif independently from the rest of the structure of E6AP. This type of interaction is present in the recruitment of p53 and some other cellular targets. Furthermore, type II interaction with the LXXLL peptide motif of E6AP is a bit different (Drews et al. 2020b). For this type of interaction, binding of E6 requires additional auxiliary regions of E6AP structure in a proximity of the LXXLL motif, in the direction of either amino terminus or carboxy-terminal HECT domain. There are no studies involving research whether similar LXXLL-motif accessory regions are required for E6/MAML1 interaction. Furthermore, it is yet unknown if cutaneous E6 oncoproteins are restructured upon binding to LXXLL, as it was above described for HPV-16 and HPV-18 (Ansari et al. 2012), which would be of a great value to be determined.

Overall, it was rather surprising to notice that HPV-16 E6 and HPV-18 E6 exhibited diverse results, even though their behavior in the previously presented overexpression results has been identical. It is likely to conclude that all amino acids in LDDLL motif are involved in the association with E6s and that the interactions of different E6 oncoproteins with MAML1, even of the same genus and oncogenic risk, cannot not be generalized and could have potentially somewhat different impact. A comparison with E6/E6AP interaction may be relevant to explain this effect, as studies have shown that HPV-16 E6 has a stronger affinity for E6AP in comparison to HPV-18 E6, but both E6s exhibit comparable effects on the degradation of p53 (Huibregtse et al. 1991).

As described above, the performed assays which included ectopically expressed E6, MAML1 and E6AP demonstrated that  $\alpha$ - and  $\beta$ -E6s bind to MAML1, and this binding resulted in upregulation of E6 protein levels. However, since the overexpression experiments cannot entirely recapitulate naturally occurring cellular system, it was necessary to additionally verify whether the same effect on increased E6 protein levels can be observed in the cell lines that endogenously express E6/E7 oncoproteins. Silencing endogenous MAML1 in HPV-18 positive HeLa cells resulted in downregulation of E6 protein levels. Strikingly, this downregulation of E6 protein levels was not accompanied by a subsequent effect on the regulation of p53 protein levels. As degradation of p53 is one of the main HR E6 functions (Scheffner et al. 1990b), it would have

been expected that a decrease in the E6 levels would result in an increase in p53 protein levels as a result of a reduction in HR E6-mediated p53 degradation, but that was not the case with MAML1 silencing. This particular result was the first one to suggest that MAML1 does not affect HPV-18 E6 cellular pool involved in p53 degradation. It also confirmed that E6 was stabilized at the protein level, as blocking of the proteasome function with bortezomib nullified the observed effect. Since the same experimental setting in HPV-16-positive CaSki cells yield the same result, this confirmed that lack of the increase in p53 protein levels as a consequence of MAML1 silencing was not an HPV-18 E6 exclusive effect. Silencing MAML1 in HPV-8 E6 expressing HT1080 cell line (Hufbauer et al. 2015b) decreased the amount of endogenous 8 E6 protein levels, while silencing E6AP had no effect on HPV-8 E6 protein levels and protein stabilization. Levels of p53 were not monitored since it is known that  $\beta$ -HPV E6s do not degrade p53 (Wallace et al. 2014b; White et al. 2014b). The obtained results in HT1080 HPV-8 E6-expressing cells were expected, since it was previously demonstrated that the majority of  $\beta$ -HPV E6s do not interact with E6AP (Miranda Thomas et al. 2013a), but no such studies have been performed including HPV-8 E6 so far. At this point of research these results created a basis to hypothesize that HPV-infected cells exhibit two distinct cellular pools of HR E6. One of the HR E6 pools is MAML1-associated, resulting in upregulation of E6 protein levels and protein stabilization. This E6/MAML1 complex seems not to be involved in well-established HR E6/E6AP-dependent functions, such as the principal p53 degradation. The remaining cellular pool of HR E6 is bound to E6AP and is involved in well-characterized E6 oncogenic functions, which are described in detail in the introduction of this thesis. As demonstrated also by immunofluorescence experiments, HR E6/E6AP-bound pool functions include E6 protein stabilization and p53 degradation. Using confocal microscopy, the restoration of p53 levels was observed in HeLa cells following E6AP silencing. Silencing MAML1 did not affect the HPV-18 E6 pool involved in p53 degradation, as no changes in cellular localization and protein levels of p53 were observed. E6AP silencing in HT1080 HPV-8 E6-expressing cells did not have an evident effect on HPV-8 E6 protein localization, while MAML1 silencing resulted in the downregulation of nuclear HPV-8 E6. This observation additionally corroborated with previous results indicating that there is likely only one cellular pool of HPV-8 E6, which exclusively interacts with MAML1 and is involved in  $\beta$ -E6 oncoprotein stabilization.

The immunofluorescence experiments were conducted in HPV-18 positive cells, so it was decided to further investigate the two pool hypotheses by using HPV-16 E6 as an additional way

to verify this hypothesis. Hence, the analyses were expanded by examining p53 degradation and degradation of another well-defined  $\alpha$ -E6 oncoprotein target, a PDZ domain-containing protein DLG1. As mentioned in Part I of the discussion, current studies have shown that p53 is degraded exclusively in the presence of E6AP (Huibregtse et al. 1993a), whilst degradation of DLG1 is E6AP-independent (Grm and Banks 2004). In addition to this, a recent study expanded this knowledge by showing that E6 can mediate the degradation of DLG1 independently of E6AP ubiquitin ligase activity, utilizing currently still unknown E6AP-independent mechanism (Vats et al. 2019). So, the following assays included individually overexpressed HPV-16 E6, or in combination with either MAML1 or E6AP in HEK-293 E6AP KO cells. Downregulation of endogenous p53 protein levels was observed in the presence of ectopically expressed HPV-16 E6 alone or with E6AP. However, on the contrary, overexpression of MAML1 with HPV-16 E6 led to restoration of the initial p53 levels. This result suggested that the overexpression of MAML1 can lead to its abundant presence within the cell, potentially occupying both cellular pools of HPV-16 E6 molecules. As a result of this, E6 may be prevented from interacting with E6AP and driving p53 proteasomal degradation. Importantly, this finding suggests that MAML1 has no effect on the degradation of E6's targets mediated by E6AP.

As it was expected, DLG1, as an E6AP-independent E6's target, was efficiently degraded in the presence of HPV-16 E6 alone and in the combination with E6AP, while no changes in DLG1 levels were detected when HPV-16 E6 was overexpressed with MAML1. This result indicated, same as for p53, that HPV-16 E6 pool that is stabilized by MAML1 is not involved in the regulation of DLG1 degradation. Both results of the degradation assays, including p53 and DLG1 suggest that E6/MAML1 complex is likely to be involved in other cellular activities which do not involve degradation of some of the well-known E6 substrates. Taken together with all previously discussed results, these observations suggest that, while both E6AP and MAML1 stabilize HPV-16 and -18 E6, they do not promote stability of the same cellular pools of E6. When MAML1 is silenced, the remaining pool of E6 is still in complex with E6AP and retains its catalytic activities involving degradation of some of the well-characterized cellular targets, such as p53 and DLG1. However, when MAML1 is overexpressed together with HR E6, the stability of the E6 pool bound to MAML1 is increased, but it appears that this cellular pool of E6 is not catalytically active in targeting cellular substrates such as p53 or DLG1. These findings suggest that the interaction between MAML1 and HR E6 may be involved in regulating other cellular processes beyond the

degradation of specific substrates, highlighting the need for the further research to fully understand the implications of these findings.

To further verify the effects of silencing MAML1 on E6 protein levels for both  $\alpha$ - and  $\beta$ -HPV genus with a confirmed proteasome-dependent regulation, the following experiment included determination of E6 half-life in the presence or absence of MAML1 by performing cycloheximide chase assays. In this experiment, E6AP was included as a control for the comparison of the effects of MAML1 silencing on E6 protein turnover, with E6 turnover in the absence of E6AP. This setting allowed to directly compare the impact of MAML1 on E6 half-life with the well-established role of E6AP in regulating E6 protein turnover. The results of these analyses showed that ablating MAML1 caused a decrease in the half-life of both HPV-18 and -8 E6, while silencing E6AP only decreased HPV-18 E6 half-life. HPV-18 E6 protein downregulation as a consequence of silencing E6AP is in agreement with previously published results (Tomaić, Pim, and Banks 2009a). The result of this cycloheximide chase assay agrees with the presented hypothesis of the existence of one cellular pool of HPV-8 E6 which is exclusively regulated via MAML1. Moreover, silencing both MAML1 and E6AP had the synergistic impact on HPV-18 E6 turnover, as the mutual silencing resulted in a further decrease in the protein half-life, when compared with individually silenced E6AP or MAML1. These findings also corroborate the two-pool hypothesis for HR E6s, so when either MAML1 or E6AP are depleted, HPV-18 E6 half-life is shorter than when both are present. Furthermore, the results presented in this doctoral thesis are consistent with a previous study that demonstrated the differential expression levels of E6 between HR mucosal and cutaneous HPVs. Specifically, a previous study showed that the steady-state expression levels of mucosal HPV-16 E6 were lower compared to cutaneous HPV-8 E6 (Kehmeier et al. 2002). This observation is consistent with the results of the described half-life experiments, which also confirmed differences between mucosal and cutaneous E6s, with HPV-18 E6 half-life being shorter than the half-life of HPV-8 E6.

The results obtained by blocking the protein synthesis using cyclohexamide suggested that increased protein levels and E6 stabilization by MAML1 occurs at the protein level, rather than at transcriptional level. Concerning the E6 stabilization and whether it occurs at the protein level, it is important to explain that the stabilization effect of E6 protein levels as a consequence of  $\beta$ -E6 interaction with MAML1 could be also attributed to the fact that MAML1 is a known co-activator of p300/CBP, which are histone acetyltransferases, that can stabilize and enhance the

transcriptional activity of E6 oncoproteins (Meyers et al. 2013). It is important to note that this mechanism is proposed for  $\beta$ -E6 oncoproteins, while it is not clear if the same mechanism can be applied to  $\alpha$ -HPV E6 oncoproteins. In the case of HPV-18 E6, it has been shown that interaction with Scrib leads to both increase in E6 transcription levels and an increase in the rate of E6 translation (Kranjec et al. 2016). However, this doctoral dissertation explored those aspects and the half-life experiments confirmed that E6 stabilization by MAML1 occurred on the protein level for both  $\alpha$  and  $\beta$  types of E6, despite the possibility of regulation at the transcriptional level.

The association of cellular proteins with their interacting partners can induce shuttling of the associated complex to other cellular compartment, leading even to modulations in protein functions. HPV-16 and HPV-18 E6 were reported to localize in the cytoplasmic perinuclear region (Daniels et al. 1998), to co-localize in the cytoplasm with p53 (Liang et al. 1993), as well as being evenly distributed in the cell cytoplasm and the nucleus (Guccione et al. 2002). Those inconsistent results can be assigned to the different cell lines used in the experiments, potential individual differences of HPV-16 and HPV-18 E6, different cell cycle phases and specific E6-fusion proteins and antibodies that were used in different studies. It is also highly likely that E6 oncoproteins undergo continuous localization changes within the cell and that cellular localization of HPV-16 and -18 E6 oncoproteins is not always uniform, but rather a snapshot of their dynamic distribution, considering the range of their different functions and the number of interaction partners. An additional study suggested that the subcellular localization of E6 is essential for p53 degradation activity revealing that the monomeric forms of HPV-16 and HPV-18 E6 exhibit predominant localization in the cell nucleus (García-Alai et al. 2007). Those monomeric species promote degradation of p53 in proteasome-dependent manner, which correlates with their nuclear localization. In contrast, the oligomeric E6 species do not promote p53 degradation, which is consistent with their localization in the cytoplasm (García-Alai et al. 2007). There is also a report indicating that the formation of HPV-18 E6/p53 complex causes protein shuttling from the nucleus to the cytoplasm (Stewart et al. 2005). Thus, E6 mediates the accumulation of polyubiquitinated p53 in the nucleus, but it is co-exported with p53 from the nucleus to the cytoplasm, and afterwards E6-driven p53 degradation can be mediated by both nuclear and cytoplasmic proteasomes (Stewart et al. 2005). Interestingly, MAML1 and E6AP are both usually found in the nucleus, but can be found in the cytoplasm as well (Kim et al. 2020; Hatakeyama et al. 1997).



Therefore, it was of interest to investigate if MAML1 and E6 interplay affects their cellular distribution. To determine whether E6 distribution and the accumulation in cellular compartments is changed by complexing with MAML1, in the comparison to binding with E6AP, a fractionation assay was performed. The assay showed that HPV-16 E6 distribution was primarily detected in the cytosolic fraction, while co-transfection of 16 E6 with MAML1 resulted in a change in the distribution of 16 E6. Specifically, there was an increase in the amounts of 16 E6 detected in the nucleic and membrane fractions, in addition to the cytosolic fraction where it was primarily detected. MAML1 by itself is predominantly present in the cytosolic fraction, while a smaller proportion is also present in the microtubule fraction. The analysis of MAML1 when it was co-transfected with 16 E6 demonstrated that changes in 16 E6 distribution, were accompanied by an accumulation of MAML1 in the same fractions, indicating that the two proteins interact and E6 affects MAML1's distribution. The increase of 16 E6 in the nucleus and membranes in the presence of MAML1 can be explained with the fact that MAML1 increases the amount of E6 protein levels because it stabilizes one particular pool and thus increases its total amount. The observed increase of HPV-16 E6 in the nuclear fraction may impact E6 functions by exposing it to different binding partners. On the other hand, E6AP is hijacked by 16 E6 and used as a molecular helper for performing diverse cellular functions including target degradation in the cytoplasm, so the 16 E6/E6AP complex is primarily found in that part of the cell. Overall, stabilization of HPV-16 E6 by MAML1 resulted in a drastic increase of 16 E6 distributed in the nucleus and membranes, while 16 E6 stabilization induced by E6AP increased the E6 cytosolic fraction, indicating that the two different pools are distributed in different cellular compartments. The results of the fractionation assay additionally supported the observation that MAML1 and E6AP stabilize two distinct pools of HPV-16 E6, which are also distributed differently within the cell.

HPV-8 E6, like HPV-16 E6, has been observed to have a predominant nuclear distribution with a lower presence in the cytoplasm (Mesplede et al. 2012). When examining HPV-8 E6 overexpressed in HEK-293 cells using the fractionation assays, again it was noticed that the distribution of HPV-8 E6 changes depending on the presence of MAML1. Expressed alone, HPV-8 E6 was mostly found in the nucleus, while when co-expressed with MAML1, HPV-8 E6 was distributed in the cytosolic and nuclear fractions. The immunofluorescence assay also revealed that HPV-8 E6 predominantly localized in the nucleus, and smaller amount with the cytoplasmic localization. Furthermore, when MAML1 was silenced in the immunofluorescence assay, the

HPV-8 E6 signal was significantly weakened, indicating that MAML1 plays a crucial role in regulating the stability of HPV-8 E6 oncoprotein. Furthermore, considering that HPV-8 E6 interacts with proteins distributed in the nucleus and cytoplasm, it would be of interest in future analyses to investigate effects of HPV-8 E6 binding to some other targets and whether the absence of MAML1 impacts the interaction profile of HPV-8 E6. Potential interaction of HPV-8 E6 with proteins both in the nucleus and cytoplasm suggests that this viral oncoprotein may have a wide range of effects on different cellular processes. Identifying additional targets of HPV-8 E6 may gain a better understanding of the molecular mechanisms underlying HPV-8-associated diseases, such as epidermodysplasia verruciformis and non-melanoma squamous cell carcinoma. Furthermore, the absence of MAML1 could impact the interaction profile of HPV-8 E6 because of the impaired HPV-8 E6 stabilization, and also due to the fact that MAML1 is known interactor of several transcription factors and co-activators. It is possible that MAML1 could modulate the ability of HPV-8 E6 to bind to certain targets or affect downstream signaling pathways. A complete depletion of MAML1, which is not achieved in siRNA experiments, could potentially result in the complete loss of HPV-8 E6 and its associated functions. This raises the question what role HPV-8 E7 plays in such a situation, which would be interesting to investigate. Additionally, studying the effects of MAML1 depletion on some other  $\beta$ -types, such as HPV-38 E6 (for which is confirmed that binds E6AP), would imply that a portion of HPV-38 E6 would probably remain in cells and be bound to E6AP in the absence of MAML1, and this could provide important insights into the functions of those E6 types, which could then be compared to HR E6 oncoproteins. On the contrary, when HPV-8 E6 was expressed with E6AP there was no changes in HPV-8 E6 localization, additionally confirming that E6AP does not influence HPV-8 E6 protein pool nor cellular shuttling between the compartments.

So far, the effects of E6/MAML1 binding on the stability, localization and distribution of both  $\alpha$ - and  $\beta$ -HPVs were discussed. However, it remains an open question whether and how this interaction translates into biological functions. Therefore, the focus of this doctoral thesis was also directed towards revealing the cellular and biological effects of HR E6/MAML1 complex formation. Silencing MAML1 or E6AP does not have an impact on cellular apoptosis both in HeLa and HT1080 HPV-8 E6 cells. Even though it would be expected that the decrease in E6 stability, as a consequence of MAML1/E6AP silencing, would result in an increase of cellular apoptosis

levels, in the case of HPV-18 E6 mostly as a result of a restoration of p53 levels (Garnett and Duerksen-Hughes 2006b). A slight induction in apoptosis was seen in HeLa cells treated with both MAML1 and E6AP, possibly as a synergic effect of their silencing on decreased HPV-18 E6 protein levels. The introduction of this thesis extensively describes the mechanisms by which  $\alpha$ -HPVs protect infected cells from apoptosis (Alfandari et al. 1999; Evan and Vousden 2001; Garnett and Duerksen-Hughes 2006b; Underbrink et al. 2008a; Yamato et al. 2006). The absence of increased apoptosis levels in HeLa and HT1080 HPV-8 E6 cells may can be understood in the light of a study done on HPV-16 E6 and -8 E6 (Underbrink et al. 2008a). Hence, this particular study showed that HPV-8 E6, same as HPV-16 E6 possess the ability to protect keratinocytes from apoptosis by reducing levels of Bak in those cells, via blocking the intrinsic apoptotic pathway (Underbrink et al. 2008a). Importantly, the expression of  $\beta$ -HPV-8 E6 oncoproteins protected keratinocytes from the apoptosis to the same extent as HPV-16 E6-expressing cells. Since it was previously described that Bak levels are normally regulated by E6AP (M. Thomas and Banks 1998b), as well as that E6-driven Bak degradation is also dependent upon the E6AP presence in the cells, it can partly explain why in this doctoral thesis silencing E6AP in HeLa and HT1080 HPV-8 E6 cells did not have an impact on apoptosis. Since cellular levels of E6AP were downregulated, subsequently also decreasing E6s protein levels, HPV-18 E6 and 8 E6 were unable to reduce Bak thus preventing and protecting HPV-positive cells from apoptosis. This implies that the basal, or constitutive, levels of Bak in E6-expressing cells, and with that also the levels of apoptosis, compared to those of siLuc-treated control cells, remained unaffected. Furthermore, to ensure that the protective effect seen for cells expressing HPV-8 E6 is limited to the ability to degrade Bak, in the mentioned study other Bcl-2 family members that are important for apoptosis signaling were also examined and it was found that their expression is not affected by the presence of HPV-8 E6 (Underbrink et al. 2008a). On the other hand, it is plausible that the restoration of p53 levels through E6AP silencing may require a longer time period than 72 hours to observe the impact on cellular apoptosis in HeLa cells.

On the contrary to the silencing of E6AP, it seems that silencing MAML1 cannot be explained by not mentioning the broader context of Notch signaling. In the case of silencing MAML1 in HeLa and HT1080 8 E6 it is necessary to emphasize once again that response to Notch differs greatly between cell types, with Notch promoting cell proliferation in some contexts, and apoptosis in others (Radtke and Raj 2003b). In brief, the interplay between Notch signaling and

HPV in the context of cervical carcinogenesis is a complex process, and the exact molecular mechanisms underlying their roles in cervical cancer are still a subject of a debate and research. In respect to HeLa cells that were analyzed for the apoptosis rates, it is important to mention that activated Notch signaling is detected in cells derived from cervical cancers, highlighting the likelihood of Notch activation as one of the complements to E6 and E7 towards cellular transformation (Zagouras et al. 1995; Lathion et al. 2003), as well as the notion that continued NOTCH1 expression is necessary to maintain neoplastic properties of CaSki, a cervical cancer derived cell line (Weijzen et al. 2002). Furthermore, it was shown that activated Notch cooperates with HPV-16 E6 and E7, and inhibits p53-induced apoptosis exhibiting an oncogenic role (Nair et al. 2003b). Those observations consolidate the fact that activated Notch in cervical cancers can have an oncogenic function (Radtke and Raj 2003b; Zagouras et al. 1995; Weijzen et al. 2002), that seems to be the opposite with Notch tumor suppressor role in murine skin. All of this implies that the role of Notch signaling in apoptosis is complex and not yet fully understood, with studies suggesting that it can have both pro- and anti-apoptotic effects depending on the cellular context and the stage of tumorigenesis. Therefore, it is possible that the interaction between E6 and MAML1 may indirectly influence apoptosis through its modulation of Notch signaling, but the precise mechanisms and effects are still not clarified, even though the experimental settings used in this doctoral dissertation may have required a longer time period than 72 hours to observe the impact of MAML silencing on cellular apoptosis. Additionally, the HT1080 HPV-8 E6 line was established from an immortalized cancer cell line, suggesting that the reduction of HPV-8 E6 stabilization by silencing MAML1 may not exert a substantial effect on apoptosis in this experimental context. Moreover, it is not expected that cutaneous HPV types would have an excessive impact on apoptosis, as HPV-8 E6 is less efficient in utilizing these pathways compared to HR E6 types. Additionally, the silencing of MAML1 led to a reduction in HPV-8 E6 protein levels, and cells lacking MAML1 control achieved by HPV-8 E6 binding would presumably undergo the process of differentiation due to activated Notch signaling. Furthermore, the process of apoptosis in HPV-positive cells, even though is mainly an E6-controlled function, depends also upon the effects of E7, and therefore it is a result of a joint interplay between E6 and E7 oncoproteins. Hence, as for the cellular proliferation that only partly depends on the effects of E6 (Chang et al. 2010; Lea et al. 2007), reducing the amount of E6 by silencing E6AP and MAML1 can also influence the cellular apoptosis to a limited degree and in cooperation with E7.

Previous reports have indicated the molecular consequences of the interaction between HPV-8 E6 and MAML1 on the Notch signaling pathway. These studies have revealed downstream effects, including repression of the transactivation of Notch-responsive genes, impacts on cell proliferation, and delay in keratinocyte differentiation (Brimer et al. 2012b; Tan et al. 2012b). To explore the effects of HR E6/MAML1 interaction on cell proliferation, HEK-293 E6AP KO cells were transfected with HPV-16 E6 and -18 E6 alone, or in combination with MAML1, E6AP or both. E6AP KO cells were utilized to eliminate any potential influence of endogenous E6AP and to rule out the possibility that the stabilization of E6 could be facilitated by the naturally occurring levels of E6AP. When overexpressed, E6AP-mediated E6 stabilization led to a statistically significant increase in cell proliferation. This effect of increased cell proliferation can be explained with the previously published results, which indicated that HPV-16 and HPV-18 E6 can induce cellular proliferation in epithelial cells by deregulation of G1/S cell cycle transition via impacting p27 (Saidu et al. 2019). A cyclin-dependent kinase inhibitor p27 is a critical cell cycle regulator which acts as an inhibitor of CDK2 and CDK4. E6 oncoproteins can stimulate cell proliferation by indirectly regulating p27 through targeting of a PDZ domain-containing protein NHERF-2 (Saidu et al. 2019). Revealing that E6 can induce cellular proliferation by deregulating the G1/S transition was rather surprising because it was thought to be mainly an E7-controlled function (Malanchi et al. 2002). HPV-16 E6 can overcome the antiproliferative signals by gaining the ability to drive p27-overexpressing cells into S phase. Hence, S phase entry required for viral DNA replication, is not exclusively controlled by E7, but involves also the actions of E6 (Malanchi et al. 2002). Furthermore, HPV-16 E6 promotes proliferation of keratinocytes in the basal layer through the combined inactivation of p53 and NOTCH1 (Kranjec et al. 2017). The inactivation of Notch signaling provides an insight into the possible mechanism that HR  $\alpha$ -HPV E6 oncoproteins can utilize to contribute to the basal cell proliferation.

MAML1-mediated stabilization of E6 did not exhibit noticeable effects on cellular proliferation, when compared with the effects of the analyzed HR HPV E6s alone. This effect can be augmented by the study which showed that expression of DN-MAML, a dominant negative form of MAML1 that blocks its coactivator activity, neither had any effects on cell proliferation of CaSki cells, nor an effect on cell cycle progression, preferably it only induced increase in cell viability (Kuncharin et al. 2011). These findings suggest that the interaction between E6 and MAML1 may not play a significant role in promoting cellular proliferation, but rather may have

other effects on cellular functions such as cell survival. Notably, when HPV-16 E6 or 18 E6 were co-expressed with both MAML1 and E6AP, the effect on cell proliferation was more pronounced than the effect of E6AP alone. This could be attributed to MAML1-mediated increase in E6 stability, which in turn may increase the amount of E6 within a cell, leading to an increased interaction between E6 and E6AP.

Evaluation of E6AP silencing in a scratch assay performed in HeLa cells resulted in a decreased rate of wound closure, due to growth suppression by p53, whose protein levels within the cell increase as a consequence of decreased E6 stability. This effect was confirmed in a study in which silencing E6AP resulted in the accumulation of p53 and growth suppression of HeLa cells (Hengstermann et al. 2005). Again, the plausible reason why apoptosis levels were not detected in these analyses could be that restored p53 initially affected cell proliferation and suppressed further growth in HeLa cells. Furthermore, the data from the scratch assay suggest that the anti-growth-suppressive effects of E6AP are reliant on its capability to facilitate the degradation of p53. In the same experimental settings, silencing MAML1 also led to a decrease in wound healing process, comparable to the decrease achieved by silencing E6AP. The same effect of reduced wound healing rate has been also previously reported in HeLa cells and the authors suggested that it was associated with the inhibition of Notch signaling (Yu et al. 2007). It is possible that abrogation of Notch signaling by silencing MAML1 leads to a growth arrest and loss of epithelial integrity, as Notch signaling is very finely tuned and modulations can be detrimental for cell proliferation (Talora et al. 2005; Yu et al. 2007). However, it is worth noting that the effect of MAML1 silencing on wound healing may be HPV-18 E6-specific since HPV-16 E6 has established altering role in Notch signaling, but the underlying mechanism does not involve MAML1 (Kranjec et al. 2017). Interestingly, MAML1 and E6AP did not exhibit synergistic effects, as silencing of both did not lead to an additional decrease in the percentage of the healed wound. It is possible that MAML1 silencing has an impact on cell proliferation through decreasing the stability and availability of E6 for binding to E6AP, through which it exerts most of its functions. Furthermore, the proliferation of HeLa cells is primarily driven by the actions of E7, while the effects of E6 play a smaller part in cell proliferation, meaning that reducing the amount of E6 can have a limited impact on cellular proliferation. E7, as the main driver of proliferation, is still abundantly present in HeLa cells what could be the explanation for the observed effects (Jones et al. 1997; Barbosa and Schlegel 1989).

Taken together, and summarized in **Figure 42**, presented results imply the existence of two distinct pools of HR E6 oncoproteins. One pool, consisting of E6/E6AP, has been well-characterized, while the other pool, comprising of E6/MAML1, requires further investigation to better understand its complete functions. E6/E6AP complex allows the viral oncoprotein to exert its oncogenic functions, while  $\alpha$ -E6/MAML1 complex does not have the same effect, even though it does increase the overall stability of E6. The proportion of  $\alpha$ -E6 that is stabilized by MAML1 presumably has some distinct, currently unknown cellular functions, and possibly interacts with different partners than  $\alpha$ -E6 stabilized by E6AP. This is further supported by the fact that HR E6 stabilized by MAML1 is distributed differently within the cell compared to E6 stabilized by E6AP.

Future research focused on exploring the specific cellular functions and molecular interactions of  $\alpha$ - and  $\beta$ -E6/MAML1 pools is needed for a more complete understanding of their functions and potential roles in HPV-associated cancers. One possible avenue is to investigate the effect of HR E6/MAML1 interaction on other cellular pathways beyond those investigated in this doctoral dissertation, possibly cell cycle control since Notch signaling has important role in cell cycle progression. Another direction for future research could be to identify additional proteins that interact specifically with the E6/MAML1 complex, since the presented results indicate that there may be distinct cellular functions associated with the pool of HR E6 oncoproteins stabilized by MAML1. To enhance comprehension of E6 stabilization, it would be valuable to identify whether other E6 target proteins that utilize same LXXLL motif for E6 interaction (such as IRF-3, E6BP and paxillin) have potential roles in stabilizing E6 protein levels and to investigate the broader implications of such interactions. Additionally, further studies could explore the effects of other cellular factors on the stability and activity of the E6/MAML1 pool, such as the histone acetyltransferase p300/CBP, which is a known coactivator of MAML1 (Jin et al. 2017). Furthermore, to gain a more comprehensive understanding of the role of MAML1 in HPV-associated cancers, it would be beneficial to investigate the interactions between MAML1 and other HR HPV types beyond HR HPV-16 and -18 investigated in this doctoral thesis, and also oncogenic  $\beta$ -HPV types such as HPV-5 and -38, in addition to the investigated  $\beta$ -HPV-8. Even though for HPV-16 was shown not to influence Notch signaling pathway, this may not be the case with other HR E6 oncoproteins that can potentially form stronger interactions with MAML1, and thus may be able to influence Notch-responsive genes.

Overall, these novel studies could shed light on the broader network of molecular interactions and signaling pathways that regulate the activity of E6 oncoproteins in HPV-infected cells.

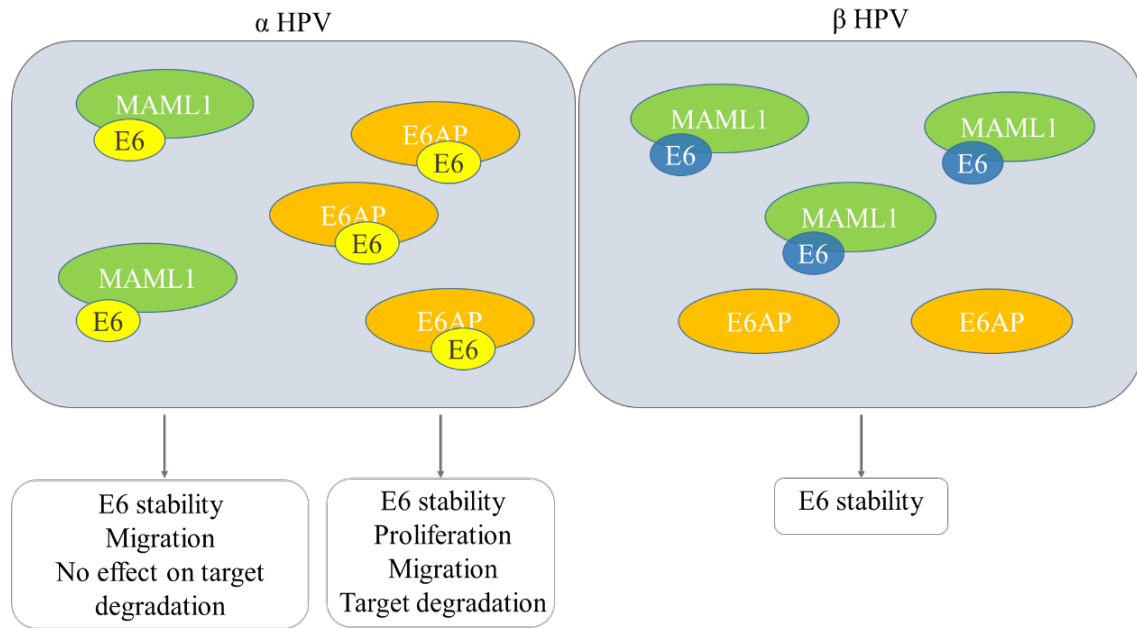


**Figure 42. A proposed model mechanism for  $\alpha$ - and  $\beta$ -HPV E6 interplay with MAML1.** The majority of  $\beta$ -E6 oncoproteins exclusively associate with MAML1 (right panel), while  $\alpha$ -E6 oncoproteins can bind both MAML1 and E6AP (left panel). MAML1-dependent protein stability of both  $\alpha$ -HPV E6 and  $\beta$ -HPV E6 impacts cell migration of HPV-18 positive cells, but it does not have an effect upon well-known HR E6 cellular target degradation.



## 6. CONCLUSIONS

Investigating the carcinogenic potential of naturally occurring variants of 16 E6 can provide insights into the association between genetic alterations and the elevated risk of cervical neoplasia, thereby emphasizing the significance of assessing cervical cancer risk. Part I of this doctoral dissertation provides insights into the functional mechanistic analyses of three genetic variants of HPV-16 E6: HPV-16 E6 D25N, E6 L83V, and E6 D25N L83V. The study demonstrated that these naturally occurring amino acid variations in the HPV-16 E6 oncoprotein can modify the level of activity of the E6 oncoprotein in various functional assays.

Based on these findings, it is possible that the naturally occurring variants of HPV-16 E6 may exhibit additional biological functions beyond those investigated in this doctoral study, which could potentially contribute to their pathogenicity. These results could guide future structural and biochemical analyses of naturally occurring HPV-16 E6 variants to comprehensively investigate their biological functions, as well as their role in modulating the progression of carcinogenesis,

The main concluding remarks of Part I are as follows:

- HPV-16 E6 D25N L83V variant exhibits an increased capacity to interact with E6AP
- HPV-16 E6 D25N L83V variant is the most efficient in triggering E6AP degradation among investigated E6 expression plasmids
- HPV-16 E6 D25N L83V variant shows higher protein levels in comparison 16 E6 D25N, 16 E6 L83V and wild-type 16 E6, but it also displays a more rapid protein turnover rate in comparison to 16 E6
- Cellular localization of ectopically expressed HPV-16 E6 and D25N, L83V, and D25N L83V mutants was found to be similar
- HPV-16 E6 D25N L83V is less effective in degrading p53 and PDZ-domain containing substrates *in vitro* in comparison to the other mutants and 16 E6
- HPV-16 E6 and the corresponding mutants efficiently target p53 and PDZ-domain containing substrates MAGI-1 and DLG1 for proteasome-mediated degradation in cultured cells

The Part II of doctoral thesis was focused on the previously uninvestigated effects of the interaction between HR E6 and MAML1 on E6 protein stability and function. It appears that this interaction is critical for maintenance of E6 protein levels and for its mediated biological activities such as cell proliferation and migration.

The main concluding remarks of Part II are as follows:

- HPV E6 oncoproteins from  $\alpha$ -HPV types interact with MAML1
- MAML1 increases protein stability of both  $\alpha$ - and  $\beta$ -HPV E6s in overexpression assays and in HPV-positive CaSki, HeLa and HT1080 8 E6 cells
- Intact LXXLL motif of MAML1 is required for E6 protein stabilization
- HPV E6 protein turnover is regulated by MAML1
- MAML1 stabilizes a distinctive cellular pool of HPV-18 E6 and an exclusive single cellular pool of HPV-8 E6
- MAML1 and HR E6 interaction does not affect p53 and DLG1 degradation
- E6 cellular localization and distribution of both  $\alpha$ - and  $\beta$ - HPV types is changed in presence of MAML1
- MAML1 ablation has no effect on apoptosis in HPV-positive HeLa and HT1080 8 E6 cells
- HR E6/MAML1 complex upregulates cell proliferation synergistically with E6AP
- 18 E6/MAML1 complex increases cell migration in HeLa cells

## 7. REFERENCES

- Accardi, Rosita, Wen Dong, Anouk Smet, Rutao Cui, Agnes Hautefeuille, Anne-Sophie Gabet, Bakary S. Sylla, Lutz Gissmann, Pierre Hainaut, and Massimo Tommasino. 2006. "Skin Human Papillomavirus Type 38 Alters P53 Functions by Accumulation of DeltaNp73." *EMBO Reports* 7 (3): 334–40. <https://doi.org/10.1038/sj.embor.7400615>.
- Aldabagh, Bishr, Jorge Gil C. Angeles, Adela R. Cardones, and Sarah T. Arron. 2013. "Cutaneous Squamous Cell Carcinoma and Human Papillomavirus: Is There an Association?" *Dermatologic Surgery: Official Publication for American Society for Dermatologic Surgery [et Al.]* 39 (1 Pt 1): 1–23. <https://doi.org/10.1111/j.1524-4725.2012.02558.x>.
- Alfandari, Jacklin, Sharon Shnitman Magal, Anna Jackman, Richard Schlegel, Pinhas Gonen, and Levana Sherman. 1999. "HPV16 E6 Oncoprotein Inhibits Apoptosis Induced during Serum–Calcium Differentiation of Foreskin Human Keratinocytes." *Virology* 257 (2): 383–96. <https://doi.org/10.1006/viro.1999.9675>.
- Anastas, J. N., T. L. Biechele, M. Robitaille, J. Muster, K. H. Allison, S. Angers, and R. T. Moon. 2012. "A Protein Complex of SCRIB, NOS1AP and VANGL1 Regulates Cell Polarity and Migration, and Is Associated with Breast Cancer Progression." *Oncogene* 31 (32): 3696–3708. <https://doi.org/10.1038/onc.2011.528>.
- Androphy, E. J., N. L. Hubbert, J. T. Schiller, and D. R. Lowy. 1987. "Identification of the HPV-16 E6 Protein from Transformed Mouse Cells and Human Cervical Carcinoma Cell Lines." *The EMBO Journal* 6 (4): 989–92. <https://doi.org/10.1002/j.1460-2075.1987.tb04849.x>.
- Ansari, Tina, Nicole Brimer, and Scott B. Vande Pol. 2012. "Peptide Interactions Stabilize and Restructure Human Papillomavirus Type 16 E6 to Interact with P53." *Journal of Virology* 86 (20): 11386–91. <https://doi.org/10.1128/JVI.01236-12>.
- Araujo-Arcos, Lilian Esmeralda, Sarita Montaña, Ciresthel Bello-Rios, Olga Lilia Garibay-Cerdenares, Marco Antonio Leyva-Vázquez, and Berenice Illades-Aguilar. 2022. "Molecular Insights into the Interaction of HPV-16 E6 Variants against MAGI-1 PDZ1 Domain." *Scientific Reports* 12 (1): 1898. <https://doi.org/10.1038/s41598-022-05995-1>.
- Arroyo Mühr, L. Sara, Emilie Hultin, Davit Bzhalava, Carina Eklund, Camilla Lagheden, Johanna Ekström, Hanna Johansson, Ola Forsslund, and Joakim Dillner. 2015. "Human Papillomavirus Type 197 Is Commonly Present in Skin Tumors." *International Journal of Cancer* 136 (11): 2546–55. <https://doi.org/10.1002/ijc.29325>.
- Artandi, Steven E., and Ronald A. DePinho. 2010. "Telomeres and Telomerase in Cancer." *Carcinogenesis* 31 (1): 9–18. <https://doi.org/10.1093/carcin/bgp268>.
- Artavanis-Tsakonas, Spyros, and Marc A. T. Muskavitch. 2010. "Chapter One - Notch: The Past, the Present, and the Future." In *Current Topics in Developmental Biology*, edited by Raphael Kopan, 92:1–29. Notch Signaling. Academic Press. [https://doi.org/10.1016/S0070-2153\(10\)92001-2](https://doi.org/10.1016/S0070-2153(10)92001-2).
- Asadurian, Yulia, Helena Kurilin, Hava Lichtig, Anna Jackman, Pinhas Gonen, Massimo Tommasino, Ingeborg Zehbe, and Levana Sherman. 2007a. "Activities of Human Papillomavirus 16 E6 Natural Variants in Human Keratinocytes." *Journal of Medical Virology* 79 (11): 1751–60. <https://doi.org/10.1002/jmv.20978>.
- Aster, Jon C., Warren S. Pear, and Stephen C. Blacklow. 2017. "The Varied Roles of Notch in Cancer." *Annual Review of Pathology* 12 (January): 245–75. <https://doi.org/10.1146/annurev-pathol-052016-100127>.
- Auslander, Noam, Yuri I. Wolf, Svetlana A. Shabalina, and Eugene V. Koonin. 2019. "A Unique Insert in the Genomes of High-Risk Human Papillomaviruses with a Predicted Dual Role in Conferring Oncogenic Risk." *F1000Research*. <https://doi.org/10.12688/f1000research.19590.2>.
- Avantaggiati, M. L., V. Ogryzko, K. Gardner, A. Giordano, A. S. Levine, and K. Kelly. 1997. "Recruitment of P300/CBP in P53-Dependent Signal Pathways." *Cell* 89 (7): 1175–84. [https://doi.org/10.1016/s0092-8674\(00\)80304-9](https://doi.org/10.1016/s0092-8674(00)80304-9).

- Barbosa, M. S., C. Edmonds, C. Fisher, J. T. Schiller, D. R. Lowy, and K. H. Vousden. 1990. "The Region of the HPV E7 Oncoprotein Homologous to Adenovirus E1a and Sv40 Large T Antigen Contains Separate Domains for Rb Binding and Casein Kinase II Phosphorylation." *The EMBO Journal* 9 (1): 153–60. <https://doi.org/10.1002/j.1460-2075.1990.tb08091.x>.
- Barbosa, M. S., and R. Schlegel. 1989. "The E6 and E7 Genes of HPV-18 Are Sufficient for Inducing Two-Stage in Vitro Transformation of Human Keratinocytes." *Oncogene* 4 (12): 1529–32.
- Basile, J. R., V. Zacny, and K. Münger. 2001. "The Cytokines Tumor Necrosis Factor-Alpha (TNF-Alpha) and TNF-Related Apoptosis-Inducing Ligand Differentially Modulate Proliferation and Apoptotic Pathways in Human Keratinocytes Expressing the Human Papillomavirus-16 E7 Oncoprotein." *The Journal of Biological Chemistry* 276 (25): 22522–28. <https://doi.org/10.1074/jbc.M010505200>.
- Bedard, Kristin M., Michael P. Underbrink, Heather L. Howie, and Denise A. Galloway. 2008. "The E6 Oncoproteins from Human Betapapillomaviruses Differentially Activate Telomerase through an E6AP-Dependent Mechanism and Prolong the Lifespan of Primary Keratinocytes." *Journal of Virology* 82 (8): 3894. <https://doi.org/10.1128/JVI.01818-07>.
- Bennett Saidu, Nathaniel Edward, Vedrana Filić, Miranda Thomas, Vanessa Sarabia-Vega, Anamaria Đukić, Frane Miljković, Lawrence Banks, and Vjekoslav Tomaić. 2019. "PDZ Domain-Containing Protein NHERF-2 Is a Novel Target of Human Papillomavirus Type 16 (HPV-16) and HPV-18." *Journal of Virology*, October. <https://doi.org/10.1128/JVI.00663-19>.
- Bergvall, Monika, Thomas Melendy, and Jacques Archambault. 2013. "The E1 Proteins." *Virology* 445 (1–2): 35–56. <https://doi.org/10.1016/j.virol.2013.07.020>.
- Bernard, H. U., S. Y. Chan, M. M. Manos, C. K. Ong, L. L. Villa, H. Delius, C. L. Peyton, H. M. Bauer, and C. M. Wheeler. 1994. "Identification and Assessment of Known and Novel Human Papillomaviruses by Polymerase Chain Reaction Amplification, Restriction Fragment Length Polymorphisms, Nucleotide Sequence, and Phylogenetic Algorithms." *The Journal of Infectious Diseases* 170 (5): 1077–85.
- Bernard, Hans-Ulrich. 2013. "Regulatory Elements in the Viral Genome." *Virology* 445 (1–2): 197–204. <https://doi.org/10.1016/j.virol.2013.04.035>.
- Bernard, Hans-Ulrich, Itzel E. Calleja-Macias, and S. Terence Dunn. 2006. "Genome Variation of Human Papillomavirus Types: Phylogenetic and Medical Implications." *International Journal of Cancer* 118 (5): 1071–76. <https://doi.org/10.1002/ijc.21655>.
- Bernard, Xavier, Philip Robinson, Yves Nominé, Murielle Masson, Sebastian Charbonnier, Juan Ramon Ramirez-Ramos, Francois Deryckere, Gilles Travé, and Georges Orfanoudakis. 2011. "Proteasomal Degradation of P53 by Human Papillomavirus E6 Oncoprotein Relies on the Structural Integrity of P53 Core Domain." *PLoS ONE* 6 (10): e25981. <https://doi.org/10.1371/journal.pone.0025981>.
- Bilder, David, Markus Schober, and Norbert Perrimon. 2003. "Integrated Activity of PDZ Protein Complexes Regulates Epithelial Polarity." *Nature Cell Biology* 5 (1): 53–58. <https://doi.org/10.1038/ncb897>.
- Blanpain, Cédric, William E. Lowry, H. Amalia Pasolli, and Elaine Fuchs. 2006. "Canonical Notch Signaling Functions as a Commitment Switch in the Epidermal Lineage." *Genes & Development* 20 (21): 3022–35. <https://doi.org/10.1101/gad.1477606>.
- Boda, Daniel, Anca Oana Docea, Daniela Calina, Mihaela Adriana Ilie, Constantin Caruntu, Sabina Zurac, Monica Neagu, et al. 2018. "Human Papilloma Virus: Apprehending the Link with Carcinogenesis and Unveiling New Research Avenues (Review)." *International Journal of Oncology* 52 (3): 637–55. <https://doi.org/10.3892/ijo.2018.4256>.
- Boon, Siaw Shi, and Lawrence Banks. 2013. "High-Risk Human Papillomavirus E6 Oncoproteins Interact with 14-3-3 $\zeta$  in a PDZ Binding Motif-Dependent Manner." *Journal of Virology* 87 (3): 1586–95. <https://doi.org/10.1128/JVI.02074-12>.
- Boon, Siaw Shi, Vjekoslav Tomaić, Miranda Thomas, Sally Roberts, and Lawrence Banks. 2015. "Cancer-Causing Human Papillomavirus E6 Proteins Display Major Differences in the Phospho-Regulation

- of Their PDZ Interactions.” *Journal of Virology* 89 (3): 1579–86. <https://doi.org/10.1128/JVI.01961-14>.
- Borggreffe, Tilman, and Robert Liefke. 2012. “Fine-Tuning of the Intracellular Canonical Notch Signaling Pathway.” *Cell Cycle (Georgetown, Tex.)* 11 (2): 264–76. <https://doi.org/10.4161/cc.11.2.18995>.
- Bottalico, Danielle, Zigui Chen, Boštjan J. Kocjan, Katja Seme, Mario Poljak, and Robert D. Burk. 2012. “Characterization of Human Papillomavirus Type 120: A Novel Betapapillomavirus with Tropism for Multiple Anatomical Niches.” *The Journal of General Virology* 93 (Pt 8): 1774–79. <https://doi.org/10.1099/vir.0.041897-0>.
- Bouvard, Véronique, Robert Baan, Kurt Straif, Yann Grosse, Béatrice Secretan, Fatiha El Ghissassi, Lamia Benbrahim-Tallaa, et al. 2009. “A Review of Human Carcinogens--Part B: Biological Agents.” *The Lancet. Oncology* 10 (4): 321–22.
- Boxman, Ingeborg L.A., Ron J.M. Berkhout, Linda H.C.Mulder, Monika C. Wolkers, Jan N. Bouwes Bavinck, Bert Jan Vermeer, and Jan ter Schegget. 1997. “Detection of Human Papillomavirus DNA in Plucked Hairs from Renal Transplant Recipients and Healthy Volunteers.”
- Braunstein, T. H., B. S. Madsen, B. Gavnholt, M. W. Rosenstjerne, C. Koefoed Johnsen, and B. Norrild. 1999. “Identification of a New Promoter in the Early Region of the Human Papillomavirus Type 16 Genome.” *The Journal of General Virology* 80 ( Pt 12) (December): 3241–50. <https://doi.org/10.1099/0022-1317-80-12-3241>.
- Bray, Sarah J. 2016. “Notch Signalling in Context.” *Nature Reviews. Molecular Cell Biology* 17 (11): 722–35. <https://doi.org/10.1038/nrm.2016.94>.
- Brimer, N., C. Lyons, A. E. Wallberg, and S. B. Vande Pol. 2012a. “Cutaneous Papillomavirus E6 Oncoproteins Associate with MAML1 to Repress Transactivation and NOTCH Signaling.” *Oncogene* 31 (43): 4639–46. <https://doi.org/10.1038/onc.2011.589>.
- Brimer, Nicole, Camille M. Drews, and Scott B. Vande Pol. 2017a. “Association of Papillomavirus E6 Proteins with Either MAML1 or E6AP Clusters E6 Proteins by Structure, Function, and Evolutionary Relatedness.” *PLoS Pathogens* 13 (12): 1–27. <https://doi.org/10.1371/journal.ppat.1006781>.
- Brimer, Nicole, Charles Lyons, and Scott B. Vande Pol. 2007a. “Association of E6AP (UBE3A) with Human Papillomavirus Type 11 E6 Protein.” *Virology* 358 (2): 303–10. <https://doi.org/10.1016/j.virol.2006.08.038>.
- Brimer, Nicole, Ramon Wade, and Scott Vande Pol. 2014. “Interactions between E6, FAK, and GIT1 at Paxillin LD4 Are Necessary for Transformation by Bovine Papillomavirus 1 E6.” *Journal of Virology* 88 (17): 9927–33. <https://doi.org/10.1128/JVI.00552-14>.
- Bruni, Laia, Mireia Diaz, Xavier Castellsagué, Elena Ferrer, F. Xavier Bosch, and Silvia de Sanjosé. 2010. “Cervical Human Papillomavirus Prevalence in 5 Continents: Meta-Analysis of 1 Million Women with Normal Cytological Findings.” *The Journal of Infectious Diseases* 202 (12): 1789–99. <https://doi.org/10.1086/657321>.
- Buck, Christopher B., Naiqian Cheng, Cynthia D. Thompson, Douglas R. Lowy, Alasdair C. Steven, John T. Schiller, and Benes L. Trus. 2008. “Arrangement of L2 within the Papillomavirus Capsid.” *Journal of Virology* 82 (11): 5190–97. <https://doi.org/10.1128/JVI.02726-07>.
- Burk, Robert D., Ariana Harari, and Zigui Chen. 2013a. “Human Papillomavirus Genome Variants.” *Virology* 445 (1–2): 232–43. <https://doi.org/10.1016/j.virol.2013.07.018>.
- Butz, K., C. Geisen, A. Ullmann, D. Spitkovsky, and F. Hoppe-Seyler. 1996. “Cellular Responses of HPV-Positive Cancer Cells to Genotoxic Anti-Cancer Agents: Repression of E6/E7-Oncogene Expression and Induction of Apoptosis.” *International Journal of Cancer* 68 (4): 506–13. [https://doi.org/10.1002/\(SICI\)1097-0215\(19961115\)68:4<506::AID-IJC17>3.0.CO;2-2](https://doi.org/10.1002/(SICI)1097-0215(19961115)68:4<506::AID-IJC17>3.0.CO;2-2).
- Butz, Karin, Tutik Ristriani, Arnd Hengstermann, Claudia Denk, Martin Scheffner, and Felix Hoppe-Seyler. 2003. “SiRNA Targeting of the Viral E6 Oncogene Efficiently Kills Human Papillomavirus-Positive Cancer Cells.” *Oncogene* 22 (38): 5938–45. <https://doi.org/10.1038/sj.onc.1206894>.

- Caldeira, S., E. M. de Villiers, and M. Tommasino. 2000. "Human Papillomavirus E7 Proteins Stimulate Proliferation Independently of Their Ability to Associate with Retinoblastoma Protein." *Oncogene* 19 (6): 821–26. <https://doi.org/10.1038/sj.onc.1203375>.
- Caldeira, Sandra, Ingeborg Zehbe, Rosita Accardi, Ilaria Malanchi, Wen Dong, Marianna Giarrè, Ethel-Michele de Villiers, Raffaele Filotico, Petra Boukamp, and Massimo Tommasino. 2003a. "The E6 and E7 Proteins of the Cutaneous Human Papillomavirus Type 38 Display Transforming Properties." *Journal of Virology* 77 (3): 2195–2206. <https://doi.org/10.1128/JVI.77.3.2195-2206.2003>.
- Campos, Samuel K. 2017. "Subcellular Trafficking of the Papillomavirus Genome during Initial Infection: The Remarkable Abilities of Minor Capsid Protein L2." *Viruses* 9 (12): E370. <https://doi.org/10.3390/v9120370>.
- Chakrabarti, Oishee, Karthikeyan Veerarahavalu, Vinay Tergaonkar, Yun Liu, Elliot J. Androphy, Margaret A. Stanley, and Sudhir Krishna. 2004. "Human Papillomavirus Type 16 E6 Amino Acid 83 Variants Enhance E6-Mediated MAPK Signaling and Differentially Regulate Tumorigenesis by Notch Signaling and Oncogenic Ras." *Journal of Virology* 78 (11): 5934–45. <https://doi.org/10.1128/JVI.78.11.5934-5945.2004>.
- Chang, J T-C, T-F Kuo, Y-J Chen, C-C Chiu, Y-C Lu, H-F Li, C-R Shen, and A-J Cheng. 2010. "Highly Potent and Specific siRNAs against E6 or E7 Genes of HPV16- or HPV18-Infected Cervical Cancers." *Cancer Gene Therapy* 17 (12): 827–36. <https://doi.org/10.1038/cgt.2010.38>.
- Chen, Alyce A., Tarik Gheit, Silvia Franceschi, Massimo Tommasino, Gary M. Clifford, and IARC HPV Variant Study Group. 2015. "Human Papillomavirus 18 Genetic Variation and Cervical Cancer Risk Worldwide." *Journal of Virology* 89 (20): 10680–87. <https://doi.org/10.1128/JVI.01747-15>.
- Chen, J. J., Y. Hong, E. Rustamzadeh, J. D. Baleja, and E. J. Androphy. 1998. "Identification of an Alpha Helical Motif Sufficient for Association with Papillomavirus E6." *The Journal of Biological Chemistry* 273 (22): 13537–44. <https://doi.org/10.1074/jbc.273.22.13537>.
- Chen, J. J., C. E. Reid, V. Band, and E. J. Androphy. 1995. "Interaction of Papillomavirus E6 Oncoproteins with a Putative Calcium-Binding Protein." *Science (New York, N.Y.)* 269 (5223): 529–31. <https://doi.org/10.1126/science.7624774>.
- Chen, Shan, Xiao Li, Junpu Qin, Yuan Chen, Longyang Liu, Dongqing Zhang, Minyi Wang, Maocai Wang, and Dikai Zhang. 2015. "APOBEC3A Possesses Anticancer and Antiviral Effects by Differential Inhibition of HPV E6 and E7 Expression on Cervical Cancer." *International Journal of Clinical and Experimental Medicine* 8 (7): 10548–57.
- Chiang, Cindy, Eva-Katharina Pauli, Jennifer Biryukov, Katharina F. Feister, Melissa Meng, Elizabeth A. White, Karl Munger, Peter M. Howley, Craig Meyers, and Michaela U. Gack. 2018. "The Human Papillomavirus E6 Oncoprotein Targets USP15 and TRIM25 To Suppress RIG-I-Mediated Innate Immune Signaling." *Journal of Virology* 92 (6). <https://doi.org/10.1128/JVI.01737-17>.
- Chiarugi, Paola, and Elisa Giannoni. 2008. "Anoikis: A Necessary Death Program for Anchorage-Dependent Cells." *Biochemical Pharmacology* 76 (11): 1352–64. <https://doi.org/10.1016/j.bcp.2008.07.023>.
- Chien, W. M., J. N. Parker, D. C. Schmidt-Grimminger, T. R. Broker, and L. T. Chow. 2000. "Casein Kinase II Phosphorylation of the Human Papillomavirus-18 E7 Protein Is Critical for Promoting S-Phase Entry." *Cell Growth & Differentiation: The Molecular Biology Journal of the American Association for Cancer Research* 11 (8): 425–35.
- Ciccia, Alberto, and Stephen J. Elledge. 2010. "The DNA Damage Response: Making It Safe to Play with Knives." *Molecular Cell* 40 (2): 179–204. <https://doi.org/10.1016/j.molcel.2010.09.019>.
- Ciechanover, Aaron. 2005. "Intracellular Protein Degradation: From a Vague Idea, through the Lysosome and the Ubiquitin-Proteasome System, and onto Human Diseases and Drug Targeting (Nobel Lecture)." *Angewandte Chemie - International Edition* 44 (37): 5944–67. <https://doi.org/10.1002/anie.200501428>.
- Clancy, Jennifer L., Michelle J. Henderson, Amanda J. Russell, David W. Anderson, Ronaldo J. Bova, Ian G. Campbell, David Y. H. Choong, et al. 2003. "EDD, the Human Orthologue of the Hyperplastic

- Discs Tumour Suppressor Gene, Is Amplified and Overexpressed in Cancer.” *Oncogene* 22 (32): 5070–81. <https://doi.org/10.1038/sj.onc.1206775>.
- Clemens, Karen E., Roger Brent, Jenó Gyuris, and Karl Munger. 1995. “Dimerization of the Human Papillomavirus E7 Oncoprotein in Vivo.” *Virology* 214 (1): 289–93. <https://doi.org/10.1006/viro.1995.9926>.
- Cochicho, Daniela, Rui Gil da Costa, and Ana Felix. 2021. “Exploring the Roles of HPV16 Variants in Head and Neck Squamous Cell Carcinoma: Current Challenges and Opportunities.” *Virology Journal* 18 (1): 217. <https://doi.org/10.1186/s12985-021-01688-9>.
- Cole, S. T., and O. Danos. 1987. “Nucleotide Sequence and Comparative Analysis of the Human Papillomavirus Type 18 Genome. Phylogeny of Papillomaviruses and Repeated Structure of the E6 and E7 Gene Products.” *Journal of Molecular Biology* 193 (4): 599–608. [https://doi.org/10.1016/0022-2836\(87\)90343-3](https://doi.org/10.1016/0022-2836(87)90343-3).
- Contreras-Cornejo, Humberto, Germán Saucedo-Correa, Javier Oviedo-Boyso, Juan José Valdez-Alarcón, Víctor Manuel Baizabal-Aguirre, Marcos Cajero-Juárez, and Alejandro Bravo-Patiño. 2016. “The CSL Proteins, Versatile Transcription Factors and Context Dependent Corepressors of the Notch Signaling Pathway.” *Cell Division* 11: 12. <https://doi.org/10.1186/s13008-016-0025-2>.
- Cooper, Brooke, Steven Schneider, Joanna Bohl, Yong hui Jiang, Arthur Beaudet, and Scott Vande Pol. 2003. “Requirement of E6AP and the Features of Human Papillomavirus E6 Necessary to Support Degradation of P53.” *Virology* 306 (1): 87–99. [https://doi.org/10.1016/s0042-6822\(02\)00012-0](https://doi.org/10.1016/s0042-6822(02)00012-0).
- Cornet, Iris, Véronique Bouvard, Maria Saveria Campo, Miranda Thomas, Lawrence Banks, Lutz Gissmann, Jérôme Lamartine, Bakary S. Sylla, Rosita Accardi, and Massimo Tommasino. 2012. “Comparative Analysis of Transforming Properties of E6 and E7 from Different Beta Human Papillomavirus Types.” *Journal of Virology* 86 (4): 2366–70. <https://doi.org/10.1128/JVI.06579-11>.
- Cornet, Iris, Tarik Gheit, Silvia Franceschi, Jerome Vignat, Robert D. Burk, Bakary S. Sylla, Massimo Tommasino, Gary M. Clifford, and IARC HPV Variant Study Group. 2012. “Human Papillomavirus Type 16 Genetic Variants: Phylogeny and Classification Based on E6 and LCR.” *Journal of Virology* 86 (12): 6855–61. <https://doi.org/10.1128/JVI.00483-12>.
- Coursey, Tami L., and Alison A. McBride. 2019. “Hitchhiking of Viral Genomes on Cellular Chromosomes.” *Annual Review of Virology* 6 (1): 275–96. <https://doi.org/10.1146/annurev-virology-092818-015716>.
- Craig, Stephanie G., Lesley A. Anderson, Andrew G. Schache, Michael Moran, Laura Graham, Keith Currie, Keith Rooney, et al. 2019. “Recommendations for Determining HPV Status in Patients with Oropharyngeal Cancers under TNM8 Guidelines: A Two-Tier Approach.” *British Journal of Cancer* 120 (8): 827–33. <https://doi.org/10.1038/s41416-019-0414-9>.
- Crook, T., J. A. Tidy, and K. H. Vousden. 1991. “Degradation of P53 Can Be Targeted by HPV E6 Sequences Distinct from Those Required for P53 Binding and Trans-Activation.” *Cell* 67 (3): 547–56. [https://doi.org/10.1016/0092-8674\(91\)90529-8](https://doi.org/10.1016/0092-8674(91)90529-8).
- Culp, Timothy D., Nancy M. Cladel, Karla K. Balogh, Lynn R. Budgeon, Andres F. Mejia, and Neil D. Christensen. 2006. “Papillomavirus Particles Assembled in 293TT Cells Are Infectious In Vivo.” *Journal of Virology* 80 (22): 11381–84. <https://doi.org/10.1128/JVI.01328-06>.
- Daniels, P. R., C. M. Sanders, and N. J. Maitland. 1998. “Characterization of the Interactions of Human Papillomavirus Type 16 E6 with P53 and E6-Associated Protein in Insect and Human Cells.” *The Journal of General Virology* 79 ( Pt 3) (March): 489–99. <https://doi.org/10.1099/0022-1317-79-3-489>.
- Day, Patricia M., and Mario Schelhaas. 2014. “Concepts of Papillomavirus Entry into Host Cells.” *Current Opinion in Virology* 4 (February): 24–31. <https://doi.org/10.1016/j.coviro.2013.11.002>.
- Degenhardt, Y. Y., and S. Silverstein. 2001. “Interaction of Zyxin, a Focal Adhesion Protein, with the E6 Protein from Human Papillomavirus Type 6 Results in Its Nuclear Translocation.” *Journal of Virology* 75 (23): 11791–802. <https://doi.org/10.1128/JVI.75.23.11791-11802.2001>.

- Delury, Craig P., Elizabeth K. Marsh, Claire D. James, Siaw Shi Boon, Lawrence Banks, Gillian L. Knight, and Sally Roberts. 2013. "The Role of Protein Kinase A Regulation of the E6 PDZ-Binding Domain during the Differentiation-Dependent Life Cycle of Human Papillomavirus Type 18." *Journal of Virology* 87 (17): 9463–72. <https://doi.org/10.1128/JVI.01234-13>.
- Demarest, R. M., F. Ratti, and A. J. Capobianco. 2008. "It's T- ALL about Notch." *Oncogene* 27 (38): 5082–91. <https://doi.org/10.1038/onc.2008.222>.
- DeMasi, Joseph, Kyung-Won Huh, Yoshihiro Nakatani, Karl Münger, and Peter M. Howley. 2005. "Bovine Papillomavirus E7 Transformation Function Correlates with Cellular P600 Protein Binding." *Proceedings of the National Academy of Sciences of the United States of America* 102 (32): 11486–91. <https://doi.org/10.1073/pnas.0505322102>.
- DiGiuseppe, Stephen, Malgorzata Bienkowska-Haba, Lucile G. M. Guion, Timothy R. Keiffer, and Martin Sapp. 2017. "Human Papillomavirus Major Capsid Protein L1 Remains Associated with the Incoming Viral Genome throughout the Entry Process." *Journal of Virology* 91 (16): e00537-17. <https://doi.org/10.1128/JVI.00537-17>.
- Dobrosotskaya, Irina, Rodney K. Guy, and Guy L. James. 1997. "MAGI-1, a Membrane-Associated Guanylate Kinase with a Unique Arrangement of Protein-Protein Interaction Domains\*." *Journal of Biological Chemistry* 272 (50): 31589–97. <https://doi.org/10.1074/jbc.272.50.31589>.
- Dongre, Anushka, and Robert A. Weinberg. 2019. "New Insights into the Mechanisms of Epithelial–Mesenchymal Transition and Implications for Cancer." *Nature Reviews Molecular Cell Biology* 20 (2): 69–84. <https://doi.org/10.1038/s41580-018-0080-4>.
- Doorbar, John. 2005a. "The Papillomavirus Life Cycle." *Journal of Clinical Virology: The Official Publication of the Pan American Society for Clinical Virology* 32 Suppl 1 (March): S7-15. <https://doi.org/10.1016/j.jcv.2004.12.006>.
- . 2006. "Molecular Biology of Human Papillomavirus Infection and Cervical Cancer." *Clinical Science (London, England: 1979)* 110 (5): 525–41. <https://doi.org/10.1042/CS20050369>.
- . 2013. "The E4 Protein; Structure, Function and Patterns of Expression." *Virology* 445 (1–2): 80–98. <https://doi.org/10.1016/j.virol.2013.07.008>.
- Doorslaer, Koenraad Van, Rob DeSalle, Mark H. Einstein, and Robert D. Burk. 2015. "Degradation of Human PDZ-Proteins by Human Alphapapillomaviruses Represents an Evolutionary Adaptation to a Novel Cellular Niche." *PLOS Pathogens* 11 (6): e1004980. <https://doi.org/10.1371/journal.ppat.1004980>.
- Dotto, G. Paolo. 2009. "Crosstalk of Notch with P53 and P63 in Cancer Growth Control." *Nature Reviews. Cancer* 9 (8): 587–95. <https://doi.org/10.1038/nrc2675>.
- Dreer, Marcel, Saskia van de Poel, and Frank Stubenrauch. 2017. "Control of Viral Replication and Transcription by the Papillomavirus E8<sup>E2</sup> Protein." *Virus Research* 231 (March): 96–102. <https://doi.org/10.1016/j.virusres.2016.11.005>.
- Drews, Camille M., Nicole Brimer, and Scott B. Vande Pol. 2020a. "Multiple Regions of E6AP (UBE3A) Contribute to Interaction with Papillomavirus E6 Proteins and the Activation of Ubiquitin Ligase Activity." *PLoS Pathogens* 16 (1): 1–25. <https://doi.org/10.1371/journal.ppat.1008295>.
- Du, Xiao, Zhong Cheng, Yi-Han Wang, Zi-Heng Guo, Si-Qin Zhang, Jian-Kun Hu, and Zong-Guang Zhou. 2014. "Role of Notch Signaling Pathway in Gastric Cancer: A Meta-Analysis of the Literature." *World Journal of Gastroenterology: WJG* 20 (27): 9191. <https://doi.org/10.3748/wjg.v20.i27.9191>.
- Duensing, Anette, Nicole Spardy, Payel Chatterjee, Leon Zheng, Joshua Parry, Rolando Cuevas, Nina Korzeniewski, and Stefan Duensing. 2009. "Centrosome Overduplication, Chromosomal Instability, and Human Papillomavirus Oncoproteins." *Environmental and Molecular Mutagenesis* 50 (8): 741–47. <https://doi.org/10.1002/em.20478>.
- Duensing, S., L. Y. Lee, A. Duensing, J. Basile, S. Piboonniyom, S. Gonzalez, C. P. Crum, and K. Munger. 2000. "The Human Papillomavirus Type 16 E6 and E7 Oncoproteins Cooperate to Induce Mitotic Defects and Genomic Instability by Uncoupling Centrosome Duplication from the Cell Division



- Cycle.” *Proceedings of the National Academy of Sciences of the United States of America* 97 (18): 10002–7. <https://doi.org/10.1073/pnas.170093297>.
- Duensing, Stefan, Anette Duensing, David C. Lee, Kirsten M. Edwards, Siribang-On Piboonniyom, Edwin Manuel, Leandros Skaltsounis, Laurent Meijer, and Karl Münger. 2004. “Cyclin-Dependent Kinase Inhibitor Indirubin-3'-Oxime Selectively Inhibits Human Papillomavirus Type 16 E7-Induced Numerical Centrosome Anomalies.” *Oncogene* 23 (50): 8206–15. <https://doi.org/10.1038/sj.onc.1208012>.
- Duensing, Stefan, and Karl Münger. 2003. “Human Papillomavirus Type 16 E7 Oncoprotein Can Induce Abnormal Centrosome Duplication through a Mechanism Independent of Inactivation of Retinoblastoma Protein Family Members.” *Journal of Virology* 77 (22): 12331–35. <https://doi.org/10.1128/JVI.77.22.12331-12335.2003>.
- Đukić, Anamaria, Lucija Lulić, Miranda Thomas, Josipa Skelin, Nathaniel Edward Bennett Saidu, Magdalena Grce, Lawrence Banks, and Vjekoslav Tomaić. 2020. “HPV Oncoproteins and the Ubiquitin Proteasome System: A Signature of Malignancy?” *Pathogens* 9 (2): 133. <https://doi.org/10.3390/pathogens9020133>.
- Dyson, N., P. M. Howley, K. Münger, and E. Harlow. 1989. “The Human Papilloma Virus-16 E7 Oncoprotein Is Able to Bind to the Retinoblastoma Gene Product.” *Science (New York, N.Y.)* 243 (4893): 934–37.
- Egawa, Nagayasu, and John Doorbar. 2017. “The Low-Risk Papillomaviruses.” *Virus Research* 231: 119–27. <https://doi.org/10.1016/j.virusres.2016.12.017>.
- Egawa, Nagayasu, Kiyofumi Egawa, Heather Griffin, and John Doorbar. 2015. “Human Papillomaviruses; Epithelial Tropisms, and the Development of Neoplasia.” *Viruses* 7 (7): 3863–90. <https://doi.org/10.3390/v7072802>.
- Egawa, Nagayasu, Qian Wang, Heather M. Griffin, Isao Murakami, Deborah Jackson, Radma Mahmood, and John Doorbar. 2017. “HPV16 and 18 Genome Amplification Show Different E4-Dependence, with 16E4 Enhancing E1 Nuclear Accumulation and Replicative Efficiency via Its Cell Cycle Arrest and Kinase Activation Functions.” *PLoS Pathogens* 13 (3): e1006282. <https://doi.org/10.1371/journal.ppat.1006282>.
- Elston, R. C., S. Naphine, and J. Doorbar. 1998. “The Identification of a Conserved Binding Motif within Human Papillomavirus Type 16 E6 Binding Peptides, E6AP and E6BP.” *The Journal of General Virology* 79 ( Pt 2) (February): 371–74. <https://doi.org/10.1099/0022-1317-79-2-371>.
- Elsum, Imogen, Laura Yates, Patrick O. Humbert, and Helena E. Richardson. 2012. “The Scribble-Dlg-Lgl Polarity Module in Development and Cancer: From Flies to Man.” *Essays in Biochemistry* 53: 141–68. <https://doi.org/10.1042/bse0530141>.
- Evan, Gerard I., and Karen H. Vousden. 2001. “Proliferation, Cell Cycle and Apoptosis in Cancer.” *Nature* 411 (6835): 342–48. <https://doi.org/10.1038/35077213>.
- Fehrmann, Frauke, David J. Klumpp, and Laimonis A. Laimins. 2003. “Human Papillomavirus Type 31 E5 Protein Supports Cell Cycle Progression and Activates Late Viral Functions upon Epithelial Differentiation.” *Journal of Virology* 77 (5): 2819–31. <https://doi.org/10.1128/jvi.77.5.2819-2831.2003>.
- Feltkamp, Mariet C.W., Maurits N.C. de Koning, Jan Nico Bouwes Bavinck, and Jan ter Schegget. 2008. “Betapapillomaviruses: Innocent Bystanders or Causes of Skin Cancer.” *Journal of Clinical Virology* 43 (4): 353–60. <https://doi.org/10.1016/j.jcv.2008.09.009>.
- Filippova, Maria, Lindsey Parkhurst, and Penelope J. Duerksen-Hughes. 2004a. “The Human Papillomavirus 16 E6 Protein Binds to Fas-Associated Death Domain and Protects Cells from Fas-Triggered Apoptosis.” *The Journal of Biological Chemistry* 279 (24): 25729–44. <https://doi.org/10.1074/jbc.M401172200>.
- Finley, Daniel. 2009. “Recognition and Processing of Ubiquitin-Protein Conjugates by the Proteasome.” *Annual Review of Biochemistry* 78: 477–513. <https://doi.org/10.1146/annurev.biochem.78.081507.101607>.

- Firzlaff, J. M., B. Lüscher, and R. N. Eisenman. 1991. "Negative Charge at the Casein Kinase II Phosphorylation Site Is Important for Transformation but Not for Rb Protein Binding by the E7 Protein of Human Papillomavirus Type 16." *Proceedings of the National Academy of Sciences of the United States of America* 88 (12): 5187–91. <https://doi.org/10.1073/pnas.88.12.5187>.
- Gammoh, Noor, Helena Sterlinko Grm, Paola Massimi, and Lawrence Banks. 2006. "Regulation of Human Papillomavirus Type 16 E7 Activity through Direct Protein Interaction with the E2 Transcriptional Activator." *Journal of Virology* 80 (4): 1787–97. <https://doi.org/10.1128/JVI.80.4.1787-1797.2006>.
- Ganti, Ketaki, Justyna Broniarczyk, Wiem Manoubi, Paola Massimi, Suruchi Mittal, David Pim, Anita Szalmas, et al. 2015a. "The Human Papillomavirus E6 PDZ Binding Motif: From Life Cycle to Malignancy." *Viruses* 7 (7): 3530–51. <https://doi.org/10.3390/v7072785>.
- Ganti, Ketaki, Paola Massimi, Joaquin Manzo-merino, Vjekoslav Tomai, David Pim, Lawrence Banks, Vjekoslav Tomaić, et al. 2016. "Interaction of the Human Papillomavirus E6 Oncoprotein with Sorting Nexin 27 Modulates Endocytic Cargo Transport Pathways." *PLoS Pathogens* 12 (9): 1–22. <https://doi.org/10.1371/journal.ppat.1005854>.
- García-Alai, María M., Karina I. Dantur, Clara Smal, Lía Pietrasanta, and Gonzalo de Prat-Gay. 2007. "High-Risk HPV E6 Oncoproteins Assemble into Large Oligomers That Allow Localization of Endogenous Species in Prototypic HPV-Transformed Cell Lines." *Biochemistry* 46 (2): 341–49. <https://doi.org/10.1021/bi602457q>.
- Gardiol, D., C. Kühne, B. Glaunsinger, S. S. Lee, R. Javier, and L. Banks. 1999. "Oncogenic Human Papillomavirus E6 Proteins Target the Discs Large Tumour Suppressor for Proteasome-Mediated Degradation." *Oncogene* 18 (40): 5487–96. <https://doi.org/10.1038/sj.onc.1202920>.
- Garnett, TO, and PJ Duerksen-Hughes. 2006a. "Modulation of Apoptosis by Human Papillomavirus (HPV) Oncoproteins." *Archives of Virology* 151 (12): 2321–35. <https://doi.org/10.1007/s00705-006-0821-0>.
- Geisen, C., and T. Kahn. 1996. "Promoter Activity of Sequences Located Upstream of the Human Papillomavirus Types of 16 and 18 Late Regions." *The Journal of General Virology* 77 ( Pt 9) (September): 2193–2200. <https://doi.org/10.1099/0022-1317-77-9-2193>.
- Gewin, Lindy, and Denise A. Galloway. 2001. "E Box-Dependent Activation of Telomerase by Human Papillomavirus Type 16 E6 Does Not Require Induction of c-Myc." *Journal of Virology* 75 (15): 7198–7201. <https://doi.org/10.1128/JVI.75.15.7198-7201.2001>.
- Gheit, Tarik. 2019a. "Mucosal and Cutaneous Human Papillomavirus Infections and Cancer Biology." *Frontiers in Oncology* 9. <https://doi.org/10.3389/fonc.2019.00355>.
- Gheit, Tarik, Francesca Rollo, Rosario N. Brancaccio, Alexis Robitaille, Luisa Galati, Massimo Giuliani, Alessandra Latini, et al. 2020. "Oral Infection by Mucosal and Cutaneous Human Papillomaviruses in the Men Who Have Sex with Men from the OHMAR Study." *Viruses* 12 (8): E899. <https://doi.org/10.3390/v12080899>.
- Giampieri, Silvia, Ramon García-Escudero, Judith Green, and Alan Storey. 2004. "Human Papillomavirus Type 77 E6 Protein Selectively Inhibits P53-Dependent Transcription of Proapoptotic Genes Following UV-B Irradiation." *Oncogene* 23 (34): 5864–70. <https://doi.org/10.1038/sj.onc.1207711>.
- Gillespie, Kenric A., Kavi P. Mehta, Laimonis A. Laimins, and Cary A. Moody. 2012. "Human Papillomaviruses Recruit Cellular DNA Repair and Homologous Recombination Factors to Viral Replication Centers." *Journal of Virology* 86 (17): 9520–26. <https://doi.org/10.1128/JVI.00247-12>.
- Glaunsinger, B. A., S. S. Lee, M. Thomas, L. Banks, and R. Javier. 2000. "Interactions of the PDZ-Protein MAGI-1 with Adenovirus E4-ORF1 and High-Risk Papillomavirus E6 Oncoproteins." *Oncogene* 19 (46): 5270–80. <https://doi.org/10.1038/sj.onc.1203906>.
- Graham, Sheila V. 2016. "Human Papillomavirus E2 Protein: Linking Replication, Transcription, and RNA Processing." *Journal of Virology* 90 (19): 8384–88. <https://doi.org/10.1128/JVI.00502-16>.

- Graham, Sheila V., and Arwa Ali A. Faizo. 2017. "Control of Human Papillomavirus Gene Expression by Alternative Splicing." *Virus Research* 231 (March): 83–95. <https://doi.org/10.1016/j.virusres.2016.11.016>.
- Grassmann, K., B. Rapp, H. Maschek, K. U. Petry, and T. Iftner. 1996. "Identification of a Differentiation-Inducible Promoter in the E7 Open Reading Frame of Human Papillomavirus Type 16 (HPV-16) in Raft Cultures of a New Cell Line Containing High Copy Numbers of Episomal HPV-16 DNA." *Journal of Virology* 70 (4): 2339–49. <https://doi.org/10.1128/JVI.70.4.2339-2349.1996>.
- Grm, Helena Sterlinko, and Lawrence Banks. 2004. "Degradation of HDlg and MAGIs by Human Papillomavirus E6 Is E6-AP-Independent." *The Journal of General Virology* 85 (Pt 10): 2815–19. <https://doi.org/10.1099/vir.0.80035-0>.
- Grodzki, Martha, Guillaume Besson, Christine Clavel, Annie Arslan, Silvia Franceschi, Philippe Birembaut, Massimo Tommasino, and Ingeborg Zehbe. 2006. "Increased Risk for Cervical Disease Progression of French Women Infected with the Human Papillomavirus Type 16 E6-350G Variant." *Cancer Epidemiology, Biomarkers & Prevention: A Publication of the American Association for Cancer Research, Cosponsored by the American Society of Preventive Oncology* 15 (4): 820–22. <https://doi.org/10.1158/1055-9965.EPI-05-0864>.
- Gross-Mesilaty, S., E. Reinstein, B. Bercovich, K. E. Tobias, A. L. Schwartz, C. Kahana, and A. Ciechanover. 1998. "Basal and Human Papillomavirus E6 Oncoprotein-Induced Degradation of Myc Proteins by the Ubiquitin Pathway." *Proceedings of the National Academy of Sciences of the United States of America* 95 (14): 8058–63. <https://doi.org/10.1073/pnas.95.14.8058>.
- Guccione, Ernesto, Paola Massimi, Agnieszka Bernat, and Lawrence Banks. 2002. "Comparative Analysis of the Intracellular Location of the High- and Low-Risk Human Papillomavirus Oncoproteins." *Virology* 293 (1): 20–25. <https://doi.org/10.1006/viro.2001.1290>.
- Gutierrez-Xicotencatl, Lourdes, Adolfo Pedroza-Saavedra, Lilia Chihu-Ampan, Azucena Salazar-Piña, Minerva Maldonado-Gama, and Fernando Esquivel-Guadarrama. 2021. "Cellular Functions of HPV16 E5 Oncoprotein during Oncogenic Transformation." *Molecular Cancer Research: MCR* 19 (2): 167–79. <https://doi.org/10.1158/1541-7786.MCR-20-0491>.
- Hampras, Shalaka S., Dana E. Rollison, Anna R. Giuliano, Sandrine McKay-Chopin, Lucia Minoni, Karen Sereday, Tarik Gheit, and Massimo Tommasino. 2017. "Prevalence and Concordance of Cutaneous Beta Human Papillomavirus Infection at Mucosal and Cutaneous Sites." *The Journal of Infectious Diseases* 216 (1): 92–96. <https://doi.org/10.1093/infdis/jix245>.
- Hatakeyama, S., J. P. Jensen, and A. M. Weissman. 1997. "Subcellular Localization and Ubiquitin-Conjugating Enzyme (E2) Interactions of Mammalian HECT Family Ubiquitin Protein Ligases." *The Journal of Biological Chemistry* 272 (24): 15085–92. <https://doi.org/10.1074/jbc.272.24.15085>.
- Hausen, H. zur. 1976. "Condylomata Acuminata and Human Genital Cancer." *Cancer Research* 36 (2 pt 2): 794.
- . 1996. "Papillomavirus Infections--a Major Cause of Human Cancers." *Biochimica Et Biophysica Acta* 1288 (2): F55-78.
- Hausen, Harald zur. 2002. "Papillomaviruses and Cancer: From Basic Studies to Clinical Application." *Nature Reviews Cancer* 2 (5): 342–50. <https://doi.org/10.1038/nrc798>.
- Hayman, Thomas J., Alan C. Hsu, Tatiana B. Kolesnik, Laura F. Dagley, Joschka Willemsen, Michelle D. Tate, Paul J. Baker, et al. 2019. "RIPLET, and Not TRIM25, Is Required for Endogenous RIG-I-Dependent Antiviral Responses." *Immunology and Cell Biology*, July. <https://doi.org/10.1111/imcb.12284>.
- Heery, David M., Eric Kalkhoven, Susan Hoare, and Malcolm G. Parker. 1997. "A Signature Motif in Transcriptional Co-Activators Mediates Binding to Nuclear Receptors." *Nature* 387 (6634): 733–36. <https://doi.org/10.1038/42750>.
- Helt, Anna-Marija, Jens Oliver Funk, and Denise A. Galloway. 2002. "Inactivation of Both the Retinoblastoma Tumor Suppressor and P21 by the Human Papillomavirus Type 16 E7 Oncoprotein

- Is Necessary To Inhibit Cell Cycle Arrest in Human Epithelial Cells.” *Journal of Virology* 76 (20): 10559–68. <https://doi.org/10.1128/JVI.76.20.10559-10568.2002>.
- Hengstermann, Arnd, Michael A D’silva, Petric Kuballa, Karin Butz, Felix Hoppe-Seyler, and Martin Scheffner. 2005. “Growth Suppression Induced by Downregulation of E6-AP Expression in Human Papillomavirus-Positive Cancer Cell Lines Depends on P53.” *Journal of Virology* 79 (14): 9296–9300. <https://doi.org/10.1128/JVI.79.14.9296-9300.2005>.
- Hershko, Avram, and Aaron Ciechanover. 1997. “The Ubiquitin System.” *Annu. Rev. Biochem.*, 425–79. [https://doi.org/10.1016/S0968-0004\(97\)01122-5](https://doi.org/10.1016/S0968-0004(97)01122-5).
- Hildesheim, Allan, and Sophia S. Wang. 2002. “Host and Viral Genetics and Risk of Cervical Cancer: A Review.” *Virus Research* 89 (2): 229–40. [https://doi.org/10.1016/s0168-1702\(02\)00191-0](https://doi.org/10.1016/s0168-1702(02)00191-0).
- Holloway, Amy, Mark Simmonds, Abul Azad, Joanna L. Fox, and Alan Storey. 2015. “Resistance to UV-Induced Apoptosis by  $\beta$ -HPV5 E6 Involves Targeting of Activated BAK for Proteolysis by Recruitment of the HERC1 Ubiquitin Ligase.” *International Journal of Cancer* 136 (12): 2831–43. <https://doi.org/10.1002/ijc.29350>.
- Howie, Heather L., Rachel A. Katzenellenbogen, and Denise A. Galloway. 2009. “Papillomavirus E6 Proteins.” *Virology* 384 (2): 324–34. <https://doi.org/10.1016/j.virol.2008.11.017>.
- Howley, Peter M., and Herbert J. Pfister. 2015. “Beta Genus Papillomaviruses and Skin Cancer.” *Virology* 479–480 (May): 290–96. <https://doi.org/10.1016/j.virol.2015.02.004>.
- Hu, Zheng, Da Zhu, Wei Wang, Weiyang Li, Wenlong Jia, Xi Zeng, Wencheng Ding, et al. 2015. “Genome-Wide Profiling of HPV Integration in Cervical Cancer Identifies Clustered Genomic Hot Spots and a Potential Microhomology-Mediated Integration Mechanism.” *Nature Genetics* 47 (2): 158–63. <https://doi.org/10.1038/ng.3178>.
- Hufbauer, Martin, James Cooke, Gijsbertus T. J. van der Horst, Herbert Pfister, Alan Storey, and Baki Akgül. 2015a. “Human Papillomavirus Mediated Inhibition of DNA Damage Sensing and Repair Drives Skin Carcinogenesis.” *Molecular Cancer* 14 (October). <https://doi.org/10.1186/s12943-015-0453-7>.
- Huh, Kyung-Won, Joseph DeMasi, Hidesato Ogawa, Yoshihiro Nakatani, Peter M. Howley, and Karl Münger. 2005. “Association of the Human Papillomavirus Type 16 E7 Oncoprotein with the 600-KDa Retinoblastoma Protein-Associated Factor, P600.” *Proceedings of the National Academy of Sciences of the United States of America* 102 (32): 11492–97. <https://doi.org/10.1073/pnas.0505337102>.
- Huh, Kyungwon, Xiaobo Zhou, Hiroyuki Hayakawa, Je-Yoel Cho, Towia A. Libermann, Jianping Jin, J. Wade Harper, and Karl Munger. 2007. “Human Papillomavirus Type 16 E7 Oncoprotein Associates with the Cullin 2 Ubiquitin Ligase Complex, Which Contributes to Degradation of the Retinoblastoma Tumor Suppressor.” *Journal of Virology* 81 (18): 9737–47. <https://doi.org/10.1128/JVI.00881-07>.
- Huibregtse, J. M., M. Scheffner, and P. M. Howley. 1991. “A Cellular Protein Mediates Association of P53 with the E6 Oncoprotein of Human Papillomavirus Types 16 or 18.” *The EMBO Journal* 10 (13): 4129–35. <https://doi.org/10.1002/j.1460-2075.1991.tb04990.x>.
- Huibregtse, J M, M Scheffner, and P M Howley. 1993a. “Cloning and Expression of the CDNA for E6-AP, a Protein That Mediates the Interaction of the Human Papillomavirus E6 Oncoprotein with P53.” *Molecular and Cellular Biology* 13 (2): 775–84. <https://doi.org/10.1128/mcb.13.2.775>.
- . 1993d. “Localization of the E6-AP Regions That Direct Human Papillomavirus E6 Binding, Association with P53, and Ubiquitination of Associated Proteins.” *Molecular and Cellular Biology* 13 (8): 4918–27. <https://doi.org/10.1128/mcb.13.8.4918>.
- Hummel, M., J. B. Hudson, and L. A. Laimins. 1992. “Differentiation-Induced and Constitutive Transcription of Human Papillomavirus Type 31b in Cell Lines Containing Viral Episomes.” *Journal of Virology* 66 (10): 6070–80. <https://doi.org/10.1128/JVI.66.10.6070-6080.1992>.

I

International Agency for Research on Cancer (IARC). n.d. *Monographs on the Evaluation of Carcinogenic Risks to Humans*. 2012th ed. Vol. 100B: 255-314. Lyon, France: IARC Press.

- Jabbar, Sean, Katerina Strati, Myeong Kyun Shin, Henry C. Pitot, and Paul F. Lambert. 2010. "Human Papillomavirus Type 16 E6 and E7 Oncoproteins Act Synergistically to Cause Head and Neck Cancer in Mice." *Virology* 407 (1): 60–67. <https://doi.org/10.1016/j.virol.2010.08.003>.
- Jackson, S., C. Harwood, M. Thomas, L. Banks, and A. Storey. 2000a. "Role of Bak in UV-Induced Apoptosis in Skin Cancer and Abrogation by HPV E6 Proteins." *Genes & Development* 14 (23): 3065–73. <https://doi.org/10.1101/gad.182100>.
- James, Claire D., and Sally Roberts. 2016. "Viral Interactions with PDZ Domain-Containing Proteins—An Oncogenic Trait?" *Pathogens* 5 (1): 8. <https://doi.org/10.3390/pathogens5010008>.
- James, Michael A., John H. Lee, and Aloysius J. Klingelhutz. 2006. "Human Papillomavirus Type 16 E6 Activates NF-KappaB, Induces CIAP-2 Expression, and Protects against Apoptosis in a PDZ Binding Motif-Dependent Manner." *Journal of Virology* 80 (11): 5301–7. <https://doi.org/10.1128/JVI.01942-05>.
- Javier, RT. 2008. "Cell Polarity Proteins: Common Targets for Tumorigenic Human Viruses." *Oncogene* 27 (55): 7031–46. <https://doi.org/10.1038/onc.2008.352>.
- Jewers, R. J., P. Hildebrandt, J. W. Ludlow, B. Kell, and D. J. McCance. 1992. "Regions of Human Papillomavirus Type 16 E7 Oncoprotein Required for Immortalization of Human Keratinocytes." *Journal of Virology* 66 (3): 1329–35.
- Jin, Jing, F. Donelson Smith, Chris Stark, Clark D. Wells, James P. Fawcett, Sarang Kulkarni, Pavel Metalnikov, et al. 2004. "Proteomic, Functional, and Domain-Based Analysis of in Vivo 14-3-3 Binding Proteins Involved in Cytoskeletal Regulation and Cellular Organization." *Current Biology: CB* 14 (16): 1436–50. <https://doi.org/10.1016/j.cub.2004.07.051>.
- Jin, Ke, Wen Zhou, Xiaoqing Han, Zhiqiang Wang, Bin Li, Shawn Jeffries, Wensi Tao, David J. Robbins, and Anthony J. Capobianco. 2017. "Acetylation of Mastermind-like 1 by P300 Drives the Recruitment of NACK to Initiate Notch-Dependent Transcription." *Cancer Research* 77 (16): 4228–37. <https://doi.org/10.1158/0008-5472.CAN-16-3156>.
- Jones, D L, R M Alani, and K Münger. 1997. "The Human Papillomavirus E7 Oncoprotein Can Uncouple Cellular Differentiation and Proliferation in Human Keratinocytes by Abrogating P21Cip1-Mediated Inhibition of Cdk2." *Genes & Development* 11 (16): 2101–11. <https://doi.org/10.1101/gad.11.16.2101>.
- K, Van Doorslaer, Sidi Ao, Zanier K, Rybin V, Deryckère F, Rector A, Burk Rd, Lienau Ek, van Ranst M, and Travé G. 2009. "Identification of Unusual E6 and E7 Proteins within Avian Papillomaviruses: Cellular Localization, Biophysical Characterization, and Phylogenetic Analysis." *Journal of Virology* 83 (17): 8759–70. <https://doi.org/10.1128/JVI.01777-08>.
- Kanda, T., S. Watanabe, S. Zanma, H. Sato, A. Furuno, and K. Yoshiike. 1991. "Human Papillomavirus Type 16 E6 Proteins with Glycine Substitution for Cysteine in the Metal-Binding Motif." *Virology* 185 (2): 536–43. [https://doi.org/10.1016/0042-6822\(91\)90523-e](https://doi.org/10.1016/0042-6822(91)90523-e).
- Kao, W. H., S. L. Beaudenon, A. L. Talis, J. M. Huibregtse, and P. M. Howley. 2000. "Human Papillomavirus Type 16 E6 Induces Self-Ubiquitination of the E6AP Ubiquitin-Protein Ligase." *Journal of Virology* 74 (14): 6408–17.
- Katzenellenbogen, Rachel. 2017. "Telomerase Induction in HPV Infection and Oncogenesis." *Viruses* 9 (7): 180. <https://doi.org/10.3390/v9070180>.
- Katzenellenbogen, Rachel A., Erin M. Egelkrout, Portia Vliet-Gregg, Lindy C. Gewin, Philip R. Gafken, and Denise A. Galloway. 2007. "NFX1-123 and Poly(A) Binding Proteins Synergistically Augment Activation of Telomerase in Human Papillomavirus Type 16 E6-Expressing Cells." *Journal of Virology* 81 (8): 3786–96. <https://doi.org/10.1128/JVI.02007-06>.
- Kehmeier, Eva, Heiko Rühl, Britta Voland, Melissa Conrad Stöppler, Elliot Androphy, and Hubert Stöppler. 2002. "Cellular Steady-State Levels of 'High Risk' but Not 'Low Risk' Human Papillomavirus (HPV) E6 Proteins Are Increased by Inhibition of Proteasome-Dependent Degradation Independent of Their P53- and E6AP-Binding Capabilities." *Virology* 299 (1): 72–87. <https://doi.org/10.1006/viro.2002.1502>.

- Kelley, Melissa L., Kerri E. Keiger, Chan Jae Lee, and Jon M. Huibregtse. 2005. "The Global Transcriptional Effects of the Human Papillomavirus E6 Protein in Cervical Carcinoma Cell Lines Are Mediated by the E6AP Ubiquitin Ligase." *Journal of Virology* 79 (6): 3737–47. <https://doi.org/10.1128/JVI.79.6.3737-3747.2005>.
- Kho, Eun-Young, Hsu-Kun Wang, N. Sanjib Banerjee, Thomas R. Broker, and Louise T. Chow. 2013. "HPV-18 E6 Mutants Reveal P53 Modulation of Viral DNA Amplification in Organotypic Cultures." *Proceedings of the National Academy of Sciences* 110 (19): 7542–49. <https://doi.org/10.1073/pnas.1304855110>.
- Khoury, George A., Richard C. Baliban, and Christodoulos A. Floudas. 2011. "Proteome-Wide Post-Translational Modification Statistics: Frequency Analysis and Curation of the Swiss-Prot Database." *Scientific Reports* 1 (1): 90. <https://doi.org/10.1038/srep00090>.
- Kim, Jiyoung, Hyeryun Kwon, You Keun Shin, Gahyeon Song, Taebok Lee, Youngeun Kim, Wonyoung Jeong, et al. 2020. "MAML1/2 Promote YAP/TAZ Nuclear Localization and Tumorigenesis." *Proceedings of the National Academy of Sciences of the United States of America* 117 (24): 13529–40. <https://doi.org/10.1073/pnas.1917969117>.
- King, Andrew M.Q., Micheal J. Adams, Eric B. Carstens, and Elliot J. Lefkowitz. 2005. "Virus Taxonomy: Classification and Nomenclature of Viruses." In *Virus Taxonomy*, II. <https://doi.org/10.1016/B978-0-12-249951-7.50001-8>.
- Kirnbauer, R, F Booy, N Cheng, D R Lowy, and J T Schiller. 1992. "Papillomavirus L1 Major Capsid Protein Self-Assembles into Virus-like Particles That Are Highly Immunogenic." *Proceedings of the National Academy of Sciences of the United States of America* 89 (24): 12180–84.
- Kiyono, T., A. Hiraiwa, M. Fujita, Y. Hayashi, T. Akiyama, and M. Ishibashi. 1997a. "Binding of High-Risk Human Papillomavirus E6 Oncoproteins to the Human Homologue of the Drosophila Discs Large Tumor Suppressor Protein." *Proceedings of the National Academy of Sciences of the United States of America* 94 (21): 11612–16. <https://doi.org/10.1073/pnas.94.21.11612>.
- Klingelutz, Aloysius J., and Ann Roman. 2012. "Cellular Transformation by Human Papillomaviruses: Lessons Learned by Comparing High- and Low-Risk Viruses." *Virology* 424 (2): 77–98. <https://doi.org/10.1016/j.virol.2011.12.018>.
- Kojika, Satoru, and James D. Griffin. 2001. "Notch Receptors and Hematopoiesis." *Experimental Hematology* 29 (9): 1041–52. [https://doi.org/10.1016/S0301-472X\(01\)00676-2](https://doi.org/10.1016/S0301-472X(01)00676-2).
- Kottaridi, Christine, Panagiota Resta, Danai Leventakou, Katerina Gioti, Ioannis Zygouras, Alina-Roxani Gouloumi, Georgios Sakagiannis, et al. 2022. "The T350G Variation of Human Papillomavirus 16 E6 Gene Prevails in Oropharyngeal Cancer from a Small Cohort of Greek Patients." *Viruses* 14 (8): 1724. <https://doi.org/10.3390/v14081724>.
- Kranjec, Christian, and Lawrence Banks. 2011. "A Systematic Analysis of Human Papillomavirus (HPV) E6 PDZ Substrates Identifies MAGI-1 as a Major Target of HPV Type 16 (HPV-16) and HPV-18 Whose Loss Accompanies Disruption of Tight Junctions." *Journal of Virology* 85 (4): 1757–64. <https://doi.org/10.1128/JVI.01756-10>.
- Kranjec, Christian, Christina Hollywood, Diane Libert, Heather Griffin, Radma Mahmood, Erin Isaacson, and John Doorbar. 2017. *The Journal of Pathology* 242 (4): 448–62. <https://doi.org/10.1002/path.4917>.
- Kranjec, Christian, Paola Massimi, and Lawrence Banks. 2014. "Restoration of MAGI-1 Expression in Human Papillomavirus-Positive Tumor Cells Induces Cell Growth Arrest and Apoptosis." *Journal of Virology* 88 (13): 7155–69. <https://doi.org/10.1128/JVI.03247-13>.
- Kranjec, Christian, Vjekoslav Tomaić, Paola Massimi, Lietta Nicolaidis, John Doorbar, and Lawrence Banks. 2016. "The High-Risk HPV E6 Target Scribble (HScrib) Is Required for HPV E6 Expression in Cervical Tumour-Derived Cell Lines." *Papillomavirus Research (Amsterdam, Netherlands)* 2 (December): 70–77. <https://doi.org/10.1016/j.pvr.2016.04.001>.
- Kühne, C., D. Gardiol, C. Guarnaccia, H. Amenitsch, and L. Banks. 2000. "Differential Regulation of Human Papillomavirus E6 by Protein Kinase A: Conditional Degradation of Human Discs Large Protein by Oncogenic E6." *Oncogene* 19 (51): 5884–91. <https://doi.org/10.1038/sj.onc.1203988>.

- Kumar, Ajay, Yongtong Zhao, Gaoyuan Meng, Musheng Zeng, Seetha Srinivasan, Laurie M. Delmolino, Qingshen Gao, et al. 2002. "Human Papillomavirus Oncoprotein E6 Inactivates the Transcriptional Coactivator Human ADA3." *Molecular and Cellular Biology* 22 (16): 5801–12. <https://doi.org/10.1128/MCB.22.16.5801-5812.2002>.
- Kuncharin, Yanin, Naunpun Sangphech, Patipark Kueanjinda, Parvapan Bhattarakosol, and Tanapat Palaga. 2011. "MAML1 Regulates Cell Viability via the NF-KB Pathway in Cervical Cancer Cell Lines." *Experimental Cell Research* 317 (13): 1830–40. <https://doi.org/10.1016/j.yexcr.2011.05.005>.
- Lambert, Paul F., Karl Münger, Frank Rösl, Daniel Hasche, and Massimo Tommasino. 2020. "Beta Human Papillomaviruses and Skin Cancer." *Nature* 588 (7838): E20–21. <https://doi.org/10.1038/s41586-020-3023-0>.
- Lange, Christian E., Claude Favrot, Mathias Ackermann, Jessica Gull, Elisabeth Vetsch, and Kurt Tobler. 2011. "Novel Snake Papillomavirus Does Not Cluster with Other Non-Mammalian Papillomaviruses." *Virology Journal* 8 (September): 436. <https://doi.org/10.1186/1743-422X-8-436>.
- Laprise, Patrick. 2011. "Emerging Role for Epithelial Polarity Proteins of the Crumbs Family as Potential Tumor Suppressors." *Journal of Biomedicine & Biotechnology* 2011: 868217. <https://doi.org/10.1155/2011/868217>.
- Lathion, Stéphanie, Janina Schaper, Peter Beard, and Kenneth Raj. 2003. "Notch1 Can Contribute to Viral-Induced Transformation of Primary Human Keratinocytes." *Cancer Research* 63 (24): 8687–94.
- Lavezzo, Enrico, Giulia Masi, Stefano Toppo, Elisa Franchin, Valentina Gazzola, Alessandro Sinigaglia, Serena Masiero, et al. 2016. "Characterization of Intra-Type Variants of Oncogenic Human Papillomaviruses by Next-Generation Deep Sequencing of the E6/E7 Region." *Viruses* 8 (3). <https://doi.org/10.3390/v8030079>.
- Lea, Jayanthi S., Noriaki Sunaga, Mitsuo Sato, Geetha Kalahasti, David S. Miller, John D. Minna, and Carolyn Y. Muller. 2007. "Silencing of HPV 18 Oncoproteins With RNA Interference Causes Growth Inhibition of Cervical Cancer Cells." *Reproductive Sciences (Thousand Oaks, Calif.)* 14 (1): 20–28. <https://doi.org/10.1177/1933719106298189>.
- Lechner, M. S., and L. A. Laimins. 1994. "Inhibition of P53 DNA Binding by Human Papillomavirus E6 Proteins." *Journal of Virology* 68 (7): 4262–73.
- Lechner, Matt, Jacklyn Liu, Liam Masterson, and Tim R. Fenton. 2022. "HPV-Associated Oropharyngeal Cancer: Epidemiology, Molecular Biology and Clinical Management." *Nature Reviews Clinical Oncology*, February. <https://doi.org/10.1038/s41571-022-00603-7>.
- Lee, Choongho, and Laimonis A. Laimins. 2004. "Role of the PDZ Domain-Binding Motif of the Oncoprotein E6 in the Pathogenesis of Human Papillomavirus Type 31." *Journal of Virology* 78 (22): 12366–77. <https://doi.org/10.1128/JVI.78.22.12366-12377.2004>.
- Lee, Choongho, Tonia R. Wooldridge, and Laimonis A. Laimins. 2007. "Analysis of the Roles of E6 Binding to E6TP1 and Nuclear Localization in the Human Papillomavirus Type 31 Life Cycle." *Virology* 358 (1): 201–10. <https://doi.org/10.1016/j.virol.2006.08.028>.
- Lee, S. S., R. S. Weiss, and R. T. Javier. 1997. "Binding of Human Virus Oncoproteins to HDlg/SAP97, a Mammalian Homolog of the Drosophila Discs Large Tumor Suppressor Protein." *Proceedings of the National Academy of Sciences of the United States of America* 94 (13): 6670–75. <https://doi.org/10.1073/pnas.94.13.6670>.
- Lefort, Karine, Anna Mandinova, Paola Ostano, Vihren Kolev, Valerie Calpini, Ingrid Kolfshoten, Vikram Devgan, et al. 2007. "Notch1 Is a P53 Target Gene Involved in Human Keratinocyte Tumor Suppression through Negative Regulation of ROCK1/2 and MRCKalpha Kinases." *Genes & Development* 21 (5): 562–77. <https://doi.org/10.1101/gad.1484707>.
- Legouis, Renaud, Fanny Jaulin-Bastard, Sonia Schott, Christel Navarro, Jean-Paul Borg, and Michel Labouesse. 2003. "Basolateral Targeting by Leucine-Rich Repeat Domains in Epithelial Cells." *EMBO Reports* 4 (11): 1096–1102. <https://doi.org/10.1038/sj.embor.7400006>.

- Li, X, and P Coffino. 1996. "High-Risk Human Papillomavirus E6 Protein Has Two Distinct Binding Sites within P53, of Which Only One Determines Degradation." *Journal of Virology* 70 (7): 4509–16. <https://doi.org/10.1128/jvi.70.7.4509-4516.1996>.
- Liang, X. H., M. Volkman, R. Klein, B. Herman, and S. J. Lockett. 1993. "Co-Localization of the Tumor-Suppressor Protein P53 and Human Papillomavirus E6 Protein in Human Cervical Carcinoma Cell Lines." *Oncogene* 8 (10): 2645–52.
- Liao, Shujie, Dongrui Deng, Weina Zhang, Xiaoji Hu, Wei Wang, Hui Wang, Yunping Lu, Shixuan Wang, Li Meng, and Ding Ma. 2013. "Human Papillomavirus 16/18 E5 Promotes Cervical Cancer Cell Proliferation, Migration and Invasion in Vitro and Accelerates Tumor Growth in Vivo." *Oncology Reports* 29 (1): 95–102. <https://doi.org/10.3892/or.2012.2106>.
- Lichtig, Hava, Meirav Algrisi, Liat Edri Botzer, Tal Abadi, Yulia Verbitzky, Anna Jackman, Massimo Tommasino, Ingeborg Zehbe, and Levana Sherman. 2006a. "HPV16 E6 Natural Variants Exhibit Different Activities in Functional Assays Relevant to the Carcinogenic Potential of E6." *Virology* 350 (1): 216–27. <https://doi.org/10.1016/j.virol.2006.01.038>.
- Lilley, Caroline E., Rachel A. Schwartz, and Matthew D. Weitzman. 2007. "Using or Abusing: Viruses and the Cellular DNA Damage Response." *Trends in Microbiology* 15 (3): 119–26. <https://doi.org/10.1016/j.tim.2007.01.003>.
- Lingle, W. L., W. H. Lutz, J. N. Ingle, N. J. Maihle, and J. L. Salisbury. 1998. "Centrosome Hypertrophy in Human Breast Tumors: Implications for Genomic Stability and Cell Polarity." *Proceedings of the National Academy of Sciences of the United States of America* 95 (6): 2950–55. <https://doi.org/10.1073/pnas.95.6.2950>.
- Liu, Xuefeng, Aleksandra Dakic, Yiyu Zhang, Yuhai Dai, Renxiang Chen, and Richard Schlegel. 2009. "HPV E6 Protein Interacts Physically and Functionally with the Cellular Telomerase Complex." *Proceedings of the National Academy of Sciences* 106 (44): 18780–85. <https://doi.org/10.1073/pnas.0906357106>.
- Liu, Xuefeng, Hang Yuan, Baojin Fu, Gary L. Disbrow, Tania Apolinario, Vjekoslav Tomaic, Melissa L. Kelley, Carl C. Baker, Jon Huibregtse, and Richard Schlegel. 2005. "The E6AP Ubiquitin Ligase Is Required for Transactivation of the HTERT Promoter by the Human Papillomavirus E6 Oncoprotein." *The Journal of Biological Chemistry* 280 (11): 10807–16. <https://doi.org/10.1074/jbc.M410343200>.
- Liu, Yun, Jason J. Chen, Qingshen Gao, Sorab Dalal, Yihui Hong, Claire P. Mansur, Vimla Band, and Elliot J. Androphy. 1999. "Multiple Functions of Human Papillomavirus Type 16 E6 Contribute to the Immortalization of Mammary Epithelial Cells." *Journal of Virology* 73 (9): 7297–7307.
- Lobry, Camille, Philmo Oh, and Iannis Aifantis. 2011. "Oncogenic and Tumor Suppressor Functions of Notch in Cancer: It's NOTCH What You Think." *The Journal of Experimental Medicine* 208 (10): 1931–35. <https://doi.org/10.1084/jem.20111855>.
- Longworth, Michelle S., and Laimonis A. Laimins. 2004. "Pathogenesis of Human Papillomaviruses in Differentiating Epithelia." *Microbiology and Molecular Biology Reviews: MMBR* 68 (2): 362–72. <https://doi.org/10.1128/MMBR.68.2.362-372.2004>.
- Lont, Anne P., Bin K. Kroon, Simon Horenblas, Maarten P. W. Gallee, Johannes Berkhof, Chris J. L. M. Meijer, and Peter J. F. Snijders. 2006. "Presence of High-Risk Human Papillomavirus DNA in Penile Carcinoma Predicts Favorable Outcome in Survival." *International Journal of Cancer* 119 (5): 1078–81. <https://doi.org/10.1002/ijc.21961>.
- López-Bueno, Alberto, Carla Mavian, Alejandro M. Labella, Dolores Castro, Juan J. Borrego, Antonio Alcami, and Alí Alejo. 2016. "Concurrence of Iridovirus, Polyomavirus, and a Unique Member of a New Group of Fish Papillomaviruses in Lymphocystis Disease-Affected Gilthead Sea Bream." Edited by S. R. Ross. *Journal of Virology* 90 (19): 8768–79. <https://doi.org/10.1128/JVI.01369-16>.
- Lou, Zhifeng, and Sheng Wang. 2014. "E3 Ubiquitin Ligases and Human Papillomavirus-Induced Carcinogenesis." *Journal of International Medical Research* 42 (2): 247–60. <https://doi.org/10.1177/0300060513506655>.



- Lowell, S., P. Jones, I. Le Roux, J. Dunne, and F. M. Watt. 2000a. “Stimulation of Human Epidermal Differentiation by Delta-Notch Signalling at the Boundaries of Stem-Cell Clusters.” *Current Biology: CB* 10 (9): 491–500. [https://doi.org/10.1016/s0960-9822\(00\)00451-6](https://doi.org/10.1016/s0960-9822(00)00451-6).
- Madsen, Birgitte S., Helle L. Jensen, Adriaan J. C. van den Brule, Jan Wohlfahrt, and Morten Frisch. 2008. “Risk Factors for Invasive Squamous Cell Carcinoma of the Vulva and Vagina--Population-Based Case-Control Study in Denmark.” *International Journal of Cancer* 122 (12): 2827–34. <https://doi.org/10.1002/ijc.23446>.
- Malanchi, Ilaria, Sandra Caldeira, Maja Krützfeldt, Marianna Giarre, Marianna Alunni-Fabbroni, and Massimo Tommasino. 2002. “Identification of a Novel Activity of Human Papillomavirus Type 16 E6 Protein in Deregulating the G1/S Transition.” *Oncogene* 21 (37): 5665–72. <https://doi.org/10.1038/sj.onc.1205617>.
- Marsh, Elizabeth K., Craig P. Delury, Nicholas J. Davies, Christopher J. Weston, Mohammed A. L. Miah, Lawrence Banks, Joanna L. Parish, Martin R. Higgs, and Sally Roberts. 2017. “Mitotic Control of Human Papillomavirus Genome-Containing Cells Is Regulated by the Function of the PDZ-Binding Motif of the E6 Oncoprotein.” *Oncotarget* 8 (12): 19491–506. <https://doi.org/10.18632/oncotarget.14469>.
- Martel, Catherine de, Damien Georges, Freddie Bray, Jacques Ferlay, and Gary M. Clifford. 2020. “Global Burden of Cancer Attributable to Infections in 2018: A Worldwide Incidence Analysis.” *The Lancet. Global Health* 8 (2): e180–90. [https://doi.org/10.1016/S2214-109X\(19\)30488-7](https://doi.org/10.1016/S2214-109X(19)30488-7).
- Martínez-Noël, Gustavo, Jeffrey T. Galligan, Mathew E. Sowa, Verena Arndt, Thomas M. Overton, J. Wade Harper, and Peter M. Howley. 2012. “Identification and Proteomic Analysis of Distinct UBE3A/E6AP Protein Complexes.” *Molecular and Cellular Biology* 32 (15): 3095–3106. <https://doi.org/10.1128/MCB.00201-12>.
- Martínez-Zapien, Denise, Francesc Xavier Ruiz, Juline Poirson, André Mitschler, Juan Ramirez, Anne Forster, Alexandra Cousido-Siah, et al. 2016. “Structure of the E6/E6AP/P53 Complex Required for HPV-Mediated Degradation of P53.” *Nature* 529 (7587): 541–45. <https://doi.org/10.1038/nature16481>.
- Massimi, Paola, Nisha Narayan, Miranda Thomas, Noor Gammoh, Susanne Strand, Dennis Strand, and Lawrence Banks. 2008. “Regulation of the HD1g/HScrib/Hugl-1 Tumour Suppressor Complex.” *Experimental Cell Research* 314 (18): 3306–17. <https://doi.org/10.1016/j.yexcr.2008.08.016>.
- Maufort, John P., Anny Shai, Henry Pitot, and Paul F. Lambert. 2010. “A Role for HPV 16 E5 in Cervical Carcinogenesis.” *Cancer Research* 70 (7): 2924–31. <https://doi.org/10.1158/0008-5472.CAN-09-3436>.
- Maufort, John P., Sybil M. Genter Williams, Henry C. Pitot, and Paul F. Lambert. 2007. “Human Papillomavirus 16 E5 Oncogene Contributes to Two Stages of Skin Carcinogenesis.” *Cancer Research* 67 (13): 6106–12. <https://doi.org/10.1158/0008-5472.CAN-07-0921>.
- McBride, Alison A. 2013. “The Papillomavirus E2 Proteins.” *Virology* 445 (1–2): 57–79. <https://doi.org/10.1016/j.virol.2013.06.006>.
- . 2017. “Mechanisms and Strategies of Papillomavirus Replication.” *Biological Chemistry* 398 (8): 919–27. <https://doi.org/10.1515/hsz-2017-0113>.
- . 2022. “Human Papillomaviruses: Diversity, Infection and Host Interactions.” *Nature Reviews. Microbiology* 20 (2): 95–108. <https://doi.org/10.1038/s41579-021-00617-5>.
- McCormack, S. J., S. E. Brazinski, J. L. Moore, B. A. Werness, and D. J. Goldstein. 1997. “Activation of the Focal Adhesion Kinase Signal Transduction Pathway in Cervical Carcinoma Cell Lines and Human Genital Epithelial Cells Immortalized with Human Papillomavirus Type 18.” *Oncogene* 15 (3): 265–74. <https://doi.org/10.1038/sj.onc.1201186>.
- McElhinny, A. S., J.-L. Li, and L. Wu. 2008. “Mastermind-like Transcriptional Co-Activators: Emerging Roles in Regulating Cross Talk among Multiple Signaling Pathways.” *Oncogene* 27 (38): 5138–47. <https://doi.org/10.1038/onc.2008.228>.
- McLaughlin, Margaret, and Karl Münger. 2010. “The Human Papillomavirus E7 Oncoprotein.” *Virology* 384 (2): 335–44. <https://doi.org/10.1016/j.virol.2008.10.006>.

- Mesplede, T., D. Gagnon, F. Bergeron-Labrecque, I. Azar, H. Senechal, F. Coutlee, and J. Archambault. 2012. "P53 Degradation Activity, Expression, and Subcellular Localization of E6 Proteins from 29 Human Papillomavirus Genotypes." *Journal of Virology* 86 (1): 94–107. <https://doi.org/10.1128/jvi.00751-11>.
- Meyers, Jordan M., and Karl Munger. 2014. "The Viral Etiology of Skin Cancer." *The Journal of Investigative Dermatology* 134 (e1): E29–32. <https://doi.org/10.1038/skinbio.2014.6>.
- Meyers, Jordan M., Jennifer M. Spangle, and Karl Munger. 2013a. "The Human Papillomavirus Type 8 E6 Protein Interferes with NOTCH Activation during Keratinocyte Differentiation." *Journal of Virology* 87 (8): 4762–67. <https://doi.org/10.1128/JVI.02527-12>.
- Meyers, Jordan M., Aayushi Uberoi, Miranda Grace, Paul F. Lambert, and Karl Munger. 2017a. "Cutaneous HPV8 and MmuPV1 E6 Proteins Target the NOTCH and TGF- $\beta$  Tumor Suppressors to Inhibit Differentiation and Sustain Keratinocyte Proliferation." *PLoS Pathogens* 13 (1): 1–29. <https://doi.org/10.1371/journal.ppat.1006171>.
- Moody, Cary. 2017. "Mechanisms by Which HPV Induces a Replication Competent Environment in Differentiating Keratinocytes." *Viruses* 9 (9): 261. <https://doi.org/10.3390/v9090261>.
- Moody, Cary A., and Laimonis A. Laimins. 2010a. "Human Papillomavirus Oncoproteins: Pathways to Transformation." *Nature Reviews. Cancer* 10 (8): 550–60. <https://doi.org/10.1038/nrc2886>.
- Morgan, Ethan L., Christopher W. Wasson, Lucy Hanson, David Kealy, Ieisha Pentland, Victoria McGuire, Cinzia Scarpini, et al. 2018. *STAT3 Activation by E6 Is Essential for the Differentiation-Dependent HPV18 Life Cycle*. *PLoS Pathogens*. Vol. 14. <https://doi.org/10.1371/journal.ppat.1006975>.
- Morris, E. J., and N. J. Dyson. 2001. "Retinoblastoma Protein Partners." *Advances in Cancer Research* 82: 1–54. [https://doi.org/10.1016/s0065-230x\(01\)82001-7](https://doi.org/10.1016/s0065-230x(01)82001-7).
- Muench, Peter, Sonja Probst, Johanna Schuetz, Natalie Leiprecht, Martin Busch, Sebastian Wesselborg, Frank Stubenrauch, and Thomas Iftner. 2010. "Cutaneous Papillomavirus E6 Proteins Must Interact with P300 and Block P53-Mediated Apoptosis for Cellular Immortalization and Tumorigenesis." *Cancer Research* 70 (17): 6913–24. <https://doi.org/10.1158/0008-5472.CAN-10-1307>.
- Muslin, A. J., J. W. Tanner, P. M. Allen, and A. S. Shaw. 1996. "Interaction of 14-3-3 with Signaling Proteins Is Mediated by the Recognition of Phosphoserine." *Cell* 84 (6): 889–97. [https://doi.org/10.1016/s0092-8674\(00\)81067-3](https://doi.org/10.1016/s0092-8674(00)81067-3).
- Nair, Pradip, Kumaravel Somasundaram, and Sudhir Krishna. 2003a. "Activated Notch1 Inhibits P53-Induced Apoptosis and Sustains Transformation by Human Papillomavirus Type 16 E6 and E7 Oncogenes through a PI3K-PKB/Akt-Dependent Pathway." *Journal of Virology* 77 (12): 7106–12. <https://doi.org/10.1128/JVI.77.12.7106-7112.2003>.
- Nakagawa, Shunsuke, and Jon M. Huibregtse. 2000. "Human Scribble (Vartul) Is Targeted for Ubiquitin-Mediated Degradation by the High-Risk Papillomavirus E6 Proteins and the E6AP Ubiquitin-Protein Ligase." *Molecular and Cellular Biology* 20 (21): 8244–53. <https://doi.org/10.1128/MCB.20.21.8244-8253.2000>.
- Nam, Yunsun, Piotr Sliz, Luyan Song, Jon C. Aster, and Stephen C. Blacklow. 2006. "Structural Basis for Cooperativity in Recruitment of MAML Coactivators to Notch Transcription Complexes." *Cell* 124 (5): 973–83. <https://doi.org/10.1016/j.cell.2005.12.037>.
- Neal, Christopher L., and Dihua Yu. 2010. "14-3-3 $\zeta$  as a Prognostic Marker and Therapeutic Target for Cancer." *Expert Opinion on Therapeutic Targets* 14 (12): 1343–54. <https://doi.org/10.1517/14728222.2010.531011>.
- Neumüller, Ralph A., and Juergen A. Knoblich. 2009. "Dividing Cellular Asymmetry: Asymmetric Cell Division and Its Implications for Stem Cells and Cancer." *Genes & Development* 23 (23): 2675–99. <https://doi.org/10.1101/gad.1850809>.
- Nguyen, Marie L., Minh M. Nguyen, Denis Lee, Anne E. Griep, and Paul F. Lambert. 2003. "The PDZ Ligand Domain of the Human Papillomavirus Type 16 E6 Protein Is Required for E6's Induction of Epithelial Hyperplasia in Vivo." *Journal of Virology* 77 (12): 6957–64. <https://doi.org/10.1128/jvi.77.12.6957-6964.2003>.

- Nicolas, Michael, Anita Wolfer, Kenneth Raj, J. Alain Kummer, Pleasantine Mill, Mascha van Noort, Chichung Hui, Hans Clevers, G. Paolo Dotto, and Freddy Radtke. 2003. "Notch1 Functions as a Tumor Suppressor in Mouse Skin." *Nature Genetics* 33 (3): 416–21. <https://doi.org/10.1038/ng1099>.
- Nominé, Yves, Murielle Masson, Sebastian Charbonnier, Katia Zanier, Tutik Ristriani, François Deryckère, Annie-Paule Sibler, et al. 2006a. "Structural and Functional Analysis of E6 Oncoprotein: Insights in the Molecular Pathways of Human Papillomavirus-Mediated Pathogenesis." *Molecular Cell* 21 (5): 665–78. <https://doi.org/10.1016/j.molcel.2006.01.024>.
- Oh, Stephen T., Saturo Kyo, and Laimonis A. Laimins. 2001. "Telomerase Activation by Human Papillomavirus Type 16 E6 Protein: Induction of Human Telomerase Reverse Transcriptase Expression through Myc and GC-Rich Sp1 Binding Sites." *Journal of Virology* 75 (12): 5559–66. <https://doi.org/10.1128/JVI.75.12.5559-5566.2001>.
- Oh, Stephen T., Michelle S. Longworth, and Laimonis A. Laimins. 2004. "Roles of the E6 and E7 Proteins in the Life Cycle of Low-Risk Human Papillomavirus Type 11." *Journal of Virology* 78 (5): 2620–26. <https://doi.org/10.1128/JVI.78.5.2620-2626.2004>.
- Orth, G., S. Jablonska, M. Favre, O. Croissant, M. Jarzabek-Chorzelska, and G. Rzesza. 1978. "Characterization of Two Types of Human Papillomaviruses in Lesions of Epidermodysplasia Verruciformis." *Proceedings of the National Academy of Sciences of the United States of America* 75 (3): 1537–41. <https://doi.org/10.1073/pnas.75.3.1537>.
- Orth, Gérard. 1987. "Epidermodysplasia Verruciformis." In *The Papovaviridae: The Papillomaviruses*, edited by Norman P. Salzman and Peter M. Howley, 199–243. The Viruses. Boston, MA: Springer US. [https://doi.org/10.1007/978-1-4757-0584-3\\_8](https://doi.org/10.1007/978-1-4757-0584-3_8).
- Ortiz-Ortiz, Julio, Luz del Carmen Alarcón-Romero, Marco Antonio Jiménez-López, Víctor Hugo Garzón-Barrientos, Itzel Calleja-Macías, Hugo Alberto Barrera-Saldaña, Marco Antonio Leyva-Vázquez, and Berenice Illades-Aguilar. 2015. "Association of Human Papillomavirus 16 E6 Variants with Cervical Carcinoma and Precursor Lesions in Women from Southern Mexico." *Virology Journal* 12 (February). <https://doi.org/10.1186/s12985-015-0242-3>.
- Ozbun, M. A., and C. Meyers. 1998. "Temporal Usage of Multiple Promoters during the Life Cycle of Human Papillomavirus Type 31b." *Journal of Virology* 72 (4): 2715–22. <https://doi.org/10.1128/JVI.72.4.2715-2722.1998>.
- Pan, Yonghua, Meei-Hua Lin, Xiaolin Tian, Hui-Teng Cheng, Thomas Gridley, Jie Shen, and Raphael Kopan. 2004. "Gamma-Secretase Functions through Notch Signaling to Maintain Skin Appendages but Is Not Required for Their Patterning or Initial Morphogenesis." *Developmental Cell* 7 (5): 731–43. <https://doi.org/10.1016/j.devcel.2004.09.014>.
- Pande, Shailja, Neeraj Jain, Bhupesh K. Prusty, Suresh Bhambhani, Sanjay Gupta, Rajyashri Sharma, Swaraj Batra, and Bhudev C. Das. 2008. "Human Papillomavirus Type 16 Variant Analysis of E6, E7, and L1 Genes and Long Control Region in Biopsy Samples from Cervical Cancer Patients in North India." *Journal of Clinical Microbiology* 46 (3): 1060–66. <https://doi.org/10.1128/JCM.02202-07>.
- Parker, D., M. Rivera, T. Zor, A. Henrion-Caude, I. Radhakrishnan, A. Kumar, L. H. Shapiro, P. E. Wright, M. Montminy, and P. K. Brindle. 1999. "Role of Secondary Structure in Discrimination between Constitutive and Inducible Activators." *Molecular and Cellular Biology* 19 (8): 5601–7. <https://doi.org/10.1128/MCB.19.8.5601>.
- Parkin, D. Maxwell, and Freddie Bray. 2006. "Chapter 2: The Burden of HPV-Related Cancers." *Vaccine* 24 Suppl 3 (August): S3/11-25. <https://doi.org/10.1016/j.vaccine.2006.05.111>.
- Patel, D, S M Huang, L A Baglia, and D J McCance. 1999. "The E6 Protein of Human Papillomavirus Type 16 Binds to and Inhibits Co-Activation by CBP and P300." *The EMBO Journal* 18 (18): 5061–72. <https://doi.org/10.1093/emboj/18.18.5061>.
- Patel, Daksha, Angela Incassati, Nancy Wang, and Dennis J. McCance. 2004. "Human Papillomavirus Type 16 E6 and E7 Cause Polyploidy in Human Keratinocytes and Up-Regulation of G2-M-Phase Proteins." *Cancer Research* 64 (4): 1299–1306. <https://doi.org/10.1158/0008-5472.can-03-2917>.

- Patrick, D. R., A. Oliff, and D. C. Heimbrook. 1994. "Identification of a Novel Retinoblastoma Gene Product Binding Site on Human Papillomavirus Type 16 E7 Protein." *The Journal of Biological Chemistry* 269 (9): 6842–50.
- Phelps, William C., Karl Munger, Carole L Yee, Julie A Barnes, and Peter M Howley. 1992. "Structure-Function Analysis of the Human Papillomavirus Type 16 E7 Oncoprotein." *Journal of Virology* 66 (4): 2418–27.
- Phelps, William C., Carole L. Yee, Karl Munger, and Peter M. Howley. 1988. "The Human Papillomavirus Type 16 E7 Gene Encodes Transactivation and Transformation Functions Similar to Those of Adenovirus E1A." *Cell* 53 (4): 539–47. [https://doi.org/10.1016/0092-8674\(88\)90570-3](https://doi.org/10.1016/0092-8674(88)90570-3).
- Pietsch, E. Christine, and Maureen E. Murphy. 2008. "Low Risk HPV-E6 Traps P53 in the Cytoplasm and Induces P53-Dependent Apoptosis." *Cancer Biology & Therapy* 7 (12): 1916–18.
- Pillai, M. R., R. Hariharan, Janki Mohan Babu, S. Lakshmi, S. V. Chiplunkar, M. Patkar, H. Tongaonkar, et al. 2009. "Molecular Variants of HPV-16 Associated with Cervical Cancer in Indian Population." *International Journal of Cancer* 125 (1): 91–103. <https://doi.org/10.1002/ijc.24322>.
- Pim, David, Martina Bergant, Siaw S. Boon, Ketaki Ganti, Christian Kranjec, Paola Massimi, Vanitha K. Subbaiah, Miranda Thomas, Vjekoslav Tomaić, and Lawrence Banks. 2012. "Human Papillomaviruses and the Specificity of PDZ Domain Targeting." *The FEBS Journal* 279 (19): 3530–37. <https://doi.org/10.1111/j.1742-4658.2012.08709.x>.
- Pim, David, Paola Massimi, and Lawrence Banks. 1997. "Alternatively Spliced HPV-18 E6\* Protein Inhibits E6 Mediated Degradation of P53 and Suppresses Transformed Cell Growth." *Oncogene* 15 (3): 257–64. <https://doi.org/10.1038/sj.onc.1201202>.
- Plevin, Michael J., Morgon M. Mills, and Mitsuhiro Ikura. 2005. "The LxxLL Motif: A Multifunctional Binding Sequence in Transcriptional Regulation." *Trends in Biochemical Sciences* 30 (2): 66–69. <https://doi.org/10.1016/j.tibs.2004.12.001>.
- Plummer, Martyn, Mark Schiffman, Philip E. Castle, Delphine Maucort-Boulch, Cosette M. Wheeler, and ALTS Group. 2007. "A 2-Year Prospective Study of Human Papillomavirus Persistence among Women with a Cytological Diagnosis of Atypical Squamous Cells of Undetermined Significance or Low-Grade Squamous Intraepithelial Lesion." *The Journal of Infectious Diseases* 195 (11): 1582–89. <https://doi.org/10.1086/516784>.
- Portal, Daniel, Bo Zhao, Michael A. Calderwood, Thomas Sommermann, Eric Johannsen, and Elliott Kieff. 2011. "EBV Nuclear Antigen EBNA1 Dismisses Transcription Repressors NCoR and RBPJ from Enhancers and EBNA2 Increases NCoR-Deficient RBPJ DNA Binding." *Proceedings of the National Academy of Sciences of the United States of America* 108 (19): 7808–13. <https://doi.org/10.1073/pnas.1104991108>.
- Pozuelo Rubio, Mercedes, Kathryn M. Geraghty, Barry H. C. Wong, Nicola T. Wood, David G. Campbell, Nick Morrice, and Carol Mackintosh. 2004. "14-3-3-Affinity Purification of over 200 Human Phosphoproteins Reveals New Links to Regulation of Cellular Metabolism, Proliferation and Trafficking." *The Biochemical Journal* 379 (Pt 2): 395–408. <https://doi.org/10.1042/BJ20031797>.
- Prathapam, Kuhne, and Banks. 2001. "The HPV-16 E7 Oncoprotein Binds Skip and Suppresses Its Transcriptional Activity." *Oncogene (2001)* 20, 7677 ± 7685, 7677 ± 7685.
- Proweller, Aaron, Lili Tu, John J. Lepore, Lan Cheng, Min Min Lu, John Seykora, Sarah E. Millar, Warren S. Pear, and Michael S. Parmacek. 2006. "Impaired Notch Signaling Promotes De Novo Squamous Cell Carcinoma Formation." *Cancer Research* 66 (15): 7438–44. <https://doi.org/10.1158/0008-5472.CAN-06-0793>.
- Pyeon, Dohun, Shane M. Pearce, Simon M. Lank, Paul Ahlquist, and Paul F. Lambert. 2009. "Establishment of Human Papillomavirus Infection Requires Cell Cycle Progression." *PLoS Pathogens* 5 (2): e1000318. <https://doi.org/10.1371/journal.ppat.1000318>.
- Quint, Koen D., Roel E. Genders, Maurits N. C. de Koning, Cinzia Borgogna, Marisa Gariglio, Jan Nico Bouwes Bavinck, John Doorbar, and Mariet C. Feltkamp. 2015. "Human Beta-Papillomavirus Infection and Keratinocyte Carcinomas." *The Journal of Pathology* 235 (2): 342–54. <https://doi.org/10.1002/path.4425>.

- Radtke, Freddy, and Kenneth Raj. 2003a. "The Role of Notch in Tumorigenesis: Oncogene or Tumour Suppressor?" *Nature Reviews Cancer* 3 (10): 756–67. <https://doi.org/10.1038/nrc1186>.
- Rangarajan, A., C. Talora, R. Okuyama, M. Nicolas, C. Mammucari, H. Oh, J. C. Aster, et al. 2001a. "Notch Signaling Is a Direct Determinant of Keratinocyte Growth Arrest and Entry into Differentiation." *The EMBO Journal* 20 (13): 3427–36. <https://doi.org/10.1093/emboj/20.13.3427>.
- Raudenská, Martina, Jan Balvan, and Michal Masařík. 2021. "Cell Death in Head and Neck Cancer Pathogenesis and Treatment." *Cell Death & Disease* 12 (2): 1–17. <https://doi.org/10.1038/s41419-021-03474-5>.
- Rector, Annabel, and Marc Van Ranst. 2013. "Animal Papillomaviruses." *Virology* 445 (1–2): 213–23. <https://doi.org/10.1016/j.virol.2013.05.007>.
- Reichrath, Jörg, and Sandra Reichrath. 2012. "Notch-Signaling and Nonmelanoma Skin Cancer: An Ancient Friend, Revisited." *Advances in Experimental Medicine and Biology* 727: 265–71. [https://doi.org/10.1007/978-1-4614-0899-4\\_20](https://doi.org/10.1007/978-1-4614-0899-4_20).
- Richard, C., C. Lanner, S. N. Naryzhny, L. Sherman, H. Lee, P. F. Lambert, and I. Zehbe. 2010. "The Immortalizing and Transforming Ability of Two Common Human Papillomavirus 16 E6 Variants with Different Prevalences in Cervical Cancer." *Oncogene* 29 (23): 3435–45. <https://doi.org/10.1038/onc.2010.93>.
- Riley, Rebecca R., Stefan Duensing, Tiffany Brake, Karl Münger, Paul F. Lambert, and Jeffrey M. Arbeit. 2003. "Dissection of Human Papillomavirus E6 and E7 Function in Transgenic Mouse Models of Cervical Carcinogenesis." *Cancer Research* 63 (16): 4862–71.
- Roberts, Jeffrey N., Christopher B. Buck, Cynthia D. Thompson, Rhonda Kines, Marcelino Bernardo, Peter L. Choyke, Douglas R. Lowy, and John T. Schiller. 2007. "Genital Transmission of HPV in a Mouse Model Is Potentiated by Nonoxynol-9 and Inhibited by Carrageenan." *Nature Medicine* 13 (7): 857–61. <https://doi.org/10.1038/nm1598>.
- Roberts, Sally, Craig Delury, and Elizabeth Marsh. 2012. "The PDZ Protein Discs-Large (DLG): The 'Jekyll and Hyde' of the Epithelial Polarity Proteins." *The FEBS Journal* 279 (19): 3549–58. <https://doi.org/10.1111/j.1742-4658.2012.08729.x>.
- Rodríguez, Ana Cecilia, Mark Schiffman, Rolando Herrero, Sholom Wacholder, Allan Hildesheim, Philip E. Castle, Diane Solomon, Robert Burk, and Proyecto Epidemiológico Guanacaste Group. 2008. "Rapid Clearance of Human Papillomavirus and Implications for Clinical Focus on Persistent Infections." *Journal of the National Cancer Institute* 100 (7): 513–17. <https://doi.org/10.1093/jnci/djn044>.
- Rodríguez-Ruiz, Hugo Alberto, Olga Lilia Garibay-Cerdenares, Berenice Illades-Aguiar, Sarita Montaña, Xiaowei Jiang, and Marco Antonio Leyva-Vázquez. 2019. "In Silico Prediction of Structural Changes in Human Papillomavirus Type 16 (HPV16) E6 Oncoprotein and Its Variants." *BMC Molecular and Cell Biology* 20 (1): 35. <https://doi.org/10.1186/s12860-019-0217-0>.
- Roman, Ann, and Karl Munger. 2013. "The Papillomavirus E7 Proteins." *Virology* 445 (1–2): 138–68. <https://doi.org/10.1016/j.virol.2013.04.013>.
- Ronco, L. V., A. Y. Karpova, M. Vidal, and P. M. Howley. 1998. "Human Papillomavirus 16 E6 Oncoprotein Binds to Interferon Regulatory Factor-3 and Inhibits Its Transcriptional Activity." *Genes & Development* 12 (13): 2061–72. <https://doi.org/10.1101/gad.12.13.2061>.
- Rosenberger, Simone, Johanna De-Castro Arce, Lutz Langbein, Renske D. M. Steenbergen, and Frank Rösl. 2010. "Alternative Splicing of Human Papillomavirus Type-16 E6/E6\* Early mRNA Is Coupled to EGF Signaling via Erk1/2 Activation." *Proceedings of the National Academy of Sciences* 107 (15): 7006–11. <https://doi.org/10.1073/pnas.1002620107>.
- Rousseau, Adrien, and Anne Bertolotti. 2018. "Regulation of Proteasome Assembly and Activity in Health and Disease." *Nature Reviews Molecular Cell Biology* 19 (11): 697–712. <https://doi.org/10.1038/s41580-018-0040-z>.
- Rozenblatt-Rosen, Orit, Rahul C. Deo, Megha Padi, Guillaume Adelmant, Michael A. Calderwood, Thomas Rolland, Miranda Grace, et al. 2012a. "Interpreting Cancer Genomes Using Systematic

- Host Network Perturbations by Tumour Virus Proteins.” *Nature* 487 (7408): 491–95. <https://doi.org/10.1038/nature11288>.
- Sabio, Guadalupe, James Simon Campbell Arthur, Yvonne Kuma, Mark Pegg, Julia Carr, Vicky Murray-Tait, Francisco Centeno, Michel Goedert, Nicholas A Morrice, and Ana Cuenda. 2005. “P38 $\gamma$  Regulates the Localisation of SAP97 in the Cytoskeleton by Modulating Its Interaction with GKAP.” *The EMBO Journal* 24 (6): 1134–45. <https://doi.org/10.1038/sj.emboj.7600578>.
- Saidu, Nathaniel Edward Bennett, Vedrana Filić, Miranda Thomas, Vanessa Sarabia-Vega, Anamaria Đukić, Frane Miljković, Lawrence Banks, and Vjekoslav Tomaić. 2019. “PDZ Domain-Containing Protein NHERF-2 Is a Novel Target of Human Papillomavirus 16 (HPV-16) and HPV-18.” *Journal of Virology* 94 (1). <https://doi.org/10.1128/JVI.00663-19>.
- Saint Just Ribeiro, Mariana, Magnus L. Hansson, and Annika E. Wallberg. 2007. “A Proline Repeat Domain in the Notch Co-Activator MAML1 Is Important for the P300-Mediated Acetylation of MAML1.” *Biochemical Journal* 404 (Pt 2): 289–98. <https://doi.org/10.1042/BJ20061900>.
- Sanjose, Silvia de, Wim Gv Quint, Laia Alemany, Daan T. Geraets, Jo Ellen Klaustermeier, Belen Lloveras, Sara Tous, et al. 2010. “Human Papillomavirus Genotype Attribution in Invasive Cervical Cancer: A Retrospective Cross-Sectional Worldwide Study.” *The Lancet. Oncology* 11 (11): 1048–56. [https://doi.org/10.1016/S1470-2045\(10\)70230-8](https://doi.org/10.1016/S1470-2045(10)70230-8).
- Saras, Jan, and Carl-Henrik Heldin. 1996. “PDZ Domains Bind Carboxy-Terminal Sequences of Target Proteins.” *Trends in Biochemical Sciences* 21 (12): 455–58. [https://doi.org/10.1016/S0968-0004\(96\)30044-3](https://doi.org/10.1016/S0968-0004(96)30044-3).
- Savkur, R. S., and T. P. Burris. 2004. “The Coactivator LXXLL Nuclear Receptor Recognition Motif.” *The Journal of Peptide Research: Official Journal of the American Peptide Society* 63 (3): 207–12. <https://doi.org/10.1111/j.1399-3011.2004.00126.x>.
- Scarth, James A., Molly R. Patterson, Ethan L. Morgan, and Andrew Macdonald. 2021. “The Human Papillomavirus Oncoproteins: A Review of the Host Pathways Targeted on the Road to Transformation.” *The Journal of General Virology* 102 (3): 001540. <https://doi.org/10.1099/jgv.0.001540>.
- Schache, Andrew G., Ned G. Powell, Kate S. Cuschieri, Max Robinson, Sam Leary, Hisham Mehanna, Davy Rapozo, et al. 2016. “HPV-Related Oropharynx Cancer in the United Kingdom: An Evolution in the Understanding of Disease Etiology.” *Cancer Research* 76 (22): 6598–6606. <https://doi.org/10.1158/0008-5472.CAN-16-0633>.
- Scheffner, M., J. M. Huibregtse, R. D. Vierstra, and P. M. Howley. 1993. “The HPV-16 E6 and E6-AP Complex Functions as a Ubiquitin-Protein Ligase in the Ubiquitination of P53.” *Cell* 75 (3): 495–505. [https://doi.org/10.1016/0092-8674\(93\)90384-3](https://doi.org/10.1016/0092-8674(93)90384-3).
- Scheffner, M., B. A. Werness, J. M. Huibregtse, A. J. Levine, and P. M. Howley. 1990a. “The E6 Oncoprotein Encoded by Human Papillomavirus Types 16 and 18 Promotes the Degradation of P53.” *Cell* 63 (6): 1129–36.
- Scheffner, Martin, and Sharad Kumar. 2014. “Mammalian HECT Ubiquitin-Protein Ligases: Biological and Pathophysiological Aspects.” *Biochimica Et Biophysica Acta* 1843 (1): 61–74. <https://doi.org/10.1016/j.bbamcr.2013.03.024>.
- Schiffman, Mark, Philip E. Castle, Jose Jeronimo, Ana C. Rodriguez, and Sholom Wacholder. 2007. “Human Papillomavirus and Cervical Cancer.” *Lancet (London, England)* 370 (9590): 890–907. [https://doi.org/10.1016/S0140-6736\(07\)61416-0](https://doi.org/10.1016/S0140-6736(07)61416-0).
- Schiffman, Mark, John Doorbar, Nicolas Wentzensen, Silvia de Sanjosé, Carole Fakhry, Bradley J. Monk, Margaret A. Stanley, and Silvia Franceschi. 2016. “Carcinogenic Human Papillomavirus Infection.” *Nature Reviews Disease Primers* 2 (1): 16086. <https://doi.org/10.1038/nrdp.2016.86>.
- Sekaric, Pedja, Jonathan J. Cherry, and Elliot J. Androphy. 2008a. “Binding of Human Papillomavirus Type 16 E6 to E6AP Is Not Required for Activation of HTERT.” *Journal of Virology* 82 (1): 71–76. <https://doi.org/10.1128/JVI.01776-07>.
- Senkomago, Virginia, S. Jane Henley, Cheryll C. Thomas, Jacqueline M. Mix, Lauri E. Markowitz, and Mona Saraiya. 2019. “Human Papillomavirus-Attributable Cancers - United States, 2012-2016.”

- MMWR. Morbidity and Mortality Weekly Report* 68 (33): 724–28. <https://doi.org/10.15585/mmwr.mm6833a3>.
- Shai, Anny, Tiffany Brake, Chamorro Somoza, and Paul F. Lambert. 2007. “The Human Papillomavirus E6 Oncogene Dysregulates the Cell Cycle and Contributes to Cervical Carcinogenesis through Two Independent Activities.” *Cancer Research* 67 (4): 1626–35. <https://doi.org/10.1158/0008-5472.CAN-06-3344>.
- Shang, Qinglong, Yan Wang, Yong Fang, Lanlan Wei, Sijia Chen, Yuhui Sun, Baoxin Li, Fengmin Zhang, and Hongxi Gu. 2011. “Human Papillomavirus Type 16 Variant Analysis of E6, E7, and L1 [Corrected] Genes and Long Control Region in [Corrected] Cervical Carcinomas in Patients in Northeast China.” *Journal of Clinical Microbiology* 49 (7): 2656–63. <https://doi.org/10.1128/JCM.02203-10>.
- Shay, Jerry W., and Woodring E. Wright. 2005. “Senescence and immortalization: Role of Telomeres and Telomerase.” *Carcinogenesis* 26 (5): 867–74. <https://doi.org/10.1093/carcin/bgh296>.
- Sherman, L., and R. Schlegel. 1996. “Serum- and Calcium-Induced Differentiation of Human Keratinocytes Is Inhibited by the E6 Oncoprotein of Human Papillomavirus Type 16.” *Journal of Virology* 70 (5): 3269–79.
- Sichero, Laura, João Simão Sobrinho, and Luisa Lina Villa. 2012. “Oncogenic Potential Diverge among Human Papillomavirus Type 16 Natural Variants.” *Virology* 432 (1): 127–32. <https://doi.org/10.1016/j.virol.2012.06.011>.
- Sidi, Abdellahi Ould M’hamed Ould, Khaled Ould Babah, Nicole Brimer, Yves Nominé, Christophe Romier, Bruno Kieffer, Scott Vande Pol, Gilles Travé, and Katia Zanier. 2011. “Strategies for Bacterial Expression of Protein-Peptide Complexes: Application to Solubilization of Papillomavirus E6.” *Protein Expression and Purification* 80 (1): 8–16. <https://doi.org/10.1016/j.pep.2011.06.013>.
- Simmonds, Mark, and Alan Storey. 2008. “Identification of the Regions of the HPV 5 E6 Protein Involved in Bak Degradation and Inhibition of Apoptosis.” *International Journal of Cancer. Journal International Du Cancer* 123 (10): 2260–66. <https://doi.org/10.1002/ijc.23815>.
- Skelin, Josipa, Ivan Sabol, and Vjekoslav Tomaić. 2022. “Do or Die: HPV E5, E6 and E7 in Cell Death Evasion.” *Pathogens* 11 (9): 1027. <https://doi.org/10.3390/pathogens11091027>.
- Sluder, Greenfield, and Joshua J. Nordberg. 2004. “The Good, the Bad and the Ugly: The Practical Consequences of Centrosome Amplification.” *Current Opinion in Cell Biology* 16 (1): 49–54. <https://doi.org/10.1016/j.ceb.2003.11.006>.
- Smotkin, D., and F. O. Wettstein. 1986. “Transcription of Human Papillomavirus Type 16 Early Genes in a Cervical Cancer and a Cancer-Derived Cell Line and Identification of the E7 Protein.” *Proceedings of the National Academy of Sciences of the United States of America* 83 (13): 4680–84. <https://doi.org/10.1073/pnas.83.13.4680>.
- Snijders, P. J., M. van Duin, J. M. Walboomers, R. D. Steenbergen, E. K. Risse, T. J. Helmerhorst, R. H. Verheijen, and C. J. Meijer. 1998. “Telomerase Activity Exclusively in Cervical Carcinomas and a Subset of Cervical Intraepithelial Neoplasia Grade III Lesions: Strong Association with Elevated Messenger RNA Levels of Its Catalytic Subunit and High-Risk Human Papillomavirus DNA.” *Cancer Research* 58 (17): 3812–18.
- Snijders, Peter J.F., Renske D.M. Steenbergen, Daniëlle A.M. Heideman, and Chris J.L.M. Meijer. 2006. “HPV-Mediated Cervical Carcinogenesis: Concepts and Clinical Implications.” *Journal of Pathology* 208 (2): 152–64. <https://doi.org/10.1002/path.1866>.
- Song, S., H. C. Pitot, and P. F. Lambert. 1999. “The Human Papillomavirus Type 16 E6 Gene Alone Is Sufficient to Induce Carcinomas in Transgenic Animals.” *Journal of Virology* 73 (7): 5887–93. <https://doi.org/10.1128/JVI.73.7.5887-5893.1999>.
- South, Andrew P., Karin J. Purdie, Stephen A. Watt, Sam Haldenby, Nicoline den Breems, Michelle Dimon, Sarah T. Arron, et al. 2014. “NOTCH1 Mutations Occur Early during Cutaneous Squamous Cell Carcinogenesis.” *The Journal of Investigative Dermatology* 134 (10): 2630–38. <https://doi.org/10.1038/jid.2014.154>.

- Stanley, Margaret. 2010. "Pathology and Epidemiology of HPV Infection in Females." *Gynecologic Oncology* 117 (2 Suppl): S5-10. <https://doi.org/10.1016/j.ygyno.2010.01.024>.
- Steben, Marc, and Eliane Duarte-Franco. 2007. "Human Papillomavirus Infection: Epidemiology and Pathophysiology." *Gynecologic Oncology* 107 (2 SUPPL.): S2. <https://doi.org/10.1016/j.ygyno.2007.07.067>.
- Stewart, Deborah, Anirban Ghosh, and Greg Matlashewski. 2005. "Involvement of Nuclear Export in Human Papillomavirus Type 18 E6-Mediated Ubiquitination and Degradation of P53." *Journal of Virology* 79 (14): 8773–83. <https://doi.org/10.1128/jvi.79.14.8773-8783.2005>.
- Stöppler, M. C., K. Ching, H. Stöppler, K. Clancy, R. Schlegel, and J. Icenogle. 1996. "Natural Variants of the Human Papillomavirus Type 16 E6 Protein Differ in Their Abilities to Alter Keratinocyte Differentiation and to Induce P53 Degradation." *Journal of Virology* 70 (10): 6987–93.
- Stracker, Travis H., Takehiko Usui, and John H.J. Petrini. 2009. "Taking the Time to Make Important Decisions: The Checkpoint Effector Kinases Chk1 and Chk2 and the DNA Damage Response." *DNA Repair* 8 (9): 1047–54. <https://doi.org/10.1016/j.dnarep.2009.04.012>.
- Strati, Katerina, and Paul F. Lambert. 2007a. "Role of Rb-Dependent and Rb-Independent Functions of Papillomavirus E7 Oncogene in Head and Neck Cancer." *Cancer Research* 67 (24): 11585–93. <https://doi.org/10.1158/0008-5472.CAN-07-3007>.
- Stubenrauch, Frank, Hock B. Lim, and Laimonis A. Laimins. 1998. "Differential Requirements for Conserved E2 Binding Sites in the Life Cycle of Oncogenic Human Papillomavirus Type 31." *Journal of Virology* 72 (2): 1071–77.
- Sung, Hyuna, Jacques Ferlay, Rebecca L. Siegel, Mathieu Laversanne, Isabelle Soerjomataram, Ahmedin Jemal, and Freddie Bray. 2021. "Global Cancer Statistics 2020: GLOBOCAN Estimates of Incidence and Mortality Worldwide for 36 Cancers in 185 Countries." *CA: A Cancer Journal for Clinicians* 71 (3): 209–49. <https://doi.org/10.3322/caac.21660>.
- Szalmás, Anita, Vjekoslav Tomaić, Om Basukala, Paola Massimi, Suruchi Mittal, József Kónya, and Lawrence Banks. 2017. "The PTPN14 Tumor Suppressor Is a Degradation Target of Human Papillomavirus E7." *Journal of Virology* 91 (7). <https://doi.org/10.1128/JVI.00057-17>.
- Taberna, M., M. Mena, M. A. Pavón, L. Alemany, M. L. Gillison, and R. Mesía. 2017. "Human Papillomavirus-Related Oropharyngeal Cancer." *Annals of Oncology: Official Journal of the European Society for Medical Oncology* 28 (10): 2386–98. <https://doi.org/10.1093/annonc/mdx304>.
- Talora, Claudio, Samantha Cialfi, Oreste Segatto, Stefania Morrone, John Kim Choi, Luigi Frati, Gian Paolo Dotto, Alberto Gulino, and Isabella Screpanti. 2005. "Constitutively Active Notch1 Induces Growth Arrest of HPV-Positive Cervical Cancer Cells via Separate Signaling Pathways." *Experimental Cell Research* 305 (2): 343–54. <https://doi.org/10.1016/j.yexcr.2005.01.015>.
- Tan, Min Jie Alvin, Elizabeth A. White, Mathew E. Sowa, J. Wade Harper, Jon C. Aster, and Peter M. Howley. 2012a. "Cutaneous  $\beta$ -Human Papillomavirus E6 Proteins Bind Mastermind-like Coactivators and Repress Notch Signaling." *Proceedings of the National Academy of Sciences of the United States of America* 109 (23): E1473-1480. <https://doi.org/10.1073/pnas.1205991109>.
- Thatte, Jayashree, and Lawrence Banks. 2017. "Human Papillomavirus 16 (HPV-16), HPV-18, and HPV-31 E6 Override the Normal Phosphoregulation of E6AP Enzymatic Activity." *Journal of Virology* 91 (22). <https://doi.org/10.1128/JVI.01390-17>.
- Thatte, Jayashree, Paola Massimi, Miranda Thomas, Siaw Shi Boon, and Lawrence Banks. 2018. "The Human Papillomavirus E6 PDZ Binding Motif Links DNA Damage Response Signaling to E6 Inhibition of P53 Transcriptional Activity." *Journal of Virology* 92 (16). <https://doi.org/10.1128/JVI.00465-18>.
- Thomas, J. T., and L. A. Laimins. 1998. "Human Papillomavirus Oncoproteins E6 and E7 Independently Abrogate the Mitotic Spindle Checkpoint." *Journal of Virology* 72 (2): 1131–37. <https://doi.org/10.1128/JVI.72.2.1131-1137.1998>.
- Thomas, M., and L. Banks. 1998a. "Inhibition of Bak-Induced Apoptosis by HPV-18 E6." *Oncogene* 17 (23): 2943–54. <https://doi.org/10.1038/sj.onc.1202223>.



- Thomas, M., B. Glaunsinger, D. Pim, R. Javier, and L. Banks. 2001. "HPV E6 and MAGUK Protein Interactions: Determination of the Molecular Basis for Specific Protein Recognition and Degradation." *Oncogene* 20 (39): 5431–39. <https://doi.org/10.1038/sj.onc.1204719>.
- Thomas, M., N. Narayan, D. Pim, V. Tomaić, P. Massimi, K. Nagasaka, C. Kranjec, N. Gammoh, and L. Banks. 2008a. "Human Papillomaviruses, Cervical Cancer and Cell Polarity." *Oncogene* 27 (55): 7018–30. <https://doi.org/10.1038/onc.2008.351>.
- Thomas, Mary C., and Cheng-Ming Chiang. 2005. "E6 Oncoprotein Represses P53-Dependent Gene Activation via Inhibition of Protein Acetylation Independently of Inducing P53 Degradation." *Molecular Cell* 17 (2): 251–64. <https://doi.org/10.1016/j.molcel.2004.12.016>.
- Thomas, Miranda, and Lawrence Banks. 2015. "PDZRN3/LNX3 Is a Novel Target of Human Papillomavirus Type 16 (HPV-16) and HPV-18 E6." *Journal of Virology* 89 (2): 1439–44. <https://doi.org/10.1128/JVI.01743-14>.
- Thomas, Miranda, Paola Massimi, Christel Navarro, Jean-Paul Borg, and Lawrence Banks. 2005. "The HScrib/Dlg Apico-Basal Control Complex Is Differentially Targeted by HPV-16 and HPV-18 E6 Proteins." *Oncogene* 24 (41): 6222–30. <https://doi.org/10.1038/sj.onc.1208757>.
- Thomas, Miranda, Michael P. Myers, Paola Massimi, Corrado Guarnaccia, and Lawrence Banks. 2016. "Analysis of Multiple HPV E6 PDZ Interactions Defines Type-Specific PDZ Fingerprints That Predict Oncogenic Potential." *PLOS Pathogens* 12 (8): e1005766. <https://doi.org/10.1371/journal.ppat.1005766>.
- Thomas, Miranda, Vjekoslav Tomaić, David Pim, Michael P. Myers, Massimo Tommasino, and Lawrence Banks. 2013a. "Interactions between E6AP and E6 Proteins from Alpha and Beta HPV Types." *Virology* 435 (2): 357–62. <https://doi.org/10.1016/j.virol.2012.11.004>.
- Tirosh, Osnat, Sean Conlan, Clay Deming, Shih-Queen Lee-Lin, Xin Huang, NISC Comparative Sequencing Program, Helen C. Su, Alexandra F. Freeman, Julia A. Segre, and Heidi H. Kong. 2018. "Expanded Skin Virome in DOCK8-Deficient Patients." *Nature Medicine* 24 (12): 1815–21. <https://doi.org/10.1038/s41591-018-0211-7>.
- Togtema, Melissa, Robert Jackson, Christina Richard, Sarah Niccoli, and Ingeborg Zehbe. 2015. "The Human Papillomavirus 16 European-T350G E6 Variant Can Immortalize but Not Transform Keratinocytes in the Absence of E7." *Virology* 485 (November): 274–82. <https://doi.org/10.1016/j.virol.2015.07.025>.
- Tomaić, Vjekoslav. 2016a. "Functional Roles of E6 and E7 Oncoproteins in HPV-Induced Malignancies at Diverse Anatomical Sites." *Cancers* 8 (10). <https://doi.org/10.3390/cancers8100095>.
- Tomaić, Vjekoslav, David Pim, and Lawrence Banks. 2009a. "The Stability of the Human Papillomavirus E6 Oncoprotein Is E6AP Dependent." *Virology* 393 (1): 7–10. <https://doi.org/10.1016/j.virol.2009.07.029>.
- Tomaić, Vjekoslav, David Pim, Miranda Thomas, Paola Massimi, Michael P. Myers, and Lawrence Banks. 2011. "Regulation of the Human Papillomavirus Type 18 E6/E6AP Ubiquitin Ligase Complex by the HECT Domain-Containing Protein EDD." *Journal of Virology* 85 (7): 3120–27. <https://doi.org/10.1128/JVI.02004-10>.
- Tommasino, Massimo. 2017. "The Biology of Beta Human Papillomaviruses." *Virus Research* 231: 128–38. <https://doi.org/10.1016/j.virusres.2016.11.013>.
- Tong, Xiao, and Peter M. Howley. 1997. "The Bovine Papillomavirus E6 Oncoprotein Interacts with Paxillin and Disrupts the Actin Cytoskeleton." *Proceedings of the National Academy of Sciences* 94 (9): 4412–17. <https://doi.org/10.1073/pnas.94.9.4412>.
- Torchia, J., D. W. Rose, J. Inostroza, Y. Kamei, S. Westin, C. K. Glass, and M. G. Rosenfeld. 1997. "The Transcriptional Co-Activator p/CIP Binds CBP and Mediates Nuclear-Receptor Function." *Nature* 387 (6634): 677–84. <https://doi.org/10.1038/42652>.
- Tsou, Meng-Fu Bryan, and Tim Stearns. 2006. "Mechanism Limiting Centrosome Duplication to Once per Cell Cycle." *Nature* 442 (7105): 947–51. <https://doi.org/10.1038/nature04985>.

- Tsvetkov, Peter, Nina Reuven, Carol Prives, and Yosef Shaul. 2009. "Susceptibility of P53 Unstructured N Terminus to 20 S Proteasomal Degradation Programs the Stress Response." *The Journal of Biological Chemistry* 284 (39): 26234–42. <https://doi.org/10.1074/jbc.M109.040493>.
- Underbrink, Michael P., Crystal Dupuis, Jia Wang, and Stephen K. Tying. 2016. "E6 Proteins from Low-Risk Human Papillomavirus Types 6 and 11 Are Able to Protect Keratinocytes from Apoptosis via Bak Degradation." *The Journal of General Virology* 97 (Pt 3): 715–24. <https://doi.org/10.1099/jgv.0.000392>.
- Underbrink, Michael P., Heather L. Howie, Kristin M. Bedard, Jennifer I. Koop, and Denise A. Galloway. 2008a. "E6 Proteins from Multiple Human Betapapillomavirus Types Degrade Bak and Protect Keratinocytes from Apoptosis after UVB Irradiation." *Journal of Virology* 82 (21): 10408–17. <https://doi.org/10.1128/JVI.00902-08>.
- Vaccarella, S., S. Franceschi, G. Engholm, S. Lönnberg, S. Khan, and F. Bray. 2014. "50 Years of Screening in the Nordic Countries: Quantifying the Effects on Cervical Cancer Incidence." *British Journal of Cancer* 111 (5): 965–69. <https://doi.org/10.1038/bjc.2014.362>.
- Van Doorslaer, Koenraad, and Alison A. McBride. 2016. "Molecular Archeological Evidence in Support of the Repeated Loss of a Papillomavirus Gene." *Scientific Reports* 6: 33028. <https://doi.org/10.1038/srep33028>.
- Vande Pol, S. B., M. C. Brown, and C. E. Turner. 1998a. "Association of Bovine Papillomavirus Type 1 E6 Oncoprotein with the Focal Adhesion Protein Paxillin through a Conserved Protein Interaction Motif." *Oncogene* 16 (1): 43–52. <https://doi.org/10.1038/sj.onc.1201504>.
- Vande Pol, Scott B., and Aloysius J. Klingelhutz. 2013a. "Papillomavirus E6 Oncoproteins." *Virology*, Special Issue: The Papillomavirus Episteme, 445 (1): 115–37. <https://doi.org/10.1016/j.virol.2013.04.026>.
- Van Doorslaer, Koenraad, Zhiwen Li, Sandhya Xirasagar, Piet Maes, David Kaminsky, David Liou, Qiang Sun, Ramandeep Kaur, Yentram Huyen, and Alison A. McBride. 2017. "The Papillomavirus Episteme: A Major Update to the Papillomavirus Sequence Database." *Nucleic Acids Research* 45 (Database issue): D499–506. <https://doi.org/10.1093/nar/gkw879>.
- Vats, Arushi, Jayashree Thatte, and Lawrence Banks. 2019. "Identification of E6AP-Independent Degradation Targets of HPV E6." *The Journal of General Virology* 100 (12): 1674–79. <https://doi.org/10.1099/jgv.0.001331>.
- Vats, Arushi, Jayashree V. Thatte, and Lawrence Banks. 2023. "Molecular Dissection of the E6 PBM Identifies Essential Residues Regulating Chk1 Phosphorylation and Subsequent 14-3-3 Recognition." *Tumour Virus Research*, February, 200257. <https://doi.org/10.1016/j.tvr.2023.200257>.
- Vats, Arushi, Oscar Trejo-Cerro, Paola Massimi, and Lawrence Banks. 2022. "Regulation of HPV E7 Stability by E6-Associated Protein (E6AP)." *Journal of Virology* 96 (16): e0066322. <https://doi.org/10.1128/jvi.00663-22>.
- Veldman, T., I. Horikawa, J. C. Barrett, and R. Schlegel. 2001. "Transcriptional Activation of the Telomerase HTERT Gene by Human Papillomavirus Type 16 E6 Oncoprotein." *Journal of Virology* 75 (9): 4467–72. <https://doi.org/10.1128/JVI.75.9.4467-4472.2001>.
- Veldman, Tim, Xuefeng Liu, Hang Yuan, and Richard Schlegel. 2003. "Human Papillomavirus E6 and Myc Proteins Associate in Vivo and Bind to and Cooperatively Activate the Telomerase Reverse Transcriptase Promoter." *Proceedings of the National Academy of Sciences of the United States of America* 100 (14): 8211–16. <https://doi.org/10.1073/pnas.1435900100>.
- Viarisio, Daniele, Karin Mueller-Decker, Ulrich Kloz, Birgit Aengeneyndt, Annette Kopp-Schneider, Hermann-Josef Gröne, Tarik Gheit, Christa Flechtenmacher, Lutz Gissmann, and Massimo Tommasino. 2011. "E6 and E7 from Beta HPV38 Cooperate with Ultraviolet Light in the Development of Actinic Keratosis-like Lesions and Squamous Cell Carcinoma in Mice." *PLoS Pathogens* 7 (7): e1002125. <https://doi.org/10.1371/journal.ppat.1002125>.
- Viarisio, Daniele, Karin Müller-Decker, Rosita Accardi, Alexis Robitaille, Matthias Dürst, Katrin Beer, Lars Jansen, et al. 2018. "Beta HPV38 Oncoproteins Act with a Hit-and-Run Mechanism in

- Ultraviolet Radiation-Induced Skin Carcinogenesis in Mice.” *PLoS Pathogens* 14 (1): e1006783. <https://doi.org/10.1371/journal.ppat.1006783>.
- Villiers, Ethel Michele De, Claude Fauquet, Thomas R. Broker, Hans Ulrich Bernard, and Harald Zur Hausen. 2004. “Classification of Papillomaviruses.” *Virology* 324 (1): 17–27. <https://doi.org/10.1016/j.virol.2004.03.033>.
- Villiers, Ethel-Michele de, Robert D. Burk, Hans-Ulrich Bernard, Zigui Chen, Koenraad van Doorslaer, and Harald zur Hausen. 2010. “Classification of Papillomaviruses (PVs) Based on 189 PV Types and Proposal of Taxonomic Amendments.” *Virology* 401 (1): 70–79. <https://doi.org/10.1016/j.virol.2010.02.002>.
- Vogt, M., K. Butz, S. Dymalla, J. Semzow, and F. Hoppe-Seyler. 2006. “Inhibition of Bax Activity Is Crucial for the Antiapoptotic Function of the Human Papillomavirus E6 Oncoprotein.” *Oncogene* 25 (29): 4009–15. <https://doi.org/10.1038/sj.onc.1209429>.
- Voltaggio, Lysandra, W. Glenn McCluggage, Jeffrey S. Iding, Brock Martin, Teri A. Longacre, and Brigitte M. Ronnett. 2020. “A Novel Group of HPV-Related Adenocarcinomas of the Lower Anogenital Tract (Vagina, Vulva, and Anorectum) in Women and Men Resembling HPV-Related Endocervical Adenocarcinomas.” *Modern Pathology* 33 (5): 944–52. <https://doi.org/10.1038/s41379-019-0437-z>.
- Vos, R. M., J. Altreuter, E. A. White, and P. M. Howley. 2009. “The Ubiquitin-Specific Peptidase USP15 Regulates Human Papillomavirus Type 16 E6 Protein Stability.” *Journal of Virology* 83 (17): 8885–92. <https://doi.org/10.1128/jvi.00605-09>.
- Wade, Ramon, Nicole Brimer, and Scott Vande Pol. 2008. “Transformation by Bovine Papillomavirus Type 1 E6 Requires Paxillin.” *Journal of Virology* 82 (12): 5962–66. <https://doi.org/10.1128/JVI.02747-07>.
- Wallace, Nicholas A., Kristin Robinson, and Denise A. Galloway. 2014a. “Beta Human Papillomavirus E6 Expression Inhibits Stabilization of P53 and Increases Tolerance of Genomic Instability.” *Journal of Virology* 88 (11): 6112–27. <https://doi.org/10.1128/JVI.03808-13>.
- Wallace, Nicholas A., Kristin Robinson, Heather L. Howie, and Denise A. Galloway. 2012. “HPV 5 and 8 E6 Abrogate ATR Activity Resulting in Increased Persistence of UVB Induced DNA Damage.” *PLoS Pathogens* 8 (7): e1002807. <https://doi.org/10.1371/journal.ppat.1002807>.
- . 2015. “ $\beta$ -HPV 5 and 8 E6 Disrupt Homology Dependent Double Strand Break Repair by Attenuating BRCA1 and BRCA2 Expression and Foci Formation.” *PLoS Pathogens* 11 (3): e1004687. <https://doi.org/10.1371/journal.ppat.1004687>.
- Wang, J., A. Sampath, P. Raychaudhuri, and S. Bagchi. 2001. “Both Rb and E7 Are Regulated by the Ubiquitin Proteasome Pathway in HPV-Containing Cervical Tumor Cells.” *Oncogene* 20 (34): 4740–49. <https://doi.org/10.1038/sj.onc.1204655>.
- Wang, Nicholas J., Zachary Sanborn, Kelly L. Arnett, Laura J. Bayston, Wilson Liao, Charlotte M. Proby, Irene M. Leigh, et al. 2011. “Loss-of-Function Mutations in Notch Receptors in Cutaneous and Lung Squamous Cell Carcinoma.” *Proceedings of the National Academy of Sciences of the United States of America* 108 (43): 17761–66. <https://doi.org/10.1073/pnas.1114669108>.
- Wang, Xin, Mei Qi, Xiuping Yu, Yan Yuan, and Weiming Zhao. 2012. “Type-Specific Interaction between Human Papillomavirus Type 58 E2 Protein and E7 Protein Inhibits E7-Mediated Oncogenicity.” *The Journal of General Virology* 93 (Pt 7): 1563–72. <https://doi.org/10.1099/vir.0.039354-0>.
- Weijzen, Sanne, Paola Rizzo, Mike Braid, Radhika Vaishnav, Suzanne M. Jonkheer, Andrei Zlobin, Barbara A. Osborne, et al. 2002. “Activation of Notch-1 Signaling Maintains the Neoplastic Phenotype in Human Ras-Transformed Cells.” *Nature Medicine* 8 (9): 979–86. <https://doi.org/10.1038/nm754>.
- Weitzman, Matthew D, and Jonathan B Weitzman. 2014. “What’s the Damage? The Impact of Pathogens on Pathways That Maintain Host Genome Integrity.” *Cell Host & Microbe* 15 (3): 283–94. <https://doi.org/10.1016/j.chom.2014.02.010>.
- White, E. A., M. E. Sowa, M. J. A. Tan, S. Jeudy, S. D. Hayes, S. Santha, K. Munger, J. W. Harper, and P. M. Howley. 2012. “Systematic Identification of Interactions between Host Cell Proteins and E7

- Oncoproteins from Diverse Human Papillomaviruses.” *Proceedings of the National Academy of Sciences* 109 (5): E260–67. <https://doi.org/10.1073/pnas.1116776109>.
- White, Elizabeth A. 2019. “Manipulation of Epithelial Differentiation by HPV Oncoproteins.” *Viruses* 11 (4): 369. <https://doi.org/10.3390/v11040369>.
- White, Elizabeth A., Rebecca E. Kramer, Min Jie Alvin Tan, Sebastian D. Hayes, J. Wade Harper, and Peter M. Howley. 2012. “Comprehensive Analysis of Host Cellular Interactions with Human Papillomavirus E6 Proteins Identifies New E6 Binding Partners and Reflects Viral Diversity.” *Journal of Virology* 86 (24): 13174–86. <https://doi.org/10.1128/JVI.02172-12>.
- White, Elizabeth A., Johanna Walther, Hassan Javanbakht, and Peter M. Howley. 2014a. “Genus Beta Human Papillomavirus E6 Proteins Vary in Their Effects on the Transactivation of P53 Target Genes.” *Journal of Virology* 88 (15): 8201–12. <https://doi.org/10.1128/JVI.01197-14>.
- Wilson, Regina, Frauke Fehrmann, and Laimonis A. Laimins. 2005. “Role of the E1–E4 Protein in the Differentiation-Dependent Life Cycle of Human Papillomavirus Type 31.” *Journal of Virology* 79 (11): 6732–40. <https://doi.org/10.1128/JVI.79.11.6732-6740.2005>.
- Wise-Draper, Trisha M., and Susanne I. Wells. 2008. “Papillomavirus E6 and E7 Proteins and Their Cellular Targets.” *Frontiers in Bioscience: A Journal and Virtual Library* 13 (January): 1003–17. <https://doi.org/10.2741/2739>.
- Wu, L., J. C. Aster, S. C. Blacklow, R. Lake, S. Artavanis-Tsakonas, and J. D. Griffin. 2000. “MAML1, a Human Homologue of Drosophila Mastermind, Is a Transcriptional Co-Activator for NOTCH Receptors.” *Nature Genetics* 26 (4): 484–89. <https://doi.org/10.1038/82644>.
- Xie, Jian, Pengwei Zhang, Mac Crite, and Daniel DiMaio. 2020. “Papillomaviruses Go Retro.” *Pathogens (Basel, Switzerland)* 9 (4): E267. <https://doi.org/10.3390/pathogens9040267>.
- Xu, Mei, Weifeng Luo, David J. Elzi, Carla Grandori, and Denise A. Galloway. 2008. “NFX1 Interacts with MSin3A/Histone Deacetylase To Repress HTERT Transcription in Keratinocytes.” *Molecular and Cellular Biology* 28 (15): 4819–28. <https://doi.org/10.1128/MCB.01969-07>.
- Yadav, Rashi, Lukai Zhai, and Ebenezer Tumban. 2019. “Virus-like Particle-Based L2 Vaccines against HPVs: Where Are We Today?” *Viruses* 12 (1): 18. <https://doi.org/10.3390/v12010018>.
- Yamamoto, Norio, Kenji Tanigaki, Hua Han, Hiroshi Hiai, and Tasuku Honjo. 2003. “Notch/RBP-J Signaling Regulates Epidermis/Hair Fate Determination of Hair Follicular Stem Cells.” *Current Biology: CB* 13 (4): 333–38. [https://doi.org/10.1016/s0960-9822\(03\)00081-2](https://doi.org/10.1016/s0960-9822(03)00081-2).
- Yamato, K., J. Fen, H. Kobuchi, Y. Nasu, T. Yamada, T. Nishihara, Y. Ikeda, M. Kizaki, and M. Yoshinouchi. 2006. “Induction of Cell Death in Human Papillomavirus 18-Positive Cervical Cancer Cells by E6 siRNA.” *Cancer Gene Therapy* 13 (3): 234–41. <https://doi.org/10.1038/sj.cgt.7700891>.
- Yi, Ja Woon, Mi Jang, Sung Jin Kim, Sung Soon Kim, and Jee Eun Rhee. 2013. “Degradation of P53 by Natural Variants of the E6 Protein of Human Papillomavirus Type 16.” *Oncology Reports* 29 (4): 1617–22. <https://doi.org/10.3892/or.2013.2281>.
- Yu, H, X Zhao, S Huang, L Jian, G Qian, and S Ge. 2007. “Blocking Notch1 Signaling by RNA Interference Can Induce Growth Inhibition in HeLa Cells.” *International Journal of Gynecological Cancer* 17 (2): 511–16. <https://doi.org/10.1111/j.1525-1438.2007.00813.x>.
- Yuan, Xun, Hua Wu, Hanxiao Xu, Na Han, Qian Chu, Shiyong Yu, Yuan Chen, and Kongming Wu. 2015. “Meta-Analysis Reveals the Correlation of Notch Signaling with Non-Small Cell Lung Cancer Progression and Prognosis.” *Scientific Reports* 5 (May): 10338. <https://doi.org/10.1038/srep10338>.
- Yuan, Xun, Mingsheng Zhang, Hua Wu, Hanxiao Xu, Na Han, Qian Chu, Shiyong Yu, Yuan Chen, and Kongming Wu. 2015. “Expression of Notch1 Correlates with Breast Cancer Progression and Prognosis.” *PLOS ONE* 10 (6): e0131689. <https://doi.org/10.1371/journal.pone.0131689>.
- Yugawa, Takashi, Keisuke Handa, Mako Narisawa-Saito, Shin-ichi Ohno, Masatoshi Fujita, and Tohru Kiyono. 2007. “Regulation of Notch1 Gene Expression by P53 in Epithelial Cells.” *Molecular and Cellular Biology* 27 (10): 3732–42. <https://doi.org/10.1128/MCB.02119-06>.
- Zacapala-Gómez, Ana Elvira, Oscar Del Moral-Hernández, Nicolás Villegas-Sepúlveda, Alfredo Hidalgo-Miranda, Sandra Lorena Romero-Córdoba, Fredy Omar Beltrán-Anaya, Marco Antonio Leyva-

- Vázquez, Luz del Carmen Alarcón-Romero, and Berenice Illades-Aguilar. 2016. "Changes in Global Gene Expression Profiles Induced by HPV 16 E6 Oncoprotein Variants in Cervical Carcinoma C33-A Cells." *Virology* 488 (January): 187–95. <https://doi.org/10.1016/j.virol.2015.11.017>.
- Zagouras, P, S Stifani, C M Blaumueller, M L Carcangiu, and S Artavanis-Tsakonas. 1995. "Alterations in Notch Signaling in Neoplastic Lesions of the Human Cervix." *Proceedings of the National Academy of Sciences of the United States of America* 92 (14): 6414–18.
- Zanier, Katia, Sebastian Charbonnier, Mireille Baltzinger, Yves Nominé, Danièle Altschuh, and Gilles Travé. 2005. "Kinetic Analysis of the Interactions of Human Papillomavirus E6 Oncoproteins with the Ubiquitin Ligase E6AP Using Surface Plasmon Resonance." *Journal of Molecular Biology* 349 (2): 401–12. <https://doi.org/10.1016/j.jmb.2005.03.071>.
- Zanier, Katia, Sebastian Charbonnier, Abdellahi Ould, M Ould, G Alastair, Maria Giovanna Ferrario, Pierre Poussin, et al. 2013. "Structural Basis for Hijacking of Cellular LxxLL Motifs by Papillomavirus E6 Oncoproteins." *Science* 339 (6120): 694–98. <https://doi.org/10.1126/science.1229934.Structural>.
- Zanier, Katia, Christine Ruhlmann, Frederic Melin, Murielle Masson, Abdellahi Ould M'hamed Ould Sidi, Xavier Bernard, Benoit Fischer, et al. 2010. "E6 Proteins from Diverse Papillomaviruses Self-Associate Both in Vitro and in Vivo." *Journal of Molecular Biology* 396 (1): 90–104. <https://doi.org/10.1016/j.jmb.2009.11.022>.
- Zehbe, Ingeborg, Christina Richard, Correne A. DeCarlo, Anny Shai, Paul F. Lambert, Hava Lichtig, Massimo Tommasino, and Levana Sherman. 2009. "Human Papillomavirus 16 E6 Variants Differ in Their Dysregulation of Human Keratinocyte Differentiation and Apoptosis." *Virology* 383 (1): 69–77. <https://doi.org/10.1016/j.virol.2008.09.036>.
- Zhang, Lei, Hong Liao, Binlie Yang, Christopher P Geffre, Ai Zhang, Aizhi Zhou, Huimin Cao, Jieru Wang, Zhenbo Zhang, and Wenxin Zheng. 2015. "Variants of Human Papillomavirus Type 16 Predispose toward Persistent Infection." *International Journal of Clinical and Experimental Pathology* 8 (7): 8453–59.
- Zhang, Min, Sangita Biswas, Xin Qin, Wenrong Gong, Wenbing Deng, and Hongjun Yu. 2016. "Does Notch Play a Tumor Suppressor Role across Diverse Squamous Cell Carcinomas?" *Cancer Medicine* 5 (8): 2048–60. <https://doi.org/10.1002/cam4.731>.
- Zhang, Yi, Jhimli Dasgupta, Runlin Z. Ma, Lawrence Banks, Miranda Thomas, and Xiaojiang S. Chen. 2007. "Structures of a Human Papillomavirus (HPV) E6 Polypeptide Bound to MAGUK Proteins: Mechanisms of Targeting Tumor Suppressors by a High-Risk HPV Oncoprotein." *Journal of Virology* 81 (7): 3618–26. <https://doi.org/10.1128/JVI.02044-06>.
- Zhao, Yongtong, Rebecca B. Katzman, Laurie M. Delmolino, Ishfaq Bhat, Ying Zhang, Channabasavaiah B. Gurumurthy, Aleksandra Germaniuk-Kurowska, et al. 2007. "The Notch Regulator MAML1 Interacts with P53 and Functions as a Coactivator." *The Journal of Biological Chemistry* 282 (16): 11969–81. <https://doi.org/10.1074/jbc.M608974200>.
- Zimmermann, H., R. Degenkolbe, H. U. Bernard, and M. J. O'Connor. 1999. "The Human Papillomavirus Type 16 E6 Oncoprotein Can Down-Regulate P53 Activity by Targeting the Transcriptional Coactivator CBP/P300." *Journal of Virology* 73 (8): 6209–19.

## 8. LIST OF TABLES AND FIGURES

### LIST OF TABLES

**Table 1.** Buffers and solutions

**Table 2.** Chemicals for various experiments and cell treatment

**Table 3.** Detergents for preparation of buffers and solutions

**Table 4.** Antibiotics used for cell and bacteria culture

**Table 5.** Commercial kits and reagents

**Table 6.** Enzymes and corresponding buffers

**Table 7.** Primary antibodies

**Table 8.** Secondary antibodies

**Table 9.** DNA markers for determining the molecular weight of nucleic acids

**Table 11.** Protein inhibitors

**Table 12.** Cell and bacterial growth media and corresponding supplements

**Table 13.** Instruments

**Table 14.** Programs for data analysis and visualization

**Table 15.** Specific primers for site-directed mutagenesis of pCA:16E6 and pGEX-2T:16 E6 vectors

**Table 16.** PCR conditions for site-directed mutagenesis

**Table 17.** Cell lines used for this doctoral research

**Table 18.** Small interfering RNA molecules (siRNA) used to silence MAML1 and UBE3A genes

**Table 19.** Polyacrylamide gels composition

**Table 20.** Reaction components for in vitro protein transcription/translation

**Table 21.** The significance of the number of stars on the displayed results

### LIST OF FIGURES

**Figure 1.** Schematic representation of HPV-16 genomic organization

**Figure 2.** Linear representation of the HPV-16 genome

**Figure 3.** HPV life cycle and development of malignancy

**Figure 4.** Schematic representation of HR E7 oncoprotein structure.

**Figure 5.** Schematic representation of HR HPV E6 oncoprotein structure

**Figure 6.** The sequence alignment and 3D structure of HPV-16 E6 European-Prototype with indicated L83V and D25N/L83V mutations

**Figure 7.** Schematic representation of HR HPV-16 E6 protein structure, including the binding sites involved in interactions with its cellular targets and the corresponding functions of E6

**Figure 8.** HPV E6 oncoprotein interfere with apoptosis through a variety of mechanisms

**Figure 9.** HPV E6 oncoprotein regulation of cell polarity complexes

**Figure 10.** Schematic representation of the cellular protein targets and signaling pathways affected by E6 oncoproteins

**Figure 11.** Canonical Notch signaling pathway vs. Notch signaling in HPV-infected cells

**Figure 12.** Schematic representation of human Mastermind-like transcriptional coactivator 1 (MAML1) protein structure

**Figure 13.** Schematic representation of a model mechanism by which HPV-8 E6 gets access to the regulatory regions of Notch target genes

**Figure 14.** DNA sequence alignment analysis after performing site directed mutagenesis using pCA:16E6 and pGEX-2T:16E6 plasmids as templates

**Figure 15.** HPV-16 E6 D25N L83V variant exhibits an increased capacity to interact and with E6AP

**Figure 16.** HPV-16 E6 D25N L83V variant exhibits an increased capacity to change E6AP turnover

**Figure 17.** HPV-16E6 D25N L83V exhibits higher protein levels, but shorter protein half-life

**Figure 18.** Cellular localization of ectopically expressed HPV-16 E6, wild type and 16 E6 L83V, D25N and D25N L83V oncoproteins

**Figure 19.** HPV-16 E6 wild-type and the corresponding 16 E6 D25N, 16 E6 L83V and 16 E6 D25N L83V mutants efficiently degrade p53 *in vitro*

**Figure 20.** HPV 16 E6 D25N, E6 L83V and E6 D25N L83V variants efficiently degrade MAGI-1 *in vitro*

**Figure 21.** HPV 16 E6 D25N, E6 L83V and E6 D25N L83V variants efficiently degrade DLG1 *in vitro*

**Figure 22.** HPV 16 E6 wild-type and E6 D25N L83V variant efficiently degrade Scrib *in vitro*

**Figure 23.** D25N and L83V mutations in HPV-16 E6 do not affect E6 ability to target p53 for a proteasome mediated degradation

**Figure 24.** HPV-16 E6 D25N L83V variant was least efficient in targeting MAGI- for proteasome-mediated degradation

**Figure 25.** D25N and L83V mutations in HPV-16 E6 do not affect E6 ability to target DLG1 for a proteasome mediated degradation

**Figure 26.** Both  $\alpha$ - and  $\beta$ - HPV E6 oncoproteins bind to MAML1

**Figure 27.** MAML1 mediates the increase in E6 protein amounts from both  $\alpha$ - and  $\beta$ - HPV types

**Figure 28.** MAML1-mediated upregulation of  $\alpha$ - and  $\beta$ -E6 protein levels are E6AP-independent

**Figure 29.** Schematic representation of MAML1 protein structure with indicated point mutations in LXXLL motif

**Figure 30.** MAML1 is involved in the regulation of E6 protein amounts via LXXLL motif

**Figure 31.** MAML1 regulates endogenous E6 protein levels in HeLa, CaSki and HT1080 HPV-8 E6-expressing cells

**Figure 32.** MAML1 stabilizes distinctive cellular pools of HPV-18 E6

**Figure 33.** MAML1 stabilizes an exclusive single cellular pool of HPV-8 E6



**Figure 34.** 16 E6/MAML1 complex does not induce p53 degradation

**Figure 35.** E6/MAML1 complex does not induce DLG1 degradation

**Figure 36.** MAML1 and E6AP exhibit a synergistic effect on HPV-18 E6 half-life

**Figure 37.** HPV-8 E6 protein half-life is exclusively regulated by MAML1

**Figure 38.** MAML1 causes changes in HPV-16 E6 and HPV-8 E6 cellular accumulation

**Figure 39.** Silencing MAML1 has no effect on cell apoptosis

**Figure 40.** MAML1 and E6AP cooperate in increasing E6-dependent cellular proliferation

**Figure 41.** Silencing MAML1 impacts cell migration in HPV-18 positive cells

**Figure 42.** Proposed model mechanism for  $\alpha$ - and  $\beta$ -HPV E6 interplay with MAML1.

**Supplementary Figure 1.** Negative controls for Figure 27A.

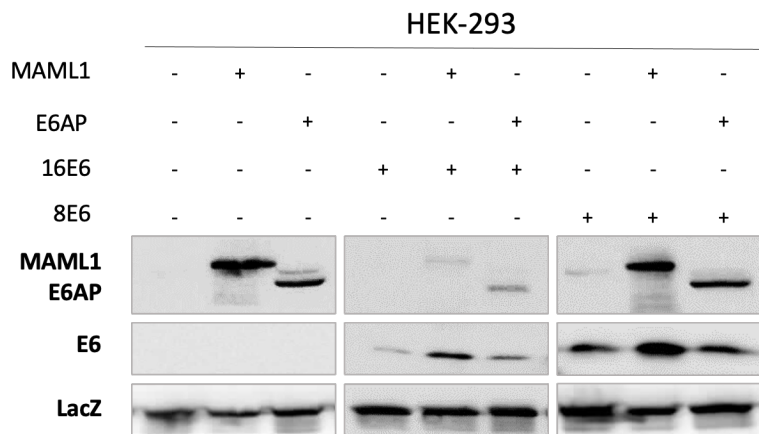
**Supplementary Figure 2.** Negative controls for Figure 28A.

**Supplementary Figure 4.** Negative controls for Figure 30C.

**Supplementary Figure 3.** Negative controls for Figures 30A and 30B.

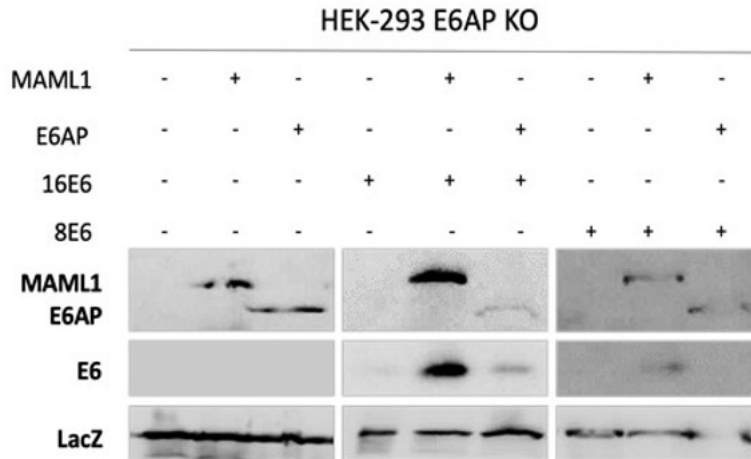
## 9. SUPPLEMENTARY DATA

In addition to the results of an extensive analysis of  $\alpha$ - and  $\beta$ -E6 protein stability in the presence of either MAML1 or E6AP (**Figure 27A**), the following figure separately presents additional negative controls (**Supplementary Figure 1**). The control samples included HEK-293 cell transfected with empty pcDNA3 plasmid, FLAG- or Myc-tagged MAML1 or E6AP alone. Along with those negative controls, samples with MAML1 and E6AP in combination with HA-tagged HPV-16 E6 and HPV-8 E6 are also depicted as a part of the same experiment (**Supplementary Figure 1**).



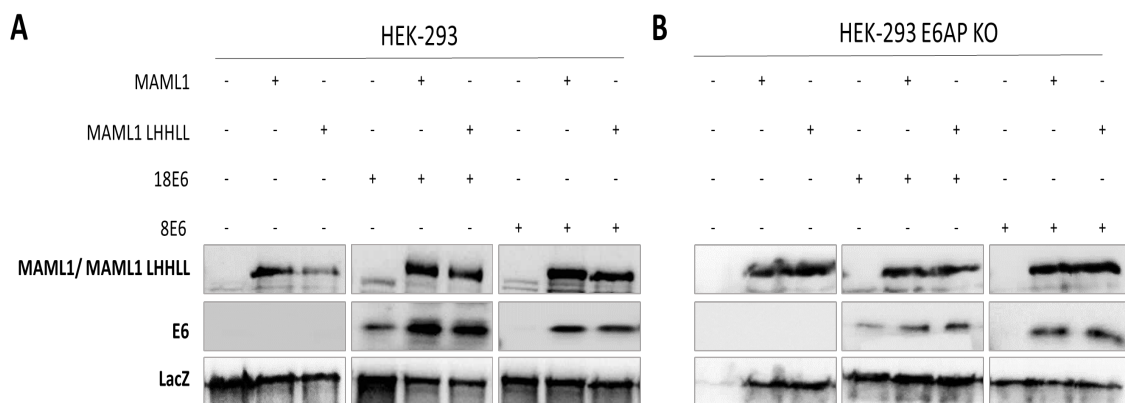
**Supplementary Figure 1. Negative controls for Figure 27A.** HEK-293 cells were transfected with empty pcDNA3 plasmid, FLAG- or Myc-tagged MAML1 or E6AP, alone or in combination with HA-tagged HPV-16 E6 and HPV-8 E6. After 24 hours cells were harvested and isolated proteins separated on SDS-PAGE, processed for western blot analysis using anti-HA, anti-FLAG or anti-Myc antibodies and visualized by chemiluminescence.  $\beta$ -galactosidase (LacZ) was used as loading control.

Same as for the experiment presented in **Figure 27A**, in addition to the results of an extensive analysis of E6 protein stability in presence or absence of MAML1 or E6AP in HEK-293 E6AP KO cells (**Figure 28A**), in **Supplementary Figure 2** negative controls are separately showed. The control samples included HEK-293 E6AP KO cell transfected with empty pcDNA3 plasmid, FLAG- or Myc-tagged MAML1 or E6AP alone, along with samples co-transfected with HA-tagged HPV-16 E6 and HPV-8 E6 (**Supplementary Figure 2**).



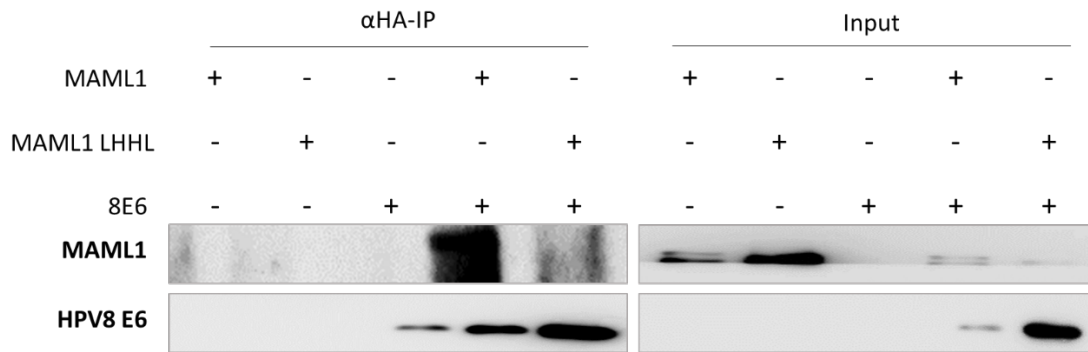
**Supplementary Figure 2. Negative controls for Figure 28A.** HEK-293 E6AP KO cells were transfected with either FLAG- or Myc-tagged MAML1 or E6AP, alone or in combination with HA-tagged HPV-16 E6 or HPV-8 E6. After 24 hours cells were harvested, isolated proteins from complete cell lysates separated on SDS-PAGE, detected by anti-HA, anti-FLAG and anti-Myc antibodies and visualized by chemiluminescence.  $\beta$ -galactosidase (LacZ) was used as the control to monitor transfection efficiency and loading.

The results of evaluating the significance of the LDDLL motif in the stabilizing effect on E6 are presented in **Figures 30A and 30B**. **Supplementary Figure 3** shows negative controls separately. The control samples included HEK-293 cell and HEK2-93 E6AP KO cells transfected with empty pcDNA3 plasmid, Myc-tagged MAML1 or FLAG-tagged MAML1 LHHLL alone. As a part of the same experiment additional samples were co-transfected in combination with HA-tagged HPV-18 E6 or HPV-8 E6.



**Supplementary Figure 3. Negative controls for Figures 30A and 30B.** (A) HEK-293 and (B) HEK-293 E6AP KO cells were transfected with Myc-tagged MAML1 or FLAG-tagged MAML1 LHHLL, alone or in combination with HA-tagged HPV18 E6 or HPV-8 E6. After 24 hours cells were harvested, isolated proteins from complete cell lysates were separated on SDS-PAGE and analysed by western blotting. MAML1 and MAML1 LHHLL were detected by anti-Myc and anti-FLAG antibodies, while HPV-18 E6 and HPV-8 E6 were detected by HRP-linked anti-HA antibody.  $\beta$ -galactosidase (LacZ) was used as the control for the transfection efficiency and loading control.

In addition to the co-immunoprecipitation analysis conducted to determine if an intact LXXLL motif on MAML1 is necessary for HPV-8 E6 binding, as presented in **Figure 31C**, negative controls for this experiment are displayed separately in **Supplementary Figure 4**. The experiment was performed using HEK-293 cells transfected with an empty plasmid, FLAG-tagged MAML1 and a mutated MAML1 LHHLL form either alone, or in combination with plasmid expressing HA-tagged HPV-8 E6 (**Supplementary Figure 4**).



**Supplementary Figure 4. Negative controls for Figure 30C.** HEK-293 cells were transfected with either an empty plasmid, Myc-tagged MAML1, FLAG-tagged MAML1 LHHLL mutant, as well as with HA-tagged HPV-8 E6 alone or in combination with MAML1 and MAML1 LHHLL. Twenty-four hours post transfection the cells were harvested, lysed in E1A buffer and incubated with anti-HA beads on a rotating wheel overnight at 4°C. The beads were extensively washed and co-immunoprecipitated complexes were subjected to western blot analysis with anti-Myc, anti-FLAG and anti-HA antibodies to compare the amount of MAML1, MAML1 LHHLL or 8 E6 present in 10% of the input.

## 10. ABBREVIATIONS

$\alpha$ -HPV – Alpha human papillomavirus

$\beta$ -HPV – Beta human papillomavirus

aa - Amino Acid

ADAM – A Disintegrin and Metalloprotease

ADC - Adenocarcinoma

AKT - AKT Serine/Threonine Kinase

ATM - Ataxia Telangiectasia Mutated

ATR – Ataxia Telangiectasia And Rad3-Related Protein

aPKC - atypical Protein Kinase C

APOBEC - Apolipoprotein B mRNA Editing Enzyme, Catalytic Polypeptide-like

Bcl-2 - B-cell Lymphoma 2

b-HLH - basic Helix-Loop-Helix

BPV - Bovine papillomavirus

CBF1 – other name for RBP-J $\kappa$

CBP – CREB-binding Protein

CDK - Cyclin-Dependent Kinase

CD1 - Conserved Domain 1

CD2 - Conserved Domain 2

CD3 - Conserved Domain 3

Chk - Checkpoint Kinase

CKII - Casein Kinase II

CIN - Cervical intraepithelial neoplasia

CSCC - Cutaneous Squamous Cell Carcinoma

CSL - an acronym for CBF-1/RBP-J $\kappa$

CUL2 - Cullin 2

DDR - DNA Damage Response

DISC - Death-Inducing Signaling Complex

DLG - Discs Large protein

DLL1-3-4 - Delta-like 1, 3, and 4

DSB - Double-strand breaks in DNA

ECM - Extracellular Matrix

EDD/UBR5 - E3 Ubiquitin Ligase Identified by Differential Display; UBR5 (Ubiquitin Protein Ligase E3 Component n-recogin 5)

EGFR - Epidermal Growth Factor Receptor

EMT - Epithelial-mesenchymal Transition

E6AP - E6-associated Protein; UBE3A (Ubiquitin Protein Ligase E3A)

E6BP - E6-binding Protein, Calcium-binding Protein ERC-55

FADD - FAS-associated Protein With Death Domain

FAK - Focal Adhesion Kinase

FCS- Forward Scatter

h - hours

HECT - Homologous to the E6-AP Carboxyl Terminus

HERC - HECT and RLD Domain Containing E3 Ubiquitin Protein Ligase Family Member

HES - Hairy and Enhancer of Split

HEY - Hairy Ears, Y-Linked

HNC - Head-And-Neck Cancer

HNSCC – Head-and-neck squamous cell carcinoma

HPV - Human papillomavirus

HR - High-risk

HSPG – Heparan Sulfate Chains of Proteoglycans

hTERT – human Telomerase Reverse Transcriptase

IAP2 - Inhibitor of Apoptosis Protein 2

ICTV - International Committee on the Taxonomy of Viruses

IRF-3 - Interferon Regulatory Factor

JAG1-2 - Jagged-1 and 2

MAGI-1 - Membrane-associated Guanylate Kinase, WW and PDZ domain-containing protein 1

MAML1 – Mastermind-like Protein 1

MHC – Major Histocompatibility Complex

MAPK - Mitogen-activated Protein Kinase

NFX1 - Nuclear Transcription Factor, X-Box Binding 1

NHEJ - Non-Homologous End Joining

NMSC - Non-Melanoma Skin Cancer

NICD - NOTCH Intracellular Domain

NIKS - Normal Immortal Keratinocytes

NTC - NOTCH-RBPJK Transcriptional Complex

LCR - Long Control Region

LR – Low risk

OPSCC - Oropharyngeal Squamous Cell Carcinoma

OIS - Oncogene-induced senescence

ORF – Open Reading Frame

PBM - PDZ-domain Binding Motif

PDZ – PSD95/Dlg/ZO-1 Binding Domain

PI – Propidium iodide

PKA – Protein Kinase A

PKB - Protein Kinase B

PSD95 - Post Synaptic Density 95

pRb – protein Retinoblastoma

PTPN14 - Protein Tyrosine Phosphatase Non-Receptor Type 14

PXN - Paxillin

p53 – protein 53

RBP-J $\kappa$  - Recombination Signal Binding Protein for Immunoglobulin Kappa J Region/suppressor of hairless

RING - Really Interesting New Gene (RING) finger E3 ubiquitin ligases

RT – Room temperature

SSC – Side scatter

SSC – Squamous Cell Carcinoma

STAT3 - Signal Transducer and Activator of Transcription 3

SV40 T - Simian Vacuolating Virus 40 Large Tumor Antigen

TNF $\alpha$  - Tumor Necrosis Factor  $\alpha$

TNFR1 - Tumor Necrosis Factor Receptor 1



TRAIL - TNF-Related Apoptosis-Inducing ligand

TRIM25 - Tripartite Motif Containing 25

URR - Upstream Regulatory Region

UPS - Ubiquitin Proteasome System

USF - Upstream Stimulating Factor

UV - Ultraviolet irradiation

ZO-1 - Zona Occludens 1

## 11. CURRICULUM VITAE

**Anamaria Đukić**, mag.biotech.in.med.

**Date and place of birth:** 23/01/1993, Rijeka, Croatia

### Education

October 2017 – present

**Postgraduate interdisciplinary doctoral study of Medicinal Chemistry**  
Department of Biotechnology University of Rijeka, Croatia

October 2014 – October 2016

**MSc in Biotechnology in medicine**  
Department of Biotechnology University of Rijeka, Croatia  
Degree classification: Highest distinction “*Summa cum laude*”

October 2011 - July 2014

**BSc in Biotechnology and Drug Discovery**  
Department of Biotechnology University of Rijeka, Croatia  
Degree classification: Upper Second-Class Honours

### Work experience

February 2018 – present

**Research Assistant- PhD student** at Laboratory of molecular virology and Bacteriology, Division of Molecular Medicine, Rudjer Boskovic Institute, Zagreb, Croatia  
Supervisor: Vjekoslav Tomiać, PhD

#### **Projects:**

- 1) Biological Factors Determining Human Papillomavirus (HPV) Driven Carcinogenesis, ICGEB project, 2017-2020, PI: Vjekoslav Tomiać;
- 2) Elucidating the HPV E6/E7 Oncogenic Functions at Different Anatomical Sites, CSF project, 2017-2021, PI: Vjekoslav Tomiać

April 2017 – February 2018

**Professional Practice** at Laboratory of Molecular Virology and Bacteriology Division of Molecular Medicine, Rudjer Boskovic Institute, Zagreb  
Supervisor: Vjekoslav Tomiać, PhD  
Research interest: viral oncology, HPV infection, carcinogenesis

October 2016 – April 2017

**Erasmus+ Graduate Traineeship** in Molecular Medicine Laboratory International Centre for Genetic Engineering and Biotechnology, Trieste, Italy  
Supervisor: prof. Mauro Giacca, PhD  
Research interest: cardiovascular disorders, cardiac regeneration, adeno-associated virus (AAV), gene therapy, angiogenesis, microRNAs

December 2015 – June 2016

**Master thesis internship** at Department of Histology and Embryology, Faculty of Medicine, University of Rijeka  
**M.A. thesis:** "The dynamics of expression of molecules important for the activation of immune system in the visceral tissue in obesity"  
Supervisor: prof. Bojan Polić, PhD

### Training

October - November 2022

**Short-term scientific visit and Ruder Boskovic Institute Fellowship award**  
Sir William Dunn School of Pathology  
Oxford, UK

November 2018

**Short-term scientific visit and Ruder Boskovic Institute Fellowship award**  
Research Group – Tumor Virology  
International Centre for Genetic Engineering and Biotechnology, Trieste, Italy

## Teaching and Volunteering

- November 2018 **Organizing Committee** for *HDIR-5: Translating Science to Medicine- Targets and Therapeutics*, Zagreb, Croatia
- May 2018 – present **Scientific Communication** for Rudjer Boskovic Institute, *Open Days of the Rudjer Boskovic Institute*, Zagreb, Croatia
- April 2018 **Organizing Committee** for international symposium *Epigenetic Changes Head and Neck Cancer*, Zagreb, Croatia
- October 2019 **Scientific Communication** for Rudjer Boskovic Institute at *Festival of Science – Zagreb*

## Awards and Honours

- August 2022 **Travel grant for short-term scientific visit** to Sir William Dunn School of Pathology, Oxford, UK, awarded from Rudjer Boskovic Institute
- July 2019 **Travel grant for “ICGEB DNA Tumor Virus Meeting”**, Trieste, Italy, awarded from The Arturo Falaschi Fellowship Programme
- November 2018 **Travel grant for short-term scientific visit** to International Centre for Genetic Engineering and Biotechnology, Trieste, Italy, awarded from Rudjer Boskovic Institute
- October 2016 – April 2017 **Erasmus+ Scholarship for Traineeship** International Centre for Genetic Engineering and Biotechnology, Trieste, Italy

## Publications

- **MAML1-induced HPV E6 oncoprotein stability is required for cellular proliferation and migration of cervical tumor-derived cells**  
Skelin J., Đukić A, Filić V, Hufbauer M, Akgül B, Thomas M, Banks L, Tomaić V.  
J Med Virol. (2023), 95 (3), e28624, doi: 10.1002/jmv.28624; **IF 20.693, Q1**
- **Human Papillomaviruses-Associated Cancers: An Update of Current Knowledge**  
Pešut, E., Đukić, A., Lulić, L., Skelin, J., Šimić, I., Gašperov, N., Tomaić, V., Sabol, I., Grce, M.  
Viruses-Basel (2021), 13 (11), 2234, 32 doi:10.3390/v13112234.; **IF 5.048, Q1.**
- **ATP synthase modulation leads to an increase of spare respiratory capacity in HPV associated cancers**  
Kirschberg, M., Heuser, S., Marcuzzi, G., Hufbauer, M., Seeger, J., Đukić, A., Tomaić, V., Majewski, S., Wagner, S., Wittekindt, C., Würdemann, N., Klusmann, J., Quaas, A., Kashkar, H. & Akgül, B.  
Scientific reports (2020), 10 (1), 17339, 12 doi:10.1038/s41598-020-74311-6.; **IF 4.380, Q1.**
- **HPV Oncoproteins and the Ubiquitin Proteasome System: A Signature of Malignancy?**  
Đukić, A., Lulić, L., Thomas, M.; Skelin, J., Saidu, NEB, Grce, M., Banks, L., Tomaić, V.,  
Pathogens (2020), 9 (2), 1-27 doi:10.3390/pathogens9020133.; **IF 3.41, Q1.**
- **PDZ Domain-Containing Protein NHERF-2 is a Novel Target of Human Papillomavirus type 16 (HPV-16) and HPV-18**  
Saidu NEB., Filić V., Thomas M., Sarabia-Vega V., Đukić A., Miljković F., Banks L., Tomaić V.  
Journal of virology (2019), 94 (1), e00663-19 doi:10.1128/JVI.00663-19; ; **IF 4.501, Q1.**

## **Presentations**

### **Oral presentations**

- May 2022 – **1<sup>st</sup> Biomedicine and Health PhD Students Congress “Science and Us”** (Rijeka, Croatia) “*MAMLI-induced HPV E6 oncoprotein stability is required for cellular proliferation and migration of cervical tumor-derived cells*”
- October 2021 - **PhD Days – Doctoral study medicinal chemistry** (Rijeka, Croatia) “*MAMLI-induced HPV E6 oncoprotein stability is required for cellular proliferation and migration of cervical tumor-derived cells*”
- May 2019 – **HDIR Symposium** (Zagreb, Croatia) “*Oncogenic Potential of Naturally Occurring HPV- 16 E6 Variants*”

### **Poster presentations**

- October 2020 - **Doctoral Students Symposium** (Zagreb, Croatia) “*Human DLG1 and SCRIB Are Distinctly Regulated Independently of HPV-16 during the Progression of Oropharyngeal Squamous Cell Carcinomas: A Preliminary Analysis*”
- July 2019 - **ICGEB DNA Tumor Virus Meeting** (Trieste, Italy) “*Oncogenic Potential of Naturally Occurring HPV-16 E6 Variants*”
- November 2018. - **HDIR-5: Translating Science to Medicine – Targets and Therapeutics** (Zagreb, Croatia) “*Biochemical Differences Among Naturally Occurring HPV-16 E6 Variants*”
- May 2018 - **Power of viruses 2018** (Porec, Croatia) “*Biochemical Characterization of Naturally Occurring HPV-16 E6 and E7 Variants*”

## **Membership**

- Croatian Association for Cancer Research (CACR)
- European Association for Cancer Research (EACR)
- Croatian Society of Biochemistry and Molecular Biology